frontiers

RESEARCH TOPICS

THE LINK BETWEEN BRAIN ENERGY HOMEOSTASIS AND NEURONAL ACTIVITY

Topic Editor
Yuri Zilberter

frontiers in NEUROENERGETICS

frontiers in PHARMACOLOGY

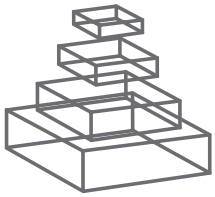

frontiers

Cover image provided by Ibbl sarl, Lausanne CH

ISSN 1664-8714
ISBN 978-2-88919-127-7
DOI 10.3389/978-2-88919-127-7

ABOUT FRONTIERS

Frontiers is more than just an open-access publisher of scholarly articles: it is a pioneering approach to the world of academia, radically improving the way scholarly research is managed. The grand vision of Frontiers is a world where all people have an equal opportunity to seek, share and generate knowledge. Frontiers provides immediate and permanent online open access to all its publications, but this alone is not enough to realize our grand goals.

FRONTIERS JOURNAL SERIES

The Frontiers Journal Series is a multi-tier and interdisciplinary set of open-access, online journals, promising a paradigm shift from the current review, selection and dissemination processes in academic publishing.
All Frontiers journals are driven by researchers for researchers; therefore, they constitute a service to the scholarly community. At the same time, the Frontiers Journal Series operates on a revolutionary invention, the tiered publishing system, initially addressing specific communities of scholars, and gradually climbing up to broader public understanding, thus serving the interests of the lay society, too.

DEDICATION TO QUALITY

Each Frontiers article is a landmark of the highest quality, thanks to genuinely collaborative interactions between authors and review editors, who include some of the world's best academicians. Research must be certified by peers before entering a stream of knowledge that may eventually reach the public - and shape society; therefore, Frontiers only applies the most rigorous and unbiased reviews.
Frontiers revolutionizes research publishing by freely delivering the most outstanding research, evaluated with no bias from both the academic and social point of view.
By applying the most advanced information technologies, Frontiers is catapulting scholarly publishing into a new generation.

WHAT ARE FRONTIERS RESEARCH TOPICS?

Frontiers Research Topics are very popular trademarks of the Frontiers Journals Series: they are collections of at least ten articles, all centered on a particular subject. With their unique mix of varied contributions from Original Research to Review Articles, Frontiers Research Topics unify the most influential researchers, the latest key findings and historical advances in a hot research area!
Find out more on how to host your own Frontiers Research Topic or contribute to one as an author by contacting the Frontiers Editorial Office: researchtopics@frontiersin.org

LINK BETWEEN BRAIN ENERGY HOMEOSTASIS AND NEURONAL ACTIVITY

Topic Editor:
Yuri Zilberter, INSERM UMR 1106 Institut de Neurosciences des Systèmes, France

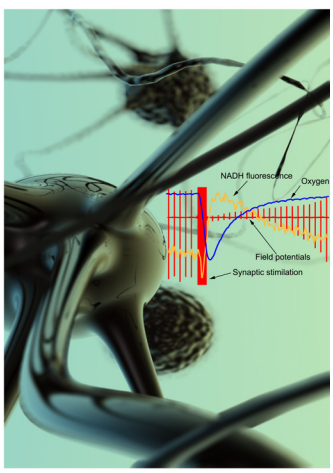

Changes in metabolic and electrophysiological parameters induced by synaptic stimulation

The brain is an extremely energy consuming part of the body, which makes it dangerously vulnerable to metabolic stress. It's no wonder then that abnormalities of brain energy metabolism are becoming the usual suspects and a hallmark of many neurodegenerative diseases. The socioeconomic burden of these alone begs for urgent measures to be taken for better understanding both fundamental and applied problems of neuroenergetics and neuroprotection. For instance, brain imaging reveals that the diseased brains of Alzheimer's patients cannot efficiently utilize the vital brain fuel, glucose. The resulting energy deficit causes neuronal hyperactivity, seizures and cognitive impairments. Administration of native energy substrates complementary to glucose is a logical (and attractive in its simplicity) approach in fighting the energy crisis in the brain*.

The two closely related aspects of brain activity -- neuronal and metabolic – are currently considered to be of utmost importance in both fundamental and applied neuroscience. Although recently the studies of both brain activity and metabolism in normal conditions, under metabolic stress, and in neurodegenerative diseases have experienced significant progress, their overlapping areas deserve further clarification by joint efforts from experts in such fields as (1) energy demands, supplies, and efficiency at the cellular level: in neurons, glial elements, micro-vessels and in the process of their coordinated interactions; (2) specific roles of energy substrates in fine-tuning of the demand-supply mechanism in the condition of metabolic stress; and (3) the macro-level of energy homeostasis and dietary manipulations possible beneficial for neurodegenerative diseases. The result of combining into a coherent whole the recent findings in these fields will hopefully bring forward a broader

view and better understanding of the knowledge continuum, which is under the threat of further fragmentation due to the unavoidable process of specialization in neuroscience.

Current issue covers the three major groups of topics:

1. The Pros and Cons of studies of neuronal activity using brain slice preparations
2. The role of particular energy substrates in metabolic support of neuronal activity
3. The macro-level of energy homeostasis and the dietary manipulations that seem promising in prevention and correction of the diseases of brain energy metabolism

Footnote

* Gulyaeva, N. V. and Stepanichev, M. Y. (2013). The anti-AD cookbook: a new recipe. Journal of Neurochemistry, 125: 4–6. doi: 10.1111/jnc.12138

Table of Contents

06 ***Understanding How the Brain Ensures its Energy Supply***
Yuri Zilberter

08 ***Excitatory GABA: How a Correct Observation May Turn Out to be an Experimental Artifact***
Piotr Bregestovski and Christophe Bernard

16 ***Metabolic Studies in Brain Slices – Past, Present, and Future***
Leif Hertz

19 ***Critical State of Energy Metabolism in Brain Slices: The Principal Role of Oxygen Delivery and Energy Substrates in Shaping Neuronal Activity***
Anton Ivanov and Yuri Zilberter

32 ***The Energy Demand of Fast Neuronal Network Oscillations: Insights from Brain Slice Preparations***
Oliver Kann

38 ***Activation of Astroglial Calcium Signaling by Endogenous Metabolites Succinate and Gamma-Hydroxybutyrate in the Nucleus Accumbens***
Tünde Molnár, László Héja, Zsuzsa Emri, Ágnes Simon, Gabriella Nyitrai, Ildikó Pál and Julianna Kardos

47 ***The Ketogenic Diet as a Treatment Paradigm for Diverse Neurological Disorders***
Carl E. Stafstrom and Jong M. Rho

55 ***The Nervous System and Metabolic Dysregulation: Emerging Evidence Converges on Ketogenic Diet Therapy***
David N. Ruskin and Susan A. Masino

67 ***Aerobic Production and Utilization of Lactate Satisfy Increased Energy Demands Upon Neuronal Activation in Hippocampal Slices and Provide Neuroprotection Against Oxidative Stress***
Avital Schurr and Evelyne Gozal

82 ***Cellular Links Between Neuronal Activity and Energy Homeostasis***
Pavan K. Shetty, Francesca Galeffi and Dennis A. Turner

96 ***Deciphering the Neuronal Circuitry Controlling Local Blood Flow in the Cerebral Cortex with Optogenetics in PV::Cre Transgenic Mice***
Alan Urban, Armelle Rancillac, Lucie Martinez and Jean Rossier

104 Energetics Based Spike Generation of a Single Neuron: Simulation Results and Analysis

Nagarajan Venkateswaran, Sudarshan Sekhar, Thiagarajan Thirupatchur Sanjayasarathy, Sharath Navalpakkam Krishnan, Dinesh Kannan Kabaleeswaran, Subbu Ramanathan, Naren Narayanasamy, Sharan Srinivas Jagathrakshakan and S. R. Vignesh

116 Carbohydrate-Biased Control of Energy Metabolism: The Darker Side of the Selfish Brain

Tanya Zilberter

frontiers in
NEUROENERGETICS

EDITORIAL
published: 20 August 2012
doi: 10.3389/fnene.2012.00009

Understanding how the brain ensures its energy supply

Yuri Zilberter*

Institut de Neuroscience des Systèmes, INSERM URM 1106, Aix-Marseille Université, Marseille, France
**Correspondence: yuri.zilberter@univmed.fr*

Edited by:
Pierre J. Magistretti, Ecole Polytechnique Fédérale De Lausanne, Switzerland

Reviewed by:
Albert Gjedde, University of Copenhagen, Denmark
Fahmeed Hyder, Yale University, USA

The theme of this research topic emerged in the hope of elucidating the mechanisms of energy supply dictated by costly neuronal activity. The versatility of the papers accepted to the topic is surprisingly broad. Three trends became evident, presumably reflecting the most vivid interests in the field: (1) the "*in vivo* versus *in vitro*" problem; (2) the role of particular energy substrates; and (3) the macro-level of energy homeostasis and how it applies to the dietary manipulations aimed at treatment of neurodegenerative disorders.

DOES THE BRAIN SLICE TELL THE TRUTH, THE WHOLE TRUTH, AND NOTHING BUT THE TRUTH?

Brain slice studies have played an important role in gaining an understanding of fundamental neuronal, synaptic, and network traits but this preparation has never been free from serious limitations. Among them repeatedly mentioned are: absence of blood flow, diffusion peculiarities, inadequate oxygenation/metabolic support, and neuronal damage due to the slicing procedure (Ivanov and Zilberter, 2011; Bregestovski and Bernard, 2012; Hertz, 2012; Kann, 2012). On the other hand, the slice preparation is still considered an appropriate model even for the high energy-demanding modes of neuronal activity such as gamma oscillations, but only when care is taken to ensure an adequate energy supply to the slice (Kann, 2012).

The problem of extrapolation of the *in vitro* results to the *in vivo* reality seems to be something more than a mere methodological technicality. In the opinion paper titled "Excitatory GABA: how a correct observation may turn out to be an experimental artifact" (Bregestovski and Bernard, 2012), the history of the problem along with the latest discoveries and an impartial discussion shed light on one sensitive issue in developmental neuroscience – the meaning of observation on excitatory GABA in ontogenesis. Shetty et al. (2012), introducing in their paper a concept of Cerebral Metabolic Unit, discussed the short- and long-term metabolic responses to neuronal stimulation as well as the coordinated regulation of synaptic functions and blood flow, which is essential *in vivo* while completely absent *in vitro*. They also stressed the "observed predicted differences in metabolic function between *in vivo* and *in vitro* preparations." In line with this notion, Ivanov and Zilberter (2011) demonstrated that neuronal activity *in vitro* requires considerably higher pO_2 compared to that *in vivo*.

THE ROLE OF PARTICULAR ENERGY SUBSTRATES

The ultimate recognized energy substrate synthesizing ATP in adults is glucose, but the view of its exact role seems to vary. The role of lactate, pyruvate, and beta-hydroxybutyrate is increasingly discussed (Schurr and Gozal, 2011; Hertz, 2012; Ruskin and Masino, 2012; Shetty et al., 2012). The fate of brain lactate *in vivo* is debated with opinions ranging from the hypothesis that lactate and not pyruvate is the end-product of aerobic glycolysis in the brain having a crucial role in coping with glutamate excitation (Schurr and Gozal, 2011) to the opinion that "exogenous lactate is not a necessary brain fuel" unable to protect from anoxic depolarization in slices (Hertz, 2012). On the other hand, in slices superfused with lactate-supplemented ACSF both oxidative metabolism and synaptic function were shown to be more efficient than in glucose-only based ACSF (Ivanov and Zilberter, 2011).

Neuronal energy demands are answered by ATP generation at a cost of energy substrate expenditure followed by metabolic signaling linking neuronal/glial activity to changes in blood flow (Shetty et al., 2012). This sequence of events is ensured by complex signaling mechanisms coordinating activities of neurons, astrocytes, and blood vessels. Molnar et al. (2011) showed a co-localization and important role of vascular and glial receptor recognizing both succinate and gamma-hydroxybutyrate, as well as the role of Ca^{2+} signaling related to energy metabolism. Urban et al. (2012), investigating BOLD signals, reported the existence of local neuronal circuits differentially controlling the blood flow in cortical barrel fields and the deeper areas.

THE MACRO-LEVEL OF ENERGY HOMEOSTASIS AND DIETARY MANIPULATIONS

Kann (2012) in his review emphasized the exceptional vulnerability of higher brain functions to metabolic stresses. From the standpoint of the control systems theory, this vulnerability calls for reliable means to counteract the threat of metabolic failure – indeed, energy homeostasis is capable of employing alternative loops of control as soon as a safety margin is approached. This capability led to the conclusion that "it is possible that a final common neurometabolic pathway might be influenced by a variety of dietary interventions" aimed at restoring energy balance by shifting the failing pathway (usually glycolytic) to an alternative one (usually lipolytic/ketogenic; Rho and Stafstrom, 2012).

Indeed, a macro-nutrient ratio (a ratio of protein plus carbohydrate grams to fat grams) that increases chances of ketogenesis (while decreasing glycolytic flux) is shown to have favorable effects on metabolic profiles, thus exerting neuroprotective properties (Zilberter, 2011). The ketone-based metabolic mode is thought to operate by "providing elevated levels of high energy molecules (e.g., ATP, phosphocreatine) and increased capacity for energy

generation (increased mitochondrial number)" and the mechanisms of its action may include increased levels of adenosine and GABA, decreased activity of glutamate as well as direct effects on ion channels (Ruskin and Masino, 2012). The assortment of neurodegenerative diseases responsive to metabolic intervention include "epilepsy, headache, neurotrauma, Alzheimer's disease, Parkinson's disease, sleep disorders, brain cancer, autism, pain, and multiple sclerosis" as listed by Rho and Stafstrom (2012).

Together, the articles comprising this Research Topic depict a complex intricately organized system with representative studies at both the macro- and micro-levels (e.g., involving molecular signaling pathways; Venkateswaran et al., 2012), which in the end ensures that the unparalleled energy demands of the brain are met in an urgent and extremely flexible manner – the trait yet to be fully understood and applied to the real life problems.

REFERENCES

Bregestovski, P., and Bernard, C. (2012). Excitatory GABA: how a correct observation may turn out to be an experimental artifact. *Front. Pharmacol.* 3:65. doi: 10.3389/fphar.2012.00065

Hertz, L. (2012). Metabolic studies in brain slices – past, present, and future. *Front. Pharmacol.* 3:26. doi: 10.3389/fphar.2012.00026

Ivanov, A., and Zilberter, Y. (2011). Critical state of energy metabolism in brain slices: the principal role of oxygen delivery and energy substrates in shaping neuronal activity. *Front. Neuroenergetics* 3:9. doi: 10.3389/fnene.2011.00009

Kann, O. (2012). The energy demand of fast neuronal network oscillations: insights from brain slice preparations. *Front. Pharmacol.* 2:90. doi: 10.3389/fphar.2011.00090

Molnar, T., Heja, L., Emri, Z., Simon, A., Nyitrai, G., Pal, I., and Kardos, J. (2011). Activation of astroglial calcium signaling by endogenous metabolites succinate and gamma-hydroxybutyrate in the nucleus accumbens. *Front. Neuroenergetics* 3:7. doi: 10.3389/fnene.2011.00007

Rho, J. M., and Stafstrom, C. E. (2012). The ketogenic diet as a treatment paradigm for diverse neurological disorders. *Front. Pharmacol.* 3:59. doi: 10.3389/fphar.2012.00059

Ruskin, D. N., and Masino, S. A. (2012). The nervous system and metabolic dysregulation: emerging evidence converges on ketogenic diet therapy. *Front. Neurosci.* 6:33. doi: 10.3389/fnins.2012.00033

Schurr, A., and Gozal, E. (2011). Aerobic production and utilization of lactate satisfy increased energy demands upon neuronal activation in hippocampal slices and provide neuroprotection against oxidative stress. *Front. Pharmacol.* 2:96. doi: 10.3389/fphar.2011.00096

Shetty, P. K., Galeffi, F., and Turner, D. A. (2012). Cellular links between neuronal activity and energy homeostasis. *Front. Pharmacol.* 3:43. doi: 10.3389/fphar.2012.00043

Urban, A., Rancillac, A., Martinez, L., and Rossier, J. (2012). Deciphering the neuronal circuitry controlling local blood flow in the cerebral cortex with optogenetics in PV: Cre transgenic mice. *Front. Pharmacol.* 3:105. doi: 10.3389/fphar.2012.00105

Venkateswaran, N., Sekhar, S., ThirupatchurSanjayasarathy, T., Krishnan, S. N., Kabaleeswaran, D. K., Ramanathan, S., Narayanasamy, N., Jagathrakshakan, S. S., and Vignesh, S. R. (2012). Energetics based spike generation of a single neuron: simulation results and analysis. *Front. Neuroenergetics* 4:2. doi: 10.3389/fnene.2012.00002

Zilberter, T. (2011). Carbohydrate-biased control of energy metabolism: the darker side of the selfish brain. *Front. Neuroenergetics* 3:8. doi: 10.3389/fnene.2011.00008

Received: 29 May 2012; accepted: 2 August 2012; published online: 20 August 2012.
Citation: Zilberter Y (2012) Understanding how the brain ensures its energy supply. Front. Neuroenerg. ***4****:9. doi: 10.3389/fnene.2012.00009*

frontiers in
PHARMACOLOGY

HYPOTHESIS AND THEORY ARTICLE
published: 19 April 2012
doi: 10.3389/fphar.2012.00065

Excitatory GABA: how a correct observation may turn out to be an experimental artifact

Piotr Bregestovski* and Christophe Bernard

INSERM URM 1106, Institut de Neuroscience des Systèmes, Aix-Marseille Université, Marseille, France

Edited by:
Yuri Zilberter, INSERM, France

Reviewed by:
Avital Schurr, University of Louisville, USA
Oliver Kann, University of Heidelberg, Germany
Jong Min Rho, University of Calgary, Canada

****Correspondence:***
Piotr Bregestovski, INSERM URM 1106, Institut de Neuroscience des Systèmes, Aix-Marseille Université, Marseille 13005, France.
e-mail: piotr.bregestovski@univmed.fr

The concept of the excitatory action of GABA during early development is based on data obtained mainly in brain slice recordings. However, *in vivo* measurements as well as observations made in intact hippocampal preparations indicate that GABA is in fact inhibitory in rodents at early neonatal stages. The apparent excitatory action of GABA seems to stem from cellular injury due to the slicing procedure, which leads to accumulation of intracellular Cl^- in injured neurons. This procedural artifact was shown to be attenuated through various manipulations such as addition of energy substrates more relevant to the *in vivo* situation. These observations question the very concept of excitatory GABA in immature neuronal networks.

Keywords: GABA, brain slices, *in vivo* versus *in vitro*, giant depolarizing potentials, energy substrates

INTRODUCTION

Brain slices are widely used to investigate basic processes of brain function. Although being a reduced preparation (i.e., there is no blood flow, oxygen levels are non-physiological, most *in vivo* metabolites are not present in the artificial cerebrospinal fluid), brain slices provide easier access to cellular phenomena than *in vivo* models. Many results obtained *in vitro* (and reproduced by different laboratories) have been verified *in vivo*, giving ground to the general thought that *in vitro* results can be generalized to the intact organism. However, although adequate in many cases, this approach may lead to misinterpretation in many others. The concept of the excitatory action of GABA at early postnatal stages of development provides a particular example of correct observations performed *in vitro* which may not apply to the *in vivo* situation.

THE CONCEPT OF EXCITATORY GABA IN THE IMMATURE BRAIN

GABA, the main inhibitory neurotransmitter in vertebrates, activates $GABA_A$ receptors ($GABA_AR$) resulting in opening of anion-selective channels and transmembrane fluxes of chloride (Cl) and bicarbonate. Normally, the direction of Cl current determines the hyperpolarizing or depolarizing effect of $GABA_AR$ activation on the membrane. If the reversal potential for Cl (E_{Cl}) is above (below) the resting membrane potential, Cl leaves (enters) the cell. An outward (inward) flux of negative charges depolarizes (hyperpolarizes) the membrane.

It is important to clarify here the difference between depolarizing and excitatory actions of GABA since there is a widespread misunderstanding of these notions. The concentration of intracellular Cl^- measured in different cell types varies from 3 to 60 mM and in mammalian neurons *in vitro* it is generally low (<10 mM, see Khirug et al., 2008; Bregestovski et al., 2009). As a result, the reversal potential of GABAergic currents, E_{GABA}, is close to the resting membrane potential and activation of $GABA_AR$ causes hyperpolarization or weak depolarization. Meanwhile, $GABA_AR$ channel opening decreases the input membrane resistance inducing "shunting inhibition" (see Andersen et al., 1980; Staley and Mody, 1992; Tang et al., 2011; Wright et al., 2011) that lowers the neuron's firing probability. Therefore, a weakly depolarizing GABA may exert an inhibitory effect. In contrast, the "excitatory" GABA action means that $GABA_AR$ activation induces a depolarization large enough to generate action potentials.

The inhibitory/hyperpolarizing effects of GABA have been extensively verified in juvenile and adult animals *in vivo*. At earlier stages of development, the picture appears to be different. *In vitro* experiments have shown an excitatory action of GABA at early stages of development in kittens (Schwartzkroin and Altschuler, 1977), rabbits (Mueller et al., 1983), and rats (Dunwiddie, 1981; Harris and Teyler, 1983; Mueller et al., 1984; Ben-Ari et al., 1989) in a large number of subsequent studies (for review, Ben-Ari et al., 2007). Experiments performed in rodent brain slices indicated that the switch from the excitatory to inhibitory action of GABA takes place during the second postnatal week (P12–P13; Ben-Ari et al., 2007). The mechanism of this switch was explained as the increased age-dependent expression of KCC2 chloride exporter which takes over the leading role in Cl homeostasis from NKCC1 chloride importer (Blaesse et al., 2009). A hypothesis on the leading role of excitatory GABA in development was proposed by Ben-Ari and co-authors who claimed it as a universal rule: "*In all developing animal species and brain structures investigated, neurons have a higher intracellular chloride concentration at an early stage leading to an efflux of chloride and excitatory actions of GABA in immature neurons*" (Ben-Ari et al., 2007). These *in vitro* findings obtained in brain slices or cell cultures were frequently taken for granted. However, several lines of evidence challenge the extrapolation of these conclusions to the intact brain.

GABA IS NOT EXCITATORY IN THE INTACT BRAIN

First, the early study performed *in vivo*, using intracellular recordings of hippocampal neurons in young kittens, suggested that inhibition is a predominant form of synaptic activity at early postnatal ages (Purpura et al., 1968). However, a high concentration of KCl was used in the pipette solution, which can alter ionic homeostasis.

Second, *in vivo* recordings using $GABA_AR$ antagonists contradict the *in vitro* observations. A study based on the analysis of more than 200 rat pups at the age of P3–P5 demonstrated that the injection of bicuculline triggered seizures in these pups (Baram and Snead, 1990). Another *in vivo* study reported that cerebellar Purkinje cells inhibit each other as early as at P5 and that bicuculline abolishes their interaction and increases their spontaneous firing activity (Bernard and Axelrad, 1993). Also, several more recent *in vivo* studies using specific agonists or antagonists of $GABA_ARs$ clearly demonstrated the inhibitory action of GABA during the first postnatal week (Minlebaev et al., 2006, 2011; Isaev et al., 2007). For instance, Minlebaev et al. (2006) wrote that in P3–P5 rats: "*Blockade of GABAA receptors by gabazine significantly increased spontaneous cortical activity by almost doubling the occurrence of spontaneous spindle-bursts. . .*" However, these results were not mentioned in the subsequent review by the same main authors (Ben-Ari et al., 2007), who instead claimed that GABA "*. . .excites immature neurons and generates primitive oscillations.*" It is difficult to state that GABA exerts an excitatory action when $GABA_AR$ blockade leads to an increased activity *in vivo*.

Third, observations on the "intact hippocampus" preparation (*in toto*) where cellular integrity and connectivity are maintained, also suggest the inhibitory action of GABA. Using recordings from the CA1 area in isolated hippocampus, Wong et al. (2005) showed that synaptically released GABA causes inhibition. Moreover, in contrast to observations made in brain slices (**Figure 1A**; Ben-Ari et al., 1989), application of bicuculline resulted in epileptiform discharges (**Figure 1C**; Wong et al., 2005). Interestingly, similar effects were observed by Ben-Ari's group in the very first study on the intact immature hippocampus (**Figure 1B**; Khalilov et al., 1997), but they were not discussed in their later publications. Recent experiments using the same preparation from P5–P7 mice confirmed these observations (Dzhala et al., 2010, 2012). Isoguvacine, a selective agonist of $GABA_ARs$, transiently reduced spontaneous neuronal activity. Thus, the net effect

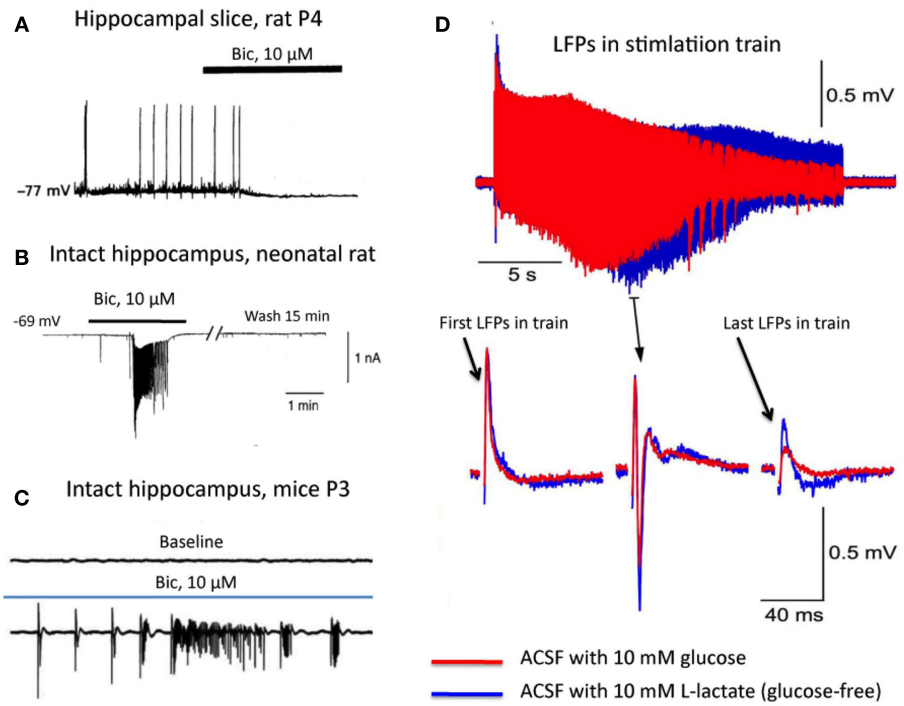

FIGURE 1 | (A–C) GABA is depolarizing in the slice preparation and hyperpolarizing in the intact hippocampus. **(A)** Microelectrode recording from hippocampal neuron in a brain slice from a 4-day-old rat (KCl-containing electrode). Note that bicuculline, a $GABA_A$ receptor antagonist, caused membrane hyperpolarization and inhibition of spontaneous synaptic activity (from Ben-Ari et al., 1989). **(B)** Whole-cell voltage-clamp recording with a pipette containing a *K*-gluconate based solution [(Cl) in the pipette was 4.2 mM] from a neuron in the intact rat hippocampus. Note that bicuculline evokes epileptiform discharges (from Khalilov et al., 1997). **(C)** GABAergic activities observed from isolated intact neonatal (P3) mouse hippocampus as seen by extracellular recordings from the CA3 area. Top: baseline field potentials. Note the absence of electrical activity. Bottom: note the presence of spontaneous activity and epileptiform discharges in the presence of bicuculline (blue line). To achieve better oxygenation of the preparation, a dual-side perfusion chamber and a fluid rate of 15 ml/min were used (from Wong et al., 2005). **(D)** Lactate without glucose maintains and even augments synaptic function. Top: local field potentials (LFPs) in response to stimulation trains when ACSF contains 10 mM glucose (red) or 10 mM lactate (blue). Bottom: examples of single LFPs at expanded time scale. Note that in the presence of lactate as the sole energy substrate, LFPs are even better maintained than under glucose-only conditions (from Ivanov et al., 2011).

of $GABA_AR$ activation in the intact hippocampal network is inhibitory.

Together, these results strongly suggest that GABA is inhibitory in the immature intact brain. On the other hand, the excitatory action of GABA has been observed in a number of studies on brain slices (Ben-Ari et al., 2007). What mechanisms may underlie this apparent discrepancy?

BRAIN SLICES ARE SEVERELY DAMAGED BRAIN TISSUE

Using brain slices implies that brain tissue will be cut, i.e., that cell processes (dendrites, axons etc.) will be severed, generating a model of traumatic brain injury. According to early histological observation in slices, there is a 50- to 100-μm deep zone of severely disrupted tissue (Garthewaite et al., 1979; Bak et al., 1980; Frotscher et al., 1981). As a consequence of mechanical injury, microglial cells in slices are rapidly activated and become highly mobile (Petersen and Dailey, 2004). This may trigger a cascade of detrimental processes due to the release of a number of neurotoxic substances including cytokines, chemokines, nitric oxide, and superoxide free radicals that generate reactive oxygen species and reactive nitrogen species (Loan and Byrnes, 2010).

While in more recent studies microtomes/vibratomes are used for slices preparation, still the regions close to the surface (30–80 μm deep) contain a large amount of damaged cells (Dzhala et al., 2012). Since most electrophysiological and imaging studies of cell body layers (like hippocampal pyramidal cells) are performed in this region, the results may be biased by the inclusion of these injured cells, thus reflecting pathological rather than physiological processes. Indeed, slicing through brain tissue invariably leads to pathological reorganizations (Hoffman et al., 1994; McKinney et al., 1997).

DAMAGED NEURONS ACCUMULATE Cl

As mentioned above, the net action of $GABA_AR$ activation depends upon E_{Cl}. Hence, the depolarizing action of GABA in slices may result from intracellular Cl accumulation in traumatized neurons located close to the surface. Indeed, after neuronal trauma, GABA, both synaptically released and exogenously applied, induced depolarization of neurons, and increased intracellular Ca^{2+} (van den Pol et al., 1996). Using gramicidin perforated-patch recordings, Nabekura et al. (2002), demonstrated that E_{GABA} was more depolarized in axotomized than in intact neurons of the vagus dorsal motor nucleus. The authors concluded that: "*axotomy led to . . . elevation of intracellular Cl, and an excitatory response to GABA. A switch of GABA action from inhibitory to excitatory might be a mechanism contributing to excitotoxicity in injured neurons*" (Nabekura et al., 2002). Direct non-invasive measurements of intracellular Cl concentration in Clomeleon-expressing mice (Dzhala et al., 2010, 2012) clearly demonstrated that axotomized and dendrotomized cells proximal to the slice surface have a much higher intracellular Cl concentration than in deeper situated and less injured cells (**Figure 2A**). In contrast, Cl levels were much lower in the intact hippocampus preparation (**Figure 2A**), in which a direct activation of $GABA_AR$ decreased neuronal firing – an observation consistent with an inhibitory/shunting action of GABA (Dzhala et al., 2012).

Finally, it is important to note that the intracellular Cl concentration may be cell type-dependent (Rohrbough and Spitzer, 1996; Sauer et al., 2012) and location-dependent in a given cell (Duebel et al., 2006). An uneven distribution of Cl ions has been described in hippocampal neurons using electrophysiological recordings (Szabadics et al., 2006; Khirug et al., 2008) and non-invasive monitoring of intracellular Cl (Waseem et al., 2010). Future studies on GABA action in the immature brain should take these factors into account.

Thus, the slicing procedure is clearly associated with damaged cells, which accumulate chloride. Slice quality critically depends upon the slicing procedure and equipment. Recent studies described conditions for better preparation (with microtomes/vibratomes) and preservation of acute slice preparations (Schurr et al., 1989; Hájos and Mody, 2009; Hájos et al., 2009; Maier et al., 2009; Ivanov and Zilberter, 2011). Still, even state-of-the-art procedures do not prevent damage inherent to slicing. For instance, using a vibratome, Taylor et al. (1999) wrote: "*Light microscopy of slices fixed immediately after Vibroslice preparation indicated significant swelling of pyramidal neurons, i.e., cell bodies, mitochondria, dendrites, and nuclei were enlarged and hydropic.*" While experimentators try to achieve recovery as much as possible after slicing (Taylor et al., 1999; Bischofberger et al., 2006), even after 1.5 h incubation in artificial cerebrospinal fluid (ACSF; typical experimental procedure for recovery of slice integrity) neurons and glial cells are still functionally and energetically defective. This point is supported by the observations of Dzhala et al. (2012) who demonstrated Cl accumulation in slice surface-proximal neurons (**Figures 2A,B**).

TRAUMATIC TISSUE NEEDS MORE ENERGY

Abnormalities induced by tissue trauma in brain slices are exacerbated by several additional factors. The lack of blood flow in slices dramatically changes the way energy substrates and oxygen are delivered to cells. Energy substrates and O_2 are instead supplied exogenously by artificial extracellular solution (ACSF), which must diffuse passively from the surface. In the intact brain, blood vessels, astrocytes, and neurons form a complex system supporting and adjusting brain metabolism (Pellerin, 2010; Turner and Adamson, 2011; Zilberter and Bregestovski, 2012) while in brain slices metabolism depends entirely on the experimental conditions. Although experimentalists are trying to create conditions maximally close to the *in vivo* environment, they are obviously far from ideal. Support normally provided by blood is not entirely compensated by perfusion of ACSF. Glucose-based composition of ACSF was empirically adjusted more than 60 years ago for relatively long-lasting preservation of neuronal function in brain slices and is, obviously, not physiological (Hájos and Mody, 2009; Zilberter et al., 2010). Slices exposed to ACSF exhibit severe abnormalities in energy metabolism. For instance, the rate of glycolysis is reduced by more than 50% in brain slices (Rolleston and Newsholme, 1967; Benjamin and Verjee, 1980) as compared to the *in vivo* estimates (Ghajar et al., 1982). In addition, the total adenine nucleotide pool is decreased by 30–50% in slices as compared to that observed *in vivo* (Whittingham et al., 1984) and this effect become less important with increasing of slice thickness (Zur Nedden et al., 2011). Remarkably, the slicing procedure causes a decrease to about 50% of the total content of ATP, creatine, and adenylate, as well as a strong

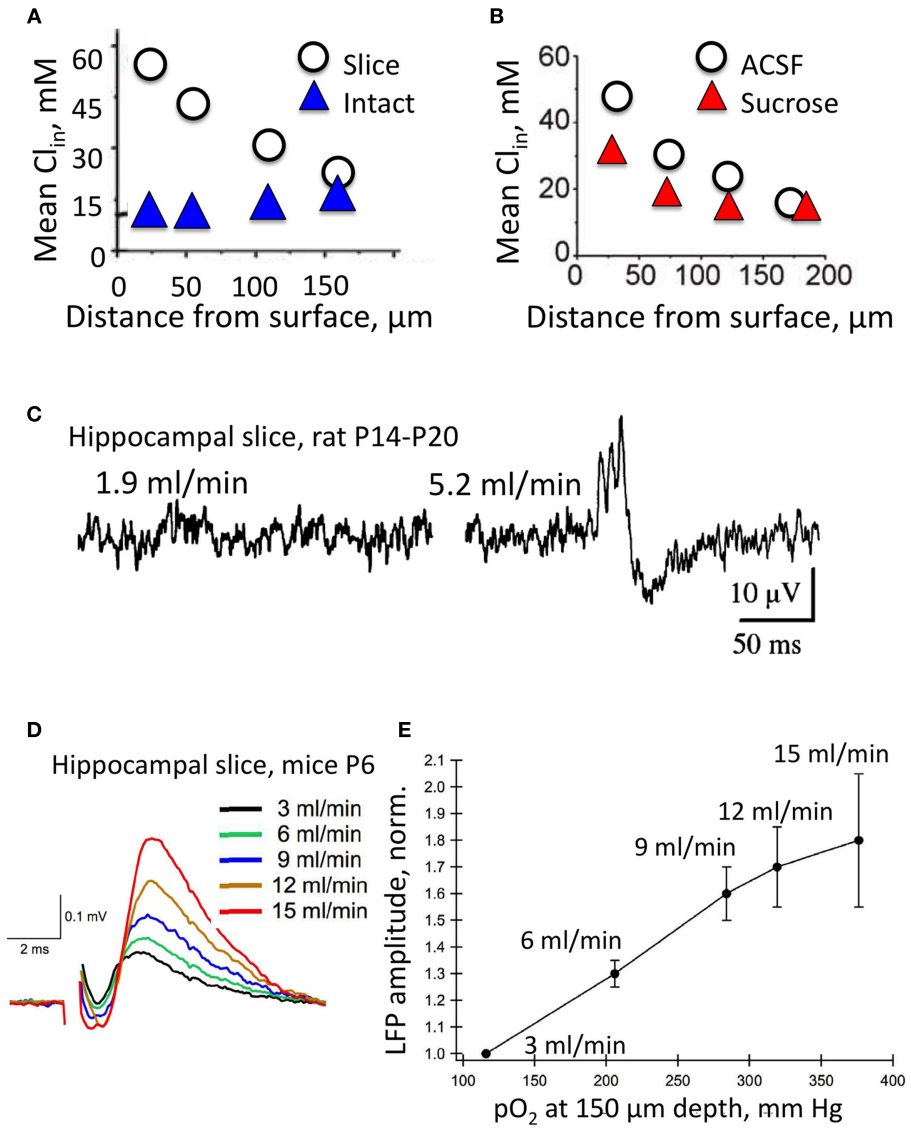

FIGURE 2 | Intracellular Cl concentration and electrical activity strongly depend on the experimental model and conditions. (A) The mean intracellular Cl concentration in neurons at different depth from the surface in the intact hippocampi (▲) and acute hippocampal slice preparations (◯) at P5–P7. Note the highly elevated Cl concentrations in neurons from the surface layers in the slice preparation (Modified from Dzhala et al., 2012). **(B)** The effects of slicing conditions on intracellular Cl concentration. Mean Cl_i as a function of depth in the hippocampal slices prepared from P5–P7 mice in control ACSF and in a high sucrose solution (Modified from Dzhala et al., 2012). **(C–E)** Genesis of network events and amplitude of local field potentials strongly depend upon the flow rate of ACSF. **(C)** Spontaneous network activity recorded at a low flow rate of 1.9 ml/min (left), and a high flow rate of 5.2 ml/min (right). Note sharp wave–ripple activity only at a high flow rate. Juvenile (P14–P20) transverse hippocampal 400–450 µm thick slices from Wistar rats were used here (from Hájos et al., 2009). **(D)** Examples of local field potentials measured in the same slice and electrode positions at different flow rates. Note the remarkable increase in amplitude when the flow rate is increased. **(E)** Summary of the dependence of local field potential (LFP) amplitudes on the oxygen levels and perfusion rates. Slices 400 µm thick from P4–P7 Swiss mice (from Ivanov et al., 2011).

change in intracellular pH from about 6.6–7.2 (Whittingham et al., 1984). Such a deficit in the cell energy supply may directly affect GABAergic action.

To test this hypothesis, Zilberter and collaborators analyzed whether improving energy supply to neurons with glucose oxidative energy substrates (OES) can modulate the response to GABA. In neocortical and hippocampal slices from neonatal (P3–P8) rats and mice, supplementing ACSF with β-hydroxybutyrate, lactate, or pyruvate significantly hyperpolarized E_{GABA}, switching the GABA action from excitatory to inhibitory (Holmgren et al., 2010). Moreover, OES inhibited giant depolarizing potentials (GDPs; Holmgren et al., 2010; Mukhtarov et al., 2011), a spontaneous network activity pattern characteristic for neonatal hippocampal slices (Ben-Ari et al., 2007). The beneficial effect of OES on energy metabolism status in neurons was confirmed by direct simultaneous measurements of oxygen consumption and NADH

fluorescence during neuronal activity (Ivanov and Zilberter, 2011; Ivanov et al., 2011). For instance, in the presence of glucose, lactate was effectively utilized as an energy substrate (Ivanov et al., 2011), causing an augmentation of oxidative metabolism (**Figure 1D**). Moreover, in the absence of glucose, lactate was fully capable of maintaining synaptic function (Schurr et al., 1988; Ivanov et al., 2011). These observations demonstrate that neuronal function can definitely be improved in both neonatal (Ivanov et al., 2011) and adult (Ivanov and Zilberter, 2011) slices by supplementing glucose with OES. Glucose alone, even at strongly hyperglycemic concentrations as in standard ACSF (10 versus 1–2 mM in the brain extracellular fluid (Abi-Saab et al., 2002; Zilberter et al., 2010) cannot fully cover energy demands during neuronal activation.

These studies have ignited a controversy (Kirmse et al., 2010; Ruusuvuori et al., 2010; Tyzio et al., 2011). However, although Tyzio and co-authors failed to reproduce the effects of b-hydroxybutyrate on E_{GABA}, they did reproduce the E_{GABA}-hyperpolarizing effect of 5 mM pyruvate. Kirmse et al. (2010) did not find any effect of β-hydroxybutyrate or pyruvate on GABA-induced Ca^{2+} fluorescent transients; but measurements for control and BHB-treated cells were performed on different slices with a slow ACSF perfusion rate leading to improper oxygenation (see Ivanov et al., 2011; Ivanov and Zilberter, 2011). Ruusuvuori et al. observed the inhibitory effect of lactate on GDP generation but suggested that this effect is induced by intracellular acidification. Indeed, OES caused pH_i changes of less than −0.05 pH units (Ivanov et al., 2011; Mukhtarov et al., 2011). However, the 0.25–0.35 reduction in pH_i obtained by substituting bicarbonate-containing solution with HEPES-based HCO_3-free solution did not eliminate GDPs (Mukhtarov et al., 2011). Therefore, a significant contribution of pH_i to the effects of OES on GDPs is unlikely (Ivanov et al., 2011; Mukhtarov et al., 2011). Certainly, the controversy needs to be resolved by independent groups. But the results clearly demonstrate that metabolic processes are central to the reorganization of cell function after making brains slices.

Altogether, these observations demonstrate that the slicing procedure injures cells and disrupts brain metabolism, leading to intracellular Cl accumulation in neurons and rendering GABA strongly depolarizing or even excitatory as has been reported during the first postnatal week in rodents.

This, however, does not rule out the possibility that GABA may be depolarizing, in particular at very early stages of development. For example, treatment of mice with bumetanide during the period of embryonic cortical developmental results in disruption of excitatory synapse formation (Wang and Kriegstein, 2011). As bumetanide antagonizes the Na^+–K^+–$2Cl^-$ cotransporter (NKCC1), which accumulates intracellular Cl, these observations suggest that Cl in embryonic neurons is elevated and plays an important signaling role in developmental processes.

GABA AND EARLY NETWORK ACTIVITIES

Oscillations/correlated neuronal discharges are a hallmark of network activity at any stage of development (Buzsáki, 1986, 2002; Spitzer, 1994; Chrobak and Buzsáki, 1998; Leinekugel et al., 2002; Khazipov et al., 2004; Adelsberger et al., 2005; Sipilä et al., 2006). At early stages of development, this synchronized activity may be important for brain maturation, regulating multiple processes including neuronal migration (Komuro and Rakic, 1998) and directing neuronal differentiation (Gu and Spitzer, 1997; Spitzer et al., 2000), dendritic growth and patterning (Katz and Shatz, 1996; Wong and Ghosh, 2002), activation of transmitter receptors (Liao et al., 2001), and the pattern of specific connections (Penn et al., 1998). The most prominent synchronized activity, early network oscillations (ENOs) associated with changes in neuronal intracellular Ca^{2+} concentration, were observed in small groups of neurons and in large populations *in vitro* (Garaschuk et al., 1998, 2000; Corlew et al., 2004) and *in vivo* (Adelsberger et al., 2005). Spindle-bursts were described in the neonatal rat neocortex *in vivo* (Khazipov et al., 2004). Thus, waves of spontaneous electrical activity propagating across many regions of the brain are a hallmark of developing networks, and actively contribute to cortical development and plasticity (Katz and Shatz, 1996; Mizuno et al., 2007). Distinct mechanisms underlie generation of synchronized events, including synaptic interaction, gap junction communication, the presence of pacemaker-like neurons as well as activation of metabotropic glutamate and ACh receptors (Kandler and Katz, 1998; Flint et al., 1999; Blankenship and Feller, 2010).

However, the reports that GABA is depolarizing/excitatory in slices from the immature brain led to a very popular theory, which inspired many researches in the neurodevelopment field and provided a conceptual framework to explain early network activities recorded *in vivo*. Excitatory GABA (i.e., its ability to drive the membrane potential to firing threshold) would be essential for developing networks. *In vitro* experiments revealed the occurrence of spontaneous network events involving large populations of neurons. This phenomenon was first described by Harris and Teyler (1983) who called it "spontaneous unison firing." It was also observed by Mueller et al. (1984), who wrote: "*Immature neurons often demonstrated spontaneous depolarizations of up to 30 mV amplitude and 30 to 60 sec duration.*" Several years later, Ben-Ari et al. (1989) also described this phenomenon in immature brain slices, which they named GDPs. GDPs were infrequent or absent after P12. It was proposed that depolarizing GABA plays a key role in the generation of GDPs and that this spontaneous activity results from the synergistic excitatory activities mediated by $GABA_A$ and glutamate *N*-methyl-D-aspartate (NMDA) receptors (Ben-Ari et al., 1997). Since GDPs were not observed after postnatal days 10–11, at the time close to the "excitation/inhibition switch," it was postulated that GDPs represent a primitive activity pattern of the developing brain and that it is "*largely based on excitatory GABA*" (Ben-Ari et al., 2007).

These observations led to the broadly accepted idea that the excitatory action of GABA underlies neuronal maturation of immature neuronal networks. According to this concept, the elevated Cl concentration and, consequently, the excitatory action of GABA, represent necessary steps in the development of the nervous system. This viewpoint is epitomized in the recent review of van Welie et al. (2011), who wrote: "*Depolarizing GABA is required for normal brain development, as it contributes to the morphological maturation of neurons* (Cancedda et al., 2007) *and neuronal circuits* (Ben-Ari, 2001; Akerman and Cline, 2006). *Depolarizing GABA can drive juvenile neurons to fire action potentials* (Ben-Ari, 2002) *and conversely, neuronal activity can regulate* E_{GABA}*, by either*

specific patterns of synaptic activation (Woodin et al., 2003; Balena and Woodin, 2008), *or alterations in postsynaptic activity levels via changes in intracellular* Ca^2+ (Fiumelli et al., 2005)."

This statement relies on the axiom that the nature of GDPs observed in brain slices correlates with network activities recorded *in vivo* in developing networks. While the general patterns of this activity may be similar *in vitro* and *in vivo*, the underlying mechanisms may be different. The presence and character of oscillatory activity in brain slices highly depend upon energy support, oxygenation, and perfusion rate (Hájos and Mody, 2009; Hájos et al., 2009; Holmgren et al., 2010; Mukhtarov et al., 2011). For instance, sharp wave (SPW) oscillations are a hallmark of hippocampal activity in developing and adult hippocampus *in vivo* (Leinekugel et al., 2002). SPWs are usually not observed or very infrequent in slices when using slow perfusion rates of ACSF (1.6–2.4 ml/min; Hájos et al., 2009; Maier et al., 2009). However, SPWs appear (or become more frequent) at high speed of perfusion (**Figure 2C**), suggesting that a proper delivery of oxygen to the whole slice is critical for the genesis of SPWs *in vitro* (Hájos et al., 2009). The importance of oxygen delivery at elevated flow rates was further demonstrated by Ivanov et al. (2011). A decrease from 15 to 3.25 ml/min in the perfusion rate resulted in strong decrease of oxygen and a two-fold reduction of the local field potential amplitude in brain slices from P6 mice (**Figures 2D,E**).

Particularly convincing arguments were obtained in a recent study demonstrating that while GDPs can be recorded both in slices and the intact hippocampus during the first postnatal week, the mechanism of their genesis is different (Dzhala et al., 2012). Isoguvacine application dramatically increased GDP frequency in brain slices (in keeping with the excitatory action of GABA); whilst in the intact hippocampus isoguvacine completely abolished GDPs (in keeping with the inhibitory action of GABA).

Since the slicing procedure also lesions superficial neurons that leads to Cl accumulation in mature networks (Dzhala et al., 2012), one would expect GDPs to occur in adult slices. However, the study by Dzhala et al. (2012) shows that, whilst superficial neurons remain connected to the network in immature slices, they are functionally disconnected in mature slices. Hence, superficial cells with high internal Cl do not contribute much to network activity in mature slice.

Together, these observations strongly suggest that ENOs do not rely upon excitatory GABA. Hence, the mechanistic insights regarding GDP genesis/propagation/function gained from slice studies should be re-evaluated. As underlined in the recent review: "*Usage of brain slice preparations has significantly contributed to a deeper understanding of neuronal functions at the cellular and network level in the recent decades. However, given factors such as absence of blood circulation, longer diffusion distances, steep interstitial pO2 gradients, and composition of the recording solution have to be kept in mind when interpreting data from slice preparations*" (Kann, 2011).

RESUME

Remaining uncertainties notwithstanding, studies utilizing the intact hippocampus preparation with more functional neurons, glial cells, and network activity, as well as the few available *in vivo* studies, suggest that GABA plays an inhibitory role in the immature brain (at least during the first postnatal week in rodents). Perhaps, the most important take-home message is that our understanding of brain function is based on experimental methods and measurements that inevitably distort/perturb the system. The observations are correct, but their interpretation may not be. The concept of excitatory GABA and its alleged role for neuronal network maturation provides a perfect example of how cautious we should be when interpreting experimental results.

ACKNOWLEDGMENTS

We would like to thank Dr. Kevin Staley for critical reading of the manuscript and valuable suggestions. This study was supported by the grant from the European Union Seventh Framework: NEUROCYPRES, HEALTH-F2-2008-202088 (to Piotr Bregestovski).

REFERENCES

Abi-Saab, W. M., Maggs, D. G., Jones, T., Jacob, R., Srihari, V., Thompson, J., Kerr, D., Leone, P., Krystal, J. H., Spencer, D. D., During, M. J., and Sherwin, R. S. (2002). Striking differences in glucose and lactate levels between brain extracellular fluid and plasma in conscious human subjects: effects of hyperglycemia and hypoglycemia. *J. Cereb. Blood Flow. Metab.* 22, 271–279.

Adelsberger, H., Garaschuk, O., and Konnerth, A. (2005). Cortical calcium waves in resting newborn mice. *Nat. Neurosci.* 8, 988–990.

Akerman, C. J., and Cline, H. T. (2006). Depolarizing GABAergic conductances regulate the balance of excitation to inhibition in the developing retinotectal circuit in vivo. *J. Neurosci.* 26, 5117–5130.

Andersen, P., Dingledine, R., Gjerstad, L., Langmoen, I. A., and Laursen, A. M. (1980). Two different responses of hippocampal pyramidal cells to application of gamma-amino butyric acid. *J. Physiol. (Lond.)* 305, 279–296.

Bak, I. J., Misgeld, U., Weiler, M., and Morgan, E. (1980). The preservation of nerve cells in rat neostriatal slices maintained in vitro: a morphological study. *Brain Res.* 197, 341–353.

Balena, T., and Woodin, M. A. (2008). Coincident pre- and postsynaptic activity downregulates NKCC1 to hyperpolarize E(Cl) during development. *Eur. J. Neurosci.* 27, 2402–2412.

Baram, T. Z., and Snead, O. C. (1990). Bicuculline induced seizures in infant rats: ontogeny of behavioral and electrocortical phenomena. *Brain Res. Dev. Brain Res.* 57, 291–295.

Ben-Ari, Y. (2001). Developing networks play a similar melody. *Trends Neurosci.* 24, 353–360.

Ben-Ari, Y. (2002). Excitatory actions of gaba during development: the nature of the nurture. *Nat. Rev. Neurosci.* 3, 728–739.

Ben-Ari, Y., Cherubini, E., Corradetti, R., and Gaiarsa, J. L. (1989). Giant synaptic potentials in immature rat CA3 hippocampal neurones. *J. Physiol.* 416, 303–325.

Ben-Ari, Y., Gaiarsa, J. L., Tyzio, R., and Khazipov, R. (2007). GABA: a pioneer transmitter that excites immature neurons and generates primitive oscillations. *Physiol. Rev.* 87, 1215–1284.

Ben-Ari, Y., Khazipov, R., Leinekugel, X., Caillard, O., and Gaiarsa, J. L. (1997). GABAA, NMDA and AMPA receptors: a developmentally regulated 'ménage à trois.' *Trends Neurosci.* 20, 523–529.

Benjamin, A. M., and Verjee, Z. H. (1980). Control of aerobic glycolysis in the brain in vitro. *Neurochem. Res.* 5, 921–934.

Bernard, C., and Axelrad, H. (1993). Effects of recurrent collateral inhibition on Purkinje cell activity in the immature rat cerebellar cortex – an in vivo electrophysiological study. *Brain Res.* 626, 234–258.

Bischofberger, J., Engel, D., Li, L., Geiger, J. R., and Jonas, P. (2006). Patch-clamp recording from mossy fiber terminals in hippocampal slices. *Nat. Protoc.* 1, 2075–2081.

Blaesse, P., Airaksinen, M. S., Rivera, C., and Kaila, K. (2009). Cation-chloride cotransporters and neuronal function. *Neuron* 61, 820–838.

Blankenship, A. G., and Feller, M. B. (2010). Mechanisms underlying spontaneous patterned activity in developing neural circuits. *Nat. Rev. Neurosci.* 11, 18–29.

Bregestovski, P., Waseem, T., and Mukhtarov, M. (2009). Genetically encoded optical sensors for monitoring of intracellular chloride and chloride-selective channel activity. *Front. Mol. Neurosci.* 2:15. doi:10.3389/neuro.02.015.2009

Buzsáki, G. (1986). Hippocampal sharp waves: their origin and significance. *Brain Res.* 398, 242–252.

Buzsáki, G. (2002). Theta oscillations in the hippocampus. *Neuron* 33, 325–340.

Cancedda, L., Fiumelli, H., Chen, K., and Poo, M. M. (2007). Excitatory GABA action is essential for morphological maturation of cortical neurons in vivo. *J. Neurosci.* 27, 5224–5235.

Chrobak, J. J., and Buzsáki, G. (1998). Gamma oscillations in the entorhinal cortex of the freely behaving rat. *J. Neurosci.* 18, 388–398.

Corlew, R., Bosma, M. M., and Moody, W. J. (2004). Spontaneous, synchronous electrical activity in neonatal mouse cortical neurones. *J. Physiol. (Lond.)* 560, 377–390.

Duebel, J., Haverkamp, S., Schleich, W., Feng, G., Augustine, G. J., Kuner, T., and Euler, T. (2006). Two-photon imaging reveals somatodendritic chloride gradient in retinal ON-type bipolar cells expressing the biosensor Clomeleon. *Neuron* 49, 81–94.

Dunwiddie, T. V. (1981). Age-related differences in the in vitro rat hippocampus: development of inhibition and the effects of hypoxia. *Dev. Neurosci.* 4, 165–175.

Dzhala, V., Valeeva, G., Glykys, J., Khazipov, R., and Staley, K. (2012). Traumatic alterations in GABA signaling disrupt hippocampal network activity in the developing brain. *J. Neurosci.* 32, 4017–4031.

Dzhala, V. I., Mail, M. E., and Staley, K. J. (2010) "Chloride imbalance in the acute hippocampal slice model of brain trauma," in *Abstract SFN Meeting 255.25/R10*, San Diego.

Fiumelli, H., Cancedda, L., and Poo, M. M. (2005). Modulation of GABAergic transmission by activity via postsynaptic Ca2+ -dependent regulation of KCC2 function. *Neuron* 48, 773–786.

Flint, A. C., Dammerman, R. S., and Kriegstein, A. R. (1999). Endogenous activation of metabotropic glutamate receptors in neocortical development causes neuronal calcium oscillations. *Proc. Natl. Acad. Sci. U.S.A.* 96, 12144–12149.

Frotscher, M., Misgeld, U., and Nitsch, C. (1981). Ultrastructure, of mossy fiber endings in in vifro hippocampal slices. *Exp. Brain Res.* 41, 247–255.

Garaschuk, O., Hanse, E., and Konnerth, A. (1998). Developmental profile and synaptic origin of early network oscillations in the CA1 region of rat neonatal hippocampus. *J. Physiol. (Lond.)* 507, 219–236.

Garaschuk, O., Linn, J., Eilers, J., and Konnerth, A. (2000). Large-scale oscillatory calcium waves in the immature cortex. *Nat. Neurosci.* 3, 452–459.

Garthewaite, J., Woodhams, P. L., Collins, M. J., and Balazs, R. (1979). On the preparation of brain slices: morphology and cyclic nucleotides. *Brain Res.* 173, 373–377.

Ghajar, J. B. G., Plum, F., and Duffy, T. E. (1982). Cerebral oxidative metabolism and blood flow during acute hypoglycemia and recovery in unanesthetized rats. *J. Neurochem.* 38, 397–409.

Gu, X., and Spitzer, N. C. (1997). Breaking the code: regulation of neuronal differentiation by spontaneous calcium transients. *Dev. Neurosci.* 19, 33–41.

Hájos, N., Ellender, T. J., Zemankovics, R., Mann, E. O., Exley, R., Cragg, S. J., Freund, T. F., and Paulsen, O. (2009). Maintaining network activity in submerged hippocampal slices: importance of oxygen supply. *Eur. J. Neurosci.* 29, 319–327.

Hájos, N., and Mody, I. (2009). Establishing a physiological environment for visualized in vitro brain slice recordings by increasing oxygen supply and modifying aCSF content. *J. Neurosci. Methods* 183, 107–113.

Harris, K. M., and Teyler, T. J. (1983). Evidence for late development of inhibition in area CA1 of the rat hippocampus. *Brain Res.* 268, 339–343.

Hoffman, S. N., Salin, P. A., and Prince, D. A. (1994). Chronic neocortical epileptogenesis in vitro. *J. Neurophysiol.* 71, 1762–1773.

Holmgren, C. D., Mukhtarov, M., Malkov, A. E., Popova, I. Y., Bregestovski, P., and Zilberter, Y. (2010). Energy substrate availability as a determinant of neuronal resting potential, GABA signaling and spontaneous network activity in the neonatal cortex in vitro. *J. Neurochem.* 112, 900–912.

Isaev, D., Isaeva, E., Khazipov, R., and Holmes, G. L. (2007). Shunting and hyperpolarizing GABAergic inhibition in the high-potassium model of ictogenesis in the developing rat hippocampus. *Hippocampus* 17, 210–219.

Ivanov, A., Mukhtarov, M., Bregestovski, P., and Zilberter, Y. (2011). Lactate effectively covers energy demands during neuronal network activity in neonatal hippocampal slices. *Front. Neuroenergetics* 3:2. doi:10.3389/fnene.2011.00002

Ivanov, A., and Zilberter, Y. (2011). Critical state of energy metabolism in brain slices: the principal role of oxygen delivery and energy substrates in shaping neuronal activity *Front. Neuroenergetics* 3:9. doi:10.3389/fnene.2011.00009

Kandler, K., and Katz, L. C. (1998). Coordination of neuronal activity in developing visual cortex by gap junction-mediated biochemical communication. *J. Neurosci.* 18, 1419–1427.

Kann, O. (2011). The energy demand of fast neuronal network oscillations: insights from brain slice preparations. *Front. Pharmacol.* 2:90. doi:10.3389/fphar.2011.00090

Katz, L. C., and Shatz, C. J. (1996). Synaptic activity and the construction of cortical circuits. *Science* 274, 1133–1138.

Khalilov, I., Khazipov, R., Esclapez, M., and Ben-Ari, Y. (1997). Bicuculline induces ictal seizures in the intact hippocampus recorded in vitro. *Eur. J. Pharmacol.* 319, R5–R6.

Khazipov, R., Sirota, A., Leinekugel, X., Holmes, G. L., Ben-Ari, Y., and Buzsáki, G. (2004). Early motor activity drives spindle bursts] in the developing somatosensory cortex. *Nature* 432, 758–761.

Khirug, S., Yamada, J., Afzalov, R., Voipio, J., Khiroug, L., and Kaila, K. (2008). GABAergic depolarization of the axon initial segment in cortical principal neurons is caused by the Na–K–2Cl cotransporter NKCC1. *J. Neurosci.* 28, 4635–4639.

Kirmse, K., Witte, O. W., and Holthoff, K. (2010). GABA depolarizes immature neocortical neurons in the presence of the ketone body ß-hydroxybutyrate. *J. Neurosci.* 30, 16002–16007.

Komuro, H., and Rakic, P. (1998). Orchestration of neuronal migration by activity of ion channels, neurotransmitter receptors, and intracellular Ca^{2+} fluctuations. *J. Neurobiol.* 37, 110–130.

Leinekugel, X., Khazipov, R., Cannon, R., Hirase, H., Ben-Ari, Y., and Buzsáki, G. (2002). Correlated bursts of activity in the neonatal hippocampus in vivo. *Science* 296, 49–52.

Liao, D., Scannevin, R. H., and Huganir, R. (2001). Activation of silent synapses by rapid activity-dependent synaptic recruitment of AMPA receptors. *J. Neurosci.* 21, 6008–6017.

Loan, D. J., and Byrnes, K. R. (2010). Role of microglia in neurotrauma. *Neurotherapeutics* 7, 366–377.

Maier, N., Morris, G., and Johenning, F. W., and Schmitz, D. (2009). An approach for reliably investigating hippocampal sharp wave-ripples in vitro. *PLoS ONE* 4, e6925. doi:10.1371/journal.pone.0006925

McKinney, R. A., Debanne, D., Gähwiler, B. H., and Thompson, S. M. (1997) Lesion-induced axonal sprouting and hyperexcitability in the hippocampus in vitro: implications for the genesis of posttraumatic epilepsy. *Nat. Med.* 3, 990–996.

Minlebaev, M., Ben-Ari, Y., and Khazipov, R. (2006). Network mechanisms of spindle-burst oscillations in the neonatal rat barrel cortex in vivo. *J. Neurophysiol.* 97, 692–700.

Minlebaev, M., Colonnese, M., Tsintsadze, T., Sirota, A., and Khazipov, R. (2011). Early γ oscillations synchronize developing thalamus and cortex. *Science.* 334, 226–229.

Mizuno, H., Hirano, T., and Tagawa, Y. (2007). Evidence for activity-dependent cortical wiring: formation of interhemispheric connections in neonatal mouse visual cortex requires projection neuron activity. *J. Neurosci.* 27, 6760–6770.

Mueller, A. L., Chesnut, R. M., and Schwartzkroin, P. A. (1983). Actions of GABA in developing rabbit hippocampus: an in vitro study. *Neurosci. Lett.* 39, 193–198.

Mueller, A. L., Taube, J. S., and Schwartzkroin, P. A. (1984). Development of hyperpolarizing inhibitory postsynaptic potentials and hyperpolarizing response to gamma-aminobutyric acid in rabbit hippocampus studied in vitro. *J. Neurosci.* 4, 860–867.

Mukhtarov, M., Ivanov, A., Zilberter, Y., and Bregestovski, P. (2011). Inhibition of spontaneous network activity in neonatal hippocampal slices by energy substrates is not correlated with intracellular acidification. *J. Neurochem.* 116, 316–321.

Nabekura, J., Ueno, T., Okabe, A., Furuta, A., Iwaki, T., Shimizu-Okabe, C., Fukuda, A., and Akaike, N. (2002). Reduction of KCC2 expression and GABAA receptor-mediated excitation after in vivo axonal injury. *J. Neurosci.* 22, 4412–4417.

Pellerin, L. (2010). Food for thought: the importance of glucose and other energy substrates for sustaining brain function under varying levels of activity. *Diabetes Metab.* 36, S59–S63.

Penn, A. A., Riquelme, P. A., Feller, M. B., and Shatz, C. J. (1998). Competition in retinogeniculate patterning driven by spontaneous activity. *Science* 279, 2108–2112.

Petersen, M. A., and Dailey, M. E. (2004). Diverse microglial motility behaviors during clearance of dead cells in hippocampal slices. *Glia* 46, 195–206.

Purpura, D. P., Prelevic, S., and Santini, M. (1968). Postsynaptic potentials and spike variations in the feline hippocampus during postnatal ontogenesis. *Exp. Neurol.* 22, 408–422.

Rohrbough, J., and Spitzer, N. C. (1996). Regulation of intracellular Cl- levels by Na(+)-dependent Cl- cotransport distinguishes depolarizing from hyperpolarizing GABAA receptor mediated responses in spinal neurons. *J. Neurosci.* 16, 82–91.

Rolleston, F. S., and Newsholme, E. A. (1967). Effects of fatty acids, ketone bodies, lactate and pyruvate on glucose utilization by guinea-pig cerebral cortex slices. *Biochem. J.* 104, 519–523.

Ruusuvuori, E., Kirilkin, I., Pandya, N., and Kaila, K. (2010). Spontaneous network events driven by depolarizing GABA action in neonatal hippocampal slices are not attributable to deficient mitochondrial energy metabolism. *J. Neurosci.* 30, 15638–15642.

Sauer, J. F., Strüber, M., and Bartos, M. (2012). Interneurons provide circuit-specific depolarization and hyperpolarization. *J. Neurosci.* 32, 4224–4229.

Schurr, A., West, C. A., and Rigor, B. M. (1988). Lactate-supported synaptic function in the rat hippocampal slice preparation. *Science* 240, 1326–1328.

Schurr, A., West, C. A., and Rigor, B. M. (1989). Electrophysiology of energy metabolism and neuronal function in the hippocampal slice preparation. *J. Neurosci. Methods* 28, 7–13.

Schwartzkroin, P. A., and Altschuler, R. J. (1977). Development of kitten hippocampal neurons. *Brain Res.* 134, 429–444.

Sipilä, S. T., Schuchmann, S., Voipio, J., Yamada, J., and Kaila, K. (2006). The cation-chloride cotransporter NKCC1 promotes sharp waves in the neonatal rat hippocampus. *J. Physiol.* 573,765–773.

Spitzer, N. C. (1994). Spontaneous Ca^{2+} spikes and waves in embryonic neurons: signaling systems for differentiation. *Trends Neurosci.* 17, 115–118.

Spitzer, N. C., Lautermilch, N. J., Smith, R. D., and Gomez, T. M. (2000). Coding of neuronal differentiation by calcium transients. *Bioessays* 22, 811–817.

Staley, K. J., and Mody, I. (1992). Shunting of excitatory input to dentate gyrus granule cells by a depolarizing GABA(A) receptor-mediated postsynaptic conductance, *J. Neurophysiol.* 68, 197–212.

Szabadics, J., Varga, C., Molnar, G., Olah, S., Barzo, P., and Tamas, G. (2006). Excitatory effect of GABAergic axo-axonic cells in cortical microcircuits. *Science* 311, 233–235.

Tang, Z. Q., Dinh, E. H., Shi, W., and Lu, Y. (2011). Ambient GABA-activated tonic inhibition sharpens auditory coincidence detection via a depolarizing shunting mechanism. *J. Neurosci.* 31, 6121–6131.

Taylor, C. P., Weber, M. L., Gaughan, C. L., Lehning, E. J., and LoPachin, R. M. (1999). Oxygen/glucose deprivation in hippocampal slices: altered intraneuronal elemental composition predicts structural and functional damage. *J. Neurosci.* 19, 619–629.

Turner, D. A., and Adamson, D. C. (2011). Neuronal-astrocyte metabolic interactions: understanding the transition into abnormal astrocytoma metabolism. *J. Neuropathol. Exp. Neurol.* 70,167–176.

Tyzio, R., Allene, C., Nardou, R., Picardo, M. A., Yamamoto, S., Sivakumaran, S., Caiati, M. D., Rheims, S., Minlebaev, M., Milh, M., Ferré, P., Khazipov, R., Romette, J. L., Lorquin, J., Cossart, R., Khalilov, I., Nehlig, A., Cherubini, E., and Ben-Ari, Y. (2011). Depolarizing actions of GABA in immature neurons depend neither on ketone bodies nor on pyruvate. *J. Neurosci.* 31, 34–45.

van den Pol, A. N., Obrietan, K., and Chen, G. (1996). Excitatory actions of GABA after neuronal trauma. *J. Neurosci.* 16, 4283–4292.

van Welie, I., Smith, I. T., and Watt, A. J. (2011). The metamorphosis of the developing cerebellar microcircuit. *Curr. Opin. Neurobiol.* 21, 245–253.

Wang, D. D., and Kriegstein, A. R. (2011). Blocking early GABA depolarization with bumetanide results in permanent alterations in cortical circuits and sensorimotor gating deficits. *Cereb. Cortex* 21, 574–587.

Waseem, T., Mukhtarov, M., Buldakova, S., Medina, I., and Bregestovski, P. (2010). Genetically encoded Cl-Sensor as a tool for monitoring of Cl-dependent processes in small neuronal compartments. *J. Neurosci. Methods* 193, 14–23.

Whittingham, T. S., Lust, W. D., Christakis, D. A., and Passonneau, J. V. (1984). Metabolic stability of hippocampal slice preparations during prolonged incubation. *J. Neurochem.* 43, 689–696.

Wong, R. O., and Ghosh, A. (2002). Activity-dependent regulation of dendritic growth and patterning. *Nat. Rev. Neurosci.* 3, 803–812.

Wong, T., Zhang, X. L., Asl, M. N., Wu, C. P., Carlen, P. L., and Zhang, L. (2005). Postnatal development of intrinsic GABAergic rhythms in mouse hippocampus. *Neuroscience* 134, 107–120.

Woodin, M. A., Ganguly, K., and Poo, M. M. (2003). Coincident pre- and postsynaptic activity modifies GABAergic synapses by postsynaptic changes in ClS transporter activity. *Neuron* 39, 807–820.

Wright, R., Raimondo, J. V., and Akerman, C. J. (2011). Spatial and temporal dynamics in the ionic driving force for GABA(A) receptors. *Neural Plast.* 2011, 728395.

Zilberter, Y., and Bregestovski, P. (2012). Fueling brain neuronal activity. *Biol. Membr.* 29, 59–64.

Zilberter, Y., Zilberter, T., and Bregestovski, P. (2010). Neuronal activity in vitro and the in vivo reality: the role of energy homeostasis. *Trends Pharmacol. Sci.* 31, 394–401.

Zur Nedden, S., Hawley, S., Pentland, N., Hardie, D. G., Doney, A. S., and Frenguelli, B. G. (2011). Intracellular ATP influences synaptic plasticity in area CA1 of rat hippocampus via metabolism to adenosine and activity-dependent activation of adenosine A1 receptors. *J. Neurosci.* 31, 6221–6234.

Conflict of Interest Statement: The authors declare that the research was conducted in the absence of any commercial or financial relationships that could be construed as a potential conflict of interest.

Received: 13 January 2012; paper pending published: 23 January 2012; accepted: 02 April 2012; published online: 19 April 2012.

*Citation: Bregestovski P and Bernard C (2012) Excitatory GABA: how a correct observation may turn out to be an experimental artifact. Front. Pharmacol. **3**:65. doi: 10.3389/fphar.2012.00065*

This article was submitted to Frontiers in Neuropharmacology, a specialty of Frontiers in Pharmacology.

frontiers in
PHARMACOLOGY

GENERAL COMMENTARY
published: 09 March 2012
doi: 10.3389/fphar.2012.00026

Metabolic studies in brain slices – past, present, and future

Leif Hertz*

Department of Clinical Pharmacology, College of Basic Medical Sciences, China Medical University, Shenyang, China
**Correspondence: leifhertz@xplornet.ca*

A commentary on

Brain slice studies in the Research Topic "The link between brain energy homeostasis and neuronal activity"

In "The link between brain energy homeostasis and neuronal activity" two papers discuss the importance of optimum energy metabolism for neuronal spike activity in brain slices incubated in glucose-containing media, with one demonstrating benefits of lactate supplementation. A third demonstrates effects of succinate and γ-hydroxybutyrate on ATP-mediated $[Ca^{2+}]_i$ gradients in astrocytes, and a fourth discusses whether lactate is the glycolytic end product and exerts neuroprotection. This commentary discusses the quantitative importance of oxidative metabolism in astrocytes, importance of their $[Ca^{2+}]_i$, and role(s) of lactate.

Metabolic brain slice studies were initiated by Warburg et al. (1924). During the 1930s several such studies showed lactate release to incubation media and stimulation of respiration by high K^+ concentrations, initially by ~65% (Ashford and Dixon, 1935; Dickens and Greville, 1935). Electrical stimulation acted similarly (McIlwain, 1951, 1955). Glutamate caused neuronal depolarization (Gibson and McIlwain, 1965), and slices displayed synaptic activity (Yamamoto and McIlwain, 1966). Hertz and Schou (1962) and Weiss et al. (1972), using Warburg equipment with rapidly oscillating tissue chambers or an oxygen electrode inserted into *intensely aerated* flasks, reported O_2 uptake rates similar to Ivanov and Zilberter's (2011) and Ca^{2+}-dependence and procaine-inhibition of the K^+-mediated stimulation. The center and both surfaces of slices showed marked cell swelling under all conditions, but especially at high extracellular K^+ concentrations (Møller et al., 1974). Elevated K^+ increased (Franck, 1970; Lund-Andersen and Hertz, 1970), and electrical stimulation decreased (Cummins and McIlwain, 1961) intracellular K^+ content. Electrical pulses evoked transition from a more oxidized to a more reduced phase in NAD(P)H and cytochromes, blockable by tetrodotoxin, whereas elevated extracellular K^+ caused a more oxidized redox state (Cummins and Bull, 1971; Galeffi et al., 2011). In ^{13}C-NMR studies, using labeled glucose and the astrocyte-specific substrate acetate, Badar-Goffer et al. (1992) concluded that the high K^+-mediated increase in O_2 consumption occurred in glial cells. This may reflect a normally occurring active astrocytic uptake of K^+ released from neurons (Somjen et al., 2008; Hertz, 2011) and depolarization-induced increase in $[Ca^{2+}]_i$, stimulating astrocytic metabolism. Electrical stimulation of brain slices also increase astrocytic $[Ca^{2+}]_i$ (Filosa et al., 2004).

Recently, several groups have measured tricarboxylic acid (TCA) cycle activity in the living, functioning brain in humans and rats using ^{13}C-NMR (reviewed by Hertz, 2011) and tabulated in **Table 1**. In awake rats total pyruvate fluxes after glycolytic conversion of glucose to pyruvate followed by pyruvate dehydrogenase (PDH-) mediated) entry into the TCA cycle (in both neurons and astrocytes) *together with* flux mediated by the astrocyte-specific pyruvate carboxylase (PC) amount to ~1.67 μmol/min/g wet wt (Öz et al., 2004; **Table 1**). With a pyruvate/O_2 ratio of 3.0, this equals 300 μmol of O_2/h/g wet wt, close to the upper limit cited by Ivanov and Zilberter (2011). As noted by them, ourselves, and Okada and Lipton (2007), this rate is substantially higher than that of oxygen uptake in brain slices. However, under anesthesia *in vivo*, respiration becomes more comparable to that in brain slices (see Choi et al., 2002; **Table 1**). Thus, the enhanced rates of oxygen consumption in slices during neuronal stimulation shown by Ivanov and Zilberter (2011), discussed by Kann (2011), and quantitated by Galeffi et al. (2011), are functionally the most meaningful. Moreover, determination of average metabolic rates in neurons (PDH_n) and astrocytes (PFH_g + PC) separately (lower two lines of **Table 1**) shows that astrocytic O_2 consumption equals one quarter of total brain energy metabolism *in vivo*, indicating that per volume astrocytes consume O_2 at least at the same rate as neurons. Additional ^{13}C-NMR studies in brain slices during different types of neuronal activation would be useful to evaluate neuronal and astrocytic responses.

Astrocytes are the topic of the non-metabolic study by Molnár et al. (2011) It describes astrocytic $[Ca^{2+}]_i$ responses to ATP and modulation of a subset of astrocytic ATP receptors by succinate and γ-aminobutyrate. Besides illustrating the high density of functioning ATP receptors, even in the young astrocytes studied, and the localization of the succinate-affected receptors to vascular-associated astrocyte processes, the study emphasizes important effects of succinate beyond its role as a TCA cycle constituent. Succinate is present in serum and its concentration is increased in diabetes, which may be of considerable importance in diabetic nephropathy (Deen and Robben, 2011), and raises the possibility of involvement of succinate and astrocytes in diabetic effects on the brain. The Molnar paper is also of interest in connection with that by Zilberter (2011), and it supports that the roles of astrocytes in brain metabolism may be underestimated in the Venkateswaran et al. (2012) paper.

Observations in brain slices by Takagaki and Tsukada (1957) that lactate sustains similar rates of oxygen consumption as glucose have been repeatedly confirmed. The Schurr and Gozal (2011) paper suggests important physiological (mitochondrial lactate oxidation) and pathological (neuroprotection) roles of lactate. However, most authors agree that lactate dehydrogenase activity in mitochondria is unlikely (Sahlin et al., 2002; Yoshida et al., 2007), and lactate cannot prevent anoxic depolarization in rat hippocampal slices, when gly-

Table 1 | Representative values for metabolic fluxes in human and rat brain *in vivo*.

Reference	Species	PDH_n	PC	% PC	PDH_g	% PDH_g
Aureli et al. (1997)	Rat[a]			10.0		
Cruz and Cerdán (1999)	Rat[a]	1.0			0.4	29
Shen et al. (1999)	Human[a]	0.71	0.04	4.9	0.06	7.4
Gruetter et al. (2001)	Human[a]	0.57	0.09	12.5	0.06	8.3
Blüml et al. (2002)	Human[a]	0.70			0.13	15.7
Lebon et al. (2002)	Human[a]	0.80			0.14	16.7
Choi et al. (2002)	Rat[b]	0.41	0.04	9.8	0.28	38
Öz et al. (2004)	Rat[a]	1.19	0.18	10.8	0.30	18
Xu et al. (2004)	Rat[a]		0.15			
Patel et al. (2005)	Rat[b]	0.52	0.06	10.3		
Mason et al. (2007)	Human[a]		0.02			
Deelchand et al. (2009)	Rat[a]				0.49	
Patel et al. (2010)	Rat[b]				0.37	
Lanz et al. (2010)	Rat[b]	0.76			0.13	14.6
Lanz et al. (2012)	Rat[b]				0.14	
Average				9.9 ± 1.0		18.5 ± 3.6
Average, awake brain				9.6 ± 1.6		15.9 ± 3.2

Absolute values are μmol/min per gram wet wt. PDH_n, pyruvate dehydrogenase-mediated pyruvate flux in neurons (equals flux in neuronal TCA cycle); PC, pyruvate carboxylase-mediated flux (astrocyte-specific);% PC, pyruvate carboxylase-mediated flux as a percentage of total measured pyruvate metabolism; PDH_g, pyruvate dehydrogenase-mediated pyruvate flux in glial cells (astrocytes);% PDH_g, pyruvate dehydrogenase-mediated pyruvate flux in astrocytes as percent of total measured pyruvate metabolism. [a]Awake, unanesthetized subjects; [b]anesthetized subjects. Slightly modified from Hertz (2011) where more details can be found.

colysis is completely inhibited (Allen et al., 2005). Techniques used during preparation of slices are important for subsequent metabolic effects of glucose and lactate (Dienel and Hertz, 2005; Okada and Lipton, 2007; Dienel, 2011). Lactate serves as a partial substrate for brain metabolism during intense exercise (when its blood concentration is increased), but this does not indicate any need for lactate in addition to glucose in brain function, including ongoing activity, since during rest there is a small lactate exit from brain (Quistorff et al., 2008). Nevertheless, if serum lactate is increased, lactate is preferentially oxidized (van Hall et al., 2009). In brain slices the question is complex, because of simultaneous lactate release. Could simple replacement of this lactate restore optimum glucose metabolism? Can results in astrocyte cultures (Sotelo-Hitschfeld et al., 2012) be similarly explained?

In conclusion, a considerable part of oxidative glucose metabolism in brain is astrocytic, exogenous lactate is not a necessary brain fuel *in vivo*, and past history of metabolic brain slice experiments may inspire future studies.

REFERENCES

Allen, N. J., Káradóttir, R., and Attwell, D. (2005). A preferential role for glycolysis in preventing the anoxic depolarization of rat hippocampal area CA1 pyramidal cells. *J. Neurosci.* 25, 848–859.

Ashford, C. A., and Dixon, K. C. (1935). The effect of potassium on the glucolysis of brain tissue with reference to the Pasteur effect. *Biochem. J.* 29, 157–168.

Aureli, T., Di Cocco, M. E., Calvani, M., and Conti, F. (1997). The entry of [1-13C]glucose into biochemical pathways reveals a complex compartmentation and metabolite trafficking between glia and neurons: a study by 13C-NMR spectroscopy. *Brain Res.* 765, 218–227.

Badar-Goffer, R. S., Ben-Yoseph, O., Bachelard, H. S., and Morris, P. G. (1992). Neuronal-glial metabolism under depolarizing conditions. A 13C-n.m.r. study. *Biochem. J.* 282(Pt 1), 225–230.

Blüml, S., Moreno-Torres, A., Shic, F., Nguy, C. H., and Ross, B. D. (2002). Tricarboxylic acid cycle of glia in the in vivo human brain. *NMR Biomed.* 15, 1–5.

Choi, I. Y., Lei, H., and Gruetter, R. (2002). Effect of deep pentobarbital anesthesia on neurotransmitter metabolism in vivo: on the correlation of total glucose consumption with glutamatergic action. *J. Cereb. Blood Flow Metab.* 22, 1343–1351.

Cruz, F., and Cerdán, S. (1999). Quantitative 13C NMR studies of metabolic compartmentation in the adult mammalian brain. *NMR Biomed.* 12, 451–462.

Cummins, J. T., and Bull, R. (1971). Spectrophotometric measurements of metabolic responses in isolated rat brain cortex. *Biochim. Biophys. Acta* 253, 29–38.

Cummins, J. T., and McIlwain, H. (1961). Electrical pulses and the potassium and other ions of isolated cerebral tissues. *Biochem. J.* 79, 330–341.

Deelchand, D. K., Shestov, A. A., Koski, D. M., Uğurbil, K., and Henry, P. G. (2009). Acetate transport and utilization in the rat brain. *J. Neurochem.* 109(Suppl. 1), 46–54.

Deen, P. M., and Ro bben, J. H. (2011). Succinate receptors in the kidney. *J. Am. Soc. Nephrol.* 22, 1416–1422.

Dickens, F., and Greville, G. D. (1935). The metabolism of normal and tumour tissue: neutral salt effects. *Biochem. J.* 29, 1468–1483.

Dienel, G. A. (2011). Brain lactate metabolism: the discoveries and the controversies. *J. Cereb. Blood Flow Metab.* doi: 10.1038/jcbfm.2011.175. [Epub ahead of print]

Dienel, G. A., and Hertz, L. (2005). Astrocytic contributions to bioenergetics of cerebral ischemia. *Glia* 50, 362–388.

Filosa, J. A., Bonev, A. D., and Nelson, M. T. (2004). Calcium dynamics in cortical astrocytes and arterioles during neurovascular coupling. *Circ. Res.* 95,e73–e81.

Franck, G. (1970). Echanges cationiques au niveau des neurones et des cellules gliales du cerveau. *Arch. Int. Physiol. Biochim.* 78, 613–866.

Galeffi, F., Somjen, G. G., Foster, K. A., and Turner, D. A. (2011). Simultaneous monitoring of tissue PO2 and NADH fluorescence during synaptic stimulation and spreading depression reveals a transient dissociation between oxygen utilization and mitochondrial redox state in rat hippocampal slices. *J. Cereb. Blood Flow Metab.* 31, 626–639.

Gibson, I. M., and McIlwain H. (1965). Continuous recordings of changes in membrane potential in mammalian cerebral tissues in vitro; recovery after

depolarization by added substrates. *J. Physiol.* 176, 261–283.

Gruetter, R., Seaquist, E. R., and Uğurbil, K. (2001). A mathematical model of compartmentalized neurotransmitter metabolism in the human brain. *Am. J. Physiol. Endocrinol. Metab.* 281, E100–E112.

Hertz, L. (2011). Astrocytic energy metabolism and glutamate formation – relevance for 13C-NMR spectroscopy and importance of cytosolic/mitochondrial trafficking. *Magn. Reson. Imaging* 29, 1319–1329.

Hertz, L., and Schou, M. (1962). Univalent cations and the respiration of brain-cortex slices. *Biochem. J.* 85, 93–104.

Ivanov, A., and Zilberter, Y. (2011). Critical state of energy metabolism in brain slices: the principal role of oxygen delivery and energy substrates in shaping neuronal activity. *Front. Neuroeng.* 3:9. doi: 10.3389/fnene. 00009

Kann, O. (2011). The energy demand of fast neuronal network oscillations: insights from brain slice preparations. *Front. Pharmacol.* 2:90. doi: 10.3389/fphar. 00090

Lanz, B., Uffmann, K. T., Wyss, M., Weber, B., Buck, A., and Gruetter, R. (2012). A two-compartment mathematical model of neuroglial metabolism using [1-11C] acetate. *J. Cereb. Blood Flow Metab.* doi: 10.1038/jcbfm.2011.162.

Lanz, B., Xin, L., Wyss, M. T., Weber, B., Buck, A., and Gruetter, R. (2010). Measurements of glial metabolic fluxes with 11C-acetate using positron emission and 1H[13C] NMR spectroscopy. *Abstracts, 9th International Conference on Brain Energy Metabolism*, Budapest, 25.

Lebon, V., Petersen, K. F., Cline, G. W., Shen, J., Mason, G. F., Dufour, S., Behar, K. L., Shulman, G. I., and Rothman, D. L. (2002). Astroglial contribution to brain energy metabolism in humans revealed by 13C nuclear magnetic resonance spectroscopy, elucidation of the dominant pathway for neurotransmitter glutamate repletion and measurement of astrocytic oxidative metabolism. *J. Neurosci.* 22, 1523–1531.

Lund-Andersen, H., and Hertz, L. (1970). Effects of potassium content in brain-cortex slices from adult rats. *Exp. Brain Res.* 11, 199–212.

Mason, G. F., Petersen, K. F., de Graaf, R. A., Shulman, G. I., and Rothman, D. L. (2007). Measurements of the anaplerotic rate in the human cerebral cortex using 13C magnetic resonance spectroscopy and [1-13C] and [2-13C] glucose. *J. Neurochem.* 100, 73–86.

McIlwain, H. (1951). Metabolic response in vitro to electrical stimulation of sections of mammalian brain. *Biochem. J.* 49, 382–393.

McIlwain, H. (1955). A transitory, rapid, production of lactate in electrically excited cerebral tissues. *Biochem. J.* 60, xxxi.

Møller, M., Møllgård, K., Lund-Andersen, H., and Hertz, L. (1974). Concordance between morphological and biochemical estimates of fluid spaces in rat brain cortex slices. *Exp. Brain Res.* 21, 299–314.

Molnár, T., Héja, L., Emri, Z., Simon, A., Nyitrai, G., Pál, I., and Kardos, J. (2011). Activation of astroglial calcium signaling by endogenous metabolites succinate and gamma-hydroxybutyrate in the nucleus accumbens. *Front. Neuroeng.* 3:7. doi: 10.3389/fnene. 00007

Okada, Y., and Lipton, P. (2007). "Glucose, oxidative metabolism and neural function in brain slices – Glycolysis plays a key role in neural activity," in *Handbook of Neurochemistry and Molecular Neurobiology, Vol. 2, Brain Energetics, Integration of Molecular and Cellular Processes*, eds G. E. Gibson and G. A. Dienel (New York/Heidelberg: Springer), 18–39.

Öz, G., Berkich, D. A., Henry, P. G., Xu, Y., LaNoue, K., Hutson, S. M., and Gruetter, R. (2004). Neuroglial metabolism in the awake rat brain: CO2 fixation increases with brain activity. *J. Neurosci.* 24, 11273–11279.

Patel, A. B., Chowdhury, G. M., de Graaf, R. A., Rothman, D. L., Shulman, R. G., and Behar, K. L. (2005). Cerebral pyruvate carboxylase flux is unaltered during bicuculline-seizures. *J. Neurosci. Res.* 79, 128–138.

Patel, A. B., de Graaf, R. A., Rothman, D. L., Behar, K. L., and Mason, G. F. (2010). Evaluation of cerebral acetate transport and metabolic rates in the rat brain in vivo using 1H-[13C]-NMR. *J. Cereb. Blood Flow Metab.* 30, 1200–1213.

Quistorff, B., Secher, N. H., and Van Lieshout, J. J. (2008). Lactate fuels the human brain during exercise. *FASEB J.* 22, 3443–3449.

Sahlin, K., Fernström, M., Svensson, M., and Tonkonogi, M. (2002). No evidence of an intracellular lactate shuttle in rat skeletal muscle. *J. Physiol.* 541, 569–574.

Schurr, A., and Gozal, E. (2011). Aerobic production and utilization of lactate satisfy increased energy demands upon neuronal activation in hippocampal slices and provide neuroprotection against oxidative stress. *Front. Pharmacol.* 2:96. doi: 10.3389/fphar. 00096

Shen, J., Petersen, K. F., Behar, K. L., Brown, P., Nixon, T. W., Mason, G. F., Petroff, O. A., Shulman, G. I., Shulman, R. G., and Rothman, D. L. (1999). Determination of the rate of the glutamate/glutamine cycle in the human brain by in vivo 13C NMR. *Proc. Natl. Acad. Sci. U.S.A.* 96, 8235–8240.

Somjen, G. G., Kager, H., and Wadman, W. J. (2008). Computer simulations of neuron-glia interactions mediated by ion flux. *J. Comput. Neurosci.* 25, 349–365.

Sotelo-Hitschfeld, T., Fernández-Moncada, I., and Barros, L. F. (2012). Acute feedback control of astrocytic glycolysis by lactate. *Glia* 60, 674–680.

Takagaki, G., and Tsukada, Y. (1957). The effect of some inorganic ions on brain slices metabolizing glucose or pyruvate. *J. Neurochem.* 2, 21–29.

van Hall, G., Strømstad, M., Rasmussen, P., Jans, O., Zaar, M., Gam, C., Quistorff, B., Secher, N. H., and Nielsen, H. B. (2009). Blood lactate is an important energy source for the human brain. *J. Cereb. Blood Flow Metab.* 29, 1121–1129.

Venkateswaran, N., Sekhar, S., Thirupatchur Sanjayasarathy, T., Krishnan, S. N., Kabaleeswaran, D. K., Ramanathan, S., Narayanasamy, N., Jagathrakshakan, S. S., and Vignesh, S. R. (2012). Energetics based spike generation of a single neuron: simulation results and analysis. *Front. Neuroeng.* 4:2. doi: 10.3389/fnene. 00002

Warburg, O., Posener, K., and Negelein, E. (1924). Ueber den Stoffwechsel der tumoren. *Biochem. Z.* 152, 319–344.

Weiss, G. B., Hertz, L., and Goodman, F. R. (1972). Drug-induced alterations in respiration of rat brain cortex and striatum slices in a carbon dioxide-bicarbonate-buffered medium. *Biochem. Pharmacol.* 21, 625–634.

Xu, Y., Öz, G., LaNoue, K. F., Keiger, C. J., Berkich, D. A., Gruetter, R., and Hutson, S. H. (2004). Whole-brain glutamate metabolism evaluated by steady-state kinetics using a double-isotope procedure: effects of gabapentin. *J. Neurochem.* 90, 1104–1116.

Yamamoto, C., and McIlwain, H. (1966). Electrical activities in thin sections from the mammalian brain maintained in chemically-defined media in vitro. *J. Neurochem.* 13, 1333–1343.

Yoshida, Y., Holloway, G. P., Ljubicic, V., Hatta, H., Spriet, L. L., Hood, D. A., and Bonen, A. (2007). Negligible direct lactate oxidation in subsarcolemmal and intermyofibrillar mitochondria obtained from red and white rat skeletal muscle. *J. Physiol. (Lond.)* 582, 1317–1335.

Zilberter, T. (2011). Carbohydrate-biased control of energy metabolism: the darker side of the selfish brain. *Front. Neuroeng.* 3:8. doi: 10.3389/fnene.2011.00008

Received: 30 January 2012; accepted: 12 February 2012; published online: 09 March 2012.

*Citation: Hertz L (2012) Metabolic studies in brain slices – past, present, and future. Front. Pharmacol. **3**:26. doi: 10.3389/fphar.2012.00026*

This article was submitted to Frontiers in Neuropharmacology, a specialty of Frontiers in Pharmacology.

frontiers in
NEUROENERGETICS

ORIGINAL RESEARCH ARTICLE
published: 29 December 2011
doi: 10.3389/fnene.2011.00009

Critical state of energy metabolism in brain slices: the principal role of oxygen delivery and energy substrates in shaping neuronal activity

Anton Ivanov and Yuri Zilberter*

INSERM UMR751, Université de la Méditerranée, Marseille, France

Edited by:
Sebastian Cerdan, Instituto de Investigaciones Biomedicas Alberto Sols, Spain

Reviewed by:
Sebastian Cerdan, Instituto de Investigaciones Biomedicas Alberto Sols, Spain
Elizabeth Hillman, Columbia University, USA
Juan C. Saez, Universidad Catolica de Chile, Chile

***Correspondence:**
Yuri Zilberter, Faculté de Médecine Timone, INSERM U751, 27 Bd Jean Moulin, 13385 Marseille Cedex 05, France.
e-mail: yuri.zilberter@univmed.fr

The interactive vasculo-neuro-glial system controlling energy supply in the brain is absent *in vitro* where energy provision is determined by experimental conditions. Despite the fact that neuronal activity is extremely energy demanding, little has been reported on the state of energy metabolism in submerged brain slices. Without this information, the arbitrarily chosen oxygenation and metabolic provisions make questionable the efficient oxidative metabolism in slices. We show that in mouse hippocampal slices (postnatal day 19–44), evoked neuronal discharges, spontaneous network activity (initiated by 4-aminopyridine), and synaptic stimulation-induced NAD(P)H autofluorescence depend strongly on the oxygen availability. Only the rate of perfusion as high as ~15 ml/min (95% O_2) provided appropriate oxygenation of a slice. Lower oxygenation resulted in the decrease of both local field potentials and spontaneous network activity as well as in significant modulation of short-term synaptic plasticity. The reduced oxygen supply considerably inhibited the oxidation phase of NAD(P)H signaling indicating that the changes in neuronal activity were paralleled by the decrease in aerobic energy metabolism. Interestingly, the dependence of neuronal activity on oxygen tension was clearly shifted toward considerably larger pO_2 values in slices when compared to *in vivo* conditions. With sufficient pO_2 provided by a high perfusion rate, partial substitution of glucose in ACSF for β-hydroxybutyrate, pyruvate, or lactate enhanced both oxidative metabolism and synaptic function. This suggests that the high pO_2 in brain slices is compulsory for maintaining oxidative metabolism, and glucose alone is not sufficient in fulfilling energy requirements during neuronal activity. Altogether, our results demonstrate that energy metabolism determines the functional state of neuronal network, highlighting the need for the adequate metabolic support to be insured in the *in vitro* experiments.

Keywords: energy substrates, brain slices, synaptic plasticity, neuronal activity, energy metabolism, oxygen, NAD(P)H, local field potential

INTRODUCTION

In the intact brain, complex machinery exists that coordinates energy substrates delivery and adjusts energy substrate pool composition to the needs of neuronal energy metabolism (Abbott et al., 2010; Pellerin, 2010; Turner and Adamson, 2011). In the acute brain slices, such a sophisticated system does not exist and the neuronal energy supply depends entirely on the experimental conditions. The primary requirement for the *in vitro* studies is to provide experimental conditions, which would approximate as close as possible the *in vivo* situation. One parameter of critical importance is the adequate slice oxygenation compulsory for aerobic energy metabolism.

For instance, it has been demonstrated that neuronal synaptic function (Yamamoto and Kurokawa, 1970; Garcia et al., 2010; Ivanov et al., 2011), networks' ability to generate physiological-like oscillations (Huchzermeyer et al., 2008; Hajos et al., 2009; Kann et al., 2011), and efficiency of glucose utilization for supporting neuronal activity (Schurr and Payne, 2007) all strongly depend on the oxygen tension in slices. In the few available electrophysiological studies with direct measurements of slice tissue oxygenation, a strong dependence of neuronal functions on oxygen was observed in the range of pO_2 (100–400 Torr; Foster et al., 2005; Hajos et al., 2009; Garcia et al., 2010; Ivanov et al., 2011; Kann et al., 2011) that exceeded the physiological pO_2 range (10–60 Torr) in brain tissue *in vivo* (Erecinska and Silver, 2001; Masamoto et al., 2003, 2007; Takano et al., 2007). This fact suggests that the oxygen requirement for neuronal function is much higher in slices than *in vivo*. In the majority of electrophysiological studies performed on submerged slices, the oxygen tension in tissue was not controlled while the solution flow rate (normally 2–4 ml/min) or chamber constructions were chosen from the assumptions not substantiated by the direct measurements. The adequacy of such approach may be especially questionable for the interpretation of multicellular activity measurements related to the functioning of neurons throughout the slice depth (Hajos and Mody, 2009).

Another important issue is the composition of energy substrate pool in ACSF. Standard ACSF contains glucose as the only energy substrate. Historically, the composition of ACSF was developed for replacement of physiological fluids in clinics (see for review Zilberter et al., 2010) but not for mimicking the extracellular neuron environment. Glucose indeed is the main energy substrate in blood circulating in the adult brain. However, the composition of energy substrate pool in the brain extracellular fluid may be complex and is defined by several factors such as network activity, neuron–glia interactions, substrate delivery across the blood brain barrier, and others. For instance, it has been recently demonstrated that lactate is the preferable neuronal fuel during the intense brain activity (Wyss et al., 2011). In slices, it is unclear whether glucose itself is able to fully cover energy demands during network activity. We have shown recently in neonatal slices that supplementing glucose in ACSF with other oxidative energy substrates enhances both the aerobic metabolism and synaptic function (Ivanov et al., 2011). These results suggest that the sole use of glucose in ACSF may not be optimal in mature slices as well. In addition, it has been demonstrated (Whittingham et al., 1984; Zur Nedden et al., 2011) that the levels of adenine nucleotides in slices is about 50% lower than those measured *in vivo*, indicating that some processes underlying neuronal energy metabolism may be disrupted.

Therefore, the critical question is how close the experimental conditions accepted for the electrophysiological studies on slices approximate the natural neuronal environment in the brain and thus with what confidence the data obtained in these experiments extrapolate to the real *in vivo* situation.

In our previous study on neonatal brain slices (Ivanov et al., 2011) we demonstrated the importance of oxidative metabolism of glucose-alternative energy substrates for the neuronal function. In the present study, we show that this conclusion is not limited to neonates but is valid for mature animals as well. In addition, we examine the influence of oxygen tension on neuronal population/spontaneous activity, our data pointing to a much stronger dependence of neuronal activity on oxygen tension in slices than that seen *in vivo*.

MATERIALS AND METHODS

TISSUE SLICE PREPARATION

Brain slices were prepared from P19 to P44 Swiss mice of both sexes. All animal protocols conformed to the French Public Health Service policy and the INSERM guidelines on the use of laboratory animals. The mouse was rapidly decapitated and the brain was removed from the skull and placed in the ice-cold ACSF oxygenated with 95% O_2/5% CO_2. The ACSF solution consisted of (in mM/l): NaCl 124, KCl 2.50, NaH_2PO_4 1.25, $NaHCO_3$ 25, $CaCl_2$ 2.00, $MgCl_2$ 1.30, and dextrose 10, pH 7.4. Sagittal slices (350 μm) were cut using a tissue slicer (Leica VT 1200 s, Leica Microsystem Vertrieb GmbH, Germany). During cutting slices were submerged in an ice-cold (<6°C) cutting solution consisted of (in mM/l): K-gluconate 140, HEPES 10, Na-gluconate 15, EGTA 0.2, NaCl 4, pH adjusted to 7.2 with KOH. Slices were transferred immediately to a multi-well, dual-sided perfusion holding camera with constantly circulating oxygenated (95% O_2/5% CO_2) ACSF maintained at room temperature (22–24°C), and allowed to recover for 2 h. The chamber was designed for minimizing the O_2 escape and providing rapid solution exchange during incubation (whole volume renewal time <3 min). Slices were then transferred to a recording chamber continuously superfused and oxygenated with 95% O_2/5% CO_2 (33–34°C).

SYNAPTIC STIMULATION AND FIELD POTENTIAL RECORDINGS

Shaffer collateral/commissural pathway was stimulated using the DS2A isolated stimulator (Digitimer Ltd., UK) with a bipolar nichrome electrode situated in the stratum radiatum (SR) of CA1 hippocampal region. Stimulus current was adjusted using single pulses (170–240 μA, 200 μs, 0.15 Hz) to produce a local field potential (LFP) of nearly 50% of maximal amplitude. LFPs were recorded using glass microelectrodes filled with ASCF, placed in stratum pyramidale at the 100- to 150-μm depth and connected to the DAM-80 amplifier (WPI, FL, USA). Synaptic stimulation consisted of a 30-s stimulus train (200 μs pulses at 10 Hz) was used to generate autofluorescence reduced pyridine nucleotide (NAD(P)H) response. LFPs were quantified by calculating their integral as described elsewhere (Ivanov et al., 2011). Field postsynaptic potentials (fPSPs) were calculated by subtracting population spikes from LFPs.

NAD(P)H FLUORESCENCE IMAGING

Reduced nicotinamide adenine dinucleotide phosphate (NADPH) and reduced nicotinamide adenine dinucleotide (NADH) have very similar optical properties, and therefore is expected that NADPH also contributes to some extent to total autofluorescence signals (Klaidman et al., 1995; Shuttleworth, 2010). Moreover, recent reports suggest the importance of pentose-phosphate pathway for neuronal glucose metabolism (Bolanos et al., 2010). Changes in NAD(P)H fluorescence in hippocampal slices were monitored using a 290- to 370-nm excitation filter and 420 nm long pass filter for emission (Omega Optical, Brattleboro, VT, USA). The light source was the Intensiligh C-HGFI illuminator (Nikon Instruments Europe B.V., UK) equipped with a mercury arc lamp. Slices were epi illuminated and imaged through a Nikon upright microscope (FN1, Eclipse) with 4×/0.10 Nikon Plan objective. Images were acquired using a linear, cooled 12-b CCD camera (Sensicam, PCO AG, Germany) with a 640 × 480 digital spatial resolution. Because of a low level of fluorescence emission for this fluorophore, NAD(P)H images were acquired every 600–800 ms as 8 × 8 binned images (effective spatial resolution of 80 × 60 pixels). The exposure time was adjusted to obtain fluorescence intensity between 2000 and 3000 optical intensity levels. Images were stored in a computer as 12-b files (0–4096 dynamic range). Fluorescence intensity changes in SR near sites of LFP and pO_2 recordings were extracted in three to five regions of interest using ImageJ software (developed by Wayne Rasband, NIH, USA). Data were expressed as the percentage changes in fluorescence over a baseline $[(\Delta F/F)\cdot 100\%]$. Signal analysis was performed using IgorPro software (WaveMetrics, Inc., OR, USA).

OXYGEN MEASUREMENTS

A Clark-style oxygen microelectrode (OX-10, tip diameter 10 μm; Unisense Ltd., Denmark) was used to measure slice tissue PO_2. The electrode was connected to a picoammeter (PA2000, Unisense Ltd., Denmark) and the cathode was polarized at −800 mV in

normal saline at 22°C for up to 12 h before the first use. A two-point calibration (in pA) was performed following polarization by inserting the electrode in normal saline solution (at 33°C) equilibrated with either 95% O_2–5% CO_2 or ambient air. Calibrations were repeated after each experiment to determine the PO_2 values. The oxygen electrode (response time 1–3 s) was positioned using motorized micromanipulator (Scientifica Ltd., UK) in SR at the proximity to field potential recording electrode (at 100–150 μM slice depth).

PHARMACOLOGY

Drugs used were purchased from Sigma (racemic mixture of DL-3-hydroxybutyric acid sodium salt, L-lactate sodium salt, pyruvate sodium salt). Within the racemic mixture, D-BHB is the primary mediator of the physiological effects of DL-BHB, and is the only form that can function as a substrate for mitochondrial BHB dehydrogenase. Consequently, only 50% of exogenous DL-BHB is expected to be utilized (Tsai et al., 2006).

STATISTICAL ANALYSIS

Group measures were expressed as means ± SEM; error bars also indicate SEM. Statistical significance was assessed using the Wilcoxon's signed paired test or Student's paired *t*-test. The level of significance was set at $p < 0.05$.

RESULTS

OXYGEN TENSION DEPTH PROFILE IN SUBMERGED SLICES DEPENDS ON THE SOLUTION FLOW RATE

To evaluate the oxygen availability at different slice depths we measured the oxygen tension in submerged slices placed in a standard round chamber (bottom diameter 17 mm, volume <1.5 ml) and superfused with solution from the upper side. **Figure 1Aa** shows the oxygen depth profile measured at 15 and 4 ml/min solution flow rates (slice is depicted by the gray color bar). Similar to our measurements on neonatal slices (Ivanov et al., 2011), pO_2 began to decrease close (200–300 μm) to the slice surface. Importantly, on the slice surface, pO_2 was already significantly lower than that in the incoming solution (~720 Torr) being 441 ± 11 Torr at 15 ml/min and 258 ± 53 Torr at 4 ml/min ($n = 5$). Note that the solution outflow was located in the vicinity of slice surface since at more distant input locations the oxygen distribution was significantly worse. At 4 ml/min, pO_2 steeply decreased within the slice depth coming close to zero at ~200 μm. The oxygen depth profile was much better at 15 ml/min with pO_2 of about 300 Torr in the slice core.

Oxygen consumption by a quiescent brain slice may be evaluated from our measurements of pO_2 at variable distance from the slice surface (**Figure 1**). Above 400 μm from the surface, pO_2 remains constant (~700 Torr). Proximal to the slice, pO_2 declines rapidly to about 440 Torr at the slice surface (at 15 ml/min flow rate). Therefore, we consider that the slice consumes O_2 from the volume defined as the slice surface (~0.6 cm^2) multiplied by 400 μm. Note that in the absence of the slice, oxygen is distributed homogeneously and its concentration is 850 μM/l as calculated from the pO_2 of 700 Torr, temperature 33°C, and ACSF salinity 12%. The total amount of O_2 in this volume is 0.02 μM. The amount of O_2 with the slice present can be obtained by the integration of O_2 distribution over this volume, which results in a value of 0.017 μM. Thus, the slice consumes 0.003 μM of oxygen from the perfusion chamber volume. Since the chamber volume is 1.5 ml and ACSF is completely renewed 10 times per minute (at 15 ml/min flow rate), the O_2 consumption is $0.003 \times 10 = 0.03$ μM/min. The mean wet weight of a 350-μm thick brain slice from a P30 mouse is about 20 mg. Assuming that the oxygen utilization is constant over the slice, the oxygen consumption is 1.5 μM/min/g of wet weight. However, it is necessary to take into account the extent of slice tissue integrity. Indeed, due to the cutting procedure, the slice edges contain mainly dead cells and the thickness of these edges has been estimated to be 35–50 μm from each side (Feig and Lipton, 1990; Frenguelli et al., 2003). Therefore, the slice volume consuming oxygen should be decreased by at least 20% (at 35 μm dead edges) and that in turn increases the estimate of O_2 consumption to 1.8 μM/min/g wet weight. The reported whole brain oxygen consumption of rats is 3.4–4.6 μM/min/g wet weight (Erecinska and Silver, 2001). Therefore, even when exposed to a relatively high oxygen tension (440 Torr at the surface and 320 Torr in the core, blue curve in **Figure 1Aa**), neuronal tissue in a "quiescent" slice consumes lesser or comparable amount of oxygen to recorded consumption *in vivo*.

In the same experiments, to examine the effect of perfusion rate on neuronal electrical activity we also measured the LFPs in CA1 region induced by single stimulation of Schaffer collaterals (SC). In line with previous observations (Garcia et al., 2010; Ivanov et al., 2011), LFPs were strongly dependent on the perfusion rate (**Figure 1Ab**) with LFP integrals 53 ± 11% smaller at 4 ml/min compared to those recorded at 15 ml/min rate (**Figure 1Ac**; $n = 5$, $p < 0.05$).

In some previous studies, scientists used the dual laminar flow slice perfusion chambers to provide better conditions for slice functioning (Hajos and Mody, 2009). We examined whether at different rates of solution flow such configuration can significantly improve slice oxygenation and electrical activity (**Figure 1B**). Indeed, dual laminar flow (chamber volume <1 ml) considerably enhances oxygenation of deep slice layers at low perfusion rates (**Figure 1B**, left) improving, therefore, the endurance of neurons in these layers. Nevertheless, at 4 ml/min perfusion rate, such an improvement in oxygenation did not appear to be sufficient enough to augment the synaptic function, as LFPs were still much smaller (by 45 ± 16%; $n = 7$, $p < 0.01$) at 4 ml/min than those at 15 ml/min (**Figure 1B**, right).

Another approach sometimes utilized for improving slice oxygenation is an exchange of air directly in contact with the bath solution to oxygen. In three experiments (data not shown), such approach did not change significantly neither the slice oxygen levels nor LFP values (LFPs were by 41 ± 17% smaller at 4 ml/min than at 15 ml/min).

To rule out a possibility that the high perfusion rate may result in a washout of some active substances from slice tissue and thus affect LFPs, we measured LFPs at the same 15 ml/min superfusion with 95% O_2 and ~50% O_2 oxygenation, partially substituting oxygen for air ($n = 3$). Similar to the experiments with different solution flow rates, lower solution oxygenation resulted in a strong reduction of LFPs (not shown).

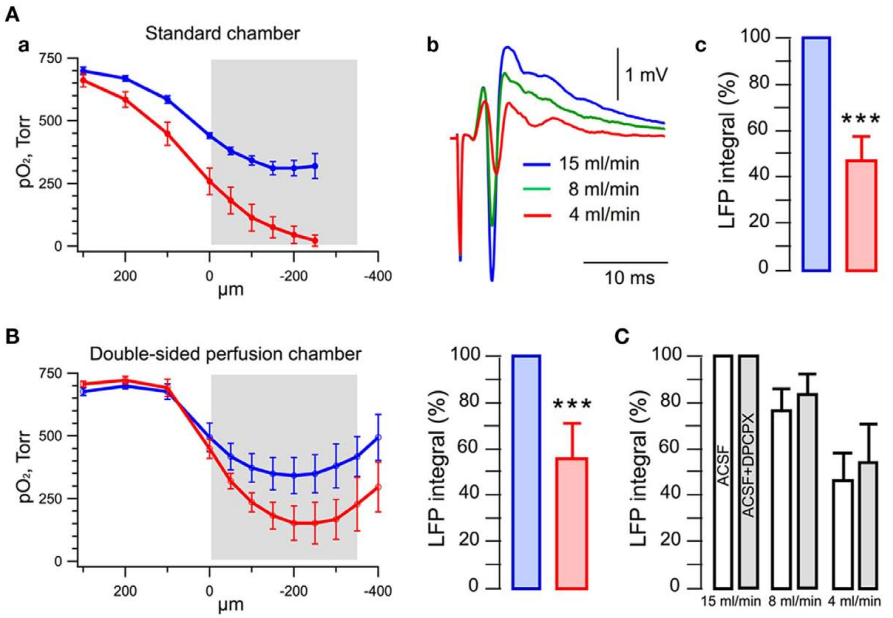

FIGURE 1 | Rate of perfusion determines oxygen distribution and LFP magnitude in a slice. (A) Measurements in a standard round chamber (1.5 ml volume) with a submerged slice. **(a)** Oxygen depth profile at 15 ml/min (blue) and 4 ml/min (red) perfusion rate. A slice is depicted in gray; **(b)** LFPs recorded in CA1 in response to 0.15 Hz stimulation of SC; **(c)** statistical summary of LFP integrals. **(B)** Oxygen depth profile in a custom chamber (<1 ml volume) with a dual-sided perfusion of submerged slice. **(C)** Blockade of adenosine receptors by DPCPX does not prevent reduction of LFPs following decrease in the perfusion rate.

Finally, inhibition of neuronal energy metabolism may result in an increase in extracellular adenosine concentration, activation of the A1 type adenosine receptors and suppression of synaptic function (Zhao et al., 1997; Coelho et al., 2000). Therefore, we performed experiments with different perfusion rates in the presence of 100 nM DPCPX, an antagonist of A1 receptors (**Figure 1C**). Blockade of adenosine receptors did not prevent the decrease of LFPs at lower perfusion rates and this effect did not differ significantly from that seen in ACSF: at 8 ml/min, LFPs decreased by $24 \pm 9\%$ in ACSF vs. $17 \pm 9\%$ in ACSF + DPCPX ($n = 5, p = 0.16$); at 4 ml/min, LFPs decreased by $55 \pm 11\%$ in ACSF vs. $47 \pm 17\%$ in ACSF + DPCPX ($n = 5$, $p = 0.27$).

Therefore, our results indicate that at low perfusion rates, the decrease in slice oxygen tension underlies the decline of synaptic function. In addition we found no alternatives to a high rate of perfusion for maintaining sufficient oxygenation in submerged slices.

OXYGEN AVAILABILITY CONTROLS ENERGY METABOLISM AND SYNAPTIC FUNCTION OF NEURONS IN SLICES

Figure 2A demonstrates the typical recordings of LFPs and oxygen pressure during a stimulation protocol that we have used for analyzing energy metabolism and electrophysiological characteristics at prolonged neuronal population activity. Following a series of single SC stimulations (1/7 s), neurons were activated by a 30-s, 10 Hz train (15 ml/min perfusion rate in **Figure 2**). The train stimulation-induced potent oxygen consumption by hippocampal cells (**Figure 2A**, blue) as indicated by a fast decrease in pO_2 by 120 Torr during first 10 s of stimulation (mean rate was 200 ± 40 Torr per 10 s, $n = 7$). LFPs in the train initially increased, presumably due to synaptic facilitation (Pitler and Landfield, 1987), but then declined strongly toward the end of train in parallel with a drop of oxygen level (by about 130 Torr). Interestingly, a slow recovery of LFPs started with a delay of about 30 s after the train and followed closely the pO_2 recovery (**Figure 2B**).

We examined the energy metabolism parameters and electrophysiological characteristics of neuronal population activity at the perfusion rate of 15 ml/min and following its reduction to 4 ml/min (**Figure 3**). Note that in this and other experiments, the presynaptic fiber volley component of LFPs did not change whatsoever, indicating that SC stimulation activated a constant number of nerve fibers throughout the experiment. At high perfusion rates, the stimulation train induced a strong oxygen consumption by hippocampal cells (**Figure 3A**, blue) and NAD(P)H autofluorescence revealed a biphasic transient characteristic for slices (Foster et al., 2006) with the pronounced dip (oxidation phase) and overshoot reflecting $NAD(P)^+$ reduction. Slowing down the rate of perfusion resulted in a considerable decrease of both oxygen consumption and NAD(P)H oxidation phase (**Figure 3A**, red). Meanwhile, the NAD(P)H overshoot did not change significantly suggesting that the overshoot may relate to some anaerobic (presumably glycolytic) part of the metabolic pathway (Kasischke et al., 2004). Modification of energy metabolism correlated with oxygen availability was also reflected in changes of neuronal electrical activity (**Figure 3B**). At lower rates of perfusion, LFPs were not only smaller throughout the train but revealed also different dynamics. This is shown in **Figure 3C**, depicting LFP integrals in

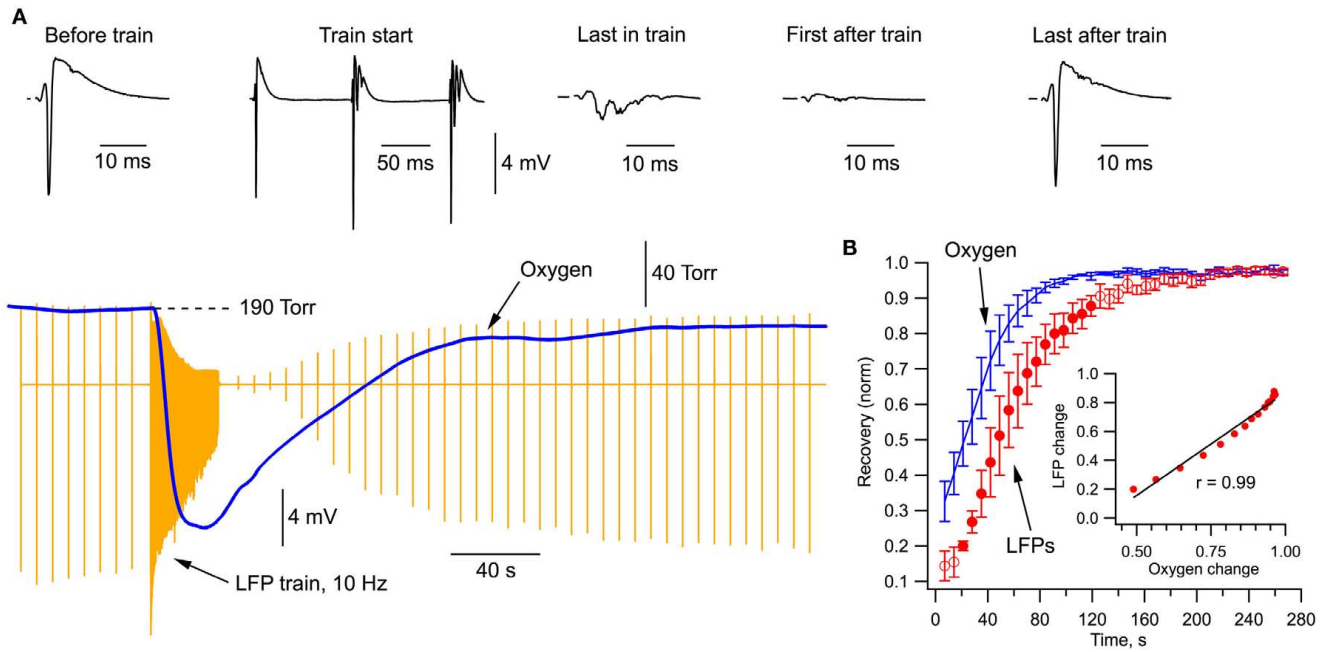

FIGURE 2 | Local field potentials and oxygen transient during stimulation protocol. (A) Simultaneous recordings of oxygen tension and LFPs (stimulation artifacts subtracted).**(B)** Time course of oxygen and LFP recovery (averaged from five experiments) after the end of stimulation train. Filled circles show the data range where LFP linearly correlates with pO_2 (see inset).

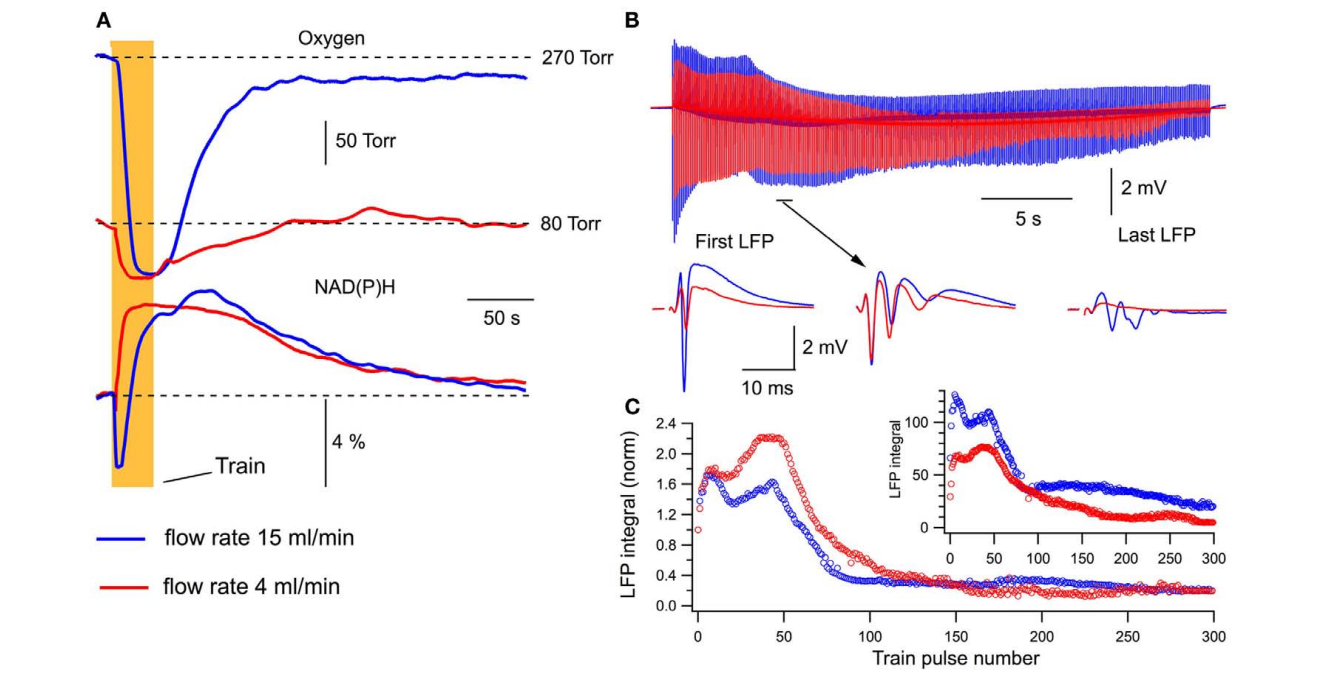

FIGURE 3 | Changes in oxygen transients, NAD(P)H signaling, and LFPs during train stimulation at different perfusion rates. (A) Oxygen transients and NAD(P)H autofluorescence recorded at different perfusion rates in the same slice. **(B)** LFPs during the stimulation train. **(C)** LFP integrals during the train stimulation calculated from original data (inset) and after normalization to the first response.

the train obtained from raw data (**Figure 3C** inset) and from data normalized to the first response. Distinctions in LFP dynamics during the train stimulation at different oxygen availability conditions indicate that modulation of energy metabolism induces

not only a "scaling" of synaptic response but also the qualitative changes in synaptic functioning. **Figure 4Aa** shows averaged normalized LFP synaptic components – fPSPs (see Materials and Methods) recorded at 15 and 4 ml/min solution flow rates in 15 slices. Note much stronger changes in synaptic responses at lower perfusion rates. **Figure 4Ab** shows a relative change of the first fPSPs in train: at 4 ml/min solution flow rate, the fPSP integral was $34 \pm 4\%$ of that at 15 ml/min ($p < 0.001$). **Figures 4B,C** show relative changes in the NAD(P)H profile and oxygen consumption at 15 and 4 ml/min superfusion: the NAD(P)H oxidation phase integral decreased by $88 \pm 4\%$ ($p < 0.001$) while the overshoot integral by $17 \pm 36\%$ (not significant, $p > 0.1$); the oxygen transient integral decreased by $67 \pm 6\%$ ($p < 0.001$) and the oxygen transient amplitude by $76 \pm 4\%$ ($p < 0.001$).

To rule out a possibility that the effect of solution flow rate on neuron electrical activity is induced by washing out of some substance(s) from slice tissue, we performed similar experiments ($n = 3$; not shown) at 15 ml/min superfusion with 95 and ~50% oxygenation of ACSF. In line with previously published results (Garcia et al., 2010), a partial oxygenation produced similar to a slow perfusion effects on LFPs.

Therefore, a solution flow rate too low to provide the adequate slice oxygenation disrupts neuronal energy metabolism and induces the qualitative changes in neuronal properties, which underlie the function of synaptic transmission and cellular excitability.

SPONTANEOUS SYNCHRONIZED NEURONAL ACTIVITY STRONGLY DEPENDS ON SLICE OXYGENATION

Since slice oxygenation causes a pronounced effect on synaptic function, this may be also reflected in synchronous neuronal network discharges. To explore this issue, we induced the interictal-like neuronal activity by 100 μM of 4-AP and measured both field potentials and pO_2 in slices superfused at different rates ($n = 5$). **Figure 5** demonstrates the original traces from such experiment. 4-AP applied at the solution flow rate of 15 ml/min evoked spontaneous discharges within a few minutes. Induced LFPs were also periodically recorded at different stages of experiment (**Figure 5**, top). After stabilization of synchronous activity, the solution flow rate was changed to 8 ml/min, inducing a significant reduction in both the oxygen level and frequency of interictal discharges. Following the reduction of solution flow rate down to 4 ml/min, pO_2 dropped further and the amplitude and frequency of discharges decreased as well. Returning superfusion to 15 ml/min recovered both pO_2 and synchronous network activity. Similar scenario was seen in five slices. Compared with 15 ml/min superfusion, the mean frequency of synchronous discharges decreased by $76 \pm 5\%$ at 4 ml/min ($p < 0.001$, $n = 5$). Therefore, insufficient

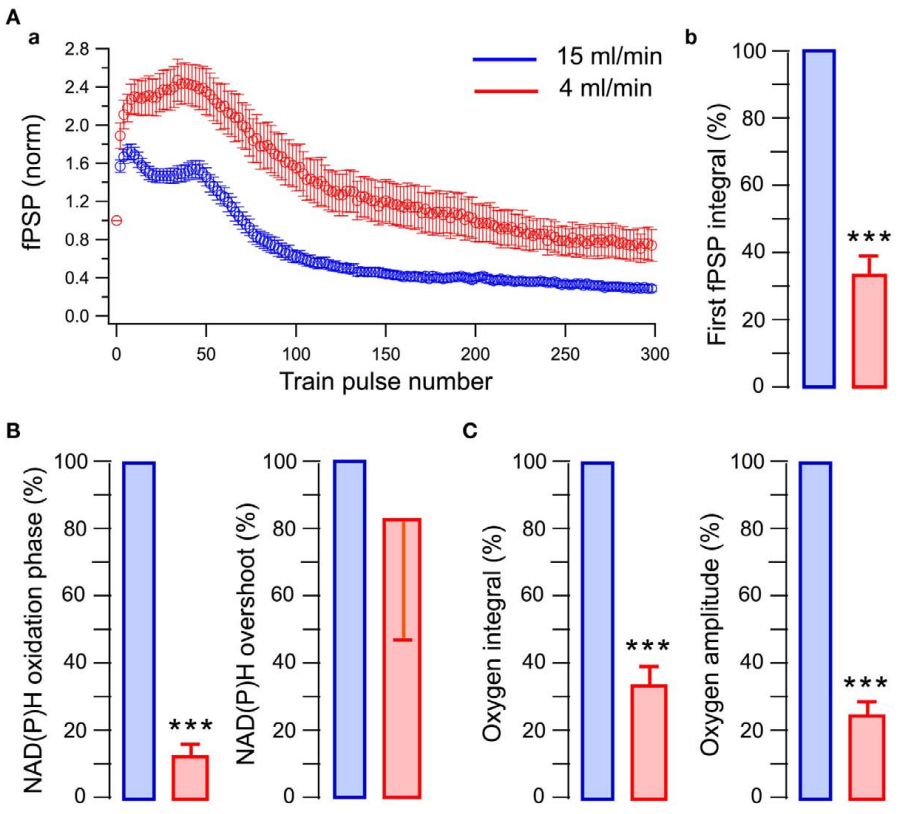

FIGURE 4 | Short-term synaptic plasticity and oxidative metabolism strongly depend on the rate of perfusion (oxygen supply). (A, a) Integrals of fPSPs induced by the train stimulation and normalized to the first response. Note much stronger relative changes in consequent fPSPs at smaller perfusion rate; **(b)** Integrals of the first fPSPs in the train. **(B)** NAD(P)H signaling parameters at different perfusion rates. **(C)** Oxygen transient parameters at different perfusion rates.

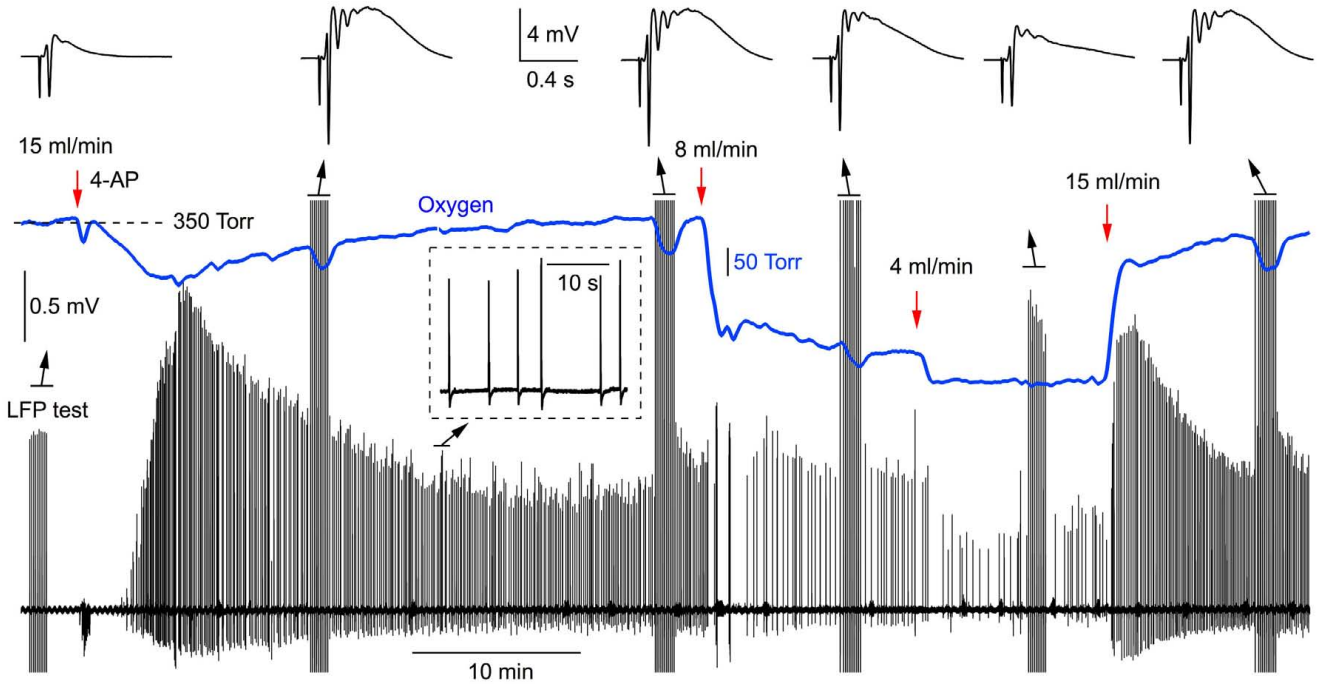

FIGURE 5 | Synchronous network activity induced by 4-AP strongly depends on the rate of perfusion (oxygen supply). Original simultaneous recordings of field potentials and oxygen tension during the 4-AP induced interictal-like network activity.

slice oxygenation strongly affects the ability of neuronal network for spontaneous synchronous activity induced by 4-AP.

OXIDATIVE METABOLISM AND SYNAPTIC FUNCTION ARE ENHANCED IN ACSF ENRICHED BY ENERGY SUBSTRATES

We have recently demonstrated in neonatal slices that supplementation of glucose in ACSF with oxidative energy substrates enhances both the oxidative metabolism and synaptic function (Ivanov et al., 2011). In the present study, we explored this issue using more mature brain slices. For this purpose, we utilized the energy substrate-enriched ACSF (eACSF; 5 mM glucose +5 mM pyruvate +4 mM DL-BHB). The composition of eACSF has been discussed elsewhere (Holmgren et al., 2010; Zilberter et al., 2010). Note that we did not attempt to reproduce the composition of extracellular brain fluid but rather attempted to provide sufficient oxidative energy substrates for neuronal energy demands.

Figure 6Aa shows that compared to standard ACSF conditions, oxygen consumption during train stimulation is increased in eACSF and this is accompanied by a considerable augmentation of the NAD(P)H oxidation phase as well as a decrease in NAD(P)H overshoot. The enhancement of oxidative metabolism is paralleled by a change in LFP dynamics throughout the train (**Figure 6Ab,c**). In six slices (**Figure 6B**), the first LFPs in the train did not differ significantly while subsequent LFPs were significantly larger in eACSF. Meanwhile, the oxygen consumption increased in eACSF by $18 \pm 3\%$ (**Figure 6C**; $p < 0.005$), NAD(P)H oxidation phase by $140 \pm 33\%$ (**Figure 6D**; $p < 0.001$) and NAD(P)H overshoot decreased by $60 \pm 7\%$ (**Figure 6D**; $p < 0.001$). Therefore, in eACSF, the aerobic energy metabolism is enhanced compared to standard ACSF.

If the last statement is correct eACSF should lose its efficacy at conditions of oxygen deficiency. In five experiments, we compared the effects of ACSF and eACSF at lower slice oxygenation using the 8-ml/min superfusion. In contrast to the results obtained at high perfusion rate (15 ml/min), LFPs did not differ significantly during the stimulation train (**Figure 7A**). In addition, transition to eACSF had no significant effect on the NAD(P)H oxidation phase (integral increased by $37 \pm 31\%$, $n = 5$, $p > 0.3$; not shown) indicating that supplemental substrates were not as efficient at lower perfusion rates when compared to their effect at 15 ml/min superfusion. This conclusion was further confirmed by comparison of NAD(P)H signals recorded in eACSF at 15 and 8 ml/min flow rates (**Figures 7B,C**). Lower perfusion rate (i.e., oxygenation) induced a substantial decrease in NAD(P)H oxidation phase integral (by $77 \pm 5\%$, $n = 5$; $p < 0.001$, **Figures 7B,C**) as well as an increase of overshoot (by $58 \pm 19\%$, $n = 5$; $p < 0.01$, **Figures 7B,C**). Importantly, these changes in the efficacy of aerobic metabolism occurred in the range of basal pO_2 (>150 Torr) considerably exceeding the physiological pO_2 levels *in vivo* (20–40 Torr; Erecinska and Silver, 2001; Masamoto et al., 2003, 2007; Takano et al., 2007), suggesting divergent oxygen requirements of neurons in slices.

LACTATE-BASED eACSF INDUCES SIMILAR TO PYRUVATE-BASED eACSF EFFECTS

Lactate has been suggested as a preferential fuel for cortical neurons during intense network activity (Wyss et al., 2011). We therefore examined the effects of a lactate-based

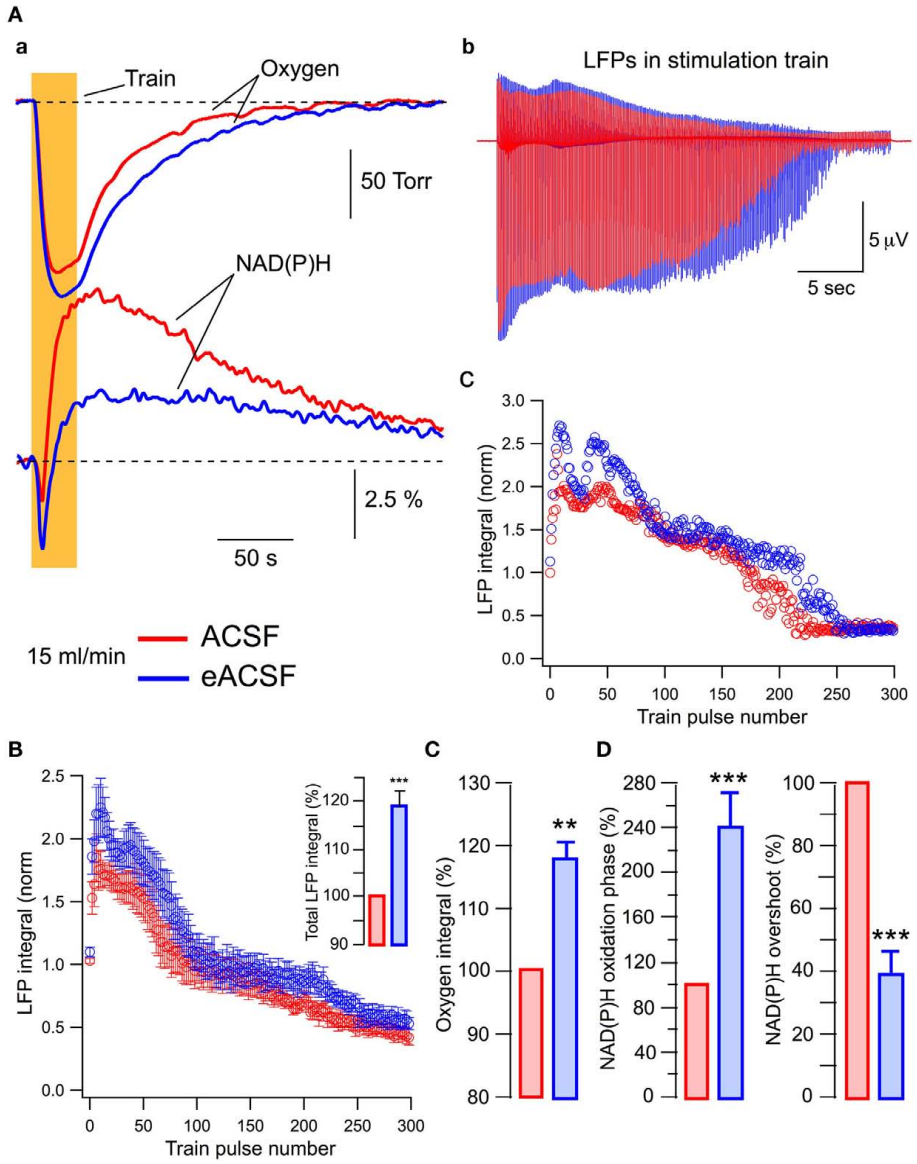

FIGURE 6 | At sufficient oxygen supply, energy substrates supplemented to glucose enhance both oxidative metabolism and synaptic function. In all experiments slices were superfused at 15 ml/min. **(A)** Original traces of **(a)** oxygen and NAD(P)H transients and **(b)** LFPs during the train (stimulation artifact subtracted) recorded in ACSF (red) and eACSF (blue). The normalized LFP integrals during the train are shown in **(c)**. **(B)** Statistical summary (six slices) of LFP integrals during the train. The inset shows total LFP integrals (summation of all LFP integrals in the train). **(C,D)** Show statistical summary of oxygen and NAD(P)H parameters.

eACSF (5 mM glucose +5 mM L-lactate +4 mM DL-BHB). Similar to the pyruvate-based eACSF, both aerobic metabolism and synaptic function were enhanced in the lactate-based eACSF compared to standard ACSF (**Figure 8**). In particular, the total LFP integral was by $27 \pm 7.5\%$ larger (**Figure 8A**; $n = 5$, $p < 0.005$). The oxygen consumption induced by stimulation train increased by $68 \pm 22\%$ (**Figure 8B**; $n = 4$, $p < 0.03$); the NAD(P)H oxidation phase increased by $143 \pm 12\%$ (**Figure 8C**; $n = 5$, $p < 0.001$) while the NAD(P)H overshoot decreased by $64 \pm 8\%$ (**Figure 8C**; $n = 5$, $p < 0.002$). Therefore, at sufficient oxygen supply, the supplementing glucose in ACSF with different combinations of energy substrates improves both oxidative metabolism and efficacy of synaptic function.

DISCUSSION

Our results demonstrate that synaptic efficacy, synaptic plasticity, and the neuronal network's potential for synchronized activity all strongly depend on oxidative energy metabolism. This conclusion is specifically important for the studies on brain slices where the oxygen delivery to neurons may be compromised by experimental conditions.

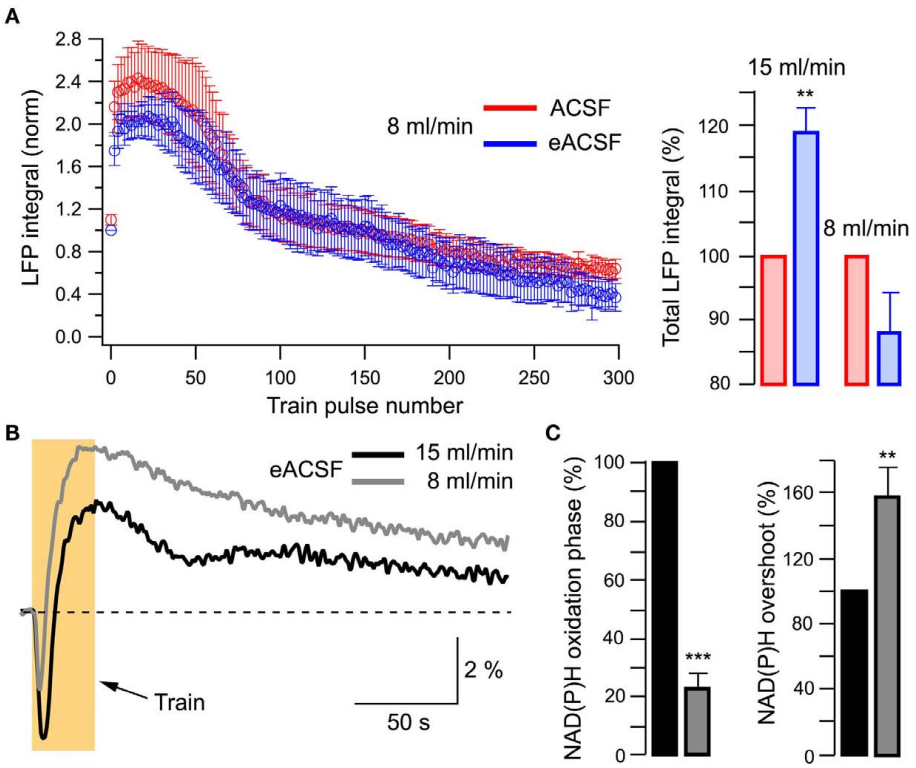

FIGURE 7 | Supplementary energy substrates are inefficient at a low perfusion rate (low oxygen supply). (A) Left: summary of LFPs recorded in ACSF and eACSF in five slices superfused at 8 ml/min. Right: comparison of total LFP integrals at 15 and 8 ml/min perfusion rate. **(B)** Example of original traces of NAD(P)H signaling recorded in eACSF at different perfusion rates. **(C)** Summary of changes in NAD(P)H signaling recorded in eACSF at different perfusion rates.

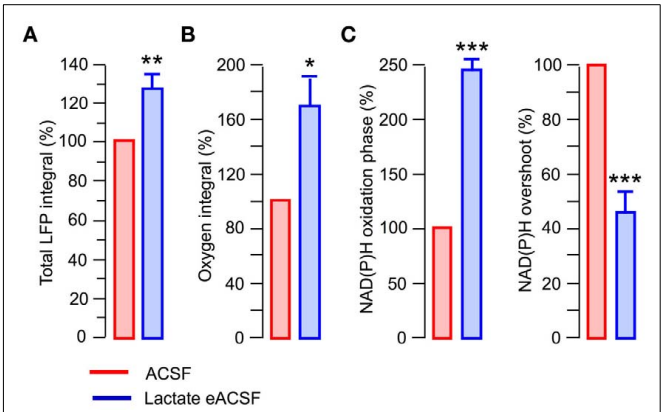

FIGURE 8 | At sufficient oxygen supply, lactate-based eACSF causes similar effects as pyruvate-based eACSF. In all experiments slices were superfused at 15 ml/min. **(A)** Total LFP integrals in the stimulation train (five slices). **(B,C)** Oxygen and NAD(P)H signaling parameters.

OXYGEN DELIVERY TO NEURONS IN SLICES AFFECTS BOTH SYNAPTIC EFFICACY AND SYNAPTIC PLASTICITY

Hippocampal LFPs revealed a strong dependence on oxygen distribution in a slice. Similar observations on P27–P40 rats (Garcia et al., 2010) and on neonatal (P4–P7) mice (Ivanov et al., 2011) have been reported previously although the underlying mechanism of synaptic function reliance on oxygen is unclear. Severe decrease in synaptic transmission was observed during slice exposure to a complete hypoxia (Pena and Ramirez, 2005) and in such cases a decline in cellular ATP level was suggested as one reason for the failure of synaptic function (Kass and Lipton, 1982; Lipton and Whittingham, 1982). It was also demonstrated that hypoxia had a direct influence on the vesicular release mechanisms (Fleidervish et al., 2001). Indeed, multiple studies of glutamatergic transmitter release from nerve terminals demonstrated prominent dependence of the release machinery on energy metabolism (Erecinska et al., 1996; Nicholls, 2003). Therefore, insufficient oxygen availability leads to the lowered oxidative metabolism and as the result may inhibit glutamate release from the pyramidal cell terminals. Interestingly, synaptic plasticity (see **Figure 4Aa**) is more striking at smaller perfusion rates (lower slice oxygenation). One possible reason for this may be an enhanced accumulation of Ca^{2+} in the nerve terminals due to its insufficient ATP-dependent extrusion between pulses. The mechanism of this phenomenon, however, requires further clarification.

SYNCHRONIZED SPONTANEOUS NETWORK ACTIVITY DEPENDS ON OXYGEN DELIVERY

Deficiency in oxidative metabolism results not only in downregulation of synaptic function but also strongly affects the ability

of neuronal network for synchronous discharges. Recently, Hajos et al. (2009) reported that both spontaneously occurring sharp wave–ripple oscillations and cholinergically induced fast oscillations in submerged hippocampal slices could be observed only at the solution flow rates providing sufficient slice oxygenation (about 6 ml/min in their custom dual-sided perfusion chamber). Strong dependence of cholinergically induced gamma oscillations on oxygen pressure was also demonstrated on the organotypic hippocampal slice cultures (Huchzermeyer et al., 2008). The importance of appropriate slice oxygenation for the approximation of physiological-like network properties was discussed recently by Hajos and Mody (2009). In our experiments (see **Figure 4**), both the amplitude and frequency of 4-AP induced spontaneous discharges decreased sharply with the drop in slice oxygenation (switch of perfusion from 15 to 4 ml/min). Therefore, these results suggest that the inadequate oxidative metabolism, e.g., due to insufficient slice oxygenation, considerably modifies network properties required for the synchronous neuronal activity, either intrinsic or induced.

NEURONAL ACTIVITY VS. OXYGEN PRESSURE *IN VIVO* AND IN SLICES

Since mitochondrial oxidative phosphorylation is coupled to oxygen reduction and is responsible for most of the cellular oxygen consumption, the rate of respiration is a measure of the rate of ATP synthesis. In brain, the respiratory rate may be controlled within a wide dynamic range and in the normal steady-state of cellular metabolism it provides ATP at precisely the rate needed to cover cell energy demands (Wilson et al., 1979; Erecinska and Silver, 2001). The ambient oxygen concentration in rat hippocampus *in vivo* is about 20–30 Torr (Erecinska and Silver, 2001; Kasischke et al., 2011). Therefore, although a relatively low oxygen environment is natural for a significant fraction of cortical neurons (Gjedde, 2002; Ndubuizu and Lamanna, 2007), this environment is still capable of efficiently supporting normal cortical function.

The obvious question therefore is how to reconcile the *in vivo* observations with the apparent much stronger oxygen dependence of neuronal activity in slices. Indeed, strong changes in LFP values occurred in slices in the range of oxygen tensions where the lower level exceeded the normal oxygen levels *in vivo* (Garcia et al., 2010; Ivanov et al., 2011). Garcia et al. (2010) observed that a single stimulation-evoked population response nearly disappeared after a switch of solution oxygenation from 0.95 ATA O_2 to 0.60 ATA O_2, although the minimal oxygen pressure in a slice core was about 100 Torr. Hyperoxic conditions were required to obtain physiological-like spontaneous gamma oscillations in acute slices (Fisahn et al., 1998; Hajos et al., 2009; Kann et al., 2011). Huchzermeyer et al. (2008) noted that gamma oscillations in cultured (organotypic) hippocampal slices strongly decreased at 20% O_2 in perfusate (compared to 95%) despite the fact that the baseline pO_2 was about 50 Torr in a slice core, decreasing during oscillations to about 20 Torr and still being in the range of interstitial pO_2 values in air-respiring rodents (Erecinska and Silver, 2001; Takano et al., 2007).

On the other hand, when oxygen tension *in vivo* is comparable to those required for neuronal function in slices, oxygen is obviously toxic. For instance, O_2 toxicity occurred in awake rats breathing oxygen at >4.0 ATA O_2 (>400 Torr in the brain; Demchenko et al., 2005), manifesting in tonic clonic seizures (Simon and Torbati, 1982). However, seizures were not observed in hippocampal slices exposed to similar (>4 ATA) pO_2 levels (Garcia et al., 2010). Contrary to LFPs recorded in slices (Garcia et al., 2010), cortical LFPs induced by somatosensory stimulation in anesthetized rats were similar at 1 (about 40 Torr pO_2), 3, or 4 ATA (>400 Torr pO_2) of breathing oxygen (Lindauer et al., 2010b), indicating much lower oxygen dependence of neuronal activity *in vivo*.

In agreement with previous reports, our results demonstrate that LFPs induced by periodic single stimulations significantly decreased with the reduction of pO_2 to values higher than the upper level of physiological range (see **Figure 1**). Spontaneous synchronous network activity revealed a pronounced sensitivity to oxygen above the physiological range (**Figure 5**).

Our data also indicate an uncoupling between oxygen pressure measured in slice tissue and neuronal energy metabolism (see also Turner et al., 2007). At oxygen tensions that might be considered as "hyperoxic," the prolonged synaptic stimulation-induced NAD(P)H signal showed dynamics abnormal for the *in vivo* observations (Rosenthal and Jobsis, 1971; Lothman et al., 1975; Lamanna et al., 1984; Mayevsky and Chance, 2007), namely the large overshoot and small oxidative phase (see **Figure 3**). Interestingly, at such oxygenation levels, supplementation of glucose with other oxidative energy substrates (pyruvate, lactate, and BHB) increased the NAD(P)H oxidation phase substantially. However, the effect of these substrates practically disappeared at lower oxygenation levels (see **Figures 6** and **7**), indicating that despite the pO_2 being above the physiological range, the oxygen supply was insufficient for oxidative phosphorylation. Therefore there exists an apparent discrepancy in the definition of "normoxic" tissue oxygen pressure between the *in vivo* and slice conditions.

One possible reason for such a discrepancy may be compromised metabolism in brain slices, presumably as a consequence of traumatic cutting procedure (Rolleston and Newsholme, 1967; Benjamin and Verjee, 1980; Whittingham et al., 1984; Zur Nedden et al., 2011). This results in a substantial decrease of high energy phosphates, in particular, about 50% lower than *in vivo* concentrations of ATP and PCr (Whittingham et al., 1984) or 40–60% smaller the total adenine nucleotide pool (Whittingham et al., 1984; Zur Nedden et al., 2011). It was also reported that the rate of glycolysis in brain slices (Rolleston and Newsholme, 1967; Benjamin and Verjee, 1980) is 50% or less of that *in vivo*.

In addition, the dynamics of pO_2 variability during neuronal activity differs radically between the intact brain and slices. *In vivo*, changes in neuronal activity are tightly coupled to changes in regional metabolism, local cerebral blood flow, and oxygenation (Raichle and Mintun, 2006; Masamoto et al., 2008; Lindauer et al., 2010b; Vazquez et al., 2010) although the factors regulating changes in cerebral blood flow during physiological activation remain the subject of debate (Raichle and Mintun, 2006; Verweij et al., 2007; Lindauer et al., 2010a,b). As the result, after the onset of neuronal activity, the tissue pO_2 can exceed the required level by 1.5–2 times (Erecinska and Silver, 2001;

Masamoto et al., 2003, 2007). Note also that the distance from any neuron to the nearest blood vessel providing oxygen supply does not exceed 25 μm (Erecinska and Silver, 2001; Masamoto et al., 2004; Abbott et al., 2010). However, even at such a favorable for the oxygen delivery situation, the oxygen distribution in cortical tissue is not homogenous and local regions of a minor hypoxia can exist (Kasischke et al., 2011). In slices, oxygen is delivered to neurons by diffusion from the superfusing solution. Compared to the rate of oxygen consumption by neurons, the rate of oxygen diffusion in slice tissue is very slow. Indeed, analysis of our data showed that at the beginning of train stimulation, pO_2 declines with a mean rate of about 20 Torr/s (see pO_2 transients in **Figures 2A**, **3A**, and **6A**). This value is likely underestimated because the response time of oxygen probe could be as long as 3 s. After the train, pO_2 recovers up to the initial level for longer than 100 s. The highest rate of recovery is about 4 Torr/s that is five times slower than O_2 consumption at the beginning of stimulation episode. Therefore, during neuronal activity, the oxygen consumption in vicinity of neurons is not followed by the oxygen recovery. Although during neuronal activity the oxygen electrode in slice tissue registers a relatively high integral oxygen pressure, the real oxygen levels in neuronal microenvironment may be extremely inhomogeneous (see also Turner et al., 2007; Huchzermeyer et al., 2008). Definitely, this issue requires further investigation. It is evident, however, that there is a substantial discrepancy between functional effects of similar oxygen levels in the brain and slices. This suggests that analyzing the link between neuronal functions and pO_2 in slices (e.g., "normoxic" or "hyperoxic"), the direct reference to pO_2 *in vivo* may be inadequate.

One very attractive, although yet speculative, explanation of the extremely high demands of slice neuronal activity for oxygen is associated with the mitochondrial anion-carrier proteins that are located on the inner mitochondrial membrane and are called uncoupling proteins (UCPs; Mattson and Liu, 2003; Andrews et al., 2005). UCPs provide a path for protons to return to the matrix without passing through ATP-synthase and therefore the energy derived from oxidation of substrates does not result in the production of ATP but is instead released as heat. UCPs can be activated by free radicals and free fatty acids. UCPs have been identified and shown to be highly expressed in the CNS including cortex and hippocampus (Andrews et al., 2005). Interestingly, strong activation of UCPs has been documented during acute brain trauma and stroke/ischemia (Sullivan et al., 2004; Kim-Han and Dugan, 2005). From these facts, it is plausible to suggest that the acute preparation of brain slices may lead to the activation of UCPs in neurons. This would result in "shunting" of mitochondrial oxidative phosphorylation and a subsequent strong increase in the amount of oxygen required for the production of necessary amount of ATP. In such a case, the dependence of neuronal activity in slices on oxygen tension would be shifted toward higher pO_2 values.

GLUCOSE DOES NOT FULLY COVER ENERGY DEMANDS DURING NEURONAL ACTIVITY

The use of high concentration (10 mM or above) of glucose as the sole energy substrate in ACSF does not seem to be adequate when mimicking *in vivo* extracellular neuronal environment (Barros et al., 2007; Hajos and Mody, 2009; Zilberter et al., 2010). For instance, it is firmly established that the glucose concentration in cortical ECF is about 1–2 mM and is comparable and even lower (during intense neuronal activity) to the concentration of lactate. A number of recent studies (Castro et al., 2009; Pellerin, 2010), including those *in vivo* (Suzuki et al., 2011; Wyss et al., 2011), provide evidence that lactate is a key energy substrate for neuronal aerobic metabolism. In the active brain, the energy substrate pool in neuronal vicinity is the result of complex blood vessel–astrocyte–neuron interaction (Abbott et al., 2010; Pellerin, 2010). Therefore, *a priori* suggestion that glucose alone is able to cover fully energy requirements during neuron activation in slices seems to be unsubstantiated. The importance of modifying the ACSF composition to better approximate physiological conditions has been highlighted in recent reviews (Hajos and Mody, 2009; Zilberter et al., 2010).

Our results demonstrate that oxidative metabolism and synaptic function are indeed both enhanced in the energy substrate-enriched solution (eACSF). At high perfusion rates, both versions of eACSF (pyruvate or lactate-based) significantly increased the oxygen consumption, NAD(P)H oxidation phase, and efficacy of synaptic transmission during prolonged stimulation (**Figures 6** and **8**). Glucose substitution also induced a decrease in NAD(P)H overshoot. It is possible that the oxidation phase of NAD(P)H enhanced in eACSF partially masks the actual reduction time course. Clarification of the origin of NAD(P)H overshoot requires further studies. We have previously observed similar effects of energy substrates on neonatal slices (Ivanov et al., 2011). Therefore, in slices as well as *in vivo*, the ability of glucose to maintain energy metabolism is limited and neuronal energy supply should be supported by other oxidative substrates.

CONCLUSION

Our results confirm that in acute brain slices, the basic neuronal parameters underlying excitability strongly depend on oxidative energy metabolism. We show that the state of energy metabolism is highly sensitive to the availability of oxygen in slice tissue. The pathway for ATP synthesis is apparently compromised in brain slices and therefore the reliance of neuronal activity on oxygen tension is clearly shifted toward considerably larger pO_2 values. In addition, during neuronal activity, glucose alone may not be able to fully cover the neuronal energy demands and therefore adequate support of oxidative metabolism by other energy substrates complementary to glucose is required. Given the fact that in a number of electrophysiological studies neither the oxygen tension in a slice nor the energy substrate composition in ACSF have been controlled, our results call for the careful reconsideration of experimental approaches to neuronal activity studies *in vitro*.

ACKNOWLEDGMENTS

We thank Dr. T. Zilberter for the valuable discussion and help in the preparation of manuscript. This study was supported by the European Union Seventh Framework "MEMOLOAD" grant (HEALTH-F2-2007-201159; Yuri Zilberter) and French National Research Agency "METANEX" grant (ANR-2010-BLAN-1443-01; Anton Ivanov and Yuri Zilberter).

REFERENCES

Abbott, N. J., Patabendige, A. A., Dolman, D. E., Yusof, S. R., and Begley, D. J. (2010). Structure and function of the blood-brain barrier. *Neurobiol. Dis.* 37, 13–25.

Andrews, Z. B., Diano, S., and Horvath, T. L. (2005). Mitochondrial uncoupling proteins in the CNS: in support of function and survival. *Nat. Rev. Neurosci.* 6, 829–840.

Barros, L. F., Bittner, C. X., Loaiza, A., and Porras, O. H. (2007). A quantitative overview of glucose dynamics in the gliovascular unit. *Glia* 55, 1222–1237.

Benjamin, A. M., and Verjee, Z. H. (1980). Control of aerobic glycolysis in the brain in vitro. *Neurochem. Res.* 5, 921–934.

Bolanos, J. P., Almeida, A., and Moncada, S. (2010). Glycolysis: a bioenergetic or a survival pathway? *Trends Biochem. Sci.* 35, 145–149.

Castro, M. A., Beltran, F. A., Brauchi, S., and Concha, I. I. (2009). A metabolic switch in brain: glucose and lactate metabolism modulation by ascorbic acid. *J. Neurochem.* 110, 423–440.

Coelho, J. E., De Mendonca, A., and Ribeiro, J. A. (2000). Presynaptic inhibitory receptors mediate the depression of synaptic transmission upon hypoxia in rat hippocampal slices. *Brain Res.* 869, 158–165.

Demchenko, I. T., Luchakov, Y. I., Moskvin, A. N., Gutsaeva, D. R., Allen, B. W., Thalmann, E. D., and Piantadosi, C. A. (2005). Cerebral blood flow and brain oxygenation in rats breathing oxygen under pressure. *J. Cereb. Blood Flow Metab.* 25, 1288–1300.

Erecinska, M., Nelson, D., and Silver, I. A. (1996). Metabolic and energetic properties of isolated nerve ending particles (synaptosomes). *Biochim. Biophys. Acta* 1277, 13–34.

Erecinska, M., and Silver, I. A. (2001). Tissue oxygen tension and brain sensitivity to hypoxia. *Respir. Physiol.* 128, 263–276.

Feig, S., and Lipton, P. (1990). N-methyl-D-aspartate receptor activation and Ca2+ account for poor pyramidal cell structure in hippocampal slices. *J. Neurochem.* 55, 473–483.

Fisahn, A., Pike, F. G., Buhl, E. H., and Paulsen, O. (1998). Cholinergic induction of network oscillations at 40 Hz in the hippocampus in vitro. *Nature* 394, 186–189.

Fleidervish, I. A., Gebhardt, C., Astman, N., Gutnick, M. J., and Heinemann, U. (2001). Enhanced spontaneous transmitter release is the earliest consequence of neocortical hypoxia that can explain the disruption of normal circuit function. *J. Neurosci.* 21, 4600–4608.

Foster, K. A., Beaver, C. J., and Turner, D. A. (2005). Interaction between tissue oxygen tension and NADH imaging during synaptic stimulation and hypoxia in rat hippocampal slices. *Neuroscience* 132, 645–657.

Foster, K. A., Galeffi, F., Gerich, F. J., Turner, D. A., and Muller, M. (2006). Optical and pharmacological tools to investigate the role of mitochondria during oxidative stress and neurodegeneration. *Prog. Neurobiol.* 79, 136–171.

Frenguelli, B. G., Llaudet, E., and Dale, N. (2003). High-resolution real-time recording with microelectrode biosensors reveals novel aspects of adenosine release during hypoxia in rat hippocampal slices. *J. Neurochem.* 86, 1506–1515.

Garcia, A. J. III, Putnam, R. W., and Dean, J. B. (2010). Hyperbaric hyperoxia and normobaric reoxygenation increase excitability and activate oxygen-induced potentiation in CA1 hippocampal neurons. *J. Appl. Physiol.* 109, 804–819.

Gjedde, A. (2002). Cerebral blood flow change in arterial hypoxemia is consistent with negligible oxygen tension in brain mitochondria. *Neuroimage* 17, 1876–1881.

Hajos, N., Ellender, T. J., Zemankovics, R., Mann, E. O., Exley, R., Cragg, S. J., Freund, T. F., and Paulsen, O. (2009). Maintaining network activity in submerged hippocampal slices: importance of oxygen supply. *Eur. J. Neurosci.* 29, 319–327.

Hajos, N., and Mody, I. (2009). Establishing a physiological environment for visualized in vitro brain slice recordings by increasing oxygen supply and modifying aCSF content. *J. Neurosci. Methods* 183, 107–113.

Holmgren, C. D., Mukhtarov, M., Malkov, A. E., Popova, I. Y., Bregestovski, P., and Zilberter, Y. (2010). Energy substrate availability as a determinant of neuronal resting potential, GABA signaling and spontaneous network activity in the neonatal cortex in vitro. *J. Neurochem.* 112, 900–912.

Huchzermeyer, C., Albus, K., Gabriel, H. J., Otahal, J., Taubenberger, N., Heinemann, U., Kovacs, R., and Kann, O. (2008). Gamma oscillations and spontaneous network activity in the hippocampus are highly sensitive to decreases in pO2 and concomitant changes in mitochondrial redox state. *J. Neurosci.* 28, 1153–1162.

Ivanov, A., Mukhtarov, M., Bregestovski, P., and Zilberter, Y. (2011). Lactate effectively covers energy demands during neuronal network activity in neonatal hippocampal slices. *Front. Neuroenergetics* 3:2. doi:10.3389/fnene.2011.00002

Kann, O., Huchzermeyer, C., Kovacs, R., Wirtz, S., and Schuelke, M. (2011). Gamma oscillations in the hippocampus require high complex I gene expression and strong functional performance of mitochondria. *Brain* 134, 345–358.

Kasischke, K. A., Lambert, E. M., Panepento, B., Sun, A., Gelbard, H. A., Burgess, R. W., Foster, T. H., and Nedergaard, M. (2011). Two-photon NADH imaging exposes boundaries of oxygen diffusion in cortical vascular supply regions. *J. Cereb. Blood Flow Metab.* 31, 68–81.

Kasischke, K. A., Vishwasrao, H. D., Fisher, P. J., Zipfel, W. R., and Webb, W. W. (2004). Neural activity triggers neuronal oxidative metabolism followed by astrocytic glycolysis. *Science* 305, 99–103.

Kass, I. S., and Lipton, P. (1982). Mechanisms involved in irreversible anoxic damage to the in vitro rat hippocampal slice. *J. Physiol. (Lond.)* 332, 459–472.

Kim-Han, J. S., and Dugan, L. L. (2005). Mitochondrial uncoupling proteins in the central nervous system. *Antioxid. Redox Signal.* 7, 1173–1181.

Klaidman, L. K., Leung, A. C., and Adams, J. D. Jr. (1995). High-performance liquid chromatography analysis of oxidized and reduced pyridine dinucleotides in specific brain regions. *Anal. Biochem.* 228, 312–317.

Lamanna, J. C., Light, A. I., Peretsman, S. J., and Rosenthal, M. (1984). Oxygen insufficiency during hypoxic hypoxia in rat brain cortex. *Brain Res.* 293, 313–318.

Lindauer, U., Dirnagl, U., Fuchtemeier, M., Bottiger, C., Offenhauser, N., Leithner, C., and Royl, G. (2010a). Pathophysiological interference with neurovascular coupling – when imaging based on hemoglobin might go blind. *Front. Neuroenergetics* 2:25. doi:10.3389/fnene.2010.00025

Lindauer, U., Leithner, C., Kaasch, H., Rohrer, B., Foddis, M., Fuchtemeier, M., Offenhauser, N., Steinbrink, J., Royl, G., Kohl-Bareis, M., and Dirnagl, U. (2010b). Neurovascular coupling in rat brain operates independent of hemoglobin deoxygenation. *J. Cereb. Blood Flow Metab.* 30, 757–768.

Lipton, P., and Whittingham, T. S. (1982). Reduced ATP concentration as a basis for synaptic transmission failure during hypoxia in the in vitro guinea-pig hippocampus. *J. Physiol. (Lond.)* 325, 51–65.

Lothman, E., Lamanna, J., Cordingley, G., Rosenthal, M., and Somjen, G. (1975). Responses of electrical potential, potassium levels, and oxidative metabolic activity of the cerebral neocortex of cats. *Brain Res.* 88, 15–36.

Masamoto, K., Kershaw, J., Ureshi, M., Takizawa, N., Kobayashi, H., Tanishita, K., and Kanno, I. (2007). Apparent diffusion time of oxygen from blood to tissue in rat cerebral cortex: implication for tissue oxygen dynamics during brain functions. *J. Appl. Physiol.* 103, 1352–1358.

Masamoto, K., Kurachi, T., Takizawa, N., Kobayashi, H., and Tanishita, K. (2004). Successive depth variations in microvascular distribution of rat somatosensory cortex. *Brain Res.* 995, 66–75.

Masamoto, K., Omura, T., Takizawa, N., Kobayashi, H., Katura, T., Maki, A., Kawaguchi, H., and Tanishita, K. (2003). Biphasic changes in tissue partial pressure of oxygen closely related to localized neural activity in guinea pig auditory cortex. *J. Cereb. Blood Flow Metab.* 23, 1075–1084.

Masamoto, K., Vazquez, A., Wang, P., and Kim, S. G. (2008). Trial-by-trial relationship between neural activity, oxygen consumption, and blood flow responses. *Neuroimage* 40, 442–450.

Mattson, M. P., and Liu, D. (2003). Mitochondrial potassium channels and uncoupling proteins in synaptic plasticity and neuronal cell death. *Biochem. Biophys. Res. Commun.* 304, 539–549.

Mayevsky, A., and Chance, B. (2007). Oxidation-reduction states of NADH in vivo: from animals to clinical use. *Mitochondrion* 7, 330–339.

Ndubuizu, O., and Lamanna, J. C. (2007). Brain tissue oxygen concentration measurements. *Antioxid. Redox Signal.* 9, 1207–1219.

Nicholls, D. G. (2003). Bioenergetics and transmitter release in the isolated nerve terminal. *Neurochem. Res.* 28, 1433–1441.

Pellerin, L. (2010). Food for thought: the importance of glucose and other energy substrates for sustaining

brain function under varying levels of activity. *Diabetes Metab.* 36(Suppl. 3), S59–S63.

Pena, F., and Ramirez, J. M. (2005). Hypoxia-induced changes in neuronal network properties. *Mol. Neurobiol.* 32, 251–283.

Pitler, T. A., and Landfield, P. W. (1987). Postsynaptic membrane shifts during frequency potentiation of the hippocampal EPSP. *J. Neurophysiol.* 58, 866–882.

Raichle, M. E., and Mintun, M. A. (2006). Brain work and brain imaging. *Annu. Rev. Neurosci.* 29, 449–476.

Rolleston, F. S., and Newsholme, E. A. (1967). Control of glycolysis in cerebral cortex slices. *Biochem. J.* 104, 524–533.

Rosenthal, M., and Jobsis, F. F. (1971). Intracellular redox changes in functioning cerebral cortex. II. Effects of direct cortical stimulation. *J. Neurophysiol.* 34, 750–762.

Schurr, A., and Payne, R. S. (2007). Lactate, not pyruvate, is neuronal aerobic glycolysis end product: an in vitro electrophysiological study. *Neuroscience* 147, 613–619.

Shuttleworth, C. W. (2010). Use of NAD(P)H and flavoprotein autofluorescence transients to probe neuron and astrocyte responses to synaptic activation. *Neurochem. Int.* 56, 379–386.

Simon, A. J., and Torbati, D. (1982). Effects of hyperbaric oxygen on heart, brain, and lung functions in rat. *Undersea Biomed. Res.* 9, 263–275.

Sullivan, P. G., Springer, J. E., Hall, E. D., and Scheff, S. W. (2004). Mitochondrial uncoupling as a therapeutic target following neuronal injury. *J. Bioenerg. Biomembr.* 36, 353–356.

Suzuki, A., Stern, S. A., Bozdagi, O., Huntley, G. W., Walker, R. H., Magistretti, P. J., and Alberini, C. M. (2011). Astrocyte-neuron lactate transport is required for long-term memory formation. *Cell* 144, 810–823.

Takano, T., Tian, G. F., Peng, W., Lou, N., Lovatt, D., Hansen, A. J., Kasischke, K. A., and Nedergaard, M. (2007). Cortical spreading depression causes and coincides with tissue hypoxia. *Nat. Neurosci.* 10, 754–762.

Tsai, Y. C., Chou, Y. C., Wu, A. B., Hu, C. M., Chen, C. Y., Chen, F. A., and Lee, J. A. (2006). Stereoselective effects of 3-hydroxybutyrate on glucose utilization of rat cardiomyocytes. *Life Sci.* 78, 1385–1391.

Turner, D. A., and Adamson, D. C. (2011). Neuronal-astrocyte metabolic interactions: understanding the transition into abnormal astrocytoma metabolism. *J. Neuropathol. Exp. Neurol.* 70, 167–176.

Turner, D. A., Foster, K. A., Galeffi, F., and Somjen, G. G. (2007). Differences in O2 availability resolve the apparent discrepancies in metabolic intrinsic optical signals in vivo and in vitro. *Trends Neurosci.* 30, 390–398.

Vazquez, A. L., Masamoto, K., Fukuda, M., and Kim, S. G. (2010). Cerebral oxygen delivery and consumption during evoked neural activity. *Front. Neuroenergetics* 2:11. doi:10.3389/fnene.2010.00011

Verweij, B. H., Amelink, G. J., and Muizelaar, J. P. (2007). Current concepts of cerebral oxygen transport and energy metabolism after severe traumatic brain injury. *Prog. Brain Res.* 161, 111–124.

Whittingham, T. S., Lust, W. D., Christakis, D. A., and Passonneau, J. V. (1984). Metabolic stability of hippocampal slice preparations during prolonged incubation. *J. Neurochem.* 43, 689–696.

Wilson, D. F., Erecinska, M., Drown, C., and Silver, I. A. (1979). The oxygen dependence of cellular energy metabolism. *Arch. Biochem. Biophys.* 195, 485–493.

Wyss, M. T., Jolivet, R., Buck, A., Magistretti, P. J., and Weber, B. (2011). In vivo evidence for lactate as a neuronal energy source. *J. Neurosci.* 31, 7477–7485.

Yamamoto, C., and Kurokawa, M. (1970). Synaptic potentials recorded in brain slices and their modification by changes in the level of tissue ATP. *Exp. Brain Res.* 10, 159–170.

Zhao, Y. T., Tekkok, S., and Krnjevic, K. (1997). 2-deoxy-D-glucose-induced changes in membrane potential, input resistance, and excitatory postsynaptic potentials of CA1 hippocampal neurons. *Can. J. Physiol. Pharmacol.* 75, 368–374.

Zilberter, Y., Zilberter, T., and Bregestovski, P. (2010). Neuronal activity in vitro and the in vivo reality: the role of energy homeostasis. *Trends Pharmacol. Sci.* 31, 394–401.

Zur Nedden, S., Hawley, S., Pentland, N., Hardie, D. G., Doney, A. S., and Frenguelli, B. G. (2011). Intracellular ATP influences synaptic plasticity in area CA1 of rat hippocampus via metabolism to adenosine and activity-dependent activation of adenosine A1 receptors. *J. Neurosci.* 31, 6221–6234.

Conflict of Interest Statement: The authors declare that the research was conducted in the absence of any commercial or financial relationships that could be construed as a potential conflict of interest.

Received: 21 September 2011; accepted: 10 December 2011; published online: 29 December 2011.

Citation: Ivanov A and Zilberter Y (2011) Critical state of energy metabolism in brain slices: the principal role of oxygen delivery and energy substrates in shaping neuronal activity. Front. Neuroenerg. ***3****:9. doi: 10.3389/fnene.2011.00009*

frontiers in
PHARMACOLOGY

MINI REVIEW ARTICLE
published: 10 January 2012
doi: 10.3389/fphar.2011.00090

The energy demand of fast neuronal network oscillations: insights from brain slice preparations

Oliver Kann*

Institute of Physiology and Pathophysiology, University of Heidelberg, Heidelberg, Germany

Edited by:
Yuri Zilberter, Faculté de Médecine Timone, France

Reviewed by:
Andre Fisahn, Karolinska Institutet, Sweden
Norbert Hajos, Hungarian Academy of Sciences, Hungary

****Correspondence:***
Oliver Kann, Institute of Physiology and Pathophysiology, University of Heidelberg, Im Neuenheimer Feld 326, D-69120 Heidelberg, Germany. e-mail: oliver.kann@physiologie.uni-heidelberg.de

Fast neuronal network oscillations in the gamma range (30–100 Hz) in the cerebral cortex have been implicated in higher cognitive functions such as sensual perception, working memory, and, perhaps, consciousness. However, little is known about the energy demand of gamma oscillations. This is mainly caused by technical limitations that are associated with simultaneous recordings of neuronal activity and energy metabolism in small neuronal networks and at the level of mitochondria *in vivo*. Thus recent studies have focused on brain slice preparations to address the energy demand of gamma oscillations *in vitro*. Here, reports will be summarized and discussed that combined electrophysiological recordings, oxygen sensor microelectrodes, and live-cell fluorescence imaging in acutely prepared slices and organotypic slice cultures of the hippocampus from both, mouse and rat. These reports consistently show that gamma oscillations can be reliably induced in hippocampal slice preparations by different pharmacological tools. They suggest that gamma oscillations are associated with high energy demand, requiring both rapid adaptation of oxidative energy metabolism and sufficient supply with oxygen and nutrients. These findings might help to explain the exceptional vulnerability of higher cognitive functions during pathological processes of the brain, such as circulatory disturbances, genetic mitochondrial diseases, and neurodegeneration.

Keywords: cognition, gamma-band synchronization, inhibitory postsynaptic potential, membrane ion current, mitochondrial respiratory chain, neuroenergetics, pyramidal cell, tissue oxygen tension

FAST NEURONAL NETWORK OSCILLATIONS AND HIGHER COGNITIVE FUNCTIONS

Fast neuronal network oscillations in the gamma frequency band (30–100 Hz) that occur in the electroencephalogram or in local field potential recordings have been observed in virtually any mammalian cortical structure, including the neocortex and the hippocampus (Gray and Singer, 1989; Traub et al., 1996; Buzsáki and Draguhn, 2004; Bartos et al., 2007; Uhlhaas and Singer, 2010). Gamma oscillations reflect synchronous membrane potential oscillations of a large number of neurons in a given neuronal network, and they have been suggested to underlie higher cognitive functions such as sensual perception, attention, and memory formation (Lisman, 1999; Axmacher et al., 2006; Mann and Paulsen, 2007; Uhlhaas and Singer, 2010). Gamma oscillations are generated in local neuronal networks by the complex interplay of excitatory neurons and specific inhibitory interneurons, both of which communicating via chemical and, perhaps, electrical synapses (Tamás et al., 2000; Whittington and Traub, 2003; Bartos et al., 2007). Functionally, gamma oscillations bind neurons into a common temporal matrix, enabling precise temporal coding, spike timing-dependent plasticity, and formation of neuronal assemblies (Paulsen and Moser, 1998; Engel and Singer, 2001; Buzsáki and Draguhn, 2004; Axmacher et al., 2006). A characteristic feature is the long-range synchronization of gamma oscillations in remote cortical areas (König et al., 1995; Bazhenov et al., 2008). This phenomenon has been suggested to underlie binding of distributed neuronal representations and, therefore, forms a crucial neuronal prerequisite for the unity of sensual perception, attention, and, perhaps, consciousness (Engel and Singer, 2001; Fries et al., 2007; Uhlhaas and Singer, 2010). Importantly, gamma oscillations can be reliably induced in brain slice preparations *in vitro* (see below).

NEURONAL INFORMATION PROCESSING AND ENERGY DEMAND

The human brain consumes about 20% of the oxygen inspired at rest while accounting for only 2% of the body weight (Erecinska and Silver, 2001). This suggests that neuronal information processing is associated with an extraordinary high metabolic rate. In more global estimations, most of the energy consumption has been attributed to action potential generation ("spiking") and excitatory synaptic transmission (Attwell and Laughlin, 2001). However, information about the energy demands of different functional brain states, i.e., the energy demands of different forms of neuronal network activity, is widely lacking (Kann and Kovács, 2007; Cunningham and Chinnery, 2011). From the clinical medicine point of view, higher cognitive functions appear to be exceptionally vulnerable during various neurological and psychiatric brain pathologies (Hansen, 1985; McFarland et al., 2010; Uhlhaas and Singer, 2010).

Abbreviations: EPSP, excitatory postsynaptic potential; FAD, flavin adenine dinucleotide; GABA, γ-aminobutyric acid; IPSP, inhibitory postsynaptic potential; NAD(P)H, nicotinamide adenine dinucleotide (phosphate); pO_2, partial oxygen pressure.

Therefore, impairment of energy metabolism by either alterations in oxygen and nutrients supply and/or dysfunction of neuronal mitochondria might be a key pathogenic factor (Kann and Kovács, 2007; DiMauro and Schon, 2008; Distelmaier et al., 2009; Nicholls, 2009; Wallace, 2010). Strikingly, neuroenergetical aspects such as energy consumption and adaptations of energy metabolism that are associated with different forms of neuronal network activity have been less defined: gamma oscillations as a cellular correlate of higher cognitive functions are a prime example (Axmacher et al., 2006; Uhlhaas and Singer, 2010; Cunningham and Chinnery, 2011). This lack of information is mainly caused by technical limitations, (i) in the accessibility to certain cortical areas, and (ii) in the high spatiotemporal resolution that is required for simultaneous local recordings of neuronal activity and energy metabolism at the level of mitochondria *in vivo* (Kann and Kovács, 2007; Cunningham and Chinnery, 2011). In the recent years, research has thus focused on brain slice preparations, in particular from the hippocampus, to address the energy demand of gamma oscillations and the associated adaptations in energy metabolism *in vitro*. Here, I will firstly describe the features of hippocampal slice preparations as a reliable model to study both, gamma oscillations and neuroenergetics, and secondly review recent reports from various groups in the field. These reports suggest that gamma oscillations are associated with high energy demand that is counterbalanced by rapid adaptations in oxidative energy metabolism.

ACUTELY PREPARED SLICES AND ORGANOTYPIC SLICE CULTURES

Living slice preparations have been successfully made from the neocortex and the hippocampus of both, rodents and humans (McIlwain, 1951; Schwartzkroin and Andersen, 1975; Fisahn et al., 1998; Kann et al., 2005; Vreugdenhil and Toescu, 2005; Ivanov et al., 2011). Hippocampal tissue is usually cut in slices with a thickness of 300–400 μm. To minimize ischemic neuronal damage because of arrest in blood circulation, the preparation of slices is carried out quickly and in cold preparation solution that contains ion concentrations similar to the cerebrospinal fluid *in vivo* (Bischofberger et al., 2006; Kann and Kovács, 2007; Hájos and Mody, 2009). Recently, the add-on of further important substrates and nutrients has been proposed (Hájos and Mody, 2009; Zilberter et al., 2010). Notably, for investigations of hippocampal slices much higher glucose concentrations (10–26 mM) have been used compared with the brain *in vivo* (0.35–2.6 mM) because it is difficult to obtain healthy slices using lower concentrations (Kann and Kovács, 2007). Oxygenation and pH adjustment of preparation solution is achieved by a gas mixture of 95% O_2 and 5% CO_2. The high oxygen fraction is routinely used to ensure sufficient oxygen supply of healthy neurons in deeper slice layers, which ultimately depends on a steep diffusion gradient. Monitoring the interstitial partial oxygen pressure (pO_2) with oxygen sensor microelectrodes in hippocampal slices during spontaneous neuronal activity revealed that oxygen was still available in excess ($pO_2 > 150$ mmHg) at the depth of 160 μm below the slice cut surface (Kann et al., 2011). However, the pO_2 at the slice cut surface is often lower than theoretically expected and might significantly vary in experimental studies because of individual experimental settings such as size and construction of the recording chamber, temperature, as well as exchange rate of gas mixture or recording solution. Notably, the pO_2 is not monitored routinely in many studies because oxygen is provided in excess, at least in the neuronal cell layers of the upper third of the slice where electrophysiological and live-cell fluorescence imaging recordings are conducted (Kann and Kovács, 2007).

After preparation, hippocampal slices are either used for experiments in the next 10–12 h ("acutely prepared slices"; McIlwain, 1951; Schwartzkroin and Andersen, 1975) or maintained under sterile conditions on a biopore membrane in an incubator for up to weeks ("organotypic slice cultures"; Stoppini et al., 1991). It is important to note that individual neurons and neuronal networks in such slice cultures show similar morphological and functional features as compared to the hippocampus *in vivo* (Caeser and Aertsen, 1991; Bahr et al., 1995; De Simoni et al., 2003; Kann et al., 2011), including preservation of the natural cellular environment, i.e., the presence of astrocytes and microglial cells ("organotypic"). However, hippocampal slice cultures widely lack input from other (sub)cortical brain areas. After 10–14 days *in vitro* slice cultures have shorter diffusion distances for oxygen and nutrients compared to acutely prepared slices because of the residual thickness of about 200 μm. Moreover, the initially damaged slice cut surface is reorganized (Bahr et al., 1995; Kann and Kovács, 2007). During electrophysiological and/or live-cell fluorescence imaging recordings slice preparations are stored either entirely in recording solution that is saturated with the gas mixture containing 95% O_2 ("submerged condition") or at the interface between recording solution and the gas mixture ("interface condition"; Kann and Kovács, 2007; Hájos and Mody, 2009). Under the interface condition, slice preparations are still covered with a thin layer of recording solution. Usage of brain slice preparations has significantly contributed to a deeper understanding of neuronal functions at the cellular and network level in the recent decades. However, given factors such as absence of blood circulation, longer diffusion distances, steep interstitial pO_2 gradients, and composition of the recording solution have to be kept in mind when interpreting data from slice preparations (Kann and Kovács, 2007; Zilberter et al., 2010).

HIPPOCAMPAL SLICE PREPARATIONS AS A RELIABLE MODEL FOR GAMMA OSCILLATIONS

In neuronal networks of the hippocampus, pyramidal cells, and granule cells are excitatory projection neurons with long-range glutamatergic connections (releasing neurotransmitter, glutamate). Besides these projection neurons there is a population of various inhibitory GABAergic interneurons [releasing neurotransmitter, γ-aminobutyric acid (GABA)], comprising about 10% of all hippocampal neurons (Caeser and Aertsen, 1991; Freund and Buzáki, 1996; Freund, 2003). Evidence from electrophysiological recordings, high-resolution functional imaging, transgenic animals, and mathematical modeling has revealed a major role of these inhibitory interneurons in the generation of coherent activity patterns. Specific types of interneurons support broad simultaneous rhythmic inhibition and thus synchronize the activity of large neuronal populations *in vitro* and *in vivo* (Freund, 2003; Whittington and Traub, 2003; Bartos et al., 2007; Sohal et al., 2009; Gulyás et al., 2010; Korotkova et al., 2010). For gamma

oscillations, perisomatic GABAergic interneurons are of central importance because the highly divergent axonal plexus allows synchronous inhibition of 1000–2000 pyramidal cells (Freund and Buzáki, 1996; Freund, 2003; Mann and Paulsen, 2007). About 50% of these interneurons are parvalbumin-containing baskets cells that are able to generate fast series of action potentials and, thus, follow almost every gamma cycle (30–100 Hz). Pyramidal cells, by contrast, show strong spiking accommodation and have typical spiking rates around 2–4 Hz during gamma oscillations *in vitro* and *in vivo* (Csicsvari et al., 1999; Freund, 2003; Hájos et al., 2004; Gulyás et al., 2010). It is important to note that the rhythmic hippocampal oscillations that occur in local field potential recordings *in vitro* primarily reflect averaged synchronized inhibitory postsynaptic potentials (IPSPs) in the perisomatic region rather than action potentials and excitatory postsynaptic potentials (EPSPs; Mann et al., 2005; Oren et al., 2010). Similar findings were reported from slices of the occipital cortex (Trevelyan, 2009).

Sustained gamma oscillations can be reliably induced in both, acutely prepared slices and slice cultures. In most of the studies, low concentrations of acetylcholine (carbachol) or kainic acid were added to the recording solution to activate muscarinic and ionotropic glutamate receptors, respectively (Fisahn et al., 1998; Fellous and Sejnowski, 2000; Vreugdenhil and Toescu, 2005; Wójtowicz et al., 2009; Kann et al., 2011). In particular, application of acetylcholine mimics cholinergic input from the septum *in vivo*. Despite some differences in the underlying synaptic mechanisms (Bartos et al., 2007) both models share important features with hippocampal gamma oscillations *in vivo* and are commonly used for analysis and mathematical modeling of cellular and network dynamics (Whittington and Traub, 2003; Bartos et al., 2007; Hájos and Paulsen, 2009). In hippocampal slice preparations, pharmacologically induced sustained gamma oscillations occur most prominently in subfield CA3 and weaker in subfield CA1, and they are absent in the dentate gyrus. This has been observed in both acutely prepared slices and slice cultures from mouse and rat (Fisahn et al., 1998; Wójtowicz et al., 2009; Kann et al., 2011). The oscillations are widely similar to gamma oscillations *in vivo*, including the sites of intrahippocampal generation and propagation. One exception is that under certain conditions input from the entorhinal cortex might also drive gamma oscillations of lower power in the dentate gyrus *in vivo* (Csicsvari et al., 2003). Gamma oscillations *in vivo* occur in the presence and the absence of theta oscillations (6–9 Hz), in brief periods as well as prolonged periods (>10 s) during running of the animal or rapid-eye-movement (REM) sleep (Penttonen et al., 1998; Buhl et al., 2003; Buzsáki et al., 2003; Chen et al., 2011).

HIGH ENERGY DEMAND OF HIPPOCAMPAL GAMMA OSCILLATIONS

Gamma oscillations *in vitro* have been reliably induced in the interface recording condition (Traub et al., 1996; Fisahn et al., 1998). Notably, under the submerged recording condition gamma oscillations could be only induced when the exchange of recording solution was significantly improved, for example by increasing the flow rate to 5–6 ml/min and by decreasing the volume of the recording chamber (Hájos et al., 2004; Huchzermeyer et al., 2008). Further studies demonstrated rapid decreases in the power of gamma oscillations in hippocampal slice preparations, (i) when the pO_2 of the ambient atmosphere was lowered to the normoxic range under the interface recording condition (Huchzermeyer et al., 2008), (ii) when the flow rate of oxygenated recording solution was too low under the submerged recording condition (Hájos et al., 2009), and (iii) when hypoxic events were induced (Fano et al., 2007; Pietersen et al., 2009). Rapid decreases in the power of gamma oscillations were also observed during pharmacological interference with mitochondrial function, namely inhibition of the respiratory chain by rotenone (acting on complex I) or potassium cyanide (acting on cytochrome *c* oxidase in complex IV), and mitochondrial uncoupling by protonophores (Kann et al., 2011; Whittaker et al., 2011). Moreover, the exquisite sensitivity of gamma oscillations to mitochondrial dysfunction has been identified because other activity forms such as electrical stimulus-evoked neuronal activation and pathological seizure-like events were more resistant to both, respiratory chain inhibition and low pO_2 (Huchzermeyer et al., 2008; Kann et al., 2011). Similar observations were recently made during unilateral hippocampal ischemia *in vivo* (Barth and Mody, 2011). These studies consistently show that hippocampal gamma oscillations are rapidly impaired during metabolic stress, indirectly suggestive for a high energy demand. Mechanistically, fast-spiking inhibitory interneurons might play a crucial role in this rapid impairment because of their key role for establishment of gamma oscillations as well as the unique electrophysiological and biochemical properties when compared to excitatory projection neurons (Gulyás et al., 2006; Alle et al., 2009; Carter and Bean, 2009; Hasenstaub et al., 2010; Kann et al., 2011; Whittaker et al., 2011).

More direct evidence for the high energy demand of gamma oscillations was recently provided by combining local field potential and pO_2 recordings. It was demonstrated that the power of gamma oscillations positively correlated with a substantial increase in oxygen consumption in both, acutely prepared slices and slice cultures. Intriguingly, the level of oxygen consumption as determined during gamma oscillations reached the level that was observed during a strong pathological form of neuronal activity, namely seizure-like events (Kann et al., 2011). These data clearly substantiate the notion that hippocampal gamma oscillations *in vitro* are associated with high oxygen consumption. This is in line with an *in vivo* study from the cat visual cortex describing tight correlations between gamma oscillations and hemodynamic responses (Niessing et al., 2005) that might reflect local adaptations in blood flow to increase oxygen and nutrients supply (Leybaert, 2005; Attwell et al., 2010; Cauli and Hamel, 2010).

The high oxygen consumption during gamma oscillations might be explained by several mechanisms underlying neuronal signaling. Both, excitatory pyramidal cells and inhibitory GABAergic interneurons increase their spiking rates from different base levels during gamma oscillations. This would increase the energy demand in these neurons, despite the fact that diverse neuronal subtypes might feature different biophysical properties for energy cost efficient generation of action potentials (Hasenstaub et al., 2010). As a consequence of increased spiking rates and highly divergent connectivity, and this might be more relevant for the increased energy demand during gamma oscillations, the incidence of EPSPs and IPSPs in the neuronal network massively

increases, and thus ion fluxes through neuronal membranes as well (De Simoni et al., 2003; Whittington and Traub, 2003; Mann and Paulsen, 2007). The ion fluxes tend to dissipate the concentration gradients of Na^+, Ca^{2+}, K^+, and Cl^- ions that exist across neuronal membranes to ensure proper neuronal function. In order to maintain ionic homeostasis, the concentration gradients are continuously reconstituted against electrochemical equilibrium by ion pumps such as Na^+/K^+-ATPase and Ca^{2+}-ATPase as well as transporters such as Na^+/Ca^{2+}-exchanger and $Na^+/K^+/Cl^-$-cotransporter. These transport processes are finally energy-dependent, leading to breakdown of cellular energy carrier, ATP (Attwell and Iadecola, 2002; Kann and Kovács, 2007). In the brain, most of the ATP generation has been attributed to oxidative phosphorylation in mitochondria (Erecinska and Silver, 2001; Attwell and Iadecola, 2002) and neurometabolic coupling is rapidly mediated by changes in substrate ratios as well as cytosolic and mitochondrial Ca^{2+}-signaling (Duchen, 1992; Kann et al., 2003; Leybaert, 2005; Kann and Kovács, 2007). Therefore, the high oxygen consumption as observed during gamma oscillations might reflect fast adaptations in mitochondrial oxidative energy metabolism. However, further experimental studies are required to determine the potential contribution of energy substrates other than glucose as well as the roles of aerobic and anaerobic glycolysis (Magistretti and Pellerin, 1999; Raichle and Mintun, 2006; Schurr, 2006; Schousboe et al., 2007; Gallagher et al., 2009; Ivanov et al., 2011).

In several reports, live-cell fluorescence imaging of nicotinamide adenine dinucleotide (phosphate) and flavin adenine dinucleotide [NAD(P)H, FAD] was applied to get insight into neuronal activity-dependent changes in mitochondrial redox state, and thus adaptations in energy metabolism (Duchen, 1992; Kann et al., 2003; Kasischke et al., 2004; Brennan et al., 2006; Ivanov et al., 2011). Using this imaging technique the changes in mitochondrial redox state during gamma oscillations were recently investigated in slice cultures. Interestingly, gamma oscillations were associated with a shift toward reduction of the dinucleotides although the interstitial pO_2 was hyperoxic (Huchzermeyer et al., 2008). This observation might reflect an increase in the availability of substrates as a result of enhanced glycolysis in neuronal and astrocytic compartments (Kasischke et al., 2004; Brennan et al., 2006; Hertz et al., 2007) or an imbalance of neuronal tricarboxylic acid cycle and mitochondrial respiratory chain activities. Moreover, repetitive electrical stimulation that was additionally applied during gamma oscillations resulted in significantly smaller shifts toward oxidation of the dinucleotides compared to controls (Kann et al., 2011). These data suggest that hippocampal gamma oscillations are associated with near-limit utilization of mitochondrial oxidative capacity, and thus provide further evidence for the high energy demand during gamma oscillations. The data might also imply that rapid and sufficient supply of oxygen and nutrients is a fundamental prerequisite for the maintenance of fast neuronal network oscillations.

Intriguingly, the electrophysiological and biochemical features of hippocampal subfield CA3, namely highest levels in gamma oscillation power, oxygen consumption, and mitochondrial performance, also correlated with the highest expression of mitochondrial complex I subunits (Kann et al., 2011; Wirtz and Schuelke, 2011). Complex I (NADH:ubiquinone oxidoreductase) is part of the mitochondrial respiratory chain and composed of up to 46 individual subunits. These subunits are encoded by both, nuclear and mitochondrial DNA (Distelmaier et al., 2009). Mitochondrial complex I has been discussed to exert major control over oxidative phosphorylation, and to play a key role in the pathogenesis of neurodegenerative diseases (Pathak and Davey, 2008). The pattern of complex I gene expression in the hippocampus might reflect unique enzymatic properties of neuronal mitochondria in subfield CA3 to match the high energy demand that is associated with the generation of gamma oscillations (Kann et al., 2011).

IMPLICATIONS FOR CLINICAL MEDICINE

It has been known from animals and humans that higher sensory and motor functions are much more vulnerable to metabolic stress than basic responses of neurons to extrinsic electrical stimuli and ion distributions in neuronal tissue (Rossen et al., 1943; Hossmann and Sato, 1970; Hansen, 1985). However, the underlying cellular mechanisms are still unknown. Gamma oscillations have been discussed as a cellular correlate of higher cognitive functions (Lisman, 1999; Axmacher et al., 2006; Mann and Paulsen, 2007; Uhlhaas and Singer, 2010). Thus, the recent neuroenergetical data on gamma oscillations in brain slice preparations and the proposed mechanisms as outlined above might contribute to a more comprehensive understanding of the exceptional vulnerability of higher brain functions during circulatory disturbances, mitochondrial diseases, and neurodegeneration.

ACKNOWLEDGMENTS

The author thanks Ismini E. Papageorgiou and Dr. Andreas Draguhn for valuable suggestions and Andrea Lewen for editing assistance. This work was supported by Deutsche Forschungsgemeinschaft in SFB 618 and SFB TR3.

REFERENCES

Alle, H., Roth, A., and Geiger, J. R. P. (2009). Energy-efficient action potentials in hippocampal mossy fibers. *Science* 325, 1405–1408.

Attwell, D., Buchan, A. M., Charpak, S., Lauritzen, M., MacVicar, B. A., and Newman, E. A. (2010). Glial and neuronal control of brain blood flow. *Nature* 468, 232–243.

Attwell, D., and Iadecola, C. (2002). The neural basis of functional brain imaging signals. *Trends Neurosci.* 25, 621–625.

Attwell, D., and Laughlin, S. B. (2001). An energy budget for signaling in the grey matter of the brain. *J. Cereb. Blood Flow Metab.* 21, 1133–1145.

Axmacher, N., Mormann, F., Fernández, G., Elger, C. E., and Fell, J. (2006). Memory formation by neuronal synchronization. *Brain Res. Rev.* 52, 170–182.

Bahr, B. A., Kessler, M., Rivera, S., Vanderklish, P. W., Hall, R. A., Mutneja, M. S., Gall, C., and Hoffman, K. B. (1995). Stable maintenance of glutamate receptors and other synaptic components in long-term hippocampal slices. *Hippocampus* 5, 425–439.

Barth, A. M. I., and Mody, I. (2011). Changes in hippocampal neuronal activity during and after unilateral selective hippocampal ischemia in vivo. *J. Neurosci.* 31, 851–860.

Bartos, M., Vida, I., and Jonas, P. (2007). Synaptic mechanisms of synchronized gamma oscillations in inhibitory interneuron networks. *Nat. Rev. Neurosci.* 8, 45–56.

Bazhenov, M., Rulkov, N. F., and Timofeev, I. (2008). Effect of synaptic connectivity on long-range synchronization of fast cortical oscillations. *J. Neurophysiol.* 100, 1562–1575.

Bischofberger, J., Engel, D., Li, L., Geiger, J. R. P., and Jonas, P. (2006). Patch-clamp recording from mossy fiber terminals in hippocampal slices. *Nat. Protoc.* 1, 2075–2081.

Brennan, A. M., Connor, J. A., and Shuttleworth, C. W. (2006). NAD(P)H fluorescence transients after synaptic activity in brain slices: predominant role of mitochondrial function. *J. Cereb. Blood Flow Metab.* 26, 1389–1406.

Buhl, D. L., Harris, K. D., Hormuzdi, S. G., Monyer, H., and Buzsáki, G. (2003). Selective impairment of hippocampal gamma oscillations in connexin-36 knock-out mouse in vivo. *J. Neurosci.* 23, 1013–1018.

Buzsáki, G., Buhl, D. L., Harris, K. D., Csicsvari, J., Czéh, B., and Morozov, A. (2003). Hippocampal network patterns of activity in the mouse. *Neuroscience* 116, 201–211.

Buzsáki, G., and Draguhn, A. (2004). Neuronal oscillations in cortical networks. *Science* 304, 1926–1929.

Caeser, M., and Aertsen, A. (1991). Morphological organization of rat hippocampal slice cultures. *J. Comp. Neurol.* 307, 87–106.

Carter, B. C., and Bean, B. P. (2009). Sodium entry during action potentials of mammalian neurons: incomplete inactivation and reduced metabolic efficiency in fast-spiking neurons. *Neuron* 64, 898–909.

Cauli, B., and Hamel, E. (2010). Revisiting the role of neurons in neurovascular coupling. *Front. Neuroenergetics* 2:9. doi: 10.3389/fnene.2010.00009

Chen, Z., Resnik, E., McFarland, J. M., Sakmann, B., and Mehta, M. R. (2011). Speed controls the amplitude and timing of the hippocampal gamma rhythm. *PLoS ONE* 6, e21408. doi:10.1371/journal.pone.0021408

Csicsvari, J., Hirase, H., Czurkó, A., Mamiya, A., and Buzsáki, G. (1999). Oscillatory coupling of hippocampal pyramidal cells and interneurons in the behaving rat. *J. Neurosci.* 19, 274–287.

Csicsvari, J., Jamieson, B., Wise, K. D., and Buzsáki, G. (2003). Mechanisms of gamma oscillations in the hippocampus of the behaving rat. *Neuron* 37, 311–322.

Cunningham, M. O., and Chinnery, P. F. (2011). Mitochondria and cortical gamma oscillations: food for thought? *Brain* 134, 330–332.

De Simoni, A., Griesinger, C. B., and Edwards, F. A. (2003). Development of rat CA1 neurones in acute versus organotypic slices: role of experience in synaptic morphology and activity. *J. Physiol. (Lond.)* 550, 135–147.

DiMauro, S., and Schon, E. A. (2008). Mitochondrial disorders in the nervous system. *Annu. Rev. Neurosci.* 31, 91–123.

Distelmaier, F., Koopman, W. J. H., van den Heuvel, L. P., Rodenburg, R. J., Mayatepek, E., Willems, P. H. G. M., and Smeitink, J. A. M. (2009). Mitochondrial complex I deficiency: from organelle dysfunction to clinical disease. *Brain* 132, 833–842.

Duchen, M. R. (1992). $Ca2^{+}$-dependent changes in the mitochondrial energetics in single dissociated mouse sensory neurons. *Biochem. J.* 283, 41–50.

Engel, A. K., and Singer, W. (2001). Temporal binding and the neural correlates of sensory awareness. *Trends Cogn. Sci.* 5, 16–25.

Erecinska, M., and Silver, I. A. (2001). Tissue oxygen tension and brain sensitivity to hypoxia. *Respir. Physiol.* 128, 263–276.

Fano, S., Behrens, C. J., and Heinemann, U. (2007). Hypoxia suppresses kainate-induced γ-oscillations in rat hippocampal slices. *Neuroreport* 18, 1827–1831.

Fellous, J.-M., and Sejnowski, T. J. (2000). Cholinergic induction of oscillations in the hippocampal slice in the slow (0.5-2 Hz), theta (5-12 Hz), and gamma (35-70 Hz) bands. *Hippocampus* 10, 187–197.

Fisahn, A., Pike, F. G., Buhl, E. H., and Paulsen, O. (1998). Cholinergic induction of network oscillations at 40 Hz in the hippocampus in vitro. *Nature* 394, 186–189.

Freund, T. F. (2003). Interneuron diversity series: rhythm and mood in perisomatic inhibition. *Trends Neurosci.* 26, 489–495.

Freund, T. F., and Buzáki, G. (1996). Interneurons of the hippocampus. *Hippocampus* 6, 347–470.

Fries, P., Nikolic, D., and Singer, W. (2007). The gamma cycle. *Trends Neurosci.* 30, 309–316.

Gallagher, C. N., Carpenter, K. L. H., Grice, P., Howe, D. J., Mason, A., Timofeev, I., Menon, D. K., Kirkpatrick, P. J., Pickard, J. D., Sutherland, G. R., and Hutchinson, P. J. (2009). The human brain utilizes lactate via the tricarboxylic acid cycle: a 13C-labelled microdialysis and high-resolution nuclear magnetic resonance study. *Brain* 132, 2839–2849.

Gray, C. M., and Singer, W. (1989). Stimulus-specific neuronal oscillations in orientation columns of cat visual cortex. *Proc. Natl. Acad. Sci. U.S.A.* 86, 1698–1702.

Gulyás, A. I., Buzsáki, G., Freund, T. F., and Hirase, H. (2006). Populations of hippocampal inhibitory neurons express different levels of cytochrome c. *Eur. J. Neurosci.* 23, 2581–2594.

Gulyás, A. I., Szabó, G. G., Ulbert, I., Holderith, N., Monyer, H., Erdélyi, F., Szabó, G., Freund, T. F., and Hájos, N. (2010). Parvalbumin-containing fast-spiking basket cells generate the field potential oscillations induced by cholinergic receptor activation in the hippocampus. *J. Neurosci.* 30, 15134–15145.

Hájos, N., Ellender, T. J., Zemankovics, R., Mann, E. O., Exley, R., Cragg, S. J., Freund, T. F., and Paulsen, O. (2009). Maintaining network activity in submerged hippocampal slices: importance of oxygen supply. *Eur. J. Neurosci.* 29, 319–327.

Hájos, N., and Mody, I. (2009). Establishing a physiological environment for visualized in vitro brain slice recordings by increasing oxygen supply and modifying aCSF content. *J. Neurosci. Methods* 183, 107–113.

Hájos, N., Pálhalmi, J., Mann, E. O., Németh, B., Paulsen, O., and Freund, T. F. (2004). Spike timing of distinct types of GABAergic interneuron during hippocampal gamma oscillations in vitro. *J. Neurosci.* 24, 9127–9137.

Hájos, N., and Paulsen, O. (2009). Network mechanisms of gamma oscillations in the CA3 region of the hippocampus. *Neural Netw.* 22, 1113–1119.

Hansen, A. J. (1985). Effect of anoxia on ion distribution in the brain. *Physiol. Rev.* 65, 101–148.

Hasenstaub, A., Otte, S., Callaway, E., and Sejnowski, T. J. (2010). Metabolic cost as a unifying principle governing neuronal biophysics. *Proc. Natl. Acad. Sci. U.S.A.* 107, 12329–12334.

Hertz, L., Peng, L., and Dienel, G. A. (2007). Energy metabolism in astrocytes: high rate of oxidative metabolism and spatiotemporal dependence on glycolysis/glycogenolysis. *J. Cereb. Blood Flow Metab.* 27, 219–249.

Hossmann, K.-A., and Sato, K. (1970). The effect of ischemia on sensorimotor cortex of cat. Electrophysiological, biochemical and electronmicroscopical observations. *Z. Neurol.* 198, 33–45.

Huchzermeyer, C., Albus, K., Gabriel, H.-J., Otáhal, J., Taubenberger, N., Heinemann, U., Kovács, R., and Kann, O. (2008). Gamma oscillations and spontaneous network activity in the hippocampus are highly sensitive to decreases in pO_2 and concomitant changes in mitochondrial redox state. *J. Neurosci.* 28, 1153–1162.

Ivanov, A., Mukhtarov, M., Bregestovski, P., and Zilberter, Y. (2011). Lactate effectively covers energy demands during neuronal network activity in neonatal hippocampal slices. *Front. Neuroenergetics* 3:2. doi:10.3389/fnene.2011.00002

Kann, O., Huchzermeyer, C., Kovács, R., Wirtz, S., and Schuelke, M. (2011). Gamma oscillations in the hippocampus require high complex I gene expression and strong functional performance of mitochondria. *Brain* 134, 345–358.

Kann, O., and Kovács, R. (2007). Mitochondria and neuronal activity. *Am. J. Physiol. Cell Physiol.* 292, C641–C657.

Kann, O., Kovács, R., Njunting, M., Behrens, C. J., Otáhal, J., Lehmann, T.-N., Gabriel, S., and Heinemann, U. (2005). Metabolic dysfunction during neuronal activation in the ex vivo hippocampus from chronic epileptic rats and humans. *Brain* 128, 2396–2407.

Kann, O., Schuchmann, S., Buchheim, K., and Heinemann, U. (2003). Coupling of neuronal activity and mitochondrial metabolism as revealed by NAD(P)H fluorescence signals in organotypic hippocampal slice cultures of the rat. *Neuroscience* 119, 87–100.

Kasischke, K. A., Vishwasrao, H. D., Fisher, P. J., Zipfel, W. R., and Webb, W. W. (2004). Neural activity triggers neuronal oxidative metabolism followed by astrocytic glycolysis. *Science* 305, 99–103.

König, P., Engel, A. K., and Singer, W. (1995). Relation between oscillatory activity and long-range synchronization in cat visual cortex. *Proc. Natl. Acad. Sci. U.S.A.* 92, 290–294.

Korotkova, T., Fuchs, E. C., Ponomarenko, A., von Engelhardt, J., and Monyer, H. (2010). NMDA receptor ablation on parvalbumin-positive interneurons impairs hippocampal synchrony, spatial representations, and working memory. *Neuron* 68, 557–569.

Leybaert, L. (2005). Neurobarrier coupling in the brain: a partner of neurovascular and neurometabolic coupling? *J. Cereb. Blood Flow Metab.* 25, 2–16.

Lisman, J. E. (1999). Relating hippocampal circuitry to function: recall of memory sequences by reciprocal dentate-CA3 interactions. *Neuron* 22, 233–242.

Magistretti, P. J., and Pellerin, L. (1999). Cellular mechanisms of brain energy metabolism and their relevance to functional brain imaging. *Philos. Trans. R. Soc. Lond. B Biol. Sci.* 354, 1155–1163.

Mann, E. O., and Paulsen, O. (2007). Role of GABAergic inhibition in hippocampal network oscillations. *Trends Neurosci.* 30, 343–349.

Mann, E. O., Suckling, J. M., Hajos, N., Greenfield, S. A., and Paulsen, O. (2005). Perisomatic feedback inhibition underlies cholinergically induced fast network oscillations in the rat hippocampus in vitro. *Neuron* 45, 105–117.

McFarland, R., Taylor, R. W., and Turnbull, D. M. (2010). A neurological perspective on mitochondrial disease. *Lancet Neurol.* 9, 829–840.

McIlwain, H. (1951). Metabolic response in vitro to electrical stimulation of sections of mammalian brain. *Biochem. J.* 49, 382–393.

Nicholls, D. G. (2009). Mitochondrial calcium function and dysfunction in the central nervous system. *Biochim. Biophys. Acta* 1787, 1416–1424.

Niessing, J., Ebisch, B., Schmidt, K. E., Niessing, M., Singer, W., and Galuske, R. A. W. (2005). Hemodynamic signals correlate tightly with synchronized gamma oscillations. *Science* 309, 948–951.

Oren, I., Hájos, N., and Paulsen, O. (2010). Identification of the current generator underlying cholinergically induced gamma frequency field potential oscillations in the hippocampal CA3 region. *J. Physiol. (Lond.)* 588, 785–797.

Pathak, R. U., and Davey, G. P. (2008). Complex I and energy thresholds in the brain. *Biochim. Biophys. Acta* 1777, 777–782.

Paulsen, O., and Moser, E. I. (1998). A model of hippocampal memory encoding and retrieval: GABAergic control of synaptic plasticity. *Trends Neurosci.* 21, 273–278.

Penttonen, M., Kamondi, A., Acsády, L., and Buzsáki, G. (1998). Gamma frequency oscillation in the hippocampus of the rat: intracellular analysis in vivo. *Eur. J. Neurosci.* 10, 718–728.

Pietersen, A. N., Lancaster, D. M., Patel, N., Hamilton, J. B., and Vreugdenhil, M. (2009). Modulation of gamma oscillations by endogenous adenosine through A1 and A2A receptors in the mouse hippocampus. *Neuropharmacology* 56, 481–492.

Raichle, M. E., and Mintun, M. A. (2006). Brain work and brain imaging. *Annu. Rev. Neurosci.* 29, 449–476.

Rossen, R., Kabat, H., and Anderson, J. P. (1943). Acute arrest of cerebral circulation in man. *Arch. Neurol. Psychiatry* 50, 510–528.

Schousboe, A., Bak, L. K., Sickmann, H. M., Sonnewald, U., and Waagepetersen, H. S. (2007). Energy substrates to support glutamatergic and GABAergic synaptic function: role of glycogen, glucose and lactate. *Neurotox. Res.* 12, 263–268.

Schurr, A. (2006). Lactate: the ultimate cerebral oxidative energy substrate? *J. Cereb. Blood Flow Metab.* 26, 142–152.

Schwartzkroin, P. A., and Andersen, P. (1975). Glutamic acid sensitivity of dendrites in hippocampal slices in vitro. *Adv. Neurol.* 12, 45–51.

Sohal, V. S., Zhang, F., Yizhar, O., and Deisseroth, K. (2009). Parvalbumin neurons and gamma rhythms enhance cortical circuit performance. *Nature* 459, 698–702.

Stoppini, L., Buchs, P.-A., and Muller, D. (1991). A simple method for organotypic cultures of nervous tissue. *J. Neurosci. Methods* 37, 173–182.

Tamás, G., Buhl, E. H., Lörincz, A., and Somogyi, P. (2000). Proximally targeted GABAergic synapses and gap junctions synchronize cortical interneurons. *Nat. Neurosci.* 3, 366–371.

Traub, R. D., Whittington, M. A., Colling, S. B., Buzsáki, G., and Jefferys, J. G. R. (1996). Analysis of gamma rhythms in the rat hippocampus in vitro and in vivo. *J. Physiol. (Lond.)* 493, 471–484.

Trevelyan, A. J. (2009). The direct relationship between inhibitory currents and local field potentials. *J. Neurosci.* 29, 15299–15307.

Uhlhaas, P. J., and Singer, W. (2010). Abnormal neural oscillations and synchrony in schizophrenia. *Nat. Rev. Neurosci.* 11, 100–113.

Vreugdenhil, M., and Toescu, E. C. (2005). Age-dependent reduction of γ oscillations in the mouse hippocampus in vitro. *Neuroscience* 132, 1151–1157.

Wallace, D. C. (2010). Mitochondrial DNA mutations in disease and aging. *Environ. Mol. Mutagen.* 51, 440–450.

Whittaker, R. G., Turnbull, D. M., Whittington, M. A., and Cunningham, M. O. (2011). Impaired mitochondrial function abolishes gamma oscillations in the hippocampus through an effect on fast-spiking interneurons. *Brain* 134, e180.

Whittington, M. A., and Traub, R. D. (2003). Interneuron diversity series: Inhibitory interneurons and network oscillations in vitro. *Trends Neurosci.* 26, 676–682.

Wirtz, S., and Schuelke, M. (2011). Region-specific expression of mitochondrial complex I genes during murine brain development. *PLoS ONE* 6, e18897. doi:10.1371/journal.pone.0018897

Wójtowicz, A. M., van den Boom, L., Chakrabarty, A., Maggio, N., ul Haq, R., Behrens, C. J., and Heinemann, U. (2009). Monoamines block kainate- and carbachol-induced γ-oscillations but augment stimulus-induced γ-oscillations in rat hippocampus in vitro. *Hippocampus* 19, 273–288.

Zilberter, Y., Zilberter, T., and Bregestovski, P. (2010). Neuronal activity in vitro and the in vivo reality: the role of energy homeostasis. *Trends Pharmacol. Sci.* 31, 394–401.

Conflict of Interest Statement: The author declares that the research was conducted in the absence of any commercial or financial relationships that could be construed as a potential conflict of interest.

Received: 08 November 2011; accepted: 20 December 2011; published online: 10 January 2012.

Citation: Kann O (2012) The energy demand of fast neuronal network oscillations: insights from brain slice preparations. Front. Pharmacol. ***2****:90. doi: 10.3389/fphar.2011.00090*

This article was submitted to Frontiers in Neuropharmacology, a specialty of Frontiers in Pharmacology.

frontiers in
NEUROENERGETICS

ORIGINAL RESEARCH ARTICLE
published: 12 December 2011
doi: 10.3389/fnene.2011.00007

Activation of astroglial calcium signaling by endogenous metabolites succinate and gamma-hydroxybutyrate in the nucleus accumbens

Tünde Molnár[1†], László Héja[1†], Zsuzsa Emri[2], Ágnes Simon[1], Gabriella Nyitrai[1], Ildikó Pál[1] and Julianna Kardos[1]*

[1] *Department of Neurochemistry, Chemical Research Center, Hungarian Academy of Sciences, Budapest, Hungary*
[2] *Department of Zoology, Eszterházy Károly College, Eger, Hungary*

Edited by:
Yuri Zilberter, INSERM U751, France

Reviewed by:
Alexej Verkhratsky, University of Manchester, UK
Mortimer Mamelak, University of Toronto, Canada

***Correspondence:**
Julianna Kardos, Department of Neurochemistry, Chemical Research Center, Hungarian Academy of Sciences, Pusztaszeri út 59-67, 1025 Budapest, Hungary.
e-mail: jkardos@chemres.hu

†Tünde Molnár and László Héja have contributed equally to this work.

Accumulating evidence suggests that different energy metabolites play a role not only in neuronal but also in glial signaling. Recently, astroglial Ca^{2+} transients evoked by the major citric acid cycle metabolite succinate (SUC) and gamma-hydroxybutyrate (GHB) that enters the citric acid cycle *via* SUC have been described in the brain reward area, the nucleus accumbens (NAc). Cells responding to SUC by Ca^{2+} transient constitute a subset of ATP-responsive astrocytes that are activated in a neuron-independent way. In this study we show that GHB-evoked Ca^{2+} transients were also found to constitute a subset of ATP-responsive astrocytes in the NAc. Repetitive Ca^{2+} dynamics evoked by GHB suggested that Ca^{2+} was released from internal stores. Similarly to SUC, the GHB response was also characterized by an effective concentration of 50 μM. We observed that the number of ATP-responsive cells decreased with increasing concentration of either SUC or GHB. Moreover, the concentration dependence of the number of ATP-responsive cells were highly identical as a function of both [SUC] and [GHB], suggesting a mutual receptor for SUC and GHB, therefore implying the existence of a distinct GHB-recognizing astroglial SUC receptor in the brain. The SUC-evoked Ca^{2+} signal remained in mice lacking $GABA_B$ receptor type 1 subunit in the presence and absence of the *N*-Methyl-d-Aspartate (NMDA) receptor antagonist (2*R*)-amino-5-phosphonovaleric acid (APV), indicating action mechanisms independent of the $GABA_B$ or NMDA receptor subtypes. By molecular docking calculations we found that residues R99, H103, R252, and R281 of the binding crevice of the kidney SUC-responsive membrane receptor SUCNR1 (GPCR91) also predict interaction with GHB, further implying similar GHB and SUC action mechanisms. We conclude that the astroglial action of SUC and GHB may represent a link between brain energy states and Ca^{2+} signaling in astrocytic networks.

Keywords: energy metabolites, succinate, gamma-hydroxybutyrate, astroglial calcium signaling, nucleus accumbens

INTRODUCTION

Using Ca^{2+} imaging in combination with immunohistochemistry, we have recently demonstrated significant co-localization of ATP-stimulated Ca^{2+} bursts with the glial marker protein connexin43 (Cx43) in slices containing the brain reward area (Berridge and Kringelbach, 2008), the nucleus accumbens (NAc) of juvenile rats (Molnár et al., 2011). Store-dependent Ca^{2+} bursting triggered by ATP was significantly reduced by an antibody raised against the Cx43 carboxy-terminal segment and by gap junction inhibitors such as carbenoxolone hemisuccinate (CBX) and flufenamic acid as well as the purinergic G protein-coupled receptor (GPCR) $P2Y_1$ subtype-selective antagonist MRS2179, but not by blocking neuronal activity with tetrodotoxin. The effect of MRS2179 implied that intercellular Ca^{2+} signaling was triggered by the activation of $P2Y_1$ receptors. Neurons within the domain of ATP-activated astrocytes did not show Ca^{2+} transients and exhibited invariant postsynaptic currents (Molnár et al., 2011). We also observed for the first time the activation of repetitive astroglial Ca^{2+} transients in response to the major intermediate of the citric acids cycle succinic acid (SUC). The apparent EC_{50} (50–60 μM) of SUC effect is within the range of physiological plasma SUC concentration (Molnár et al., 2011), since the concentration of SUC in plasma increases from 5 up to 125 μM with exercise, metabolic acidosis or hyperglycemic metabolic states (Krebs, 1950; Nordmann and Nordmann, 1961; Hochachka and Dressendorfer, 1976; Kushnir et al., 2001; Forni et al., 2005; Sadagopan et al., 2007). These data suggest that SUC-responsive Ca^{2+} transients may also have a regulatory role for cellular energy supply. SUC-responsive cells also participated in the ATP induced concerted Ca^{2+} bursts (Molnár et al., 2011). These findings conclusively suggest that astroglial Ca^{2+} bursting evoked by SUC couples astroglial activation to cerebral energy resources.

A common binding site for SUC and gamma-hydroxybutyrate (GHB), that enters the citric acid cycle *via* SUC (Rumigny et al.,

1981) has been disclosed previously (Molnár et al., 2006, 2008a,b). Additionally, intracellular Ca^{2+} store-reliant astroglial Ca^{2+} transients evoked by GHB have been described in the NAc (Molnár et al., 2009). We have shown that this action of GHB is $GABA_B$ receptor independent, since it remains in mice lacking functional $GABA_B$ receptors unlike the majority of GHB-mediated physiological and pharmacological actions including "rape drug effects" that were demonstrated to be dependent on $GABA_B$ receptors (Kaupmann et al., 2003; Wong et al., 2004). Only a few study addressed GHB receptor dependent GHB actions (Molnár et al., 2006, 2009), although high-affinity GHB binding sites were demonstrated in mice lacking $GABA_B$ receptors (Kaupmann et al., 2003) and the function of endogenous GHB has never been clearly defined. A number of studies indicate that in addition to its neurotransmitter/neuromodulatory role, GHB may function in the control of physiological states, like sleep and hibernation. Moreover, it is an endogenous protective agent when tissue energy supplies are limited (MacMillan, 1980a,b; Mamelak, 1989; references cited). The molecular identity of the GHB receptor has not been identified yet satisfactorily, the putative GHB receptor mRNA showed different brain distribution than the native GHB receptors (Andriamampandry et al., 2003, 2007). A binding site recognizing GHB and SUC has been disclosed in the NAc (Molnár et al., 2006, 2008a,b), its relationship with the G protein-coupled heptahelical kidney SUC receptor (SUCNR1:GPCR91, He et al., 2004) has not previously been conjectured.

ATP induced functional coupling of Cx43 hemichannels is known to evoke store-mediated repetitive Ca^{2+} transients triggered by activation of purinergic GPCRs *in vitro* (Stout et al., 2002; Anderson et al., 2004; Beierlein and Regehr, 2006; Piet and Jahr, 2007) and *in vivo* (Hirase et al., 2004; Takata and Hirase, 2008; Hoogland and Kuhn, 2010; Hoogland et al., 2009; Nimmerjahn, 2009; Nimmerjahn et al., 2009). Different *in vitro* paradigms, including locally administered ATP stimuli (100 μM) were found effective (Barry and Cheek, 1994; Li et al., 2001; Zur Nieden and Deitmer, 2006; D'Ascenzo et al., 2007; Fischer et al., 2009). In awake, behaving animal, three types of glial Ca^{2+}-excitation were distinguishable according to the number of networking cells and the dependence on neuronal stimulation (Nimmerjahn et al., 2009): flares (involving large networks of astrocyte fibers), sparkles (restricted to individual fibers), and bursts (expanding radial waves). Spontaneous bursting can be contrasted to sparks and flares as being independent of neuronal activity (Nimmerjahn et al., 2009). Thus, the question may also come up, how ATP-responsive glial Ca^{2+} bursting proceeds and what functions it perform in cellular communication?

In order to better understand these issues, we used different models and/or approaches to compare the effects of GHB with those of SUC and/or ATP: (i) rat brain slice containing the NAc studied by combined application of confocal Ca^{2+} imaging and Cx43 immunohistochemistry to explore and compare GHB-responsive and ATP puff-evoked astroglial Ca^{2+} bursting; (ii) evaluation of SUC/GHB- and ATP-evoked Ca^{2+} transients to disclose mechanistic clues; (iii) homology model of SUCNR1 (He et al., 2004) to simulate binding interactions between SUC/GHB and SUCNR1; (iv) slices containing the NAc from mice lacking $GABA_B$ receptor type 1 subunit in combination with confocal Ca^{2+} imaging to distinguish SUC-responsive Ca^{2+} transients and to compare with GHB-evoked Ca^{2+} signals (Molnár et al., 2009). We report on astroglial Ca^{2+} bursting linked to endogenous metabolites GHB and SUC performing similar function that might possibly be related to cellular energy states.

MATERIALS AND METHODS

BUFFERS AND TEST COMPOUNDS

Slice preparing buffer contained in mM: 250 sucrose, 2 KCl, 1.25 KH_2PO_4, 10 $MgSO_4$, 2 $CaCl_2$, 16 NaH_2CO_3, and 10 glucose. Artificial cerebrospinal fluid (ACSF) contained in mM: 129 NaCl, 2 KCl, 1.25 KH_2PO_4, 1 $MgSO_4$, 2 $CaCl_2$, 16 $NaHCO_3$, and 10 glucose.

The following drugs, applied via the ACSF perfusion including SUC, GHB, and adenosine 5′-triphosphate disodium salt (ATP) were obtained from Sigma-Aldrich (Budapest, Hungary). Fluorescence indicators Fluo-4 acetoxymethyl ester (Fluo-4 AM) was purchased from Molecular Probes (Eugene, OR, USA). Stock solutions of ester fluorescence indicators prepared in DMSO were diluted to 0.2% DMSO in the staining solution.

ANIMALS

Animal care and preparation were in accordance with the Helsinki declaration, European Council Directive of 24 November 1986 (86/609/EEC), Hungarian Animal Act 1998 and associated institutional guidelines, as approved by the local authority. BALB/c $GABA_{B1}$ (−/−) mice exhibit spontaneous seizures (Prosser et al., 2001; Schuler et al., 2001) thus BALB/c $GABA_{B1}$ (−/+) mice were bred, their offspring genotyped at the seventh day and used by the tenth day before seizure could develop in (−/−) mice. All efforts were made to minimize animal suffering and the number of animals used.

ACUTE SLICE PREPARATION AND DYE-LOADING

Coronal slices from the forebrain containing the NAc and the caudate putamen (CP) were prepared for the imaging experiments. Ten to 14-day-old male Wistar rats or 10 day-old mice were decapitated and the forebrain blocks were sliced into 300 μm thin coronal slices by a vibratome (Vibratome, Technical Products International Inc., St. Louis, MO, USA) in ice-cold preparation buffer. Slices were incubated for 1 h under humidified gas-mixture carbogen (5% CO_2 + 95% O_2) atmosphere in an interface-type holding chamber containing warmed (35°C) ACSF. After preincubation in 2% pluronic acid containing ACSF for 2 min, slices were incubated with 5 μM Fluo-4 AM in ACSF for 1 h at 35°C in the dark under humidified carbogen (5% CO_2 + 95% O_2) atmosphere (Molnár et al., 2009). In order to monitor cell death, several slices were exposed to double dye-loading protocol, performed by adding 7.5 μM propidium iodide (PI excitation: 534 nm, emission: 570–600 nm) to the Fluo-4 AM containing ACSF. In order to allow for cleavage of the AM ester group of Fluo-4, slices were transferred to dye-free ACSF at least 30 min before the start of the experiment (Porter and McCarthy, 1996).

CONFOCAL IMAGING AND DRUG TESTING PROTOCOL

Fluorescence recordings of changes in the intracellular Ca^{2+} ion level in cells loaded with Fluo-4 AM were performed as described (Molnár et al., 2009) with an upright epifluorescent

microscope (Olympus BX61WI, Olympus, Budapest, Hungary) equipped with the FluoView300 confocal laser-scanning system (Olympus, Budapest, Hungary) using 20× (0.5 numerical aperture) or 60× (0.9 numerical aperture) water immersion objectives. Image acquisition rate was controlled by a computer running FluoView 5.0 software (Olympus, Budapest, Hungary).

Freshly isolated slices were transferred to the submerge-type recording chamber mounted on the stage of the microscope and were superfused with carbogenated (5% CO_2 + 95% O_2) ACSF (3 ml/min, room temperature). Serial scanning of slices were made at 488 nm excitation wavelength and emitted green fluorescence was collected through a 510–530 nm bandpass filter. Ca^{2+} transients were initiated by application of SUC or GHB in the perfusion or by pressure-ejection of 100 μM ATP in ACSF through a glass micropipette (5–10 μM diameter) on the slice surface. Fluorescence intensity changes within a 355 μm × 355 μm field containing approximately 100 Fluo-4 AM loaded cells around the area of the ATP puff, were followed over a 10-min interval (2 s/image).

Two 10-min-long recordings were made from each slice with a 20-min resting time between the two recordings. ATP was applied 3 min after the beginning of each 10-min-long recording period. The cells showing Ca^{2+} increase after ATP applications at approximately 15–30 μm below the surface were counted (approximately 45 cells in response to the ATP stimulus) and fluorescence changes of cells that responded to ATP applications were measured. The observation threshold was 5× of the variance of the baseline fluorescence.

N denotes the number of slices in a given experimental condition. Statistical analysis was performed using the non-parametric Mann–Whitney test with Bonferroni *post hoc* test (OriginLab Corporation, Northampton, UK) and $p < 0.05$ was considered statistically significant. Unless otherwise stated, the effects of different treatments were compared to the control. Images recorded by the FluoView300 software were processed using the free ImageJ 1.41 image analysis software (http://rsbweb.nih.gov/ij/).

POST-CALCIUM IMAGING IMMUNOHISTOCHEMISTRY PROTOCOL FOR CX43 AND GFAP

In order to identify the cell types involved in Ca^{2+} bursts, we followed our recently described protocol (Molnár et al., 2011). The brain slices were immunostained with antibodies for astrocyte marker proteins (Cx43 and GFAP). However, Fluo-4 signal could not be preserved through fixation with either 0.4% paraformaldehyde or 40 mg/ml EDAC (1-ethyl-3-(3-dimethylaminopropyl)-carbodiimide, Sigma-Aldrich). Therefore co-localization between SUC/ATP-responsive cells and cell type markers could not be resolved. Hence we opted to perform the *in situ* immunostaining in non-fixed slices directly after the Ca^{2+} imaging protocol. Slices used previously to measure Ca^{2+} changes in response to SUC/ATP application were treated as follows: upon completion of the calcium-imaging experiments, each slice was kept in its original position in the recording chamber (using a ballast) and incubated with Cx43 (1:300) and GFAP (1:200) primary antibodies for 30 min, at room temperature. After 3 min × 10 min washing in ACSF, the slice was incubated with Chromeo 546 goat anti-rabbit (1:100 Abcam, Cambridge, UK, catalog number: ab60317) secondary antibody and Alexa-488 donkey anti-mouse (1:100, Molecular Probes) secondary antibody in ACSF for 30 min at room temperature. This was followed by 3 × 10 min washing in ACSF. Serial Z-scans of Cx43 – (excitation: 543 nm, emission: 570–600 nm) and GFAP – (excitation: 488 nm, emission: 510–530 nm) labeled slices were acquired between the slice surface and the maximal penetration depth of the antibodies (approximately 60–70 μm from the surface) through a 20× objective (1 μm/step). Since the fluorescence emission of both Fluo-4 and Alexa-488 dyes are collected in the 510–530 nm range, GFAP-specific staining was obtained by subtracting the Fluo-4 fluorescence from the GFAP immunolabeling signal at each Z depth. Optical sections from identical depths of Fluo-4 and Cx43 images were merged along the Z axis. Single cells, glia filaments, or blood vessels that showed double immunolabeling were recorded through a 60× objective and Z-scans were performed by alternating the excitation wavelengths between 543 nm (Cx43) and 488 m (GFAP) using FluoView 5.0 software at each depth (0.1 μm/step). Images were processed using ImageJ 1.41 and Adobe Photoshop 8.0 image analysis softwares.

SIMULATIONS

The sequence of the human kidney SUC receptor1 (SUCNR1; accession code: Q9BXA5) was downloaded from the UniprotKB database. The SUCNR1 receptor model was built based on the bovine rhodopsin (RHO) structure (PDB code 1f88; Palczewski et al., 2000). The alignment was adopted from He et al. (2004), with one manual adjustment: Asn253 of SUCNR1 was aligned to Ala269 of RHO by reducing the five residue gap of He et al. (2004). The alignment continued according to He et al. (2004), from and Ser275 of SUCNR1, and Ile286 of RHO. The model was built by Modeller9v3 (Sali and Blundell, 1993), and prepared in SYBYL8.0 (Tripos Inc., St. Louis, MO, USA). Hydrogen atoms were added to the protein, and chains were terminated by *N*-methyl and acetyl groups by the Analyze Protein menu of the Biopolymer module. His103 was protonated at both *N* atoms, corresponding to an acidic environment. SUC and GHB ligands were prepared from the PDB database (SUC ligand of 2WBP; Helmetag et al., 2009) in their protonated form according to the acidic pH of the receptor binding (Molnár et al., 2006, 2008a,b). Ligands were minimized in SYBYL until the RMS gradient reached 0.01 kcal/mol/Å. Docking was performed by GOLD5.1 (Cambridge Crystallographic Data Center). A cavity of 10 Å was searched in the docking studies containing the predicted binding crevice residues of SUCNR1 (Arg99, His103, Arg252, Arg281), see **Figure 4** GoldScore was used for evaluating the results. Figures were prepared by Pymol.

RESULTS

GHB-RESPONSIVE CELLS CONSTITUTE A SUB-POPULATION OF ASTROCYTES RESPONDING TO ATP

As outlined in the Section "Introduction," we tested the hypothesis that similarly to SUC (Molnár et al., 2011), GHB also acts on a subpopulation of ATP-responsive cells. Indeed, the presence of GHB (50 μM) in the superfusion evoked Ca^{2+} transients (**Figure 1A**), covering some astroglial Ca^{2+} bursts occurred in response to the ATP puff (100 μM, **Figure 1B**, see also Movie S1 in Supplementary Material). The ATP-evoked Ca^{2+} signal propagated circularly

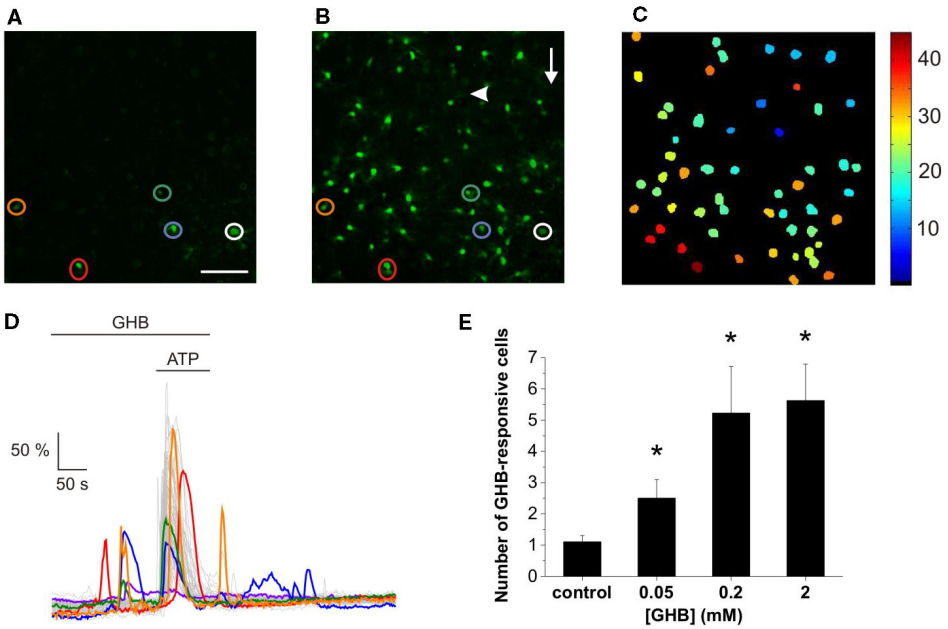

FIGURE 1 | GHB and ATP evoke overlaying Ca^{2+} transients in the rat NAc slice. Representative confocal image of GHB-responsive cells [**(A)** circled] participated in ATP-stimulated concerted Ca^{2+} burst [**(B)** circled]. Arrow indicates the direction of the superfusion buffer. Arrowhead indicates the location and direction of the ATP puff. Scale bar is 50 μm. **(C)** Pseudo-color depiction of the spatiotemporal characteristics of the astroglial Ca^{2+} transients evoked by GHB and ATP shown in **(B)** (see also Movie S1 in Supplementary Material). **(C)** Representative dF/F_0-time plots showing effects of 50 μM GHB alone **(A)** and with 100 μM ATP puff **(B)**. **(D)** Color traces correspond to the GHB-responsive cells circled in **(A)** and **(B)** while gray traces show the fluorescence changes of ATP-responsive cells. **(E)** Summary plot of the effects of increasing (GHB) on the number of cells showing GHB-responsive Ca^{2+} transients. $N = 32$ (control), $N = 13$ (0.05 mM), $N = 9$ (0.2 mM), $N = 9$ (2 mM). $^*p < 0.05$ and $^{**}p < 0.01$ compared to control.

from the point of application, independent of the perfusion direction (**Figure 1C**) with the speed of approximately 10 μm/s, 1.5 times slower than the speed of ATP diffusion as monitored by addition of the fluorescent dye sulforhodamine 101 in the ATP-containing pipette (Molnár et al., 2011). The waveform and speed of the signal propagation conclusively exclude the possibility that Ca^{2+} bursts were triggered by merely the exogenously applied ATP. Comparing the GHB- and ATP-evoked signals, the responses in the presence of GHB and ATP appeared relatively more robust than responses evoked by GHB only (**Figure 1D**). Summary plot of the effects of increasing (GHB) on the number of cells showing GHB-responsive Ca^{2+} transients indicated that similarly to SUC (Molnár et al., 2011) GHB had an EC_{50} value of approximately 50 μM, however smaller number of cells responded to GHB than to SUC, indicating lower efficacy (**Figure 1E**).

GHB AND SUC SHAPED ATP-EVOKED CA^{2+} SIGNALS IN THE SAME WAY

We observed that the number of ATP-responsive cells decreased with increasing concentration of either SUC or GHB (**Figure 2A**). Moreover, the concentration dependence of the number of ATP-responsive cells were highly identical as a function of both (SUC) and (GHB; **Figure 2A**), suggesting a mutual target for SUC and GHB actions. Increasing [SUC] may activate this mutual target, a presumable GHB-responsive astroglial SUC receptor and consequently reduce ATP-responsiveness of astrocytes (**Figures 2A,B**). Furthermore, increasing [SUC] resulted in a rise of the relative abundance of SUC- and shared SUC/ATP-responsive astroglial Ca^{2+} transients (**Figure 2B**) as well as in an increase in the number of cells showing repetitive Ca^{2+} dynamics (**Figure 2C**). The SUC-evoked repetitive Ca^{2+} transients (**Figure 3A**; Molnár et al., 2011) mimicked the GHB response dynamics described above (**Figure 1D**; Movie S1 in Supplementary Material), further suggesting the existence of a GHB-responsive astroglial SUC receptor. In a previous work we provided evidence on store-dependent astroglial Ca^{2+} transients evoked by ATP acting through the G protein-coupled purinergic $P2Y_1$ receptor subtypes in the NAc slice (Molnár et al., 2011). Therefore, SUC- and shared SUC/ATP-responsive astroglial Ca^{2+} transients may suggest co-localization of GHB-responsive SUC and $P2Y_1$ receptors on astrocytes.

THE PRESUMED GHB-RESPONSIVE ASTROGLIAL SUC RECEPTOR WAS CLASSIFIED AS BEING INDEPENDENT OF BOTH $GABA_B$ AND *N*-METHYL-D-ASPARTATE RECEPTORS

We supposed that similarly to GHB, its metabolite SUC also acts independently from $GABA_B$ receptors in the NAc. To verify this hypothesis we tested the effect of SUC (2 mM) on astroglial Ca^{2+} transients in the NAc slice prepared from mice lacking the $GABA_B$ receptor functional subunit 1 ($GABA_B$ KO). We found that similarly to GHB (Molnár et al., 2009), SUC-responsive Ca^{2+} transients were preserved in NAc slices isolated from $GABA_B$ KO mice (**Figure 3A**). Next we asked, if NMDA receptors of the NAc slice were involved in the SUC action mechanisms. We observed that SUC responses remained unaltered in the presence of NMDA

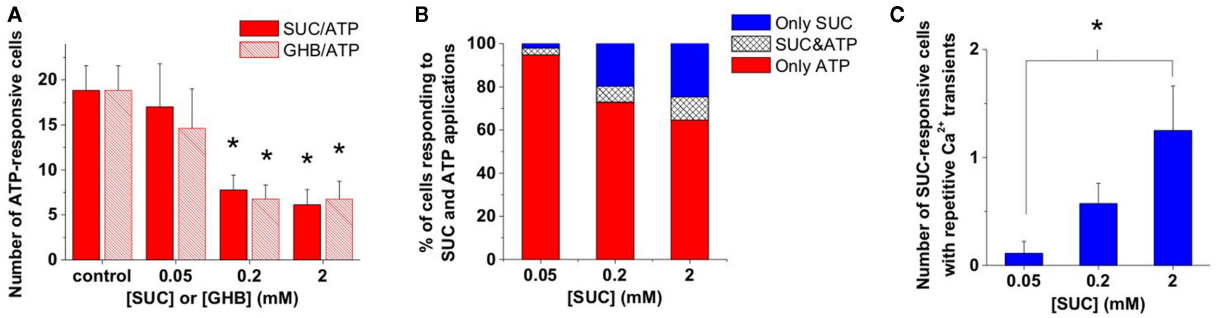

FIGURE 2 | GHB and SUC shaped ATP-evoked Ca^{2+} signals in the same way. (A) Average number of cells showing Ca^{2+} transients in response to ATP (100 μM) puff-application in the presence of different concentrations of SUC or GHB. **(B)** Average number of cells showing Ca^{2+} transients during SUC or SUC plus ATP (100 μM) application as a percent of the total number of cells showing Ca^{2+} transients during SUC or ATP application. **(C)** Average number of cells showing multiple Ca^{2+} transients during application of different SUC concentrations. $N = 32$ (control), $N = 13$ and 9 (0.05 mM), $N = 9$ and 21 (0.2 mM), $N = 9$ and 16 (2 mM) for GHB and SUC, respectively, $^{*}p < 0.05$.

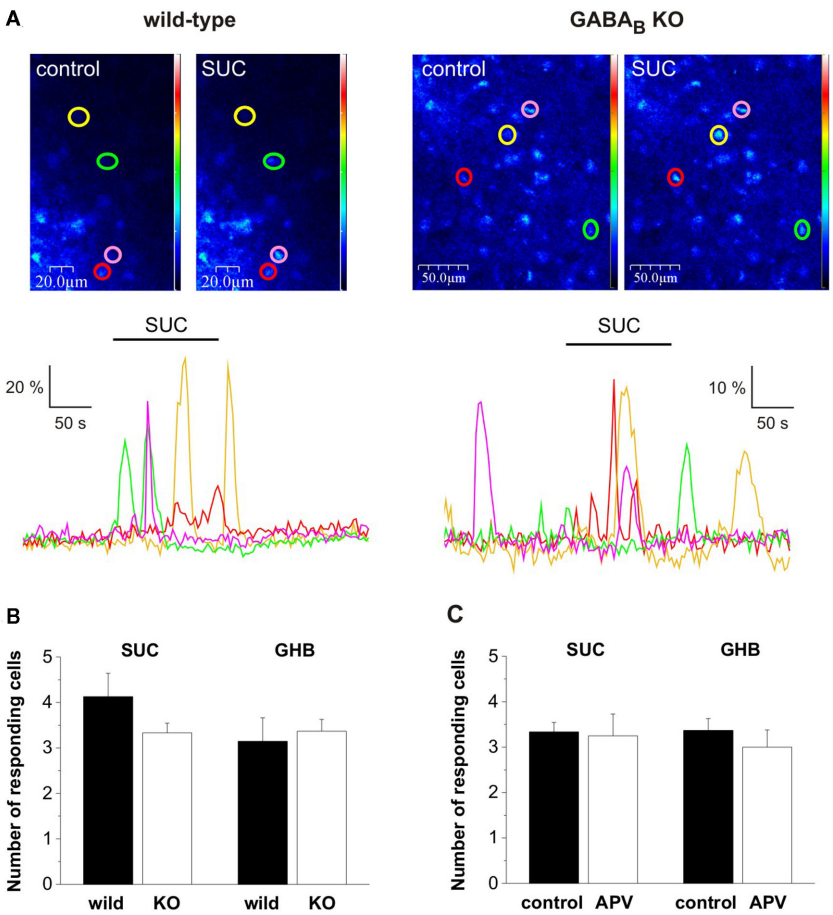

FIGURE 3 | The presumed GHB-responsive astroglial SUC receptor was classified as being independent of both $GABA_B$ and *N*-methyl-D-Aspartate (NMDA) receptors. (A) Pseudo-color images showing fluorescence in NAc astrocytes during control and SUC (2 mM) application in wild type and $GABA_BR$ type 1 subunit KO mice. Astrocytes showing SUC-evoked Ca^{2+} transients are circled and color-coded and the change in fluorescence is shown in dF/F_0-time plots below the images. **(B)** Summary plots show that SUC-evoked Ca^{2+} transients, similarly to GHB-evoked Ca^{2+} transients were preserved in $GABA_BR1$ KO mice. **(C)** Summary plots indicate that SUC/GHB-evoked Ca^{2+} transients were unaltered by the presence of NMDA receptor antagonist (2*R*)-amino-5-phosphonovaleric acid (APV, 20 μM).

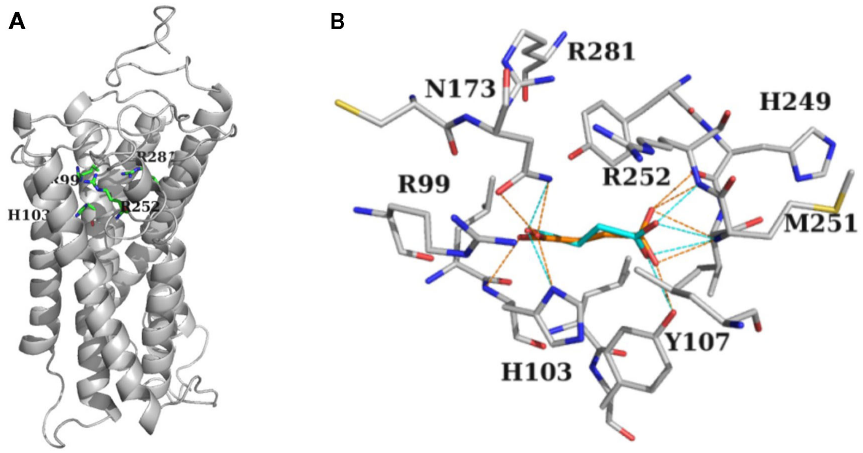

FIGURE 4 | Modeling predicted interaction of GHB with the presumed astroglial SUC receptor. (A) Stick-representation of the binding crevice residues Arg99, His103, Arg252, and Arg281 of SUCNR1 shown as gray cartoon (after He et al., 2004). **(B)** Residues forming the binding crevice of SUC (orange) and GHB (cyan). Residues in the 4 Å vicinity of the ligands together with Arg281 are shown in stick representation. H-bond interactions between ligands and the protein are shown as dotted lines, orange for SUC, and cyan for GHB. **(A,B)** Carbon atoms are gray, nitrogens, and oxygens are colored according to atom type. H atoms are not shown for clarity.

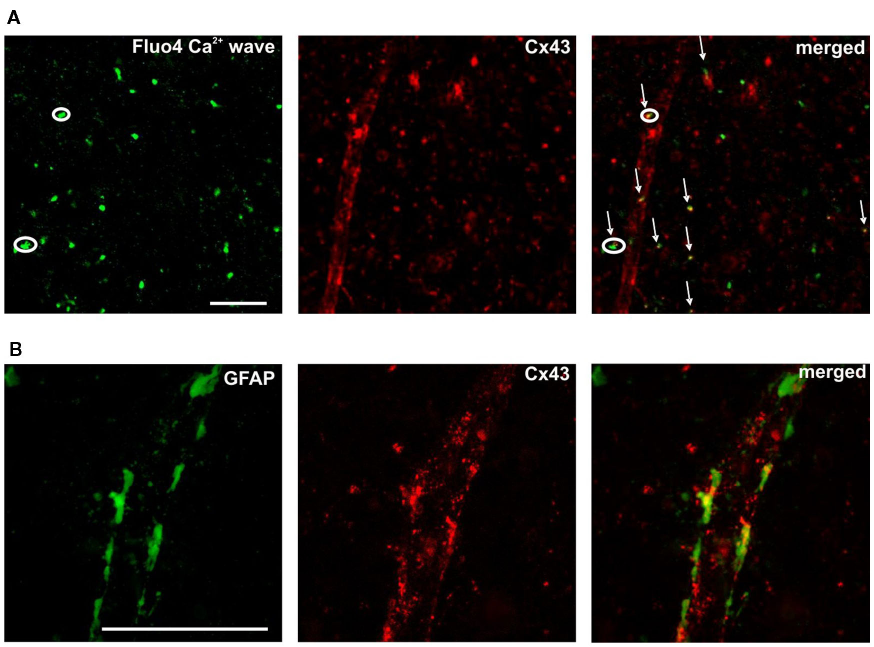

FIGURE 5 | Positioning of SUC/ATP – [(A) circles] and ATP-responsive [(A) arrows] Ca^{2+} transients along a vessel, identified by the appearance of Cx43 gap junction plaques [(A) middle and right panels). Scale bar is 50 μm. Higher magnification in **(B)** displays Cx43-immunoreactive plaques (red) interconnecting astrocytic GFAP-positive (green) end feet.

receptor antagonist (2*R*)-amino-5-phosphonovaleric acid (APV, 20 μM; **Figure 3C**). Therefore, both SUC and GHB effect on astroglial Ca^{2+} signals could be classified as being independent of $GABA_B$ and NMDA receptors. These data further strengthen the possibility that SUC and GHB act through a common target protein, the presumed GHB-responsive astroglial SUC receptor in the NAc.

MODELING PREDICTED INTERACTION OF GHB WITH THE PRESUMED ASTROGLIAL SUC RECEPTOR

To explore the possibility of a shared target protein for SUC and GHB actions, we used the kidney-type SUC receptor (SUCNR1:GPCR91) model structure (He et al., 2004) and simulated interactions of SUC and GHB with this protein. Docking of SUC and GHB into SUCNR1 resulted in similar ligand

conformations occupying the same binding site. The predicted binding crevice was formed by residues R99, H103, R252, and R281 (**Figure 4**) in accordance with previous studies (He et al., 2004). In addition, residues T107, N173, H249, and M251 were also found to be involved in the binding of SUC and GHB (**Figure 4B**). Agonist SUC participated in more extensive H-bond interactions (**Figure 4B**) enabling higher docking score value (35 for SUC vs. 31 for GHB). In addition, we also disclosed a previously unrecognized binding site appearing near to the entrance of the receptor, showing preference to GHB over SUC. However, being more distal to the agonist binding crevice, preferential GHB binding into this "vestibular" binding site is expected to be less effective in forming active receptor conformations, explaining the previously experienced lower efficacy of GHB.

DISCUSSION

Our previous (Molnár et al., 2006, 2008a,b, 2009, 2011) and recent (this work) findings conclusively suggest the existence of a SUC receptor in brain tissue that also recognizes GHB. Activation of the presumed brain type SUC receptor (as an analogy to SUCNR1 we reference this putative receptor as SUCBR1) by agonists SUC or GHB evokes repetitive Ca^{2+} transients in astrocytes independently of neuronal signaling (Molnár et al., 2009, 2011). A sub-population of SUCBR1-triggered repetitive Ca^{2+} transients can also be activated by ATP making Ca^{2+} signaling more robust. We conjecture physiological significance for the detection of these endogenous metabolites and ATP performing energy supply dependent regulation of astroglial Ca^{2+} bursting.

SUC shaped the astroglial Ca^{2+} bursting activity in different ways. Both the absolute and relative abundance of astrocytes showing ATP-evoked, $P2Y_1$ receptor-mediated Ca^{2+} release from internal stores tended to decay with increasing [SUC]. By contrast, the astroglial SUC- and SUC/ATP-responsive Ca^{2+} signals were enhanced with increasing [SUC]. These findings suggest the occurrence of distinct ATP-responsive astrocytic sub-populations that can be distinguished by their responsiveness to SUC. These findings imply several mechanistic clues reasoning reduced responsiveness to ATP: (i) refilling of Ca^{2+} stores may take longer after activation by SUC and/or (ii) SUCBR1 may desensitize slower than $P2Y_1$. These mechanistic clues, however, does not rationalize why the relative abundance of cells responsive to both SUC and ATP increases with [SUC]. Such a unique phenomenon can be explained by supposing that the presence of SUCBR1 may make desensitization of $P2Y_1$ slower, also implying co-localization of SUCBR1 and $P2Y_1$ receptors in the SUC/ATP-responsive sub-population of astrocytes.

Identity of SUC-sensitive GHB (Molnár et al., 2006) and GHB-sensitive SUC (Molnár et al., 2008a) binding sites in rat forebrain and human NAc membrane homogenates has previously been disclosed (Molnár et al., 2008b). We have shown that drug of abuse (Wong et al., 2003, 2004), dietary supplement for body builders (Camacho et al., 2005) and brain metabolite (Bessman and Fishbein, 1963) GHB also activates store-dependent astrocytic Ca^{2+} transients in the brain reward area NAc (Molnár et al., 2009). Moreover, binding of GHB and SUC can be characterized by interaction with CBX (Molnár et al., 2006, 2008a,b), a blocker of gap junctions that are major players in astroglial Ca^{2+} wave propagation (Finkbeiner, 1992). In spite of their disclosure, molecular and cellular characterization of binding effects (Molnár et al., 2006, 2008a,b, 2009, 2011), the functional significance of astroglial SUC receptor recognizing GHB was less appreciated. Thus metabolic actions of GHB may be explained by the activation of the SUCBR1 signaling route.

Understanding of the role of Ca^{2+} signaling in astrocytes at neuronal and vascular interfaces through specific intercellular communication mechanisms has grown considerably in recent years (Newman and Zahs, 1997; Scemes et al., 2000; Parri et al., 2001; Matthias et al., 2003; Verkhratsky, 2006; Fiacco et al., 2007; Iadecola and Nedergaard, 2007; Sadaogopan et al., 2007; Barres, 2008; Gordon et al., 2008; Hall and Attwell, 2008; Li et al., 2008; Doengi et al., 2009; Hoogland and Kuhn, 2010; Hoogland et al., 2009; Koehler et al., 2009; Nimmerjahn, 2009; Nimmerjahn et al., 2009; Agulhon et al., 2010; Hamilton and Attwell, 2010; Xi et al., 2010). It may have significance in this respect that we observed SUC/GHB and ATP-responsive cells around NAc vessels at the end feet of astroglial processes. Representative image indicating SUC-evoked Ca^{2+} transient in a sub-population of ATP-responsive astrocytes (**Figure 5A** circles and arrows, respectively) along with a vessel contoured by Cx43 positive plaques (**Figure 5A** middle and right panels). GFAP and Cx43 expression in cerebrocortical astrocyte end feet plastered at the vessel wall has previously been characterized (Simard et al., 2003). Accordingly, double immunolabelling for Cx43 and GFAP showed large Cx43-immunoreactive plaques interconnecting astrocytic GFAP-positive end feet along with vessels in the NAc (**Figure 5B**). Co-localization of SUC-responsive astrocytes and vessel wall may provide a mechanistic clue for cellular energy metabolite-responsive Ca^{2+} signaling activity around vessels, at the end feet of astrocyte processes interconnected by gap junctional plaques. The setting can possibly imply a role for Ca^{2+} signaling at the glio-vascular interface. Regulation of Ca^{2+} bursting through cellular energy metabolites may in turn provide a mechanism for the control of astrocyte activation and will therefore benefit from further study in awake, behaving animal.

ACKNOWLEDGMENTS

This work was supported by TECH-09-A1-2009-0117 and CRC-HAS-2009-Nanotransport grants. The authors thank Erzsébet Kútiné-Fekete for excellent technical assistance.

SUPPLEMENTARY MATERIAL

The Movie S1 for this article can be found online at http://www.frontiersin.org/neuroenergetics/10.3389/fnene.2011.00007/abstract

Movie S1 | File name: 3-31-29_PM-diff.avi. Ca^{2+} signaling evoked by GHB and ATP in the acute NAc slice from the rat brain. Movie of time measurement showing GHB (50 μM) and ATP (100 μM) application onto a Fluo-4 AM loaded acute, 300 μm thick NAc slice. GHB was applied between 0 and 2 min in the perfusion buffer. ATP was applied for 60 s starting from 1.5 min through a glass micropipette right above the tissue surface. Image acquisition frequency was 2 s in depth of ∼25 μm from the slice surface. The background fluorescence (first frame) was subtracted from all subsequent frames in the image stack. The resulting images were false colored (more red pixels represent higher dF/F_0 values) and converted to avi file by ImageJ 1.44 image processing and analysis software.

REFERENCES

Agulhon, C., Fiacco, T. A., and McCarthy, K. D. (2010). Hippocampal short- and long-term plasticity are not modulated by astrocyte $Ca2^+$ signaling. *Science* 327, 1250–1254.

Anderson, C. M., Bergher, J. P., and Swanson, R. A. (2004). ATP-induced ATP release from astrocytes. *J. Neurochem.* 88, 246–256.

Andriamampandry, C., O. Taleb, O., Kemmel, V., Humbert, J. P., Aunis, D., and M. Maitre, M. (2007). Cloning and functional characterization of a gamma-hydroxybutyrate receptor identified in the human brain. *FASEB J.* 21, 885–895.

Andriamampandry, C., Taleb, O., Viry, S., Muller, C., Humbert, J. P., Gobaille, S., Aunis, D., and Maitre, M. (2003). Cloning and characterization of a rat brain receptor that binds the endogenous neuromodulator gamma-hydroxybutyrate (GHB). *FASEB J.* 17, 1691–1693.

Barres, B. A. (2008). The mystery and magic of glia: a perspective on their roles in health and disease. *Neuron* 60, 430–440.

Barry, V. A., and Cheek, T. R. (1994). Extracellular ATP triggers two functionally distinct calcium signalling pathways in PC12 cells. *J. Cell Sci.* 107, 451–462.

Beierlein, M., and Regehr, W. G. (2006). Brief bursts of parallel fiber activity trigger calcium signals in Bergmann glia. *J. Neurosci.* 26, 6958–6967.

Berridge, K. C., and Kringelbach, M. L. (2008). Affective neuroscience of pleasure: reward in humans and animals. *Psychopharmacology* 199, 457–480.

Bessman, S. P., and Fishbein, W. N. (1963). Gamma-hydroxybutyrate, a normal brain metabolite. *Nature* 200, 1207–1208.

Camacho, A., Matthews, S. C., Murray, B., and Dimsdale, J. E. (2005). Use of GHB compounds among college students. *Am. J. Drug Alcohol Abuse* 31, 601–607.

D'Ascenzo, M., Fellin, T., Terunuma, M., Revilla-Sanchez, R., Meaney, D. F., Auberson, Y. P., Moss, S. J., and Haydon, P. G. (2007). mGluR5 stimulates gliotransmission in the nucleus accumbens. *Proc. Natl. Acad. Sci. U.S.A.* 104, 1995–2000.

Doengi, M., Hirnet, D., Coulon, P., Pape, H. P., Deitmer, J. W., and Lohr, C. (2009). GABA uptake-dependent $Ca2^+$ signaling in developing olfactory bulb astrocytes. *Proc. Natl. Acad. Sci. U.S.A.* 106, 17570–17575.

Fiacco, T. A., Agulhon, C., Taves, S. R., Petravicz, J., Casper, K. B., Dong, X., Chen, J., and McCarthy, K. D. (2007). Selective stimulation of astrocyte calcium in situ does not affect neuronal excitatory synaptic activity. *Neuron* 54, 611–626.

Finkbeiner, S. (1992). Calcium waves in astrocytes-filling in the gaps. *Neuron* 8, 1101–1108.

Fischer, W., Appelt, K., Grohmann, M., Franke, H., Nörenberg, W., and Illes, P. (2009). Increase of intracellular $Ca2^+$ by P2X and P2Y receptor-subtypes in cultured cortical astroglia of the rat. *Neuroscience* 160, 767–783.

Forni, L. G., McKinnon, W., Lord, G. A., Treacher, D. F., Peron, J. M., and Hilton, P. J. (2005). Circulating anions usually associated with the Krebs cycle in patients with metabolic acidosis. *Crit. Care* 9, 591–595.

Gordon, G. J. R., Choi, H. B., Rungta, R. L., Ellis-Davies, G. C. R., and MacVicar, B. A. (2008). Brain metabolism dictates the polarity of astrocyte control over arterioles. *Nature* 456, 745–750.

Hall, C. N., and Attwell, D. (2008). Neuroscience: brain power. *Nature* 456, 715–716.

Hamilton, N. B., and Attwell, D. (2010). Do astrocytes really exocytose neurotransmitters? *Nat. Rev. Neurosci.* 11, 227–238.

He, W., Miao, F. J. P., Lin, D. C. H., Schwandner, R. T., Wang, Z., Gao1 J, Chen, J. L., Tian, H., and Ling, L. (2004). Citric acid cycle intermediates as ligands for orphan G-protein-coupled receptors. *Nature* 429, 188–193.

Helmetag, V., Samel, S. A., Thomas, M. G., Marahiel, M. A., and Essen, L. O. (2009). Structural basis for the erythro-stereospecificity of the L-arginine oxygenase VioC in viomycin biosynthesis. *FEBS J.* 276, 3669–3682.

Hirase, H., Qian, L., and Barthó P, Buzsáki G. (2004). Calcium dynamics of cortical astrocytic networks in vivo. *PLoS Biol.* 2, 0494–0499. doi:10.1371/journal.pbio.0020096

Hochachka, P. W., and Dressendorfer, R. H. (1976). Succinate accumulation in man during exercise. *Eur. J. Appl. Physiol. Occup. Physiol.* 35, 235–242.

Hoogland, T. M., and Kuhn, B. (2010). Recent developments in the understanding of astrocyte function in the cerebellum in vivo. *Cerebellum* 9, 264–271.

Hoogland, T. M., Kuhn, B., Gobel, W., Huang, W., Nakai, J., Helmchen, F., Flint, J., and Wang, S. S. (2009). Radially expanding transglial calcium waves in the intact cerebellum. *Proc. Natl. Acad. Sci. U.S.A.* 106, 3496–3501.

Iadecola, C., and Nedergaard, M. (2007). Glial regulation of the cerebral microvasculature. *Nat. Neurosci.* 10, 1369–1376.

Kaupmann, K., Cryan, J. F., Wellendorph, P., Mombereau, C., Sansig, G., Klebs, K., M. Schmutz, M., Froestl, W., van der Putten, H., Mosbacher, J., Bräuner-Osborne, H., Waldmeier, P. B., and Bettler, B. (2003). Specific gamma-hydroxybutyrate-binding sites but loss of pharmacological effects of gamma-hydroxybutyrate in GABA(B) (1)-deficient mice. *Eur. J. Neurosci.* 18, 2722–2730.

Koehler, R. C., Roman, R. J., and Harder, D. R. (2009). Astrocytes and the regulation of cerebral blood flow. *Trends Neurosci.* 32, 160–169.

Krebs, H. A. (1950). Chemical composition of blood plasma and serum. *Annu. Rev. Biochem.* 19, 409–430.

Kushnir, M. M., Komaromy-Hiller, G., Shushan, B., Urry, F. M., and Roberts, W. L. (2001). Analysis of dicarboxylic acids by tandem mass spectrometry. High-throughput quantitative measurement of methylmalonic acid in serum, plasma, and urine. *Clin. Chem.* 47, 1993–2002.

Li, A., Xi, Q., Umstot, E. S., Bellner, L., Schwartzman, M. L., Jaggar, J. H., and Leffler, C. W. (2008). Astrocyte-derived CO is a diffusible messenger that mediates glutamate-induced cerebral arteriolar dilation by activating smooth muscle cell KCa channels. *Circ. Res.* 102, 234–241.

Li, Y., Holtzclaw, L. A., and Russell, J. T. (2001). Müller cell $Ca2^+$ waves evoked by purinergic receptor agonists in slices of rat retina. *J. Neurophysiol.* 85, 986–994.

MacMillan, V. (1980a). Sequential alterations of cerebral carbohydrate metabolism associated with gamma-hydroxybutyrate. *Brain Res.* 183, 123–134.

MacMillan, V. (1980b). Effects of gamma-hydroxybutrate and gamma-butyrolactone on cerebral energy metabolism during exposure and recovery from hypoxemia-oligemia. *Stroke* 11, 271–277.

Mamelak, M. (1989). Gamma hydroxybutyrate: an endogenous regulator of energy metabolism. *Neurosci. Biobehav. Rev.* 13, 187–198.

Matthias, K., Kirchhoff, F., Seifert, G., Huttmann, K., Matyash, M., Kettenmann, H., and Steinhauser, C. (2003). Segregated expression of AMPA-type glutamate receptors and glutamate transporters defines distinct astrocyte populations in the mouse hippocampus. *J. Neurosci.* 23, 1750–1758.

Molnár, T., Antal, K., Nyitrai, G., and Emri, Z. (2009). Gamma-hydroxybutyrate (GHB) induces GABAB receptor independent intracellular $Ca2^+$ transients in astrocytes, but has no effect on GHB or GABAB receptors of medium spiny neurons in the nucleus accumbens. *Neuroscience* 162, 268–281.

Molnár, T., Barabás, P., Héja, L., Fekete, E. K., Lasztóczi, B., Szabó P, Nyitrai, G., Simon-Trompler, E., Hajós F, Palkovits, M., and Kardos, J. (2008a). Gamma-hydroxybutyrate binds to the synaptic site recognizing succinate monocarboxylate: a new hypothesis on astrocyte-neuron interaction via the protonation of succinate. *J. Neurosci. Res.* 86, 1566–1576.

Molnár, T., Visy, J., Simon, A., Moldvai, I., Temesvári-Major, E., Dörnyei, G., Kútiné Fekete, E. K. and Kardos, J. (2008b) Validation of high-affinity binding sites for succinic acid through distinguishable binding of gamma-hydroxybutyric acid receptor-specific NCS 382 antipodes. *Bioorg. Med. Chem. Lett.* 18, 6290–6292.

Molnár, T., Dobolyi, Á., Nyitrai, G., Barabás, P., Héja, L., Emri, Z., Palkovits, M., and Kardos, J. (2011). Calcium signals in the nucleus accumbens: activation of astrocytes by ATP and succinate. *BMC Neurosci.* 12, 96. doi:10.1186/1471-2202-12-96

Molnár, T., Fekete, E. K., Kardos, J., Simon-Trompler, E., Palkovits, M., and Emri, Z. (2006). Metabolic GHB precursor succinate binds to gamma-hydroxybutyrate receptors: characterization of human basal ganglia areas nucleus accumbens and globus pallidus. *J. Neurosci. Res.* 84, 27–36.

Newman, E. A., and Zahs, K. R. (1997). Calcium waves in retinal glial cells. *Science* 275, 844–847.

Nimmerjahn, A. (2009). Astrocytes going live: advances and challenges. *J. Physiol.* 587, 1639–1647.

Nimmerjahn, A., Mukamel, E. A., and Schnitzer, M. J. (2009). Motor behavior activates bergmann glial networks. *Neuron* 62, 400–412.

Nordmann, J., and Nordmann, R. (1961). Organic acids in blood and urine. *Adv. Clin. Chem.* 4, 53–120.

Palczewski, K., Kumasaka, T., Hori, T., Behnke, C. A., Motoshima, H., Fox, B. A., Le Trong, I., Teller, D. C., Okada, T., Stenkamp, R. E., Yamamoto, M., and Miyano, M. (2000). Crystal structure of rhodopsin: a G protein-coupled receptor. *Science* 289, 739–745.

Parri, H. R., Gould, T. M., and Crunelli, V. (2001). Spontaneous astrocytic $Ca2^{+}$ oscillations in situ drive NMDAR-mediated neuronal excitation. *Nat. Neurosci.* 8, 803–812.

Piet, R., and Jahr, C. E. (2007). Glutamatergic and purinergic receptor-mediated calcium transients in Bergmann glial cells. *J. Neurosci.* 27, 4027–4035.

Porter, J. T., and McCarthy, K. D. (1996). Hippocampal astrocytes in situ respond to glutamate released from synaptic terminals. *J. Neurosci.* 16, 5073–5081.

Prosser, H. M., Gill, C. H., Hirst, W. D., Grau, E., Robbins, M., Calver, A., Soffin, E. M., Farmer, C. E., Lanneau, C., Gray, J., Schenck, E., Warmerdam, B. S., Clapham, C., Reavill, C., Rogers, D. C., Stean, T., Upton, N., Humphreys, K., Randall, A., Geppert, M., Davies, C. H., and Pangalos, M. N. (2001). Epileptogenesis and enhanced prepulse inhibition in GABA(B1)-deficient mice. *Mol. Cell. Neurosci.* 17, 1059–1070.

Rumigny, J. F., Maitre, M., Cash, C., and Mandel, P. (1981). Regional and subcellular localization in rat brain of the enzymes that can synthesize gamma-hydroxybutyric acid. *J. Neurochem.* 36, 1433–1438.

Sadagopan, N., Li, W., Roberds, S. L., Major, T., Preston, G. M., Yu, Y., and Tones, M. A. (2007). Circulating succinate is elevated in rodent models of hypertension and metabolic disease. *Am. J. Hypertens.* 20, 1209–1215.

Sali, A., and Blundell, T. L. (1993). Comparative protein modeling by satisfaction of spatial restraints. *J. Mol. Biol.* 234, 779–815.

Scemes, E., Suadicani, S. O., and Spray, D. C. (2000). Intercellular communication in spinal cord astrocytes: fine tuning between gap junctions and P2 nucleotide receptors in calcium wave propagation. *J. Neurosci.* 20, 1435–1445.

Schuler, V., Lüscher, C., Blanchet, C., Klix, N., Sansig, G., Klebs, K., Schmutz, M., Heid, J., Gentry, C., Urban, L., Fox, A., Spooren, W., Jaton, A. L., Vigouret, J., Pozza, M., Kelly, P. H., Mosbacher, J., Froestl, W., Käslin, E., Korn, R., Bischoff, S., Kaupmann, K., van der Putten, H., and Bettler, B. (2001). Epilepsy, hyperalgesia, impaired memory and loss of pre and postsynaptic GABA(B) responses in mice lacking GABA(Z(1)). *Neuron* 31, 47–58.

Simard, M., Arcuino, G., Takano, T., Liu, Q., and Nedergaard, M. (2003). Signaling at the gliovascular interface. *J. Neurosci.* 23, 9254–9262.

Stout, C. E., Costantin, J. L., Naus, C. C., and Charles, A. C. (2002). Intercellular calcium signaling in astrocytes via ATP release through connexin hemichannels. *J. Biol. Chem.* 277, 10482–10488.

Takata, N., and Hirase, H. (2008). Cortical layer 1 and layer 2/3 astrocytes exhibit distinct calcium dynamics in vivo. *PLoS ONE* 3, e2525. doi:10.1371/journal.pone.0002525

Verkhratsky, A. (2006). Glial calcium signaling in physiology and pathophysiology. *Acta Pharmacol. Sin.* 27, 773–780.

Wong, C. G., Bottiglieri, T., and Snead, OC. (2003). GABA, gamma-hydroxybutyric acid and neurological diseases. *Ann. Neurol.* 54, S3–S12.

Wong, C. G., Gibson, K. M., and Snead, O. C. (2004). From the street to the brain: neurobiology of the recreational drug gamma-hydroxybutyric acid. *Trends Pharmacol. Sci.* 25, 29–34.

Xi, Q., Umstot, E., Zhao, G., Narayanan, D., Leffler, C. W., and Jaggar, J. H. (2010). Glutamate regulates $Ca2^{+}$ signals in smooth muscle cells of newborn piglet brain slice arterioles through astrocyte- and heme oxygenase-dependent mechanisms. *Am. J. Physiol. Heart Circ. Physiol.* 298, 562–569.

Zur Nieden, R., and Deitmer, J. W. (2006). The role of metabotropic glutamate receptors for the generation of calcium oscillations in rat hippocampal astrocytes in situ. *Cereb. Cortex* 16, 676–687.

Conflict of Interest Statement: The authors declare that the research was conducted in the absence of any commercial or financial relationships that could be construed as a potential conflict of interest.

Received: 22 October 2011; accepted: 25 November 2011; published online: 12 December 2011.

Citation: Molnár T, Héja L, Emri Z, Simon Á, Nyitrai G, Pál I and Kardos J (2011) Activation of astroglial calcium signaling by endogenous metabolites succinate and gamma-hydroxybutyrate in the nucleus accumbens. Front. Neuroenerg. ***3****:7. doi: 10.3389/fnene.2011.00007*

frontiers in
PHARMACOLOGY

REVIEW ARTICLE
published: 09 April 2012
doi: 10.3389/fphar.2012.00059

The ketogenic diet as a treatment paradigm for diverse neurological disorders

Carl E. Stafstrom[1,2] and Jong M. Rho[3,4]*

[1] Department of Neurology, University of Wisconsin, Madison, WI, USA
[2] Department of Pediatrics, University of Wisconsin, Madison, WI, USA
[3] Department of Pediatrics, University of Calgary Faculty of Medicine, Calgary, AB, Canada
[4] Department of Clinical Neurosciences, University of Calgary Faculty of Medicine, Calgary, AB, Canada

Edited by:
Yuri Zilberter, INSERM U751, Faculté de Médecine Timone, France

Reviewed by:
Yuri Zilberter, INSERM U751, Faculté de Médecine Timone, France
Marta Balietti, Istituto Nazionale di Ricovero e Cura per Anziani, Italy

***Correspondence:**
Jong M. Rho, Alberta Children's Hospital, University of Calgary, 2888 Shaganappi Trail Northwest, Calgary, AB, Canada T3B 6A8.
e-mail: jmrho@ucalgary.ca

Dietary and metabolic therapies have been attempted in a wide variety of neurological diseases, including epilepsy, headache, neurotrauma, Alzheimer disease, Parkinson disease, sleep disorders, brain cancer, autism, pain, and multiple sclerosis. The impetus for using various diets to treat – or at least ameliorate symptoms of – these disorders stems from both a lack of effectiveness of pharmacological therapies, and also the intrinsic appeal of implementing a more "natural" treatment. The enormous spectrum of pathophysiological mechanisms underlying the aforementioned diseases would suggest a degree of complexity that cannot be impacted universally by any single dietary treatment. Yet, it is conceivable that alterations in certain dietary constituents could affect the course and impact the outcome of these brain disorders. Further, it is possible that a final common neurometabolic pathway might be influenced by a variety of dietary interventions. The most notable example of a dietary treatment with proven efficacy against a neurological condition is the high-fat, low-carbohydrate ketogenic diet (KD) used in patients with medically intractable epilepsy. While the mechanisms through which the KD works remain unclear, there is now compelling evidence that its efficacy is likely related to the normalization of aberrant energy metabolism. The concept that many neurological conditions are linked pathophysiologically to energy dysregulation could well provide a common research and experimental therapeutics platform, from which the course of several neurological diseases could be favorably influenced by dietary means. Here we provide an overview of studies using the KD in a wide panoply of neurologic disorders in which neuroprotection is an essential component.

Keywords: ketogenic diet, neuroplasticity, epilepsy, neurological disorders

INTRODUCTION

The ketogenic diet (KD) is now a proven therapy for drug-resistant epilepsy (Vining et al., 1998; Neal et al., 2008), and while the mechanisms underlying its anticonvulsant effects remain incompletely understood (Hartman et al., 2007; Bough and Stafstrom, 2010; Rho and Stafstrom, 2011), there is mounting experimental evidence for its broad neuroprotective properties and in turn, emerging data supporting its use in multiple neurological disease states (Baranano and Hartman, 2008). Even in patients with medically refractory epilepsy who have remained seizure-free on the KD for 2 years or more, it is not uncommon for clinicians to observe that both anticonvulsant medications and the diet can be successfully discontinued without recrudescence of seizures (Freeman et al., 2007). This intriguing clinical observation forms the basis of the hypothesis that the KD may possess anti-epileptogenic properties.

This review article explores the rationale for using the KD and related dietary treatments in neurological disorders outside of epilepsy, and summarizes the clinical experience to date. An underlying theme of such diet-based therapies is that nutrients and metabolic substrates can exert profound effects on neuronal plasticity, modifying neural circuits and cellular properties to enhance and normalize function. At a fundamental level, any disease in which the pathogenesis is influenced by abnormalities in cellular energy utilization – and this implies almost every known condition – would theoretically be amenable to the KD. It is important to acknowledge that much of the data discussed here are preliminary and anecdotal, and hence need to be validated by well-controlled prospective studies. Nevertheless, that diet and nutrition should influence brain function should not be altogether surprising, and there are already abundant clinical and laboratory data linking defects in energy metabolism to a wide variety of disease states (Waldbaum and Patel, 2010; Roth et al., 2011; Schiff et al., 2011). Thus, the potential for interesting and novel applications of the KD and related dietary therapies is almost limitless (Stafstrom, 2004).

NEUROPROTECTIVE ROLE OF THE KD

Over the past decade, investigators have identified numerous mechanisms through which the KD may provide neuroprotective activity. While a comprehensive discussion of such mechanisms is beyond the scope of this chapter, a brief discussion is warranted as such actions are intimately related to disorders that share the common feature of progressive neurodegeneration and/or cellular

bioenergetic dysfunction. The reader is referred to recent reviews for more details on this subject (Gasior et al., 2006; Acharya et al., 2008; Masino and Geiger, 2008).

Two hallmark features of KD treatment are the rise in ketone body production by the liver and a reduction in blood glucose levels. The elevation of ketones is largely a consequence of fatty acid oxidation. Specific polyunsaturated fatty acids (PUFAs) such as arachidonic acid, docosahexaenoic acid, and eicosapentaenoic acid, might themselves regulate neuronal membrane excitability by blocking voltage-gated sodium and calcium channels (Voskuyl and Vreugdenhil, 2001), reducing inflammation through activation of peroxisome proliferator-activated receptors (PPARs; Cullingford, 2008; Jeong et al., 2011), or inducing expression of mitochondrial uncoupling proteins which reduce reactive oxygen species (ROS) production (Bough et al., 2006; Kim do and Rho, 2008). Ketone bodies themselves have been shown to possess neuroprotective properties, by raising ATP levels and reducing ROS production through enhanced NADH oxidation and inhibition of mitochondrial permeability transition (mPT; Kim do et al., 2007). Along similar lines of improved bioenergetics, the KD has been shown to stimulate mitochondrial biogenesis, resulting in stabilized synaptic function (Bough et al., 2006).

The second major biochemical feature of the KD is the decrease in glycolytic flux. Reduction of glycolysis is an essential feature of calorie restriction, which has been shown to suppress seizures (Greene et al., 2001) as well as prolong the lifespan of numerous species, including primates (Kemnitz, 2011; Redman and Ravussin, 2011). While the link between calorie restriction and KD mechanisms remain controversial (Yamada, 2008; Maalouf et al., 2009), it is clear that both treatments result in reduction of blood glucose, likely involving reduced glycolytic flux. In that regard, 2-deoxy-D-glucose (2DG), an analog of glucose that blocks phosphoglucose isomerase and hence inhibits glycolysis, has been shown to block epileptogenesis in the rat kindling model by decreasing the expression of brain-derived neurotrophic factor (BDNF) and its principal receptor, tyrosine kinase B (TrkB; Garriga-Canut et al., 2006). Several other important mechanisms contribute to the neuroprotective consequences of calorie restriction, including improved mitochondrial function and decreased oxidative stress (similar to that seen with ketones and PUFAs), decreased activity of pro-apoptotic factors, and inhibition of inflammatory mediators such as interleukins and tumor necrosis factor alpha (TNFα; Maalouf et al., 2009).

In the end, there are likely many other mechanisms that could contribute to the neuroprotective properties of the KD. Many of these mechanisms are thought to relate principally to the KD's anticonvulsant effects, but some if not all of them could contribute to cellular homeostasis and preventing neuronal injury or dysfunction. An important caveat, however, is that yet unidentified mechanisms may operate in diseases outside of epilepsy, and this possibility presents further opportunities for examining the pleiotropic effects of this metabolism-based therapy at a mechanistic level.

THE KD IN EPILEPSY

There is no longer any doubt that the KD is effective in ameliorating seizures in patients, especially children, with medically refractory epilepsy (Vining, 1999; Neal et al., 2008; Freeman et al., 2009). After its introduction in 1920, the KD was used as a first or second-line treatment for severe childhood epilepsy. With the introduction of anticonvulsant medications in convenient pill form, the use of the KD waned, only to resurge later in the early 1990s, due largely to the efforts of concerned parents who brought the diet back to greater public awareness (Wheless, 2008). Recent years have witnessed a remarkable surge in research on the KD, including basic science efforts as well as clinical protocols and trials (Kim do and Rho, 2008; Neal et al., 2008; Kessler et al., 2011). The KD has now become an integral part of the armamentarium of most major epilepsy centers throughout the world (Kossoff and McGrogan, 2005).

THE KD IN AGING

Aging involves the gradual decrease in function, and at times outright degeneration, of neurons and neural circuits. It is possible that by altering energy metabolism with the KD, rates of degeneration of certain neural structures and functions might be slowed (Balietti et al., 2010a). However, KDs may induce differential morphological effects in structures such as the hippocampus, perhaps as a consequence of region-specific neuronal vulnerability during the late aging process (Balietti et al., 2008). Specifically, it has been shown that the medium-chain triglyceride (MCT) form of the KD may induce detrimental synaptic changes in CA1 stratum moleculare, but beneficial effects in the outer molecular layer of the dentate gyrus (Balietti et al., 2008). In MCT-fed aged rats compared to aged rats receiving a normal diet, mitochondrial density and function in cerebellar Purkinje cells were significantly increased, suggesting that the KD can rescue age-related mitochondrial dysfunction (Balietti et al., 2010b). These observations imply certain risks, but also potential benefits of the KD for the aging brain. However, the fact that the KD reduces oxidative stress and its downstream consequences provides a reasonable rationale for considering this type of treatment to retard the adverse consequences during aging (Freemantle et al., 2009). As an example, T-maze and object recognition performance were improved in aged rats by KD administration, suggesting a potential functional benefit in cognition (Xu et al., 2010). Finally, it should be noted that because of its similarities to calorie restriction (as noted above), the KD is likely to involve other neuroprotective mechanisms that could ameliorate pathological aging – especially when occurring in the context of neurodegeneration (Contestabile, 2009).

THE KD IN ALZHEIMER DISEASE

There is growing realization that neuronal excitability is enhanced in patients with Alzheimer disease (AD; Noebels, 2011; Roberson et al., 2011). While the essential pathological processes of AD involves neuronal degeneration with accumulation of abnormal cellular products such as fibrillary plaques and tangles, recent evidence points to alterations in the function of extant neural circuits and mitochondrial homeostasis (Kapogiannis and Mattson, 2011). This view is bolstered by the higher incidence of seizures in patients with AD as compared to the unaffected population (Palop and Mucke, 2009). Therefore, there is a rationale for hypothesizing that the KD might have a beneficial role in patients with

AD (Balietti et al., 2010a), in addition to the potential benefits to the aging process as noted above. One should note, importantly, that if ketone bodies are indeed the primary mediators that counter aging and neurodegeneration in AD, implementation of the KD should be tempered by known age-related differences in the production and extraction of ketones (i.e., this is more efficient in young animals), as well as age-specific regional differences in ketone utilization within the brain (Nehlig, 1999).

Clinical studies to date have been equivocal but promising. A randomized double-blind, placebo-controlled trial of a MCT KD resulted in significantly improved cognitive functioning in APOε4-negative patients with AD but not in patients with a APOε4 mutation (Henderson et al., 2009). In this study, the primary cognitive end-points measured were the mean change from baseline in the AD Assessment Scale-Cognitive subscale, and global scores in the AD Cooperative Study – Clinical Global Impression of Change (Henderson et al., 2009). This significant clinical improvement was considered to be secondary to improved mitochondrial function, since ketone bodies (specifically, beta-hydroxybutyrate or BHB) have been shown to protect against the toxic effects of β-amyloid on neurons in culture (Kashiwaya et al., 2000). Alternatively, the KD may actually decrease amounts of β-amyloid deposition (VanderAuwera et al., 2005). Interestingly, other diets such as the Mediterranean diet are showing some promise in AD (Gu et al., 2010), possibly through a reduction in systemic inflammation and improved metabolic profiles.

Recent studies have shown a closer linkage of AD to epilepsy. For example, animal models of AD exhibit neuronal hyperexcitability and enhanced propensity to seizures (Palop et al., 2007; Roberson et al., 2011); these models may ultimately allow for detailed analyses of both cognitive and anticonvulsant effects of the KD or other dietary manipulations such as calorie restriction. Transgenic AD mice fed 2DG demonstrated better mitochondrial function, less oxidative stress, and reduced expression of amyloid precursor protein and β-amyloid compared to control animals (Yao et al., 2011).

Another pathophysiological mechanism hypothesized to operate in AD ties together altered mitochondrial function and glucose metabolism, i.e., accumulation of advanced glycation endproducts (AGE; Srikanth et al., 2011). AGE accumulation is a process of normal aging that is accelerated in AD; proteins are non-enzymatically glycosylated and this cross-linking of proteins accentuates their dysfunction. One proposed mechanism is increased ROS and free radical formation, which, as discussed above, hampers mitochondrial function. The intriguing possibility that AGE inhibitors (e.g., aminoguanidine, tenilsetam, carnosine) could act in concert with the KD or antioxidants in retarding AD progression remains speculative at this time.

Thus, there is growing evidence that the KD may be an effective treatment for AD through a variety of metabolism-induced mechanisms that reduce oxidative stress and neuroinflammation, and enhance bioenergetic profiles – largely through enhanced mitochondrial functioning. However, caution should be exercised in extrapolating findings in animals to humans, as discrepancies in terms of both clinical efficacy and untoward side-effects have been noted. For example, adverse reactions to calorie restriction have been reported in some rodent models (Maalouf et al., 2009), and in hippocampus, abnormal morphological synaptic changes have been observed in CA1 stratum moleculare (Balietti et al., 2008).

THE KD IN PARKINSON DISEASE

The primary pathophysiology in Parkinson disease (PD) is excitotoxic degeneration of dopaminergic neurons in the substantia nigra, leading to abnormalities of movement, and to an increasing extent, in cognition and other cortical functions. How could the KD benefit patients with PD? Based on the recognition that ketone bodies may bypass defects in mitochondrial complex I activity that have been implicated in PD, a small clinical study demonstrated that 5 of 7 affected patients showed improved scores on a standard PD rating scale (Vanitallie et al., 2005); however, given the small sample size, a placebo effect cannot be ruled out. In animal models of PD produced by 1-methyl-4-phenyl-1,2,3,6-tetrahydropyridine (MPTP), BHB administration ameliorated the mitochondrial respiratory chain damage that ordinarily results from that toxin (Kashiwaya et al., 2000). Additional evidence supporting the potential benefits of ketone bodies in PD is provided by *in vitro* experiments demonstrating the protective effects of these substrates against mitochondrial respiratory chain dysfunction induced exogenously by complex I and II inhibitors rotenone and 3-nitropropionic acid, respectively (Kim do et al., 2010), and even anti-inflammatory actions of the KD on MPTP-induced neurotoxicity (Yang and Cheng, 2010). It would be of interest to determine whether commercially available treatments that augment ketonemia – e.g., the MCT-based formulation used in a recent Alzheimer's clinical trial (Henderson et al., 2009) – might benefit patients with PD.

THE KD IN AMYOTROPHIC LATERAL SCLEROSIS

Amyotrophic lateral sclerosis (ALS) is a rapidly progressive disease due to degeneration of motor neurons of the cortex and anterior horn of the spinal cord. As a consequence, voluntary motor activity gradually deteriorates, leaving the affected individual profoundly weak despite largely retained cognitive functioning. The essential pathophysiological mechanisms that underlie this relentless disorder are yet to be fully elucidated, but similar to other neurodegenerative disorders, the involvement of energy-producing systems likely play a role and mitochondrial dysfunction probably contributes to disease pathogenesis. In this regard, the KD may be a promising adjunctive treatment for this devastating disease (Siva, 2006), as evidenced in a mouse model of ALS, produced by knocking out the gene encoding the copper/zinc superoxide dismutase SOD1-G93A, causing progressive muscle weakness and death by respiratory failure. Administration of a KD to these mutant mice led to both histological (higher motor neuron counts) and functional improvements (preserved motor function on the rotorod test) compared to non-KD fed animals (Zhao et al., 2006). However, the KD did not extend survival time compared to non-KD fed control mice. Mitochondria from these mutant mice demonstrated increased ATP synthesis, countering the inhibition of complex I of the electron transport chain. It is important to note that approximately 20% of the familial cases of ALS have SOD1 mutations, and hence the possibility arises that the KD may be of benefit to patients with ALS.

One potentially important consideration in this regard – applicable to all neurodegenerative diseases – is determining whether timing of intervention is crucial for a protective effect by KD treatment. Neurological disorders in late stages of progression may have such extreme neuronal dysfunction and death to allow a "refueling" with metabolic substrates to help recover integrity and function. Certainly, this appears to be the case in a small pilot study of KD treatment in patients with Lafora body disease (Cardinali et al., 2006).

THE KD IN CANCER

Cells that exhibit the most active metabolic rates (i.e., cancer cells) are most sensitive to the lack of metabolic energy to fuel their activity, a well-recognized biochemical phenomenon known as the Warburg effect. Theoretically, depriving rapidly dividing, highly metabolic cancer cells of their usual fuel supply, e.g., glucose (by use of the KD or 2DG), could be clinically therapeutic (Aft et al., 2002; Pelicano et al., 2006; Otto et al., 2008). Despite this well documented cellular observation, the KD has only recently been considered as a clinical treatment in the oncology field.

Pioneering work by Seyfried et al. (2011) over the past decade has shown that animals with experimentally produced brain tumors placed on a KD exhibit markedly decreased tumor growth rates, and these remarkable effects appear to be a consequence of calorie restriction (i.e., reduced blood glucose levels) rather than KD-induced ketosis (i.e., fatty acid oxidation) as the principal mechanism. Other investigators have found similar effects of the KD in animal models. One group found that the KD reduces ROS production in malignant glioma cells, and gene microarray expression profiling demonstrated that the KD induces an overall reversion to patterns seen in non-tumor specimens and a reduction in the expression of genes encoding signal transduction pathways and growth factors known to be involved in glioma growth (Stafford et al., 2010). It is also interesting to note that PPARα-activated by nutrients such as fatty acids – is now a target for developing anti-cancer drugs that target mitochondrial metabolism (Grabacka et al., 2010).

While clinical validation of this phenomenon is not yet forthcoming, there are several case reports suggesting that the KD may be efficacious in humans with brain tumors. Nebeling et al. (1995) reported beneficial effects of an MCT-based diet in two pediatric patients with advanced stage malignant astrocytomas. More recently, Zuccoli et al. (2010) described a case study of an elderly woman with glioblastoma multiforme who was treated with standard radiotherapy plus concomitant temozolomide therapy together with a calorie-restricted KD, and a complete absence of brain tumor tissue was noted on FDT–PET and MRI imaging after 2 months of treatment – results the authors attributed in part to the adjunctive dietary treatment. Further, in a pilot trial of the KD in 16 patients with advanced metastatic tumors, six individuals reported improved emotional functioning and less insomnia, indicating that in some instances, the KD may lead to improved quality of life (Schmidt et al., 2011). In contrast, a retrospective examination of five patients with tuberous sclerosis complex treated with the KD indicated either a lack of tumor suppression or further tumor growth (Chu-Shore et al., 2010). Thus, it may be that distinct tumor types within different organ systems may respond differently to the KD or other dietary treatments and that such differences may reflect variations in the metabolic vulnerability of specific tumor types, perhaps through intrinsic differences in the expression of metabolism-related genes (Stafford et al., 2010).

THE KD IN STROKE

To date, no clinical trials of the KD have been performed in patients with stroke, but several animal studies of hypoxia-ischemia support the potential beneficial effect of the diet. Most of these models entail pre-treatment with the KD (or with BHB), resulting in decreased structural and functional damage from the stroke. For example, Tai et al. (2008) utilized a cardiac arrest model in rats and found significantly reduced Fluoro-Jade staining in animals that underwent 25 days of pre-treatment with the KD. These investigators later determined that these effects were not due to involvement of plasmalemmal ATP-sensitive potassium channels (Tai et al., 2009), which have been implicated in ketone body action (Ma et al., 2007). Other researchers have hypothesized that the neuroprotective properties of ketone bodies might be related to up-regulation of hypoxia inducible factor (HIF1-α) which is important in angiogenesis and anti-apoptotic activity (Puchowicz et al., 2008). In that study, pre-treatment with BHB (via intraventricular infusion, followed by middle cerebral artery occlusion) led to significant increases in brain succinate content, as well as elevations in HIF1-α and Bcl-2, an anti-apoptotic protein. To be clinically meaningful, of course, a positive effect must be demonstrable after, and not before, an ischemic event. Nevertheless, such studies imply that biochemical alterations that favor energy metabolism would be protective against acute forms of severe brain injury.

THE KD IN MITOCHONDRIAL DISORDERS

As mentioned above, given the growing evidence that the KD enhances mitochondrial functioning and biogenesis (Bough et al., 2006; Maalouf et al., 2009; Kim do et al., 2010), it is logical to ask whether patients with known mitochondrial cytopathies might derive a benefit from the KD and/or ketone bodies such as BHB. At the same time, it must be considered that inherent mitochondrial dysfunction might predispose individuals to adverse toxicities from high fatty acid loads that could overwhelm β-oxidation within the mitochondrial matrix. Experimental data described above attest to significant improvements in mitochondrial function, and many lines of evidence point to the rationale of therapeutically targeting mitochondrial bioenergetics for other disease states (Wallace et al., 2010), but is there any clinical evidence in patients with intrinsic mitochondrial disorders? Kang et al. (2007) reported that the KD was both safe and effective in 14 pediatric patients with established mitochondrial defects in complexes I, II, and IV, all of whom had medically intractable epilepsy. These authors observed that half of these patients became seizure-free on the KD, and only four patients failed to respond. Hence, these preliminary data suggest that the KD is not necessarily contraindicated in patients with mitochondrial respiratory chain abnormalities. However, KD treatment is not recommended in individuals with primary carnitine deficiencies [including mutations in carnitine palmitoyl transferase (CPT) I or II and mitochondrial translocase] and fatty acid β-oxidation abnormalities (e.g., medium-chain acyl dehydrogenase deficiency; Kossoff et al.,

2009). Thus, it is critical to determine the specific mitochondrial defect when considering treatment with the KD, to avert clinical deterioration.

THE KD IN BRAIN TRAUMA

Unfortunately, the incidence of brain injury is increasing in both civilian and military contexts. Brain injury, either due to a penetrating injury or to blunt/blast trauma, can lead to severe cognitive and motor consequences. Further, the occurrence of epilepsy months to years following brain trauma adds to the morbidity of affected individuals, and speaks to the emergence of hyperexcitable neuronal circuits over time. Hence, in light of the clinical problem of post-traumatic epileptogenesis and the fact that the KD can reduce seizure activity, the notion has emerged that dietary therapy might ameliorate brain injury and possibly, long-term consequences such as epilepsy.

Several recent animal studies support this idea, and investigators have principally focused on ketone bodies (Prins, 2008a). Using a controlled cortical impact (CCI) injury model, Prins et al. (2005) showed that pre-treatment with a KD significantly reduced cortical contusion volume in an age-related manner that correlated with maturation-dependent differences in cerebral metabolism and ketone utilization. Later, they showed that cognitive and motor functioning was also improved with KD treatment (Appelberg et al., 2009). Further, using a weight drop model, Hu et al. (2009) showed that the KD pre-treatment reduced Bcl-2 (also known as Bax) mRNA and protein levels 72 h after trauma, indicating that apoptotic neurodegeneration could be prevented with this diet. Consistent with these observations, it was found that fasting – which shares the key feature of ketosis with the KD – led to significant tissue sparing in brain following CCI injury, and that again ketosis (with improved mitochondrial functioning) rather than the relative hypoglycemia seen with fasting was the important determinant of neuroprotection (Davis et al., 2008).

With respect to anti-epileptogenesis following head injury, the data regarding KD effects are mixed. KD treatment – either before or after fluid percussion injury in rats – did not alter later seizure sensitivity to fluorothyl, even though the degree of hippocampal cell loss was reduced by pre- but not post-treatment (Schwartzkroin et al., 2010). Similarly, in the lithium–pilocarpine model of temporal lobe epilepsy, KD treatment prior to induction led to morphological neuroprotection in the hippocampus but did not affect latency to onset of spontaneous recurrent seizures (Linard et al., 2010). In contrast, Jiang et al. (2012) recently reported that the KD increased after-discharge thresholds and reduced generalized seizure occurrence in a rat amygdala kindling model. Thus, at this juncture, there is no consensus regarding whether the KD is anti-epileptogenic following a variety of traumatic insults and manipulations. However, given the recent finding that the KD inhibits the mammalian target of rapamycin (mTOR) pathway (McDaniel et al., 2011), which has been linked to modulation of epileptogenesis (McDaniel and Wong, 2011), further studies in different animal models are clearly warranted. What is unambiguous, nevertheless, is the age-dependence of the effects of the KD in ameliorating the consequences of head injury (Prins, 2008b; Deng-Bryant et al., 2011).

THE KD IN PSYCHIATRIC DISORDERS (DEPRESSION)

Mood stabilizing properties of the KD have been hypothesized (El-Mallakh and Paskitti, 2001), but no clinical studies have been conducted as of this writing. The potential role of the KD in depression has been studied in the forced choice model of depression in rats, which led to a beneficial effect similar to that afforded by conventional antidepressants (Murphy et al., 2004; Murphy and Burnham, 2006).

THE KD IN AUTISM

Autism is a neurodevelopmental disorder that affects language development and social function. The heterogeneous etiologies leading to autism spectrum disorders, plus the uncertainty about what causes autism in the majority of "idiopathic" cases, has hampered the development of a universally beneficial treatment, aside from symptomatic treatment of autism-related behaviors such as aggression or anxiety. Now, limited clinical evidence raises the intriguing possibility that the KD might be helpful to alleviate some of the abnormal behaviors seen in children with autism spectrum disorders. Using a KD variant consisting of MCT, 10 of 18 autistic children demonstrated moderate or significant behavioral improvement (by a blinded rater) after a 6-month trial of providing the diet for 4 weeks of KD diet treatment alternating with 2 weeks of normal diet, in 6-week cycles (Evangeliou et al., 2003). This study was carried out on the island of Crete, where the frequency of autism is high but the possibility of genetic inbreeding is also significant. Therefore, these findings need to be interpreted cautiously and larger longitudinal studies are needed. The potential involvement of adenosine, an endogenous neuromodulator and anticonvulsant, in ameliorating autistic behaviors raises the possibility of overlap with KD mechanisms (Masino et al., 2011). As a caveat, many children with autism poorly tolerate changes in dietary and other routines, which could impact implementation of dietary therapies, which require strict adherence.

THE KD IN MIGRAINE

Migraine is a paroxysmal neurological disorder having considerable clinical phenotypic overlap with epilepsy (Rogawski, 2008). Although the intrinsic mechanisms underlying seizures and migraine attacks differ in many fundamental respects, there are theoretical reasons to consider the KD for chronic migraine. Both disorders involve paroxysmal excitability changes in the brain, and there is considerable overlap in the array of pharmacological agents used to treat these conditions. Although it might seem unlikely that an individual with migraine would undertake such a complicated dietary regimen as the KD, in light of suboptimal alternatives, this choice is worthy of consideration, particularly in the medically refractory population (Maggioni et al., 2011).

Interestingly, the first report of using the KD for migraine came in 1928, only a few years after the diet's first use for epilepsy (Schnabel, 1928). Nine of 28 patients reported "some improvement," although the validity of this clinical study is uncertain and some patients admitted poor compliance. Compliance might be better with the less restrictive modified Atkins diet, which has also shown promise for migraine treatment (Kossoff et al., 2010). Other case reports exist but there are no large clinical series or trials. Notwithstanding this limitation, laboratory investigations

have found that both short-term and long-term treatment with either MCT or long-chain triglyceride forms of the KD resulted in a significant reduction in the velocity of cortical spreading depression (CSD) velocity in immature rats (de Almeida Rabello Oliveira et al., 2008). Another intriguing aspect of this study was the observation that triheptanoin – an anaplerotic substrate that enhances tricarboxylic acid cycle function – had a notable effect in retarding CSD, consistent with a later report that triheptanoin supplementation raised pentylenetetrazol tonic seizure threshold and delayed the development of corneal kindled seizures (Willis et al., 2010).

SUMMARY

Despite the relative lack of clinical data, there is an emerging literature supporting the broad use of the KD (and its variants) against a variety of neurological conditions. These preliminary studies are largely based on the fundamental idea that metabolic shifts may lead to neuroprotective actions (Gasior et al., 2006; Maalouf et al., 2009). How can a simple dietary change lead to improvement in disorders with such a huge span of pathophysiological mechanisms? Alterations in energy metabolism appear to be a common theme. So while the mechanisms through which the KD exerts such effects are likely diverse (Maalouf et al., 2009; Rho and Stafstrom, 2011), there may indeed be one or more common final pathways that are mechanistically shared. Ultimately, the details of how that altered metabolism reduces neuronal excitability, abrogates ongoing neurodegeneration, or mitigates functional disability remain unknown. Herein lay rich opportunities for further investigation, in both the laboratory and the clinic, in the broad realm of translational neurosciences.

REFERENCES

Acharya, M. M., Hattiangady, B., and Shetty, A. K. (2008). Progress in neuroprotective startegies for preventing epilepsy. *Prog. Neurobiol.* 84, 363–404.

Aft, R. L., Zhang, F. W., and Gius, D. (2002). Evaluation of 2-deoxy-D-glucose as a chemotherapeutic agent: mechanism of cell death. *Br. J. Cancer* 87, 805–812.

Appelberg, K. S., Hovda, D. A., and Prins, M. L. (2009). The effects of a ketogenic diet on behavioral outcome after controlled cortical impact injury in the juvenile and adult rat. *J. Neurotrauma* 26, 497–506.

Balietti, M., Casoli, T., DiStefano, G., Giorgetti, B., Aicardi, G., and Fattoretti, P. (2010a). Ketogenic diets: an historical antiepieptic therapy with promising potentialities for the aging brain. *Ageing Res. Rev.* 9, 273–279.

Balietti, M., Giorgetti, B., DiStefano, G., Casoli, T., Platano, D., Solazzi, M., Bertoni-Freddari, C., Aicardi, G., Lattanzio, F., and Fattoretti, P. (2010b). A ketogenic diet increases succinic dehydrogenase (SDH) activity and recovers age-related decrease in numeric density of SDH-positive mitochondria in cerebellar Purkinje cells of late-adult rats. *Micron* 41, 143–148.

Balietti, M., Giorgetti, B., Fattoretti, P., Grossi, Y., DiStefano, G., Casoli, T., Platano, D., Solazzi, M., Orlando, F., Aicardi, G., and Bertoni-Freddari, C. (2008). Ketogenic diets cause opposing changes in synaptic morphology in CA1 hippocampus and dentate gyrus of late-adult rats. *Rejuvenation Res.* 11, 631–640.

Baranano, K. M., and Hartman, A. L. (2008). The ketogenic diet: uses in epilepsy and other neurologic illnesses. *Curr. Treat. Options Neurol.* 10, 410–419.

Bough, K. J., and Stafstrom, C. E. (2010). "The ketogenic diet: scientific principles underlying it use," in *Epilepsy: Mechanisms, Models, and Translational Perspectives*, eds J. M. Rho, R. Sankar, and C. E. Stafstrom (Boca Raton, FL: CRC Press), 417–439.

Bough, K. J., Wetherington, J., Hassel, B., Pare, J. F., Gawryluk, J. W., Greene, J. G., Shaw, R., Smith, Y., Geiger, J. D., and Dingledine, R. J. (2006). Mitochondrial biogenesis in the anticonvulsant mechanism of the ketogenic diet. *Ann. Neurol.* 60, 223–235.

Cardinali, S., Canafoglia, L., Bertoli, S., Franceschetti, S., Lanzi, G., Tagliabue, A., and Veggiotti, P. (2006). A pilot study of a ketogenic diet in patients with Lafora body disease. *Epilepsy Res.* 69, 129–134.

Chu-Shore, C. J., Major, P., Camposano, S., Muzykewicz, D., and Thiele, E. A. (2010). The natural history of epilepsy in tuberous sclerosis complex. *Epilepsia* 51, 1236–1241.

Contestabile, A. (2009). Benefits of caloric restriction on brain aging and related pathological states: understanding mechanisms to devise novel therapies. *Curr. Med. Chem.* 16, 350–361.

Cullingford, T. (2008). Peroxisome proliferator-activated receptor alpha and the ketogenic diet. *Epilepsia* 49(Suppl. 8), 70–72.

Davis, L. M., Pauly, J. R., Readnower, R. D., Rho, J. M., and Sullivan, P. G. (2008). Fasting is neuroprotective following traumatic brain injury. *J. Neurosci. Res.* 86, 1812–1822.

de Almeida Rabello Oliveira, M., da Rocha Ataíde, T., de Oliveira, S. L., de Melo Lucena, A. L., de Lira, C. E., Soares, A. A., de Almeida, C. B., Ximenes da Silva, A. (2008). Effects of short-term and long-term treatment with medium- and long-chain triglycerides ketogenic diet on cortical spreading depression in young rats. *Neurosci. Lett.* 434, 66–70.

Deng-Bryant, Y., Prins, M. L., Hovda, D. A., and Harris, N. G. (2011). Ketogenic diet prevents alterations in brain metabolism in young but not adult rats after traumatic brain injury. *J. Neurotrauma* 28, 1813–1825.

El-Mallakh, R. S., and Paskitti, M. E. (2001). The ketogenic diet may have mood-stabilizing properties. *Med. Hypotheses* 57, 724–726.

Evangeliou, A., Vlachonikolis, I., Mihailidou, H., Spilioti, M., Skarpalezou, A., Makaronas, N., Prokopiou, A., Christodoulou, P., Liapi-Adamidou, G., Helidonis, E., Sbyrakis, S., and Smeitink, J. (2003). Application of a ketogenic diet in children with autistic behavior: pilot study. *J. Child Neurol.* 18, 113–118.

Freeman, J. M., Kossoff, E. H., Freeman, J. B., and Kelly, M. T. (2007). *The Ketogenic Diet – A Treatment for Children and Others with Epilepsy*. New York: Demos Publications.

Freeman, J. M., Vining, E. P., Kossoff, E. H., Pyzik, P. L., Ye, X., and Goodman, S. N. (2009). A blinded, crossover study of the efficacy of the ketogenic diet. *Epilepsia* 50, 322–323.

Freemantle, E., Vandal, M., TremblayMercier, J., Plourde, M., Poirier, J., and Cunnane, S. C. (2009). Metabolic response to a ketogenic breakfast in the healthy elderly. *J. Nutr. Health Aging* 13, 293–298.

Garriga-Canut, M., Schoenike, B., Qazi, R., Bergendahl, K., Daley, T. J., Pfender, R. M., Morrison, J. F., Ockuly, J., Stafstrom, C., Sutula, T., and Roopra, A. (2006). 2-Deoxy-D-glucose reduces epilepsy progression by NRSF-CtBP-dependent metabolic regulation of chromatin structure. *Nat. Neurosci.* 9, 1382–1387.

Gasior, M., Rogawski, M. A., and Hartman, A. L. (2006). Neuroprotective and disease-modifying effects of the ketogenic diet. *Behav. Pharmacol.* 17, 431–439.

Grabacka, M., Pierzchalska, M., and Reiss, K. (2010). Peroxisome proliferator activated receptor α ligands as anti-cancer drugs targeting mitochondrial metabolism. *Curr. Pharm. Biotechnol.* PMID: 21133850.

Greene, A. E., Todorova, M. T., McGowan, R., and Seyfried, T. N. (2001). Caloric restriction inhibits seizure susceptibility in epileptic EL mice by reducing blood glucose. *Epilepsia* 42, 1371–1378.

Gu, Y., Luchsinger, J. A., Stern, Y., and Scarmeas, N. (2010). Mediterranean diet, inflammatory and metabolic biomarkers, and risk of Alzheimer's disease. *J. Alzheimers Dis.* 22, 483–492.

Hartman, A. L., Gasior, M., Vining, E. P. G., and Rogawski, M. A. (2007). The neuropharmacology of the ketogenic diet. *Pediatr. Neurol.* 36, 281–292.

Henderson, S. T., Vogel, J. L., Barr, L. J., Garvin, F., Jones, J. J., and Costantini, L. C. (2009). Study of the ketogenic agent AC-1202 in mild to moderate Alzheimer's disease: a randomized, double-blind, placebo-controlled, multicenter trial. *Nutr. Metab. (Lond.)* 6, 31.

Hu, Z. G., Wang, H. D., Qiao, L., Yan, W., Tan, Q. F., and Yin, H. X. (2009). The protective effect of the ketogenic diet on traumatic brain injury-induced cell death in juvenile rats. *Brain Inj.* 23, 459–465.

Jeong, E. A., Jeon, B. T., Shin, H. J., Kim, N., Lee, D. H., Kim, H. J., Kang, S. S., Cho, G. J., Choi, W. S., and Roh, G. S. (2011). Ketogenic diet-induced peroxisome proliferator-activated receptor-γ activation decreases neuroinflammation in the mouse hippocampus after kainic acid-induced seizures. *Exp. Neurol.* 232, 195–202.

Jiang, Y., Yang, Y., Wang, S., Ding, Y., Guo, Y., Zhang, M. M., Wen, S. Q., and Ding, M. P. (2012). Ketogenic diet protects against epileptogenesis as well as neuronal loss in amygdaloid-kindling seizures. *Neurosci. Lett.* 508, 22–26.

Kang, H. C., Lee, Y. M., Kim, H. D., Lee, J. S., and Slama, A. (2007). Safe and effective use of the ketogenic diet in children with epilepsy and mitochondrial respiratory chain complex defects. *Epilepsia* 48, 82–88.

Kapogiannis, D., and Mattson, M. P. (2011). Disrupted energy metabolism and neuronal circuit dysfunction in cognitive impairment and Alzheimer's disease. *Lancet Neurol.* 10, 187–198.

Kashiwaya, Y., Takeshima, T., Mori, N., Nakashima, K., Clarke, K., and Veech, R. L. (2000). D-beta-hydroxybutyrate protects neurons in models of Alzheimer's and Parkinson's disease. *Proc. Natl. Acad. Sci. U.S.A.* 97, 5440–5444.

Kemnitz, J. W. (2011). Calorie restriction and aging in nonhuman primates. *ILAR J.* 52, 66–77.

Kessler, S. K., Neal, E. G., Camfield, C. S., and Kossoff, E. H. (2011). Dietary therapies for epilepsy: future research. *Epilepsy Behav.* 22, 17–22.

Kim do, Y., Davis, L. M., Sullivan, P. G., Maalouf, M., Simeone, T. A., van-Brederode, J., and Rho, J. M. (2007). Ketone bodies are protective against oxidative stress in neocortical neurons. *J. Neurochem.* 101, 1316–1326.

Kim do, Y., and Rho, J. M. (2008). The ketogenic diet and epilepsy. *Curr. Opin. Clin. Nutr. Metab. Care* 11, 113–120.

Kim do, Y., Vallejo, J., and Rho, J. M. (2010). Ketones prevent synaptic dysfunction induced by mitochondrial respiratory complex inhibitors. *J. Neurochem.* 114, 130–141.

Kossoff, E. H., Huffman, J., Turner, Z., and Gladstein, J. (2010). Use of the modified Atkins diet for adolescents with chronic daily headache. *Cephalalgia* 30, 1014–1016.

Kossoff, E. H., and McGrogan, J. R. (2005). Worldwide use of the ketogenic diet. *Epilepsia* 46, 280–289.

Kossoff, E. H., Zupec-Kania, B. A., Amark, P. E., Ballaban-Gil, K. R., Bergqvist, C. A. G., Blackford, R., Buchhalter, J. R., Caraballo, R. H., Cross, H. J., Dahlin, M. G., Donner, E. J., Klepper, J., Jehle, R. S., Kim, H. D., Liu, C. Y. M., Nation, J., Nordli, D. R. Jr., Pfeifer, H. H., Rho, J. M., Stafstrom, C. E., Thiele, E. A., Turner, Z., Wirrell, E. C., Wheless, J. W., Veggiotti, P., and Vining, E. P. (2009). Optimal clinical management of children receiving the ketogenic diet: recommendations of the International Ketogenic Diet Study Group. *Epilepsia* 50, 304–317.

Linard, B., Ferrandon, A., Koning, E., Nehlig, A., and Raffo, E. (2010). Ketogenic diet exhibits neuroprotective effects in hippocampus but fails to prevent epileptogenesis in the lithium-pilocarpine model of mesial temporal lobe epilepsy in adult rats. *Epilepsia* 51, 1829–1836.

Ma, W., Berg, J., and Yellen, G. (2007). Ketogenic diet metabolites reduce firing in central neurons by opening K(ATP) channels. *J. Neurosci.* 27, 3618–3625.

Maalouf, M., Rho, J. M., and Mattson, M. P. (2009). The neuroprotective properties of calorie restriction, the ketogenic diet, and ketone bodies. *Brain Res. Rev.* 59, 293–315.

Maggioni, F., Margoni, M., and Zanchin, G. (2011). Ketogenic diet in migraine treatment: a brief but ancient history. *Cephalalgia* 31, 1150–1151.

Masino, S. A., and Geiger, J. D. (2008). Are purines mediators of the anticonvulsant/neuroprotective effects of ketogenic diets? *Trends Neurosci.* 31, 273–278.

Masino, S. A., Kawamura, M. Jr., Plotkin, L. M., Svedova, J., DiMario, F. J. Jr., and Eigsti, I. M. (2011). The relationship between the neuromodulator adenosine and behavioral symptoms of autism. *Neurosci. Lett.* 500, 1–5.

McDaniel, S. S., Rensing, N. R., Thio, L. L., Yamada, K. A., and Wong, M. (2011). The ketogenic diet inhibits the mammalian target of rapamycin (mTOR) pathway. *Epilepsia* 52, e7–e11.

McDaniel, S. S., and Wong, M. (2011). Therapeutic role of mammalian target of rapamycin (mTOR) inhibition in preventing epileptogenesis. *Neurosci. Lett.* 497, 231–239.

Murphy, P., and Burnham, W. M. (2006). The ketogenic diet causes a reversible decrease in activity level in Long-Evans rats. *Exp. Neurol.* 201, 84–89.

Murphy, P., Likhodii, S., Nylen, K., and Burnham, W. M. (2004). The antidepressant properties of the ketogenic diet. *Biol. Psychiatry* 56, 981–983.

Neal, E. G., Chaffe, H., Schwartz, R. H., Lawson, M. S., Edwards, N., Fitzsimmons, G., Whitney, A., and Cross, J. H. (2008). The ketogenic diet for the treatment of childhood epilepsy: a randomised controlled trial. *Lancet Neurol.* 7, 500–506.

Nebeling, L. C., Miraldi, F., Shurin, S. B., and Lerner, E. (1995). Effects of a ketogenic diet on tumor metabolism and nutritional status in pediatric oncology patients: two case reports. *J. Am. Coll. Nutr.* 14, 202–208.

Nehlig, A. (1999). Age-dependent pathways of brain energy metabolism: the suckling rat, a natural model of the ketogenic diet. *Epilepsy Res.* 37, 211–221.

Noebels, J. L. (2011). A perfect storm: converging paths of epilepsy and Alzheimer's dementia intersect in the hippocampal formation. *Epilepsia* 52(Suppl. 1), 39–46.

Otto, C., Kaemmerer, U., Illert, B., Muehling, B., Pfetzer, N., Wittig, R., Voelker, H. U., Thiede, A., and Coy, J. F. (2008). Growth of human gastric cancer cells in nude mice is delayed by a ketogenic diet supplemented with omega-3 fatty acids and medium-chain triglycerides. *BMC Cancer* 8, 122. doi:10.1186/1471-2407-8-122

Palop, J. J., Chin, J., Roberson, E. D., Wang, J., Thwin, M. T., Bien-Ly, N., Yoo, J., Ho, K. O., Yu, G. Q., Kreitzer, A., Finkbeiner, S., Noebels, J. L., and Mucke, L. (2007). Aberrant excitatory neuronal activity and compensatory remodeling of inhibitory hippocampal circuits in mouse models of Alzheimer's disease. *Neuron* 55, 697–711.

Palop, J. J., and Mucke, L. (2009). Epilepsy and cognitive impairments in Alzheimer disease. *Arch. Neurol.* 66, 435–440.

Pelicano, H., Martin, D. S., Xu, R.-H., and Huang, P. (2006). Glycolysis inhibition for anticancer treatment. *Oncogene* 25, 4633–4646.

Prins, M. L. (2008a). Cerebral metabolic adaptation and ketone metabolism after brain injury. *J. Cereb. Blood Flow Metab.* 28, 1–16.

Prins, M. L. (2008b). Diet, ketones, and neurotrauma. *Epilepsia* 49(Suppl. 8), 111–113.

Prins, M. L., Fujima, L. S., and Hovda, D. A. (2005). Age-dependent reduction of cortical contusion volume by ketones after traumatic brain injury. *J. Neurosci. Res.* 82, 413–420.

Puchowicz, M. A., Zechel, J. L., Valerio, J., Emancipator, D. S., Xu, K., Pundik, S., LaManna, J. C., and Lust, W. D. (2008). Neuroprotection in diet-induced ketotic rat brain after focal ischemia. *J. Cereb. Blood Flow Metab.* 28, 1907–1916.

Redman, L. M., and Ravussin, E. (2011). Caloric restriction in humans: impact on physiological, psychological, and behavioral outcomes. *Antioxid. Redox Signal.* 14, 275–278.

Rho, J. M., and Stafstrom, C. E. (2011). The ketogenic diet: what has science taught us? *Epilepsy Res.* doi:10.1016/j.eplepsyres.2011.05.021

Roberson, E. D., Halabisky, B., Yoo, J. W., Yao, J., Chin, J., Yanm, F., Wu, T., Hamto, P., Devidze, N., Yu, G. Q., Palop, J. J., Noebels, J. L., and Mucke, L. (2011). Amyloid-β/Fyn-induced synaptic, network, and cognitive impairments depend on tau levels in multiple mouse models of Alzheimer's disease. *J. Neurosci.* 31, 700–711.

Rogawski, M. A. (2008). Common pathophysiologic mechanisms in migraine and epilepsy. *Arch. Neurol.* 65, 709–714.

Roth, J., Szulc, A. L., and Danoff, A. (2011). Energy, evolution, and human diseases: an overview. *Am. J. Clin. Nutr.* 93, 875S–883S.

Schiff, M., Bénit, P., Coulibaly, A., Loublier, S., El-Khoury, R., and Rustin, P. (2011). Mitochondrial response to controlled nutrition in health and disease. *Nutr. Rev.* 69, 65–75.

Schmidt, M., Pfetzer, N., Schwab, M., Strauss, I., and Kämmerer, U. (2011). Effects of a ketogenic diet on the quality of life in 16 patients with advanced cancer: a pilot trial. *Nutr. Metab. (Lond.)* 8, 54.

Schnabel, T. G. (1928). An experience with a ketogenic diet in migraine. *Ann. Int. Med.* 2, 341–347.

Schwartzkroin, P. A., Wenzel, H. J., Lyeth, B. G., Poon, C. C., Delance, A., Van, K. C., Campos, L., and Nguyen, D. V. (2010). Does ketogenic diet alter seizure sensitivity and cell loss following fluid percussion injury? *Epilepsy Res.* 92, 74–84.

Seyfried, T. N., Marsh, J., Shelton, L. M., Huysentruyt, L. C., and Mukherjee, P. (2011). Is the restricted ketogenic diet a viable alternative to the standard of care for managing malignant brain cancer? *Epilepsy Res.* [Epub ahead of print].

Siva, N. (2006). Can ketogenic diet slow progression of ALS? *Lancet Neurol.* 5, 476.

Srikanth, V., Maczurek, A., Phan, T., Steele, M., Westcott, B., Juskiw, D., and Münch, G. (2011). Advanced glycation endproducts and their

receptor RAGE in Alzheimer's disease. *Neurobiol. Aging* 32, 763–777.

Stafford, P., Abdelwahab, M. G., Kimdo, Y., Preul, M. C., Rho, J. M., and Scheck, A. C. (2010). The ketogenic diet reverses gene expression patterns and reduces reactive oxygen species levels when used as an adjuvant therapy for glioma. *Nutr. Metab. (Lond.)* 7, 74.

Stafstrom, C. E. (2004). Dietary approaches to epilepsy treatment: old and new options on the menu. *Epilepsy Curr.* 4, 215–222.

Tai, K. K., Nguyen, N., Pham, L., and Truong, D. D. (2008). Ketogenic diet prevents cardiac arrest-induced cerebral ischemic neurodegeneration. *J. Neural Transm.* 115, 1011–1017.

Tai, K. K., Pham, L., and Truong, D. D. (2009). Intracisternal administration of glibenclamide or 5-hydroxydecanoate does not reverse the neuroprotective effect of ketogenic diet against ischemic brain injury-induced neurodegeneration. *Brain Inj.* 23, 1081–1088.

VanderAuwera, I., Wera, S., VanLeuven, F., and Henderson, S. T. (2005). A ketogenic diet reduces amyloid beta 40 and 42 in a mouse model of Alzheimer's disease. *Nutr. Metab. (Lond.)* 2, 28.

Vanitallie, T. B., Nonas, C., DiRocco, A., Boyar, K., Hyams, K., and Heymsfield, S. B. (2005). Treatment of Parkinson disease with diet-induced hyperketonemia: a feasibility study. *Neurology* 64, 728–730.

Vining, E., Freeman, J., Ballaban-Gil, K., Camfield, C., Camfield, P., Holmes, G., Shinnar, S., Shuman, R., Trevathan, E., and Wheless, J. (1998). A multicenter study of the efficacy of the ketogenic diet. *Arch. Neurol.* 55, 1433–1437.

Vining, E. P. G. (1999). Clinical efficacy of the ketogenic diet. *Epilepsy Res.* 37, 181–190.

Voskuyl, R. A., and Vreugdenhil, M. (2001). "Effects of essential fatty acids on voltage-regulated ionic channels and seizure thresholds in animals," in *Fatty Acids: Physiological and Behavioral Functions*, eds D. Mostofsky, S. Yehuda, and N. Jr. Salem (Totowa, NJ: Humana Press), 63–78.

Waldbaum, S., and Patel, M. (2010). Mitochondrial dysfunction and oxidative stress: a contributing link to acquired epilepsy? *J. Bioenerg. Biomembr.* 42, 449–455.

Wallace, D. C., Fan, W., and Procaccio, V. (2010). Mitochondrial energetics and therapeutics. *Annu. Rev. Pathol.* 5, 297–348.

Wheless, J. W. (2008). History of the ketogenic diet. *Epilepsia* 49(Suppl. 8), 3–5.

Willis, S., Stoll, J., Sweetman, L., and Borges, K. (2010). Anticonvulsant effects of a triheptanoin diet in two mouse chronic seizure models. *Neurobiol. Dis.* 40, 565–572.

Xu, K., Sun, X., Eroku, B. O., Tsipis, C. P., Puchowicz, M. A., and LaManna, J. C. (2010). Diet-induced ketosis improves cognitive performance in aged rats. *Adv. Exp. Med. Biol.* 662, 71–75.

Yamada, K. A. (2008). Calorie restriction and glucose regulation. *Epilepsia* 49(Suppl. 8), 94–96.

Yang, X., and Cheng, B. (2010). Neuroprotective and anti-inflammatory activities of ketogenic diet on MPTP-induced neurotoxicity. *J. Mol. Neurosci.* 42, 145–153.

Yao, J., Chen, S., Mao, Z., Cadenas, E., and Brinton, R. D. (2011). 2-Deoxy-D-glucose treatment induces ketogenesis, sustains mitochondrial function, and reduces pathology in female mouse model of Alzheimer's disease. *PLoS ONE* 6, e21788. doi:10.1371/journal.pone.0021788

Zhao, Z., Lange, D. J., Voustianiouk, A., MacGrogan, D., Ho, L., Suh, J., Humala, N., Thiyagarajan, M., Wang, J., and Pasinetti, G. M. (2006). A ketogenic diet as a potential novel therapeutic intervention in amyotrophic lateral sclerosis. *BMC Neurosci.* 7, 29. doi:10.1186/1471-2202-7-29

Zuccoli, G., Marcello, N., Pisanello, A., Servadei, F., Vaccaro, S., Mukherjee, P., and Seyfried, T. N. (2010). Metabolic management of glioblastoma multiforme using standard therapy together with a restricted ketogenic diet: case report. *Nutr. Metab. (Lond.)* 7, 33.

Conflict of Interest Statement: The authors declare that the research was conducted in the absence of any commercial or financial relationships that could be construed as a potential conflict of interest.

Received: 17 January 2012; paper pending published: 25 January 2012; accepted: 21 March 2012; published online: 09 April 2012.

Citation: Stafstrom CE and Rho JM (2012) The ketogenic diet as a treatment paradigm for diverse neurological disorders. Front. Pharmacol. ***3****:59. doi: 10.3389/fphar.2012.00059*

This article was submitted to Frontiers in Neuropharmacology, a specialty of Frontiers in Pharmacology.

frontiers in
NEUROSCIENCE

REVIEW ARTICLE
published: 26 March 2012
doi: 10.3389/fnins.2012.00033

The nervous system and metabolic dysregulation: emerging evidence converges on ketogenic diet therapy

David N. Ruskin and Susan A. Masino*

Neuroscience Program, Department of Psychology, Trinity College, Hartford, CT, USA

Edited by:
Yuri Zilberter, INSERM U751, France

Reviewed by:
Jason B. Wu, Cedars-Sinai Medical Center, USA
Robert W. Greene, University of Texas Southwestern Medical Center and Veterans Affairs Medical Center, USA

****Correspondence:***
Susan A. Masino, Neuroscience Program, Department of Psychology, Trinity College, Life Sciences Center, 300 Summit Street, Hartford, CT 06106, USA.
e-mail: susan.masino@trincoll.edu

A link between metabolism and brain function is clear. Since ancient times, epileptic seizures were noted as treatable with fasting, and historical observations of the therapeutic benefits of fasting on epilepsy were confirmed nearly 100 years ago. Shortly thereafter a high fat, low-carbohydrate ketogenic diet (KD) debuted as a therapy to reduce seizures. This strict regimen could mimic the metabolic effects of fasting while allowing adequate caloric intake for ongoing energy demands. Today, KD therapy, which forces predominantly ketone-based rather than glucose-based metabolism, is now well-established as highly successful in reducing seizures. Cellular metabolic dysfunction in the nervous system has been recognized as existing side-by-side with nervous system disorders – although often with much less obvious cause-and-effect as the relationship between fasting and seizures. Rekindled interest in metabolic and dietary therapies for brain disorders complements new insight into their mechanisms and broader implications. Here we describe the emerging relationship between a KD and adenosine as a way to reset brain metabolism and neuronal activity and disrupt a cycle of dysfunction. We also provide an overview of the effects of a KD on cognition and recent data on the effects of a KD on pain, and explore the relative time course quantified among hallmark metabolic changes, altered neuron function and altered animal behavior assessed after diet administration. We predict continued applications of metabolic therapies in treating dysfunction including and beyond the nervous system.

Keywords: adenosine, epilepsy, glucose, inflammation, long-term potentiation, metabolism, pain, seizure

THE KETOGENIC DIET AND KETONE-BASED METABOLISM

Metabolism influences brain activity, and metabolic dysfunction is associated with a wide variety of neurological disorders. The cause-and-effect relationship between metabolic and neuronal dysfunction is often unclear, though not in the case of epilepsy and diet. Historical observations noted the therapeutic benefits of fasting on epilepsy, but fasting is necessarily a time-limited practice. Therapeutic benefits of the metabolic condition of fasting were confirmed over 90 years ago when the high fat, low-carbohydrate ketogenic diet (KD) was described as alternative to fasting which still reduced epileptic seizures (Wilder, 1921). In turn, anticonvulsant drugs debuted over the next two decades, such that since then the KD has been used mostly for inoperable and medication-resistant epilepsy, which has been estimated to be 15% up to 45% of cases (Picot et al., 2008; Dong et al., 2011).

Although used clinically for many decades, prescribed most often to children, and increasing in popularity over the last two decades, the KD's mechanism of action remains controversial. The KD was designed to produce ketosis without fasting by strictly limiting carbohydrate intake (Wilder, 1921). To make up for lost calories and augment ketosis, fat content is increased dramatically. When carbohydrate intake is strongly limited (as during the KD or fasting), the liver increases production of the ketone bodies β-hydroxybutyrate, acetoacetate, and acetone from circulating fatty acids (Aoki, 1981). Because of the β-hydroxyl substitution, β-hydroxybutyrate is not actually a ketone, although by convention it is grouped with the other two ketone bodies.

Ketone bodies are released into the circulation as an alternative energy source to generate ATP ("ketolytic" metabolism) within tissues, including the brain and spinal cord. Hallmark changes in blood chemistry are produced reliably in rodents (**Figure 1**). Formulation of the KD is calculated using a ratio of fat content to combined protein and carbohydrate content, varying in the clinic from 5:1 to 1:1 depending on a patient's individual needs (Swink et al., 1997; Vining, 1999). We found that a KD-fed *ad libitum* at ratio of 7:1 or 3:1 to rats produced similar changes in blood chemistry (**Figure 1**). Clinically, the trend has been to decrease the ratio where possible and thus make the diet more palatable (including the more liberal modified Atkins diet; Kang et al., 2007; Kossoff et al., 2008b) but more systematic research is needed. Regarding different food types, the KD has now been adapted for widely varying cultures and cuisines in different countries around the world (e.g., India, Korea, United Kingdom, Saudi Arabia, Republic of Georgia; Kang et al., 2007; Neal et al., 2008a; Sharma et al., 2009; B. Zupec-Kania, personal communication). Understanding the mechanisms by which a diet controls seizures, along with broader opportunities for metabolic therapies, remains an active research topic because of accessibility, efficacy, and economics.

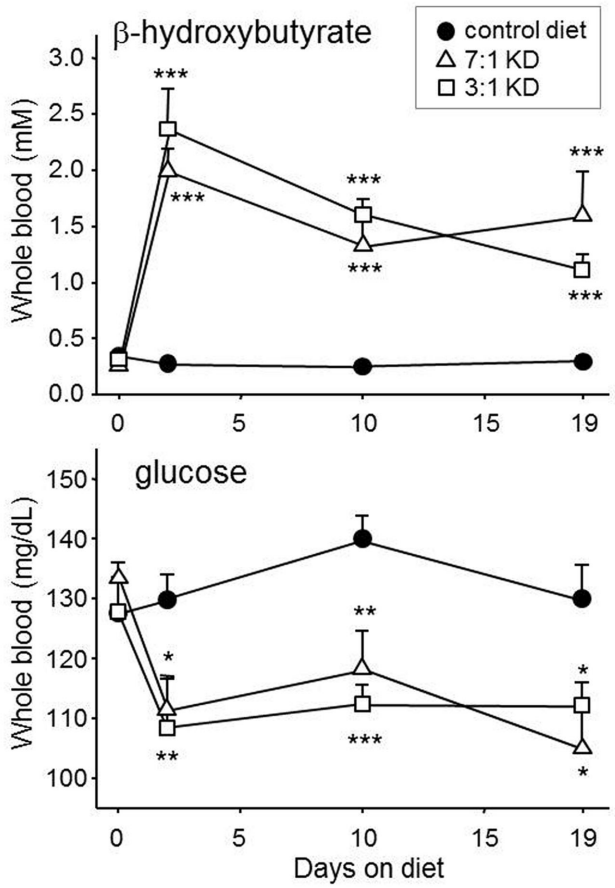

FIGURE 1 | Ketogenic diets can produce prompt and sustained ketosis and mild hypoglycemia in experimental rodents. Here, young male Sprague-Dawley rats were fed with one of two ketogenic diets for 19 days, or remained fed with normal rodent chow. Both KDs, with strengths of 3:1 and 7:1 (BioServ 5140 and 3666, respectively), produced similar and significantly increased blood ketones and reduced blood glucose within 2 days and lasting until the last test day. Number of subjects was 12–14. $*p < 0.05$, $**p < 0.01$, $***p < 0.001$, comparisons to control diet. Authors' unpublished data.

METABOLISM, PLASTICITY, AND SYNAPTIC ACTIVITY

The KD might alleviate seizures and other pathological states partially by providing elevated levels of high-energy molecules (e.g., ATP, phosphocreatine) and increased capacity for energy generation (increased mitochondrial number; Seyfried and Mukherjee, 2005; Bough and Rho, 2007; Masino and Geiger, 2008). Yet, numerous other changes due to the KD have been hypothesized to underlie increased inhibition and/or decreased excitation in brain, and thus to an anticonvulsant/neuroprotective state. In normal humans fed a KD, electroencephalography and transcranial magnetic stimulation demonstrated increased inhibition in the cerebral cortex, with a magnitude similar to that seen after benzodiazepine administration (Cantello et al., 2007). With the more extensive investigation possible in experimental animals, a KD was shown to enhance paired-pulse depression, shift the input/output relationship rightward, elevate the threshold for maximal electrical activation, and to block spreading depression-style events in the hippocampus *in vivo* (Bough et al., 2003). There have been surprisingly few detailed studies on detailed synaptic effects, likely because of the difficulty in performing such studies *in vivo*, coupled with the typical glucose-based incubation protocol for *in vitro* slices; to date, a "KD" incubation protocol has not been standardized, although recent work sampling cerebrospinal fluid in KD-fed animals might provide a starting point (Samala et al., 2011). Currently, the major proposed mechanisms for such increased inhibition and/or decreased excitation include increased levels of adenosine, a major inhibitory neuromodulator (Masino and Geiger, 2008); increased levels of γ-aminobutyric acid (GABA), a major inhibitory neurotransmitter (Yudkoff et al., 2007; Omote et al., 2011); decreased glutamate, a major excitatory neurotransmitter (Lund et al., 2009; Juge et al., 2010) and direct effects of elevated ketone bodies on ion channels (Ma et al., 2007).

Increased inhibition or decreased excitability, if sufficiently strong, might not only suppress seizures but also influence normal brain function. Many types of normal brain function, as well as recovery from injury, are thought to depend on synaptic plasticity, i.e., the malleability, either temporary or long-lasting, of the strength of neuronal communication (Davis et al., 1992; Goosens and Maren, 2002). Long-term potentiation (LTP) is a sustained increase in synaptic efficacy which can be observed in a number of brain regions including its original discovery site, the hippocampus (Bliss and Lømo, 1973; Bramham and Srebro, 1989; Clugnet and LeDoux, 1990; Bonci and Malenka, 1999; Mahon et al., 2004). Studies have linked metabolism and LTP (Potter et al., 2010); we and our collaborators characterized the effects of a KD on hippocampal LTP with the hypothesis that KD-related inhibition or reduced excitation might affect brain plasticity (Koranda et al., 2011). We recorded hippocampal signals through chronically implanted electrodes in freely moving rats. After 3 weeks on a 7:1 KD, baseline synaptic measurements were taken in the perforant path-dentate gyrus pathway and LTP was induced with tetanic stimulation and the response measured over the next 2 days. The KD had no significant effects on measures of short-term plasticity (paired-pulse depression, paired-pulse facilitation), and did not prevent LTP induction, whereas the magnitude of the potentiation was significantly smaller in KD-fed rats. The LTP magnitude remained lower in these rats out to the longest tested time point (48 h). As discussed below, cognitive effects of the diet are mixed in animals and overall positive in humans. In addition, it is important to note that 7:1 is a stronger diet ratio than that used clinically, animals used had never had seizures, and another paper looking at the KD on LTP *in vivo* in anesthetized animals did not find any differences (Thio et al., 2010).

To test the role of adenosine in the KD's ability to reduce seizures, we and our collaborators recently tested the effectiveness of a KD in a transgenic mouse with spontaneous hippocampal electrographic seizures due to adenosine deficiency. These mice overexpress the adenosine-metabolizing enzyme adenosine kinase (ADK) in brain (Fedele et al., 2005), and tonic levels of the endogenous inhibitor adenosine are therefore lower than normal. At baseline, seizures recorded with chronically implanted electrodes occur five times per hour, on average (Masino et al., 2011). After being fed on a 7:1 KD for 3 weeks, seizure frequency dropped almost

90%. This antiseizure effect depended on low glucose (seizures were restored by a peripheral injection of glucose), and activation of the adenosine A_1 receptor subtype (A_1R; seizure activity was restored by injection of a selective A_1R antagonist). Together, this evidence suggests that the KD exerts antiseizure effects by restoring adenosine levels and A_1R activation via a mechanism related to low glucose.

Further support for this idea is provided by transgenic mice lacking A_1Rs. These mice also have spontaneous electrographic seizures in the hippocampus, but the KD has no effect on seizure frequency in A_1R knockout mice, and is partially effective in mice heterozygous for the A_1R (Masino et al., 2011). Although these models all involve seizures induced by a lack of adenosinergic modulation, the results are likely generalizable: adenosine has been found to be anticonvulsive/antiseizure in virtually every seizure model in which it has been tested (excepting A_1R knockout mice – providing further evidence for the primary anticonvulsant role of A_1Rs). Adenosine in particular, and a KD in general, might offer more homeostatic "upstream" bioenergetic regulation of neuronal activity, and possibly long-term benefits on brain homeostasis, than highly specific drug therapies (Boison et al., 2011). Regarding LTP, previous results consistent with the involvement of adenosine in KD effects have shown that adenosine reduces LTP magnitude when present during induction (Mitchell et al., 1993; Costenla et al., 1999; de Mendonca and Ribeiro, 2000; Fujii et al., 2000a,b; Tabata et al., 2001; Zhang et al., 2004; Rex et al., 2005; but see Pascual et al., 2005) and, when applied after induction, promotes reversal of existing LTP (Huang et al., 1999; Fujii et al., 2000a). Yet, the lack of effects of the KD on input–output relationships and short-term plasticity seem to argue against the tonic involvement of adenosine (Koranda et al., 2011). Mechanism aside, the KD can limit excessive neuronal activity (a class into which the neuronal activity during an LTP induction burst certainly applies) and perhaps reset baseline activity.

KETOGENIC DIET FOR A BRAIN SLICE: RELAXING IN REDUCED GLUCOSE?

Compared to *in vivo*, *in vitro* paradigms can provide tighter control over experimental variables, allowing for a more thorough characterization of mechanisms. Effects of KD feeding on baseline excitability are inconsistent *in vitro*, however (Stafstrom et al., 1999; Thio et al., 2000; Bough et al., 2006; Nylen et al., 2008). Certainly, the metabolic state established by a KD might be disrupted during tissue preparation for *in vitro* work. As introduced briefly above, one of the biochemical effects associated with a KD is an abundance of high-energy molecules (DeVivo et al., 1978; Nakazawa et al., 1983; Pan et al., 1999; Masino et al., 2007), as well as increased mitochondrial biogenesis, respiration, and expression of ATP synthesis-related proteins (Noh et al., 2004; Sullivan et al., 2004; Bough et al., 2006; Nylen et al., 2009; Balietti et al., 2010). Several lines of evidence suggest that reduced glucose is critical for antiseizure effects.

We modeled key aspects of the KD *in vitro* by maintaining or increasing intracellular ATP while decreasing extracellular glucose in individual CA3 pyramidal neurons in acute hippocampal slices. We varied ATP (0.5–5.0 mM; 2 mM is standard) in the patch pipet and changed glucose concentration of the bathing solution from 11 mM (standard) to either 7 or 3 mM (Kawamura et al., 2010). Note that 3 mM glucose is still a physiological level: *in vivo* brain concentrations are near 3 mM (Hu and Wilson, 1997; Shram et al., 1997). Moderately lowered extracellular glucose has been reported to attenuate epileptiform activity in brain slices (Kirchner et al., 2006), whereas experimental studies of pathological hypoglycemia often remove glucose completely from the bathing medium (aglycemia; Tromba et al., 1992; Zhu and Krnjevic, 1993).

We found that when intracellular ATP levels were adequate or high (1.0–5.0 mM), reducing extracellular glucose provoked an outward (inhibitory) current, with a larger current found with a reduction to 3 mM versus to 7 mM (**Figure 2**). This outward current was fully reversible on return to 11 mM glucose and had a reversal potential near the equilibrium potential for K^+, and was blocked by the non-selective K^+ channel antagonist Ba^{2+} (Kawamura et al., 2010). If intracellular ATP levels were low (0.5 mM), reducing glucose produced a transient inward (excitatory) current instead (**Figure 2**). Therefore, moderately low extracellular glucose can inhibit hippocampal neurons that have sufficient or abundant energy stores. Furthermore, this inhibition was completely blocked by application of an A_1R antagonist and was not present in neurons from A_1R knockout mice (**Figure 2**; similar to observations *in vivo*: Masino et al., 2011) implying increased adenosine levels produced the inhibition (conversely, diabetic hyperglycemia seems to be related to reduced signaling through A_1Rs (Duarte et al.,

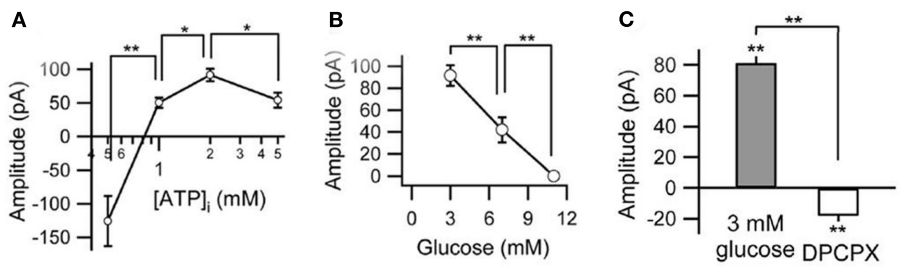

FIGURE 2 | Relationship among membrane current, intracellular ATP, and extracellular glucose. (A) Peak currents produced by lowering extracellular glucose from 11 to 3 mM depend on intracellular ATP concentration (0.5–5 mM). Current is outward, except at 0.5 mM ATP. **(B)** Concentration-dependence of glucose-related outward current (with 2 mM intracellular ATP). **(C)** Outward current produced in low-glucose buffer reversed completely (and became slightly inward) with the A_1R antagonist DPCPX. $*p < 0.05$, $**p < 0.01$. Adapted with permission from Kawamura et al. (2010).

2006). A similar consistent mechanism was reflected presynaptically (measured as decreased spontaneous postsynaptic current frequency); an A_1R-dependent presynaptic inhibition was produced by adequate/high postsynaptic intracellular ATP combined with low extracellular glucose (Kawamura et al., 2010). Together, this study and Masino et al. (2011) suggest that a KD can limit seizures (at least those involving the hippocampus) through a mechanism dependent on low glucose and abundant high-energy molecules and involving augmentation of adenosine levels.

In our *in vitro* study, we manipulated ATP only in the patched neuron, suggesting an autocrine mechanism to increase adenosine. How might this autoinhibition occur? ATP might be metabolized intracellularly to adenosine, which would then be released. Loading pyramidal neurons with adenosine + ATP versus ATP alone, however, suggested that the current was not mediated by direct adenosine release (Kawamura et al., 2010). Alternatively, ATP might be released and then metabolized to adenosine. Cells can release ATP by several mechanisms (Dubyak, 2009), and extracellular ATP is metabolized rapidly to adenosine (Dunwiddie et al., 1997). One prominent non-exocytotic ATP release mechanism in neurons and glia is ATP passage through channels composed of connexins or pannexins (Stout et al., 2002; Schock et al., 2008; Iwabuchi and Kawahara, 2011). Through a series of physiological and pharmacological experiments, we determined that pannexin channels were the source of extracellular ATP. Taken together, our data are consistent with a process by which lowered extracellular glucose promotes release of ATP via pannexins. ATP is then converted extracellularly to adenosine, which activates A_1Rs coupled, under these conditions, to K_{ATP} channels (Kawamura et al., 2010). This pathway is likely to underlie the A_1R-mediated anticonvulsant effect produced by the KD *in vivo*. Certainly, mild hypoglycemia and enhanced adenosine tone can underlie its anticonvulsant effect (Masino et al., 2011), whereas the *in vivo* involvement of pannexin channels and ATP release remains to be demonstrated directly.

KETOGENIC DIET'S EFFECT ON COGNITION AND MOOD: NEGATIVE, THEN POSITIVE?

Altered cognition and affect in children with seizure disorders has always been a concern. Regarding pharmacological therapies, several authors have shown that children with epilepsy – even those whose seizures were well-controlled with antiepileptic drugs – had decreased cognitive function compared to their peers (Devinsky, 1995; Thompson et al., 2000; Drane and Meador, 2002). The exact mechanism of cognitive decline is unknown: traditional antiepileptic drugs decrease membrane excitability, increase postsynaptic inhibition, or reduce network synchronization to decrease excessive excitability associated with seizure development (Loring, 2005). These neurophysiological mechanisms, if sufficiently strong, will not only suppress seizures but also impair normal brain function. The incidence of cognitive side effects is increased at higher dosing and with polypharmacy which might be necessary for significant seizure control (Loring and Kimford, 2001). Thus, the cognitive and affective state of a medicated epileptic patient results from a balance of forces including the negative effects of the disease state (seizures, abnormal interictal brain activity, abnormal sleep), the positive effects of the anticonvulsive medication (seizure control), and the negative side effects of the anticonvulsive mediation (which can include sedation and/or abnormal sleep).

The KD might offer fewer chronic negative side effects than medication, and given that it has been in use for over 90 years, serious or systematic negative consequences would likely have surfaced by now. In research studies, KDs (albeit at a much stronger ratio than used clinically) reduced brain mass in juvenile rodents (Cheng et al., 2004; Zhao et al., 2004) and KDs can affect body growth in children (who are typically on the diet temporarily; Liu et al., 2003; Peterson et al., 2005; Neal et al., 2008b) but to our knowledge negative KD effects on human brain development and growth have not been quantified. Notably, recurrent clinical hypoglycemia can lead to a cumulative cognitive impairment (Langan et al., 1991; Deary et al., 1993) – although this effect might not be directly applicable because the hypoglycemia in these studies was episodic and much more severe than the chronic reduced (but not abnormal) glucose levels associated with the KD. Overall, positive and negative short- and long-term effects of this strict diet on cognition and mood remain under-examined clinically, particularly in pediatric patients.

It is worthwhile to consider that any assessment of cognitive or affective state associated with a KD should occur at multiple time points, as effects of the KD (including anticonvulsive effects) clearly evolve. There are limitations to combining data from different laboratories due to differing methodologies, different KDs, etc. Yet in surveying the research literature, it seems fairly clear that there is a biphasic effect on locomotor behavior: reduced activity characterizes KD onset, whereas increased activity predominate after a few weeks. Effects of a KD on locomotion in rodents (compiled informally from the literature) are shown in **Figure 3**. Notably, a biphasic pattern over time after diet initiation

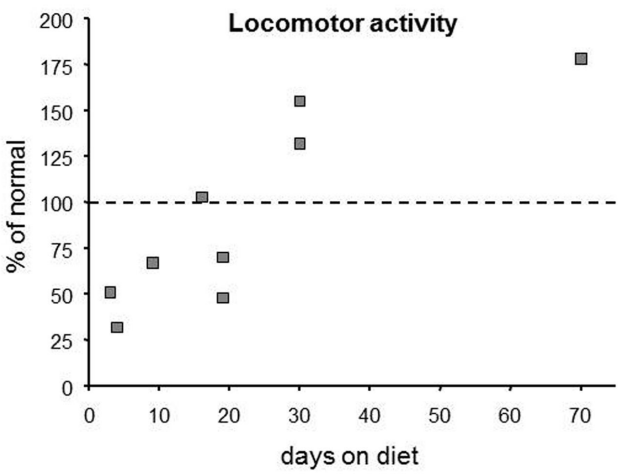

FIGURE 3 | Over time, KDs produce a biphasic effect on locomotor activity based on this compilation of published rodent data. Note that hypoactivity predominated in studies with short diet treatments (≤20 day), whereas hyperactivity predominated with longer treatments (≥30 day). Points were estimated from published graphs and tables in multiple references (Zhao et al., 2004; Murphy et al., 2005; Ziegler et al., 2005; Murphy and Burnham, 2006; Mantis et al., 2009; Oishi et al., 2010; Thio et al., 2010).

is found in clinical literature relating to cognition, mood, and vitality. Soon after beginning a KD, subjects often complain of lethargy (Vining et al., 1998; Lefevre and Aronson, 2000); in children, intolerable drowsiness is a reported side-effect that sometimes leads to cessation of KD treatment (Neal et al., 2008a). Yet, after weeks on the diet, subjects report heightened vitality, physical functioning, and alertness (Hallböök et al., 2007; Mosek et al., 2009; Yancy et al., 2009). In some cases these positive effects may be at least partially due to reduced seizure frequency, but similar positive effects are also described in non-epileptic subjects. This delay in beneficial effects is reminiscent of the delay often observed in anticonvulsant effects (Kossoff et al., 2008a).

Studies of the KD in epileptic patients rarely characterize mood, which might understandably be poor during the initial lethargic/drowsy stage. Several weight-loss studies, however, included affective measures and found positive effects of KD on mood in overweight subjects as early as 2 weeks into diet treatment, and lasting many weeks (Halyburton et al., 2007; McClernon et al., 2007; Brinkworth et al., 2009; Yancy et al., 2009). Two of these studies provide some evidence against this result simply being a psychological effect of weight loss (Brinkworth et al., 2009; Yancy et al., 2009). Thus, beneficial effects on mood (as well as weight loss) await those who conquer the early stage after KD initiation. Studies of patients with epilepsy on the KD, including children, have either reported improved cognition anecdotally (Sirven et al., 1999) or reported improvements in more general measures such as attention and social functioning (Kinsman et al., 1992; Pulsifer et al., 2001). It is difficult to determine if these effects are due to reduced seizures, to concomitantly reduced medications, or a direct action on cognition/attention. Investigations in non-epileptic adult subjects (thus without confounding antiepileptic medications) have more specifically addressed cognition and the KD. One study found a transient, moderate impairment in one cognitive task (but not two other tasks) at 1 week of diet treatment but found no impairments at later time points (Wing et al., 1995); two studies examining chronic KD treatments reported improved processing speed and working memory lasting up to 1 year (Halyburton et al., 2007; Brinkworth et al., 2009). This pattern seems to parallel the biphasic effect on activity and vitality noted above.

A minority of animal studies have reported impairments in learning and memory, specifically in a task of spatial reference memory (Su et al., 2000; Zhao et al., 2004). Other studies, however, have failed to find any detrimental effect of the KD on learning and memory in rodents in various mazes or in fear conditioning (Hori et al., 1997; Todorova et al., 2000; Silva et al., 2005; Appelberg et al., 2009; Thio et al., 2010). We tested normal mice of both sexes in a simple working memory task after feeding on a 7:1 KD at a number of time points, up to 10 weeks, and found no effect of the KD (though hyperactivity did appear beginning at 2 weeks (Ruskin et al., 2011a). It is worth noting that a KD not only does not impair but in fact reverses age-related deficits in learning and other cognitive measures in aged, but otherwise healthy, dogs and rodents (Pan et al., 2010; Xu et al., 2010). Taken together, these results largely support the beneficial nature of KD feeding on mood and cognition in patients.

NOCICEPTION AND INFLAMMATION: MULTIPLE MECHANISMS LIKELY

Converging lines of evidence suggest the utility of a KD for pain relief. First, it has long been known that reducing glucose metabolism influences pain. There is an overall increase in pain thresholds (and thus reduced pain) when glycolytic enzymes are inhibited by exogenous 2-deoxy-D-glucose (Bodnar et al., 1979). This effect is mediated centrally (Bodnar et al., 1981), and might involve increased brain/spinal cord inhibition by adenosine, the release of which is stimulated by 2-deoxy-D-glucose (Zhao et al., 1997; Minor et al., 2001). 2-Deoxy-D-glucose is also anticonvulsant (Garriga-Canut et al., 2006), and while the mechanisms might not overlap entirely with the KD (Stafstrom et al., 2009; Gasior et al., 2010) there might be some common pathways. Second, anticonvulsant drugs such as gabapentin, felbamate, and valproate are useful in treating pain, particularly neuropathic pain and migraine (Johannessen Landmark, 2008). These drugs typically act by decreasing neuronal activity or excitability, and it is clear that reducing central activity with adenosine or GABA agonists alleviates pain (Karlsten et al., 1992; Malmberg and Yaksh, 1993; Belfrage et al., 1995; Malan et al., 2002; Gwak et al., 2006). Thus, we predicted that the KD, which reduces glucose metabolism and is anticonvulsant, would reduce pain.

We fed rats a 7:1 KD in order to test the effects in the hot-plate test. In this test, the latency to withdraw a hindpaw from the warm surface indicates the animal's sensitivity to painful heat. In young rats, we found that KD feeding for 3–4 weeks increased paw withdrawal latency (i.e., decreased the sensitivity) to plate temperatures from 48 to 51°C (Ruskin et al., 2009). In adult rats, the effect seemed to be smaller in magnitude, and was significant only at 49 and 50°C. We recently found similar results with a less stringent 3:1 KD (Ruskin et al., 2011b). Curiously, another study reported increased thermal pain sensitivity (tail flick) after 12 weeks of KD feeding in young rats (Ziegler et al., 2005); methodological differences such as rat strain, body part (paw vs. tail), diet composition, and stimulus strength might be factors. The difference in diet treatment length (3 vs. 12 weeks) does not seem to explain the disparity, as subsequently we have found decreased thermal pain sensitivity present after 10–11 weeks of feeding with a 3:1 KD (Ruskin et al., 2011b). Thus far the specific mechanism of altered thermal nociception in KD-fed rats is unknown, and could involve hypoglycemia, ketosis, fatty acids, and/or adenosine.

One recently published clinical report on KD effects on "quality of life" reported that beneficial effects on self-reported general bodily pain were at the threshold of statistical significance (Yancy et al., 2009), suggesting that KD effects on overall pain might be positive. This report, however, was not a dedicated study of pain, but rather a study of overall quality of life; as such, there was no underlying painful condition to treat. In the same study, a low-fat diet also alleviated bodily pain. Overall, an assessment of pain in KD-treated patients is warranted.

A better understanding of the relationship between metabolism and pain could help multiple and comorbid conditions, and the KD might prove uniquely useful against diabetes and diabetes-related neuropathy. Although work with rodents has produced mixed results (Al-Khalifa et al., 2009, 2011; Garbow et al., 2011; Park et al., 2011; Poplawski et al., 2011), clinical

studies have found exclusively positive outcomes: after KD treatment, patients with type I or II diabetes had improved control of blood glucose, and many could have their medications reduced or eliminated (Gumbiner et al., 1996; Yancy et al., 2005; Westman et al., 2008; Dressler et al., 2010). In addition, type I diabetic patients (and, based on one report, children with epilepsy) prefer foods that are high in fat and low in carbohydrates (Amari et al., 2007; Snell-Bergeon et al., 2009), which might be attempted self-medication. The mixed animal results might result from the use of very strict KDs (Garbow et al., 2011; Park et al., 2011), or from the diabetic propensity of many laboratory rodent strains. Thus, the KD might benefit diabetic patients both by alleviating neuropathic pain and treating the underlying glycemic control dysfunction.

Finally, the KD would be predicted to be effective against inflammatory pain. Chronic inflammation is typically accompanied by pain due to the release of prostaglandins and the consequent sensitization of sensory neurons (Mense, 1983). Some of the most common sources of inflammatory pain are rheumatoid arthritis, chronic inflammatory bowel disease, pancreatitis, back pain, and some cancers. We found that a KD reduced experimental inflammation-induced swelling and plasma extravasation (Ruskin et al., 2009), and clinical studies describe positive effects of a KD on liver inflammation in non-alcoholic fatty liver disease (Tendler et al., 2007; Pérez-Guisado and Muñoz-Serrano, 2011). Regarding mechanisms linking metabolism to inflammatory pain, reactive oxygen species are a major component of inflammation, and limiting reactive oxygen species should contribute to limiting inflammation. Accordingly, ketone-based metabolism should produce fewer free radicals and reactive oxygen species through affecting the mitochondrial co-enzyme Q couple and the cytoplasmic glutathione couple (Veech, 2004). Indeed, as expected, treatment with ketones reduces the level of reactive oxygen species (Noh et al., 2006a; Kim et al., 2007, 2010; Maalouf et al., 2007; Haces et al., 2008; Maalouf and Rho, 2008), as does KD feeding (Sullivan et al., 2004).

Regarding inflammatory pain, by virtue of their high-fat content KDs should also activate peroxisome proliferator-activated receptors (PPARs). These nuclear receptors bind long-chain polyunsaturated fatty acids, and consequently induce transcriptional changes that culminate in enhanced lipid metabolism (Moya-Camarena et al., 1999; Diradourian et al., 2005; Michalik et al., 2006). Genetic knockout of a major PPAR (the α subtype) augments inflammatory reactions (Cuzzocrea et al., 2006), whereas synthetic PPAR agonists reduce experimentally induced inflammation (Cuzzocrea et al., 2003; LoVerme et al., 2005). This latter effect appears to involve reduced transcription of pro-inflammatory genes (Blanquart et al., 2003) and seems to be invoked by the KD (Jeong et al., 2011). Synthetic PPAR agonists are analgesic against inflammatory pain (LoVerme et al., 2006). In addition to these effects, PPAR activation augments expression of the enzymes involved in ketogenesis (Cullingford et al., 2002), promoting the shift to a ketone-based metabolism, in agreement with findings of stronger ketosis with a high-polyunsaturated fat KD (Fuehrlein et al., 2004). Although polyunsaturated fatty acid content of the KD seems not to be important in the diet's anticonvulsant effect (Dell et al., 2001; Dahlin et al., 2007), it might be a crucial characteristic for KD influence on inflammation.

It might seem ironic that the KD is discussed here as reducing inflammation, given that other high-fat diets and obesity are definitely linked to chronic inflammation (Thaler and Schwartz, 2010; Ding and Lund, 2011; Laugerette et al., 2011). Those high-fat diets that lead to obesity, including the so-called Western diet, include a high amount of fat along with normal amounts of carbohydrate, a crucial difference from the very low-carbohydrate KD which typically leads to weight loss (Gumbiner et al., 1996; Halyburton et al., 2007; Tendler et al., 2007; Westman et al., 2008). Thus, the high-fat-plus-carbohydrate diet promotes fat storage whereas the high fat, low-carbohydrate diet promotes fat metabolism. Nevertheless, more clinical work with the KD and inflammation is warranted, particularly regarding long-term effects. It will be crucial to determine which of the mechanisms described above is most important for the KD's alleviation of inflammation. Future work on the relationship between the KD's hallmark changes in blood chemistry, ketosis and mild hypoglycemia, and its anti-inflammatory and anti-nociceptive effects should help characterize the pertinent mechanisms.

ATTENUATING BRAIN INJURY AND NEURODEGENERATION

Animal studies have found find that the KD protects against seizure-induced neurodegeneration and related sequelae (such as aberrant neurite sprouting; Muller-Schwarze et al., 1999; Noh et al., 2003, 2005, 2006b; Linard et al., 2010). The KD is also neuroprotective against ischemic damage (Tai et al., 2008, 2009), hypoglycemic damage (Yamada et al., 2005), and traumatic brain and spinal injury (Prins et al., 2005; Appelberg et al., 2009; Hu et al., 2009a,b; Prins and Hovda, 2009; Schwartzkroin et al., 2010; Streijger et al., 2011), and improves injury-related deficits in cognition and movement after traumatic brain and spinal injury, respectively (Appelberg et al., 2009; Streijger et al., 2011). Ketosis is apparently crucial to these effects as direct application of ketones to *in vitro* tissue is also protective against hypoglycemia and ischemia (Samoilova et al., 2010), oxidative stress (Kim et al., 2007), and excitotoxicity (Massieu et al., 2003; Noh et al., 2006b; Maalouf et al., 2007; Samoilova et al., 2010). The mechanisms are likely to involve reduced reactive oxygen species, reduced tissue excitability, and enhanced production of high-energy molecules.

Based on evidence for neuroprotection against acute insults, and recognition that metabolic dysfunction accompanies chronic neurological disease, researchers are expanding into animal models of more slowly-acting neurodegenerative diseases. Positive effects of KD feeding have been found in models of amyotrophic lateral sclerosis (Zhao et al., 2006), Parkinson's disease (Cheng et al., 2009; Yang and Cheng, 2010), and Alzheimer's disease (Van der Auwera et al., 2005; Mohamed et al., 2010). In addition, KD feeding reverses aging-related impairments in brain biochemistry in animals (Studzinski et al., 2008; Balietti et al., 2010). Direct application of ketones is also beneficial in models of Parkinson's disease (Kashiwaya et al., 2000; Tieu et al., 2003) and Alzheimer's disease (Kashiwaya et al., 2000).

Huntington's disease, which involves the death of neurons in the caudate and putamen, is thought to involve excitotoxicity and mitochondrial dysfunction (Estráda-Sanchez et al., 2008;

Damiano et al., 2010). Based on findings reviewed above, we characterized the effects of a strict (7:1) KD in a rapidly progressing Huntington's disease model, the R6/2 mouse (lifespan less than 16 weeks). KD feeding began at 6 weeks of age, when motor impairments are still minor (Ruskin et al., 2011a). The KD did not increase lifespan or alleviate motor impairments, but, importantly, it did not negatively affect either. However, the KD did delay significantly the onset of progressive weight loss, which is a major problem in patients (Sanberg et al., 1981; Lanska et al., 1988). In addition, the KD reversed a modest working memory impairment in female mice, and working memory is known to be affected in patients with Huntington's disease (Lange et al., 1995; Lawrence et al., 1996) as well as other neurological disorders and aging.

The lack of effect on lifespan or locomotor activity may signal that beneficial effects of a KD might not be similar across neurodegenerative disorders, might depend on the severity or rate of progression, or might differ in different animal models of a disorder; alternatively, the KD might need to be optimized for strength and composition for different conditions. Although it seems paradoxical that the KD, normally associated with weight loss, might maintain, or increase body weight under particular conditions, our data suggest that KD feeding could alleviate Huntington's disease-associated cachexia, and, as noted above, in patients a higher body mass is associated with slower disease progression (Myers et al., 1991). Based on this finding, the KD might also deserve consideration for treatment of other cachexias; for instance, that associated with cancer (Colomer et al., 2007). Indeed, the KD is beginning to be used as an anti-tumorigenic treatment (Klement and Kammerer, 2011; Seyfried et al., 2012) and so could provide dual benefits. If the anti-neurodegenerative effects found in animal models of Parkinson's disease, Alzheimer's disease, and aging are successfully extended to humans, the KD could also have dual benefits, delaying the primary degenerative condition and alleviating the working memory problems common to these conditions (Halyburton et al., 2007; Brinkworth et al., 2009; Ruskin et al., 2011a).

LOOKING AHEAD

A KD offers known benefits for epilepsy, and it is apparent that the relationship between metabolism and brain function offers primary therapeutic opportunities. Basic and clinical research is acutely aware that metabolic dysfunction and comorbidities promulgate lifelong impacts on nervous system function. Particularly promising unrealized opportunities for intervention and restoration of metabolic homeostasis occur during development, after injury, and during disease progression – all windows with high levels of plasticity and remodeling. New insight into mechanisms could accelerate development of treatments.

ACKNOWLEDGMENTS

Supported by the National Institutes of Health (P20RR017699, R15NS065446, R15NS066392, R01NS065957), the National Science Foundation (IOS0843585), the CHDI Foundation, and Trinity College.

REFERENCES

Al-Khalifa, A., Mathew, T. C., Al-Zaid, N. S., Mathew, E., and Dashti, H. (2011). Low carbohydrate ketogenic diet prevents the induction of diabetes using streptozotocin in rats. *Exp. Toxicol. Pathol.* 63, 663–669.

Al-Khalifa, A., Mathew, T. C., Al-Zaid, N. S., Mathew, E., and Dashti, H. M. (2009). Therapeutic role of low-carbohydrate ketogenic diet in diabetes. *Nutrition* 25, 1177–1185.

Amari, A., Dahlquist, L., Kossoff, E. H., Vining, E. P. G., Trescher, W. H., and Slifer, K. J. (2007). Children with seizures exhibit preferences for foods compatible with the ketogenic diet. *Epilepsy Behav.* 11, 98–104.

Aoki, T. T. (1981). Metabolic adaptations to starvation, semistarvation, and carbohydrate restriction. *Prog. Clin. Biol. Res.* 67, 161–177.

Appelberg, K. S., Hovda, D. A., and Prins, M. L. (2009). The effects of a ketogenic diet on behavioral outcome after controlled cortical impact injury in the juvenile and adult rat. *J. Neurotrauma* 26, 497–506.

Balietti, M., Giorgetti, B., Di Stefano, G., Casoli, T., Platano, D., Solazzi, M., Bertoni-Freddari, C., Aicardi, G., Lattanzio, F., and Fattoretti, P. (2010). A ketogenic diet increases succinic dehydrogenase (SDH) activity and recovers age-related decrease in numeric density of SDH-positive mitochondria in cerebellar Purkinje cells of late-adult rats. *Micron* 41, 143–148.

Belfrage, M., Sollevi, A., Segerdahl, M., Sjölund, K. F., and Hansson, P. (1995). Systemic adenosine infusion alleviates spontaneous and stimulus evoked pain in patients with peripheral neuropathic pain. *Anesth. Analg.* 81, 713–717.

Blanquart, C., Barbier, O., Fruchart, J. C., Staels, B., and Glineur, C. (2003). Peroxisome proliferator-activated receptors: regulation of transcriptional activities and roles in inflammation. *J. Steroid Biochem. Mol. Biol.* 85, 267–273.

Bliss, T. V. P., and Lømo, T. (1973). Long-lasting potentiation of synaptic transmission in the dentate area of the anaesthetized rabbit following stimulation of the perforant path. *J. Physiol. (Lond.)* 232, 331–356.

Bodnar, R. J., Kelly, D. D., and Glusman, M. (1979). 2-Deoxy-D-glucose analgesia: influences of opiate and non-opiate factors. *Pharmacol. Biochem. Behav.* 11, 297–301.

Bodnar, R. J., Merrigan, K. P., and Wallace, M. M. (1981). Analgesia following intraventricular administration of 2-deoxy-D-glucose. *Pharmacol. Biochem. Behav.* 14, 579–581.

Boison, D., Masino, S. A., and Geiger, J. D. (2011). Homeostatic bioenergetic network regulation: a novel concept to avoid pharmacoresistance in epilepsy. *Expert Opin. Drug Discov.* 6, 713–724.

Bonci, A., and Malenka, R. C. (1999). Properties and plasticity of excitatory synapses on dopaminergic and GABAergic cells in the ventral tegmental area. *J. Neurosci.* 19, 3723–3730.

Bough, K. J., and Rho, J. M. (2007). Anticonvulsant mechanisms of the ketogenic diet. *Epilepsia* 48, 43–58.

Bough, K. J., Schwartzkroin, P. A., and Rho, J. M. (2003). Caloric restriction and ketogenic diet diminish neuronal excitability in rat dentate gyrus in vivo. *Epilepsia* 44, 752–760.

Bough, K. J., Wetherington, J., Hassel, B., Pare, J. F., Gawryluk, J. W., Greene, J. G., Shaw, R., Smith, Y., Geiger, J. D., and Dingledine, R. J. (2006). Mitochondrial biogenesis in the anticonvulsant mechanism of the ketogenic diet. *Ann. Neurol.* 60, 223–235.

Bramham, C. R., and Srebro, B. (1989). Synaptic plasticity in the hippocampus is modulated by behavioral state. *Brain Res.* 493, 74–86.

Brinkworth, G. D., Buckley, J. D., Noakes, M., Clifton, P. M., and Wilson, C. J. (2009). Long-term effects of a very low-carbohydrate diet and a low-fat diet on mood and cognitive function. *Arch. Intern. Med.* 169, 1873–1880.

Cantello, R., Varrasi, C., Tarletti, R., Cecchin, M., D'Andrea, F., Veggiotti, P., Bellomo, G., and Monaco, F. (2007). Ketogenic diet: electrophysiological effects on the normal human cortex. *Epilepsia* 48, 1756–1763.

Cheng, B., Yang, X., An, L., Gao, B., Liu, X., and Liu, S. (2009). Ketogenic diet protects dopaminergic neurons against 6-OHDA neurotoxicity via up-regulating glutathione in a rat model of Parkinson's disease. *Brain Res.* 1286, 25–31.

Cheng, C. M., Hicks, K., Wang, J., Eagles, D. A., and Bondy, C. A. (2004). Caloric restriction augments brain glutamic acid decarboxylase-65 and -67 expression. *J. Neurosci. Res.* 77, 270–276.

Clugnet, M.-C., and LeDoux, J. E. (1990). Synaptic plasticity in fear conditioning circuits: induction of LTP in the lateral nucleus of the amygdala by stimulation of the medial geniculate body. *J. Neurosci.* 10, 2818–2824.

Colomer, R., Moreno-Nogueira, J. M., García-Luna, P. P., García-Peris, P., García-De-Lorenzo, A., Zarazaga, A., Quecedo, L., Del Llano, J., Usán, L., and Casimiro, C. (2007). N-3 fatty acids, cancer and cachexia: a systematic review of the literature. *Br. J. Nutr.* 97, 823–831.

Costenla, A. R., De Mendonca, A., and Ribeiro, J. A. (1999). Adenosine modulates synaptic plasticity in hippocampal slices from aged rats. *Brain Res.* 851, 228–234.

Cullingford, T. E., Dolphin, C. T., and Sato, H. (2002). The peroxisome proliferator-activated receptor α-selective activator ciprofibrate upregulates expression of genes encoding fatty acid oxidation and ketogenesis enzymes in rat brain. *Neuropharmacology* 42, 724–730.

Cuzzocrea, S., Mazzon, E., Di Paolo, R., Peli, A., Bonato, A., Britti, D., Genovese, T., Muia, C., Crisafulli, C., and Caputi, A. P. (2006). The role of the peroxisome proliferator-activated receptor-alpha (PPAR-alpha) in the regulation of acute inflammation. *J. Leukoc. Biol.* 79, 999–1010.

Cuzzocrea, S., Mazzon, E., Dugo, L., Patel, N. S., Serraino, I., Di Paolo, R., Genovese, T., Britti, D., De Maio, M., Caputi, A. P., and Thiemermann, C. (2003). Reduction in the evolution of murine type II collagen-induced arthritis by treatment with rosiglitazone, a ligand of the peroxisome proliferator-activated receptor gamma. *Arthritis Rheum.* 48, 3544–3556.

Dahlin, M., Hjelte, L., Nilsson, S., and Åmark, P. (2007). Plasma phospholipid fatty acids are influenced by a ketogenic diet enriched with n-3 fatty acids in children with epilepsy. *Epilepsy Res.* 73, 199–207.

Damiano, M., Galvan, L., Déglon, N., and Brouillet, E. (2010). Mitochondria in Huntington's disease. *Biochim. Biophys. Acta* 1802, 52–61.

Davis, S., Butcher, S. P., and Morris, R. G. M. (1992). The NMDA receptor antagonist D-2-amino-5-phosphonopentanoate (D-AP5) impairs spatial learning and LTP in vivo at intracerebral concentrations comparable to those that block LTP in vitro. *J. Neurosci.* 12, 21–34.

de Mendonca, A., and Ribeiro, J. A. (2000). Long-term potentiation observed upon blockade of adenosine A1 receptors in rat hippocampus is N-methyl-D-aspartate receptor-dependent. *Neurosci. Lett.* 291, 81–84.

Deary, I. J., Crawford, J. R., Hepburn, D. A., Langan, S. J., Blackmore, L. M., and Frier, B. M. (1993). Severe hypoglycemia and intelligence in adult patients with insulin-treated diabetes. *Diabetes* 42, 341–344.

Dell, C. A., Likhodii, S. S., Musa, K., Ryan, M. A., Burnham, W. C., and Cunnane, S. C. (2001). Lipid and fatty acid profiles in rats consuming different high-fat ketogenic diets. *Lipids* 36, 373–378.

Devinsky, O. (1995). Cognitive and behavioral effects of antiepileptic drugs. *Epilepsia* 36, S46–S65.

DeVivo, D. C., Leckie, M. P., Ferrendelli, J. S., and McDougal, D. B. Jr. (1978). Chronic ketosis and cerebral metabolism. *Ann. Neurol.* 3, 331–337.

Ding, S., and Lund, P. K. (2011). Role of intestinal inflammation as an early event in obesity and insulin resistance. *Curr. Opin. Clin. Nutr. Metab. Care* 14, 328–333.

Diradourian, C., Girard, J., and Pegorier, J.-P. (2005). Phosphorylation of PPARs: from molecular characterization to physiological relevance. *Biochimie* 87, 33–38.

Dong, L., Luo, R., Tong, Y., Cai, X., Mao, M., and Yu, D. (2011). Lack of association between ABCB1 gene polymorphisms and pharmacoresistant epilepsy: an analysis in a western Chinese pediatric population. *Brain Res.* 1391, 114–124.

Drane, D. L., and Meador, K. J. (2002). Cognitive and behavioral effects of antiepileptic drugs. *Epilepsy Behav.* 3, S49–S53.

Dressler, A., Reithofer, E., Trimmel-Schwahofer, P., Klebermasz, K., Prayer, D., Kasprian, G., Rami, B., Schober, E., and Feucht, M. (2010). Type 1 diabetes and epilepsy: efficacy and safety of the ketogenic diet. *Epilepsia* 51, 1086–1089.

Duarte, J. M. N., Oliveira, C. R., Ambrosio, A. F., and Cunha, R. A. (2006). Modification of adenosine A1 and A2A receptor density in the hippocampus of streptozotocin-induced diabetic rats. *Neurochem. Int.* 48, 144–150.

Dubyak, G. R. (2009). Both sides now: multiple interactions of ATP with pannexin-1 hemichannels. *Am. J. Physiol. Cell Physiol.* 296, C235–C241.

Dunwiddie, T. V., Diao, L., and Proctor, W. R. (1997). Adenine nucleotides undergo rapid, quantitative conversion to adenosine in the extracellular space in rat hippocampus. *J. Neurosci.* 17, 7673–7682.

Estráda-Sanchez, A. M., Mejía-Tober, J., and Massieu, L. (2008). Excitotoxic neuronal death and the pathogenesis of Huntington's disease. *Arch. Med. Res.* 39, 265–276.

Fedele, D. E., Gouder, N., Guttinger, M., Gabernet, L., Scheurer, L., Rulicke, T., Crestani, F., and Boison, D. (2005). Astrogliosis in epilepsy leads to overexpression of adenosine kinase, resulting in seizure aggravation. *Brain* 128, 2383–2395.

Fuehrlein, B. S., Rutenberg, M. S., Silver, J. N., Warren, M. W., Theriaque, D. W., Duncan, G. E., Stacpoole, P. W., and Brantly, M. L. (2004). Differential metabolic effects of saturated versus polyunsaturated fats in ketogenic diets. *J. Clin. Endocrinol. Metab.* 89, 1641–1645.

Fujii, S., Kato, H., Ito, K.-I., Itoh, S., Yamazaki, Y., Sasaki, H., and Kuroda, Y. (2000a). Effects of A1 and A2 adenosine receptor antagonists on the induction and reversal of long-term potentiation in guinea pig hippocampal slices of CA1 neurons. *Cell. Mol. Neurobiol.* 20, 331–350.

Fujii, S., Kuroda, Y., Ito, K.-I., Yoshioka, M., Kaneko, K., Yamazaki, Y., Sasaki, H., and Kato, H. (2000b). Endogenous adenosine regulates the effects of low-frequency stimulation on the induction of long-term potentiation in CA1 neurons of guinea pig hippocampal slices. *Neurosci. Lett.* 279, 121–124.

Garbow, J. R., Doherty, J. M., Schugar, R. C., Travers, S., Weber, M. L., Wentz, A. E., Ezenwajiaku, N., Cotter, D. G., Brunt, E. M., and Crawford, P. A. (2011). Hepatic steatosis, inflammation, and ER stress in mice maintained long term on a very low-carbohydrate ketogenic diet. *Am. J. Physiol. Gastrointest. Liver Physiol.* 300, G956–G967.

Garriga-Canut, M., Schoenike, B., Qazi, R., Bergendahl, K., Daley, T. J., Pfender, R. M., Morrison, J. F., Ockuly, J., Stafstrom, C., Sutula, T., and Roopra, A. (2006). 2-Deoxy-D-glucose reduces epilepsy progression by NRSF-CtBP-dependent metabolic regulation of chromatin structure. *Nat. Neurosci.* 9, 1382–1387.

Gasior, M., Yankura, J., Hartman, A. L., French, A., and Rogawski, M. A. (2010). Anticonvulsant and proconvulsant actions of 2-deoxy-D-glucose. *Epilepsia* 51, 1385–1394.

Goosens, K. A., and Maren, S. (2002). Long-term potentiation as a substrate for memory: evidence from studies of amygdaloid plasticity and Pavlovian fear conditioning. *Hippocampus* 12, 592–599.

Gumbiner, B., Wendel, J. A., and McDermott, M. P. (1996). Effects of diet composition and ketosis on glycemia during very-low-energy-diet therapy in obese patients with non-insulin-dependent diabetes mellitus. *Am. J. Clin. Nutr.* 63, 110–115.

Gwak, Y. S., Tan, H. Y., Nam, T. S., Paik, K. S., Hulsebosch, C. E., and Leem, J. W. (2006). Activation of spinal GABA receptors attenuates chronic central neuropathic pain after spinal cord injury. *J. Neurotrauma* 23, 1111–1124.

Haces, M. L., Hernandez-Fonseca, K., Medina-Campos, O. N., Montiel, T., Pedraza-Chaverri, J., and Massieu, L. (2008). Antioxidant capacity contributes to protection of ketone bodies against oxidative damage induced during hypoglycemic conditions. *Exp. Neurol.* 211, 85–96.

Hallböök, T., Lundgren, J., and Rosén, I. (2007). Ketogenic diet improves sleep quality in children with therapy-resistant epilepsy. *Epilepsia* 48, 59–65.

Halyburton, A. K., Brinkworth, G. D., Wilson, C. J., Noakes, M., Buckley, J. D., Keogh, J. B., and Clifton, P. M. (2007). Low- and high-carbohydrate weight-loss diets have similar effects on mood but not cognitive performance. *Am. J. Clin. Nutr.* 86, 580–587.

Hori, A., Tandon, P., Holmes, G. L., and Stafstrom, C. E. (1997). Ketogenic diet: effects on expression of kindled seizures and behavior in adult rats. *Epilepsia* 38, 750–758.

Hu, Y., and Wilson, G. S. (1997). Rapid changes in local extracellular rat brain glucose observed with an in vivo glucose sensor. *J. Neurochem.* 68, 1745–1752.

Hu, Z.-G., Wang, H.-D., Qiao, L., Yan, W., Tan, Q.-F., and Yin, H.-X. (2009a). The protective effect of the ketogenic diet on traumatic brain injury-induced cell death in juvenile rats. *Brain Inj.* 23, 459–465.

Hu, Z. G., Wang, H. D., Jin, W., and Yin, H. X. (2009b). Ketogenic diet reduces cytochrome c release and cellular apoptosis following traumatic brain injury in juvenile rats. *Ann. Clin. Lab. Sci.* 39, 76–83.

Huang, C.-C., Liang, Y.-C., and Hsu, K.-S. (1999). A role for extracellular adenosine in the time-dependent reversal of long-term potentiation by low-frequency stimulation at hippocampal CA1 synapses. *J. Neurosci.* 19, 9728–9738.

Iwabuchi, S., and Kawahara, K. (2011). Functional significance of the negative-feedback regulation of ATP release via pannexin-1 hemichannels under ischemic stress in astrocytes. *Neurochem. Int.* 58, 376–384.

Jeong, E. A., Jeon, B. T., Shin, H. J., Kim, N., Lee, D. H., Kim, H. J., Kang, S. S., Cho, G. J., Choi, W. S., and Roh, G. S. (2011). Ketogenic diet-induced peroxisome proliferator-activated receptor-γ activation decreases neuroinflammation in the mouse hippocampus after kainic acid-induced seizures. *Exp. Neurol.* 232, 195–202.

Johannessen Landmark, C. (2008). Antiepileptic drugs in non-epileptic disorders: relations between mechanisms of action and clinical efficacy. *CNS Drugs* 22, 27–47.

Juge, N., Gray, J. A., Omote, H., Miyaji, T., Inoue, T., Hara, C., Uneyama, H., Edwards, R. H., Nicoll, R. A., and Moriyama, Y. (2010). Metabolic control of vesicular glutamate transport and release. *Neuron* 68, 99–112.

Kang, H.-C., Lee, H. S., You, S. J., Kang, D. C., Ko, T.-S., and Kim, H. D. (2007). Use of a modified Atkins diet in intractable childhood epilepsy. *Epilepsia* 48, 182–186.

Karlsten, R., Gordh, T., and Post, C. (1992). Local antinociceptive and hyperalgesic effects in the formalin test after peripheral administration of adenosine analogues in mice. *Pharmacol. Toxicol.* 70, 434–438.

Kashiwaya, Y., Takeshima, T., Mori, N., Nakashima, K., Clarke, K., and Veech, R. L. (2000). D-β-hydroxybutyrate protects neurons in models of Alzheimer's and Parkinson's disease. *Proc. Natl. Acad. Sci. U.S.A.* 97, 5440–5444.

Kawamura, M. Jr., Ruskin, D. N., and Masino, S. A. (2010). Metabolic autocrine regulation of neurons involves cooperation among pannexin hemichannels, adenosine receptors and KATP channels. *J. Neurosci.* 30, 3886–3895.

Kim, D. Y., Davis, L. M., Sullivan, P. G., Maalouf, M., Simeone, T. A., Van Brederode, J., and Rho, J. M. (2007). Ketone bodies are protective against oxidative stress in neocortical neurons. *J. Neurochem.* 101, 1316–1326.

Kim, D. Y., Vallejo, J., and Rho, J. M. (2010). Ketones prevent synaptic dysfunction induced by mitochondrial respiratory complex inhibitors. *J. Neurochem.* 114, 130–141.

Kinsman, S. L., Vining, E. P., Quaskey, S. A., Mellits, D., and Freeman, J. M. (1992). Efficacy of the ketogenic diet for intractable seizure disorders: review of 58 cases. *Epilepsia* 33, 1132–1136.

Kirchner, A., Veliskova, J., and Velisek, L. (2006). Differential effects of low glucose concentrations on seizures and epileptiform activity in vivo and in vitro. *Eur. J. Neurosci.* 23, 1512–1522.

Klement, R. J., and Kammerer, U. (2011). Is there a role for carbohydrate restriction in the treatment and prevention of cancer? *Nutr. Metab.* 8, 75.

Koranda, J. L., Ruskin, D. N., Masino, S. A., and Blaise, J. H. (2011). A ketogenic diet reduces long-term potentiation in the dentate gyrus of freely-behaving rats. *J. Neurophysiol.* 106, 662–666.

Kossoff, E. H., Laux, L. C., Blackford, R., Morrison, P. F., Pyzik, P. L., Hamdy, R. M., Turner, Z., and Nordli, D. R. Jr. (2008a). When do seizures usually improve with the ketogenic diet? *Epilepsia* 49, 329–333.

Kossoff, E. H., Rowley, H., Sinha, S. R., and Vining, E. P. G. (2008b). A prospective study of the modified Atkins diet for intractable epilepsy in adults. *Epilepsia* 49, 316–319.

Langan, S. J., Deary, I. J., Hepburn, D. A., and Frier, B. M. (1991). Cumulative cognitive impairment following recurrent severe hypoglycaemia in adult patients with insulin-treated diabetes mellitus. *Diabetologia* 34, 337–344.

Lange, K. W., Sahakian, B. J., Quinn, N. P., Marsden, C. D., and Robbins, T. W. (1995). Comparison of executive and visuospatial memory function in Huntington's disease and dementia of Alzheimer type matched for degree of dementia. *J. Neurol. Neurosurg. Psychiatr.* 58, 598–606.

Lanska, D. J., Lanska, M. J., Lavine, L., and Schoenberg, B. S. (1988). Conditions associated with Huntington's disease at death: a case-control study. *Arch. Neurol.* 45, 878–880.

Laugerette, F., Vors, C., Peretti, N., and Michalski, M.-C. (2011). Complex links between dietary lipids, endogenous endotoxins and metabolic inflammation. *Biochimie* 93, 39–45.

Lawrence, A. D., Sahakian, B. J., Hodges, J. R., Rosser, A. E., Lange, K. W., and Robbins, T. W. (1996). Executive and mnemonic functions in early Huntington's disease. *Brain* 119, 1633–1645.

Lefevre, F., and Aronson, N. (2000). Ketogenic diet for the treatment of refractory epilepsy in children: a systematic review of efficacy. *Pediatrics* 105, e46.

Linard, B., Ferrandon, A., Koning, E., Nehlig, A., and Raffo, E. (2010). Ketogenic diet exhibits neuroprotective effects in hippocampus but fails to prevent epileptogenesis in the lithium-pilocarpine model of mesial temporal lobe epilepsy in adult rats. *Epilepsia* 51, 1829–1836.

Liu, Y.-M. C., Williams, S., Basualdo-Hammond, C., Stephens, D., and Curtis, R. (2003). A prospective study: growth and nutritional status of children treated with the ketogenic diet. *J. Am. Diet. Assoc.* 103, 707–712.

Loring, D. W. (2005). Cognitive side effects of antiepileptic drugs in children. *Psychiatr. Times* 22, 41.

Loring, D. W., and Kimford, J. (2001). Cognitive and behavioral effects of epilepsy treatment. *Epilepsia* 42, 24–32.

LoVerme, J., Fu, J., Astarita, G., La Rana, G., Russo, R., Calignano, A., and Piomelli, D. (2005). The nuclear receptor peroxisome proliferator-activated receptor-alpha mediates the anti-inflammatory actions of palmitoylethanolamide. *Mol. Pharmacol.* 67, 15–19.

LoVerme, J., Russo, R., La Rana, G., Fu, J., Farthing, J., Mattace-Raso, G., Meli, R., Hohmann, A., Calignano, A., and Piomelli, D. (2006). Rapid broad-spectrum analgesia through activation of peroxisome-proliferator activated receptor-α. *J. Pharmacol. Exp. Ther.* 319, 1051–1061.

Lund, T. M., Risa, Ø., Sonnewald, U., Schousboe, A., and Waagepetersen, H. S. (2009). Availability of neurotransmitter glutamate is diminished when β-hydroxybutyrate replaces glucose in cultured neurons. *J. Neurochem.* 110, 80–91.

Ma, W., Berg, J., and Yellen, G. (2007). Ketogenic diet metabolites reduce firing in central neurons by opening KATP channels. *J. Neurosci.* 27, 3618–3625.

Maalouf, M., and Rho, J. M. (2008). Oxidative impairment of hippocampal long-term potentiation involves activation of protein phosphatase 2A and is prevented by ketone bodies. *J. Neurosci. Res.* 86, 3322–3330.

Maalouf, M., Sullivan, P. G., Davis, L., Kim, D. Y., and Rho, J. M. (2007). Ketones inhibit mitochondrial production of reactive oxygen species production following glutamate excitotoxicity by increasing NADH oxidation. *Neuroscience* 145, 256–264.

Mahon, S., Deniau, J.-M., and Charpier, S. (2004). Corticostriatal plasticity: life after the depression. *Trends Neurosci.* 27, 460–467.

Malan, T. P. Jr., Mata, H. P., and Porreca, F. (2002). Spinal GABAA and GABAB receptor pharmacology in a rat model of neuropathic pain. *Anesthesiology* 96, 1161–1167.

Malmberg, A. B., and Yaksh, T. L. (1993). Pharmacology of the spinal action of ketorolac, morphine, ST-91, U50488H, and L-PIA on the formalin test and an isobolographic analysis of the NSAID interaction. *Anesthesiology* 79, 270–281.

Mantis, J. G., Fritz, C. L., Marsh, J., Heinrichs, S. C., and Seyfried, T. N. (2009). Improvement in motor and exploratory behavior in Rett syndrome mice with restricted ketogenic and standard diets. *Epilepsy Behav.* 15, 133–141.

Masino, S. A., and Geiger, J. D. (2008). Are purines mediators of the anticonvulsant/neuroprotective effects of ketogenic diets? *Trends Neurosci.* 31, 273–278.

Masino, S. A., Gockel, J. A., Wasser, C. D., Pomeroy, L. T., Wagener, J. F., Gawryluk, J. W., and Geiger, J. D. (2007). The relationship among ATP, adenosine and a ketogenic diet. *Soc. Neurosci. Abstr.* 595, 512.

Masino, S. A., Li, T., Theofilas, P., Ruskin, D. N., Fredholm, B. B., Geiger, J. D., Aronica, E., and Boison, D. (2011). A ketogenic diet suppresses seizures in mice through adenosine A1 receptors. *J. Clin. Invest.* 121, 2679–2683.

Massieu, L., Haces, M. L., Montiel, T., and Hernández-Fonseca, K. (2003). Acetoacetate protects hippocampal neurons against glutamate-mediated neuronal damage during glycolysis inhibition. *Neuroscience* 120, 365–378.

McClernon, F. J., Yancy, W. S. Jr., Eberstein, J. A., Atkins, R. C., and Westman, E. C. (2007). The effects of a low-carbohydrate ketogenic diet and a low-fat diet on mood, hunger, and other self-reported symptoms. *Obesity (Silver Spring).* 15, 182–187.

Mense, S. (1983). Basic neurobiological mechanisms of pain. *Am. J. Med.* 75, 4–14.

Michalik, L., Auwerx, J., Berger, J. P., Chatterjee, V. K., Glass, C. K., Gonzalez, F. J., Grimaldi, P. A., Kadowaki, T., Lazar, M. A., O'Rahilly, S., Palmer, C. N. A., Plutzky, J., Reddy, J. K., Spiegelman, B. M., Staels, B., and Wahli, W. (2006). International Union of Pharmacology. LXI. Perixosome proliferator-activated

receptors. *Pharmacol. Rev.* 58, 726–741.

Minor, T. R., Rowe, M. K., Soames-Job, R. F., and Ferguson, E. C. (2001). Escape deficits induced by inescapable shock and metabolic stress are reversed by adenosine receptor antagonists. *Behav. Brain Res.* 120, 203–212.

Mitchell, J. B., Miller, K., and Dunwiddie, T. V. (1993). Adenosine-induced suppression of synaptic responses and the initiation and expression of long-term potentiation in the CA1 region of the hippocampus. *Hippocampus* 3, 77–86.

Mohamed, H. E., El-Swefy, S. E., Rashed, L. A., and El-Latif, S. K. A. (2010). Biochemical effect of a ketogenic diet on the brains of obese adult rats. *J. Clin. Neurosci.* 17, 899–904.

Mosek, A., Natour, H., Neufeld, M. Y., Shiff, Y., and Vaisman, N. (2009). Ketogenic diet treatment in adults with refractory epilepsy: a prospective pilot study. *Seizure* 18, 30–33.

Moya-Camarena, S. Y., Vanden Heuvel, J. P., Blanchard, S. G., Leesnitzer, L. A., and Belury, M. A. (1999). Conjugated linoleic acid is a potent naturally occurring ligand and activator of PPARα. *J. Lipid Res.* 40, 1426–1433.

Muller-Schwarze, A. B., Tandon, P., Liu, Z., Lang, Y., Holmes, G. L., and Stafstrom, C. E. (1999). Ketogenic diet reduces spontaneous seizures and mossy fiber sprouting in the kainic acid model. *Neuroreport* 10, 1517–1522.

Murphy, P., and Burnham, W. M. (2006). The ketogenic diet causes a reversible decrease in activity level in Long-Evans rats. *Exp. Neurol.* 201, 84–89.

Murphy, P., Likhodii, S. S., Hatamian, M., and Burnham, W. M. (2005). Effect of the ketogenic diet on the activity level of Wistar rats. *Pediatr. Res.* 57, 353–357.

Myers, R. H., Sax, D. S., Koroshetz, W. J., Mastromauro, C., Cupples, L. A., Kiely, D. K., Pettengill, F. K., and Bird, E. D. (1991). Factors associated with slow progression in Huntington's disease. *Arch. Neurol.* 48, 800–804.

Nakazawa, M., Kodama, S., and Matsuo, T. (1983). Effects of ketogenic diet on electroconvulsive threshold and brain contents of adenosine nucleotides. *Brain Dev.* 5, 375–380.

Neal, E. G., Chaffe, H., Schwartz, R. H., Lawson, M. S., Edwards, N., Fitzsimmons, G., Whitney, A., and Cross, J. H. (2008a). The ketogenic diet for the treatment of childhood epilepsy: a randomised controlled trial. *Lancet Neurol.* 7, 500–506.

Neal, E. G., Chaffe, H. M., Edwards, N., Lawson, M. S., Schwartz, R. H., and Cross, J. H. (2008b). Growth of children on classical and medium-chain triglyceride ketogenic diets. *Pediatrics* 122, e334–e340.

Noh, H. S., Hah, Y.-S., Nilufar, R., Han, J., Bong, J.-H., Kang, S. S., Cho, G. J., and Choi, W. S. (2006a). Acetoacetate protects neuronal cells from oxidative glutamate toxicity. *J. Neurosci. Res.* 83, 702–709.

Noh, H. S., Kim, Y. S., Kim, Y. H., Han, J. Y., Park, C. H., Kang, A. K., Shin, H. S., Kang, S. S., Cho, G. J., and Choi, W. S. (2006b). Ketogenic diet protects the hippocampus from kainic acid toxicity by inhibiting the dissociation of Bad from 14-3-3. *J. Neurosci. Res.* 84, 1829–1836.

Noh, H. S., Kang, S. S., Kim, D. W., Kim, Y. H., Park, C. H., Han, J. Y., Cho, G. J., and Choi, W. S. (2005). Ketogenic diet increases calbindin-D28k in the hippocampi of male ICR mice with kainic acid seizures. *Epilepsy Res.* 65, 153–159.

Noh, H. S., Kim, Y. S., Lee, H. P., Chung, K. M., Kim, D. W., Kang, S. S., Cho, G. J., and Choi, W. S. (2003). The protective effect of a ketogenic diet on kainic acid-induced hippocampal cell death in the male ICR mice. *Epilepsy Res.* 53, 119–128.

Noh, H. S., Lee, H. P., Kim, D. W., Kang, S. S., Cho, G. J., Rho, J. M., and Choi, W. S. (2004). A cDNA microarray analysis of gene expression profiles in rat hippocampus following a ketogenic diet. *Brain Res. Mol. Brain Res.* 129, 80–87.

Nylen, K., Velazquez, J. L. P., Likhodii, S. S., Cortez, M. A., Shen, L., Leshchenko, Y., Adeli, K., Gibson, K. M., Burnham, W. M., and Snead, O. C. III. (2008). A ketogenic diet rescues the murine succinic semialdehyde dehydrogenase deficient phenotype. *Exp. Neurol.* 210, 449–457.

Nylen, K., Velazquez, J. L. P., Sayed, V., Gibson, K. M., Burnham, W. M., and Snead, O. C. III. (2009). The effects of a ketogenic diet on ATP concentrations and the number of hippocampal mitochondria in Aldh5a1-/- mice. *Biochim. Biophys. Acta* 1790, 208–212.

Oishi, K., Sakamoto, K., Konishi, M., Murata, Y., Itoh, N., and Sei, H. (2010). FGF21 is dispensable for hypothermia induced by fasting in mice. *Neuro Endocrinol. Lett.* 31, 101–105.

Omote, H., Miyaji, T., Juge, N., and Moriyama, Y. (2011). Vesicular neurotransmitter transporter: bioenergetics and regulation of glutamate transport. *Biochemistry* 50, 5558–5565.

Pan, J. W., Bebin, E. M., Chu, W. J., and Hetherington, H. P. (1999). Ketosis and epilepsy: 31P spectroscopic imaging at 4.1 T. *Epilepsia* 40, 703–707.

Pan, Y., Larson, B., Araujo, J. A., Lau, W., De Rivera, C., Santana, R., Gore, A., and Milgram, N. W. (2010). Dietary supplementation with medium-chain TAG has long-lasting cognition-enhancing effects in aged dogs. *Br. J. Nutr.* 103, 1746–1754.

Park, S., Kim, D. S., Kang, S., and Daily, J. W. III. (2011). A ketogenic diet impairs energy and glucose homeostasis by the attenuation of hypothalamic leptin signaling and hepatic insulin signaling in a rat model of non-obese type 2 diabetes. *Exp. Biol. Med.* 236, 194–204.

Pascual, O., Casper, K. B., Kubera, C., Zhang, J., Revilla-Sanchez, R., Sul, J.-Y., Takano, H., Moss, S. J., McCarthy, K., and Haydon, P. G. (2005). Astrocytic purinergic signaling coordinates synaptic networks. *Science* 310, 113–116.

Pérez-Guisado, J., and Muñoz-Serrano, A. (2011). The effect of the Spanish Ketogenic Mediterranean Diet on nonalcoholic fatty liver disease: a pilot study. *J. Med. Food* 14, 677–680.

Peterson, S. J., Tangney, C. C., Pimentel-Zablah, E. M., Hjelmgren, B., Booth, G., and Berry-Kravis, E. (2005). Changes in growth and seizure reduction in children on the ketogenic diet as a treatment for intractable epilepsy. *J. Am. Diet. Assoc.* 105, 718–725.

Picot, M. C., Baldy-Moulinier, M., Daurès, J. P., Dujols, P., and Crespel, A. (2008). The prevalence of epilepsy and pharmacoresistant epilepsy in adults: a population-based study in a Western European country. *Epilepsia* 49, 1230–1238.

Poplawski, M. M., Mastaitis, J. W., Isoda, F., Grosjean, F., Zheng, F., and Mobbs, C. V. (2011). Reversal of diabetic nephropathy by a ketogenic diet. *PLoS ONE* 6, e18604. doi:10.1371/journal.pone.0018604

Potter, W. B., O'Riordan, K. J., Barnett, D., Osting, S. M. K., Wagoner, M., Burger, C., and Roopra, A. (2010). Metabolic regulation of neuronal plasticity by the energy sensor AMPK. *PLoS ONE* 5, e8996. doi:10.1371/journal.pone.0008996

Prins, M. L., Fujima, L. S., and Hovda, D. A. (2005). Age-dependent reduction of cortical contusion volume by ketones after traumatic brain injury. *J. Neurosci. Res.* 82, 413–420.

Prins, M. L., and Hovda, D. A. (2009). The effects of age and ketogenic diet on local cerebral metabolic rates of glucose after controlled cortical impact injury in rats. *J. Neurotrauma* 26, 1083–1093.

Pulsifer, M. B., Gordon, J. M., Brandt, J., Vining, E. P. G., and Freeman, J. M. (2001). Effects of ketogenic diet on development and behavior: preliminary report of a prospective study. *Dev. Med. Child Neurol.* 43, 301–306.

Rex, C. S., Kramar, E. A., Colgin, L. L., Lin, B., Gall, C. M., and Lynch, G. (2005). Long-term potentiation is impaired in middle-aged rats: regional specificity and reversal by adenosine receptor antagonists. *J. Neurosci.* 25, 5956–5966.

Ruskin, D. N., Kawamura, M. Jr., and Masino, S. A. (2009). Reduced pain and inflammation in juvenile and adult rats fed a ketogenic diet. *PLoS ONE* 4, e8349. doi:10.1371/journal.pone.0008349

Ruskin, D. N., Ross, J. L., Kawamura, M. Jr., Ruiz, T. L., Geiger, J. D., and Masino, S. A. (2011a). A ketogenic diet delays weight loss and does not impair working memory or motor function in the R6/2 1J mouse model of Huntington's disease. *Physiol. Behav.* 103, 501–507.

Ruskin, D. N., Suter, T. A. C. S., and Masino, S. A. (2011b). Dissociation of hypoalgesia, ketosis, and hypoglycemia with two ketogenic diets in the rat. *Soc. Neurosci. Abstr.* 383.04.

Samala, R., Klein, J., and Borges, K. (2011). The ketogenic diet changes metabolite levels in hippocampal extracellular fluid. *Neurochem. Int.* 58, 5–8.

Samoilova, M., Weisspapir, M., Abdelmalik, P., Velumian, A. A., and Carlen, P. L. (2010). Chronic in vitro ketosis is neuroprotective but not anticonvulsant. *J. Neurochem.* 113, 826–835.

Sanberg, P. R., Fibiger, H. C., and Mark, R. F. (1981). Body weight and dietary factors in Huntington's disease patients compared with matched controls. *Med. J. Aust.* 1, 407–409.

Schock, S. C., LeBlanc, D., Hakim, A. M., and Thompson, C. S. (2008). ATP release by way of connexin 36 hemichannels mediates ischemic tolerance in vitro. *Biochem. Biophys. Res. Commun.* 368, 138–144.

Schwartzkroin, P. A., Wenzel, H. J., Lyeth, B. G., Poon, C. C., DeLance, A., Van, K. C., Campos, L., and Nguyen, D. V. (2010). Does ketogenic diet alter seizure sensitivity and cell loss following fluid percussion injury? *Epilepsy Res.* 82, 74–84.

Seyfried, T. N., Marsh, J., Shelton, L. M., Huysentruyt, L. C., and Mukherjee, P. (2012). Is the restricted ketogenic diet a viable alternative to the standard of care for managing malignant brain cancer? *Epilepsy Res.* PMID: 21885251. [Epub ahead of print].

Seyfried, T. N., and Mukherjee, P. (2005). Targeting energy metabolism in brain cancer: review and hypothesis. *Nutr. Metab.* 2, 30.

Sharma, S., Gulati, S., Kalra, V., Agarwala, A., and Kabra, M. (2009). Seizure control and biochemical profile on the ketogenic diet in young children with refractory epilepsy – Indian experience. *Seizure* 18, 446–449.

Shram, N. F., Netchiporouk, L. I., Martelet, C., Jaffrezic-Renault, N., and Cespuglio, R. (1997). Brain glucose: voltammetric determination in normal and hyperglycaemic rats using a glucose microsensor. *Neuroreport* 8, 1109–1112.

Silva, M. C., Rocha, J., Pires, C. S., Ribeiro, L. C., Brolese, G., Leite, M. C., Almeida, L. M. V., Tramontina, F., Ziegler, D. R., and Gonçalves, C. A. (2005). Transitory gliosis in the CA3 hippocampal region in rats fed on a ketogenic diet. *Nutr. Neurosci.* 8, 259–264.

Sirven, J., Whedon, B., Caplan, D., Liporace, J., Glosser, D., O'Dwyer, J., and Sperling, M. R. (1999). The ketogenic diet for intractable epilepsy in adults: preliminary results. *Epilepsia* 40, 1721–1726.

Snell-Bergeon, J. K., Chartier-Logan, C., Maahs, D. M., Ogden, L. G., Hokanson, J. E., Kinney, G. L., Eckel, R. H., Ehrlich, J., and Rewers, M. (2009). Adults with type 1 diabetes eat a high fat, atherogenic diet which is associated with coronary artery calcium. *Diabetologia* 52, 801–809.

Stafstrom, C. E., Ockuly, J. C., Murphree, L., Valley, M. T., Roopra, A., and Sutula, T. P. (2009). Anticonvulsant and antiepileptic actions of 2-deoxy-d-glucose in epilepsy models. *Ann. Neurol.* 65, 435–447.

Stafstrom, C. E., Wang, C., and Jensen, F. E. (1999). Electrophysiological observations in hippocampal slices from rats treated with the ketogenic diet. *Dev. Neurosci.* 21, 393–399.

Stout, C. E., Costantin, J. L., Naus, C. C., and Charles, A. C. (2002). Intercellular calcium signaling in astrocytes via ATP release through connexin hemichannels. *J. Biol. Chem.* 277, 10482–10488.

Streijger, F., Plunet, W. T., Lee, H. T., Liu, J., Lam, C. K., Park, S., Hilton, B. J., Fransen, B. L., Matheson, K. A., Assinck, P., Kwon, B. K., and Tetzlaff, W. (2011). Ketogenic diet improves forelimb motor function after spinal cord injury. *Soc. Neurosci. Abstr.* 255.09.

Studzinski, C. M., Mackay, W. A., Beckett, T. L., Henderson, S. T., Murphy, M. P., Sullivan, P. G., and Burnham, W. M. (2008). Induction of ketosis may improve mitochondrial function and decrease steady-state amyloid-β precursor protein (APP) levels in the aged dog. *Brain Res.* 1226, 209–217.

Su, S. W., Sogawa, M. R. C. Y., Silveira, D. C., Holmes, G. L., and Stafstrom, C. E. (2000). Timing of ketogenic diet initiation in an experimental epilepsy model. *Brain Res. Dev. Brain Res.* 125, 131–138.

Sullivan, P. G., Rippy, N. A., Dorenbos, K., Concepcion, R. C., Agarwal, A. K., and Rho, J. M. (2004). The ketogenic diet increases mitochondrial uncoupling protein levels and activity. *Ann. Neurol.* 55, 576–580.

Swink, T. D., Vining, E. P., and Freeman, J. M. (1997). The ketogenic diet: 1997. *Adv. Pediatr.* 44, 297–329.

Tabata, K., Matsumoto, K., Murakami, Y., and Watanabe, H. (2001). Ameliorative effects of paeoniflorin, a major constituent of peony root, on adenosine A1 receptor-mediated impairment of passive avoidance performance and long-term potentiation in the hippocampus. *Biol. Pharm. Bull.* 24, 496–500.

Tai, K.-K., Nguyen, N., Pham, L., and Truong, D. D. (2008). Ketogenic diet prevents cardiac arrest-induced cerebral ischemic neurodegeneration. *J. Neural Transm.* 115, 1011–1017.

Tai, K.-K., Pham, L., and Truong, D. D. (2009). Intracisternal administration of glibenclamide or 5-hydroxydecanoate does not reverse the neuroprotective effect of ketogenic diet against ischemic brain injury-induced neurodegeneration. *Brain Inj.* 23, 1081–1088.

Tendler, D., Lin, S., Yancy, W. S. Jr., Mavropoulos, J., Sylvestre, P., Rockey, D. C., and Westman, E. C. (2007). The effect of a low-carbohydrate, ketogenic diet on nonalcoholic fatty liver disease: a pilot study. *Dig. Dis. Sci.* 52, 589–593.

Thaler, J. P., and Schwartz, M. W. (2010). Minireview: inflammation and obesity pathogenesis: the hypothalamus heats up. *Endocrinology* 151, 4109–4115.

Thio, L. L., Rensing, N., Maloney, S., Wozniak, D. F., Xiong, C., and Yamada, K. A. (2010). A ketogenic diet does not impair rat behavior or long-term potentiation. *Epilepsia* 51, 1619–1623.

Thio, L. L., Wong, M., and Yamada, K. A. (2000). Ketone bodies do not directly alter excitatory or inhibitory hippocampal synaptic transmission. *Neurology* 54, 325–331.

Thompson, P. J., Baxendale, S. A., Duncan, J. S., and Sander, J. W. (2000). Effects of topiramate on cognitive function. *J. Neurol. Neurosurg. Psychiatr.* 69, 636–641.

Tieu, K., Perier, C., Caspersen, C., Teismann, P., Wu, D.-C., Yan, S.-D., Niani, A., Vila, M., Jackson-Lewis, V., Ramasamy, R., and Przedborsky, S. (2003). d-β-Hydroxybutyrate rescues mitochondrial respiration and mitigates features of Parkinson disease. *J. Clin. Invest.* 112, 892–901.

Todorova, M. T., Tandon, P., Madore, R. A., Stafstrom, C. E., and Seyfried, T. N. (2000). The ketogenic diet inhibits epileptogenesis in EL mice: a genetic model for idiopathic epilepsy. *Epilepsia* 41, 933–940.

Tromba, C., Salvaggio, A., Racagni, G., and Volterra, A. (1992). Hypoglycemia-activated K^+ channels in hippocampal neurons. *Neurosci. Lett.* 143, 185–189.

Van der Auwera, I., Wera, S., Van Leuven, F., and Henderson, S. T. (2005). A ketogenic diet reduces amyloid beta 40 and 42 in a mouse model of Alzheimer's disease. *Nutr. Metab.* 2, 28.

Veech, R. L. (2004). The therapeutic implications of ketone bodies: the effects of ketone bodies in pathological conditions: ketosis, ketogenic diet, redox states, insulin resistance, and mitochondrial metabolism. *Prostaglandins Leukot. Essent. Fatty Acids* 70, 309–319.

Vining, E. P. (1999). Clinical efficacy of the ketogenic diet. *Epilepsy Res.* 37, 181–190.

Vining, E. P., Freeman, J. M., Ballaban-Gil, K., Camfield, C. S., Camfield, P. R., Holmes, G. L., Shinnar, S., Shuman, R., Trevathan, E., and Wheless, J. W. (1998). A multicenter study of the efficacy of the ketogenic diet. *Arch. Neurol.* 55, 1433–1437.

Westman, E. C., Yancy, W. S. Jr., Mavropoulos, J. C., Marquart, M., and McDuffie, J. R. (2008). The effect of a low-carbohydrate, ketogenic diet versus a low-glycemic index diet on glycemic control in type 2 diabetes mellitus. *Nutr. Metab. (Lond.)* 5, 36.

Wilder, R. M. (1921). The effects of ketonemia on the course of epilepsy. *Mayo Clin. Bull.* 2, 307–308.

Wing, R. R., Vazquez, J. A., and Ryan, C. M. (1995). Cognitive effects of ketogenic weight-reducing diets. *Int. J. Obes. Relat. Metab. Disord.* 19, 811–816.

Xu, K., Sun, X., Eroku, B. O., Tsipis, C. P., Puchowicz, M. A., and LaManna, J. C. (2010). Diet-induced ketosis improves cognitive performance in aged rats. *Adv. Exp. Med. Biol.* 662, 71–75.

Yamada, K. A., Rensing, N., and Thio, L. L. (2005). Ketogenic diet reduces hypoglycemia-induced neuronal death in young rats. *Neurosci. Lett.* 385, 210–214.

Yancy, W. S. Jr., Almirall, D., Maciejewski, M. L., Kolotkin, R. L., McDuffie, J. R., and Westman, E. C. (2009). Effects of two weight-loss diets on health-related quality of life. *Qual. Life Res.* 18, 281–289.

Yancy, W. S. Jr., Foy, M., Chalecki, A. M., Vernon, M. C., and Westman, E. C. (2005). A low-carbohydrate, ketogenic diet to treat type 2 diabetes. *Nutr. Metab.* 2, 34.

Yang, X., and Cheng, B. (2010). Neuroprotective and anti-inflammatory activities of ketogenic diet on MPTP-induced neurotoxicity. *J. Mol. Neurosci.* 42, 145–153.

Yudkoff, M., Daikhin, Y., Melø, T. M., Nissim, I., Sonnewald, U., and Nissim, I. (2007). The ketogenic diet and brain metabolism of amino acids: relationship to the anticonvulsant effect. *Annu. Rev. Nutr.* 27, 415–430.

Zhang, D. S., Ren, L. M., and Zhang, L. (2004). Relation between adenosine A1 receptor and NMDA receptor on synaptic transmission in dentate gyrus of hippocampus. *Yao Xue Xue Bao* 39, 245–249.

Zhao, Q., Stafstrom, C. E., Fu, D. D., Hu, Y., and Holmes, G. L. (2004). Detrimental effects of the ketogenic diet on cognitive function in rats. *Pediatr. Res.* 55, 498–506.

Zhao, Y. T., Tekkök, S., and Krnjevic, K. (1997). 2-Deoxy-d-glucose-induced changes in membrane potential, input resistance, and excitatory postsynaptic potentials of CA1 hippocampal neurons. *Can. J. Physiol. Pharmacol.* 75, 368–374.

Zhao, Z., Lange, D. J., Voustianiouk, A., MacGrogan, D., Ho, L., Suh, J., Humala, N., Thiyagarajan, M., Wang, J., and Pasinetti, G. M. (2006). A ketogenic diet as a potential novel therapeutic intervention in amyotrophic lateral sclerosis. *BMC Neurosci.* 7, 29. doi:10.1186/1471-2202-7-29

Zhu, P. J., and Krnjevic, K. (1993). Adenosine release is a major cause of failure of synaptic transmission during hypoglycaemia in rat hippocampal slices. *Neurosci. Lett.* 155, 128–131.

Ziegler, D. R., Gamaro, G. D., Araújo, E., Bassani, M. G., Perry, M. L. S., Dalmaz, C., and Gonçalves, C.-A. (2005). Nociception and locomotor activity are increased in ketogenic diet fed rats. *Physiol. Behav.* 84, 421–427.

Conflict of Interest Statement: The authors declare that the research was conducted in the absence of any commercial or financial relationships that could be construed as a potential conflict of interest.

Received: 23 December 2011; paper pending published: 16 January 2012; accepted: 23 February 2012; published online: 26 March 2012.

*Citation: Ruskin DN and Masino SA (2012) The nervous system and metabolic dysregulation: emerging evidence converges on ketogenic diet therapy. Front. Neurosci. **6**:33. doi: 10.3389/fnins.2012.00033*

This article was submitted to Frontiers in Neuropharmacology, a specialty of Frontiers in Neuroscience.

frontiers in
PHARMACOLOGY

ORIGINAL RESEARCH ARTICLE
published: 13 January 2012
doi: 10.3389/fphar.2011.00096

Aerobic production and utilization of lactate satisfy increased energy demands upon neuronal activation in hippocampal slices and provide neuroprotection against oxidative stress

Avital Schurr [1] **** and Evelyne Gozal*** [2,3]

[1] *Department of Anesthesiology and Perioperative Medicine, School of Medicine, University of Louisville, Louisville, KY, USA*
[2] *Department of Pediatrics, School of Medicine, University of Louisville, Louisville, KY, USA*
[3] *Department of Pharmacology and Toxicology, School of Medicine, University of Louisville, Louisville, KY, USA*

Edited by:
Yuri Zilberter, Faculté de Médecine Timone, France

Reviewed by:
Oliver Kann, University of Heidelberg, Germany
Luc Pellerin, University of Lausanne, Switzerland

****Correspondence:***
Avital Schurr, Department of Anesthesiology and Perioperative Medicine, School of Medicine, University of Louisville, 530 South Jackson Street, CCB-ULH, Room C2A03, Louisville, KY, USA.
e-mail: a0schu01@louisville.edu

Ever since it was shown for the first time that lactate can support neuronal function *in vitro* as a sole oxidative energy substrate, investigators in the field of neuroenergetics have been debating the role, if any, of this glycolytic product in cerebral energy metabolism. Our experiments employed the rat hippocampal slice preparation with electrophysiological and biochemical methodologies. The data generated by these experiments (a) support the hypothesis that lactate, not pyruvate, is the end-product of cerebral aerobic glycolysis; (b) indicate that lactate plays a major and crucial role in affording neural tissue to respond adequately to glutamate excitation and to recover unscathed post-excitation; (c) suggest that neural tissue activation is accompanied by aerobic lactate and NADH production, the latter being produced when the former is converted to pyruvate by mitochondrial lactate dehydrogenase (mLDH); (d) imply that NADH can be utilized as an endogenous scavenger of reactive oxygen species (ROS) to provide neuroprotection against ROS-induced neuronal damage.

Keywords: lactate, glycolysis, LDH, hippocampal slice, neuronal function, reactive oxygen species, NADH, neuroprotection

INTRODUCTION

Almost a quarter of century ago we demonstrated for the first time the ability of cerebral tissue *in vitro* to sustain normal neuronal function by utilizing lactate aerobically as its sole energy substrate (Schurr et al., 1988). The debate that ensued following this discovery on whether or not lactate plays a major role in cerebral energy metabolism continues, although much more evidence in favor of such a role has been accumulated over that period (Gladden, 2004; Schurr, 2006; Pellerin et al., 2007; Mangia et al., 2009; Zielke et al., 2009; Barros and Deitmer, 2010; Ivanov et al., 2011; Wyss et al., 2011). It is important to realize that lactate has never been suggested to replace glucose as the main energy substrate, but rather to play an important, maybe even a crucial role, especially in specific situations. However, for many who still hold that lactate is simply the end-product of anaerobic glycolysis, it is difficult to visualize this monocarboxylate as a major player in cerebral energy metabolism. Consequently, the debate over lactate role in energy metabolism continues unabated for almost two decades.

The findings of Pellerin and Magistretti (1994) and the hypothesis they have offered to explain them, i.e., the astrocytic-neuronal lactate shuttle hypothesis (ANLSH), have been supported by many studies over the years (Hu and Wilson, 1997a; Schurr et al., 1997a,b, 1999a,b; Mangia et al., 2003; Kasischke et al., 2004; Schurr, 2006; Atlante et al., 2007; Schurr and Payne, 2007; Larsen et al., 2008; Passarella et al., 2008; Gallagher et al., 2009). Those who disagree with the ANLSH quarrel mainly about the central role attributed to lactate in this hypothesis and the studies supporting it (Chih et al., 2001; Chih and Roberts, 2003; Hertz, 2004; Dienel and Hertz, 2005; Korf, 2006; Hertz et al., 2007; Gandhi et al., 2009). While glucose is, indisputably, the only energy substrate that can enter glycolysis, the fate of glucose in this pathway is in dispute. Many continue to hold that aerobic glycolysis's end-product is pyruvate, the monocarboxylate that is the substrate for the mitochondrial tricarboxylic acid cycle, while lactate is glycolysis's end-product only under anaerobic conditions. Accordingly, an increase in oxygen supply should occur to allow for the increase in energy demands upon neural activation. Hence, the detractors of lactate's role as an energy substrate during neural activation claim that an increase in oxygen supply could be achieved simply by an increase in cerebral blood circulation. Although an increase in microcirculation at the activation region has been correlated with a spike in oxygen consumption (Malonek and Grinvald, 1996; Vanzetta and Grinvald, 1999) and with a similar spike in NADH level measured *in vitro* (Kasischke et al., 2004), these measurements did not reveal the identity of the oxidized energy substrate. Nevertheless, the prevailing assumption of those who discount the role of lactate is that as long as there are sufficient supplies of oxygen and glucose, glycolysis should produce enough pyruvate to satisfy the heightened energy demands upon activation.

This scenario does not take into account the fact that glucose is incapable of increasing glycolytic flux and thus of up-regulating VO_2, while lactate is capable of producing a dose-dependent increase in VO_2 (Levasseur et al., 2006). The study by Hu and Wilson (1997b) actually alludes to this very phenomenon. Thus, we afforded it a closer reexamination in light of the discount and criticism it received so far (Dienel and Hertz, 2005; Fillenz, 2005; Korf, 2006). Hence, in aiming to clarify some of the contentious issues that continue to divide investigators in the field of cerebral energy metabolism, we consider here several of our own studies and postulates, including one unpublished study, along with the study of Hu and Wilson (1997b). These considerations have led us to contend that most of the disagreements as to lactate's role in cerebral energy metabolism could be easily settled if and when lactate is "allowed" to be the only end-product of glycolysis, both aerobic and anaerobic.

MATERIALS AND METHODS

The experimental portions of the studies already published by us and that are part of the considerations and elaborations herewith can be found in the respective papers. All the experiments in those studies and in the unpublished one we are detailing here employed the rat hippocampal slice preparation, using electrophysiological and biochemical modalities. Therefore, the methods described below apply to the unpublished data on the role of lactate in neuroprotection against glutamate-mediated, reactive oxygen species (ROS)-induced neuronal damage, the results of which are shown in **Figures 8–10**. Adult (200–350 g) male Sprague-Dawley rats were used with diligent attention to minimizing animal stress. Rats were housed in the animal facility at the University of Louisville School of Medicine, maintained on a 12 h light/12 h dark cycle at 22˚C and had unlimited access to food and water. All protocols were approved by the University of Louisville School of Medicine Institutional Animal Care and Use Committee. For each experiment, one rat was decapitated under ether anesthesia, its brain rapidly removed and rinsed with cold (6–8˚C) artificial cerebrospinal fluid (aCSF, see composition below) and dissected. Isolated hippocampi were sliced transversely at 400 μm with a McIlwain tissue chopper and the resulting slices (10–12 slices per hippocampus) were placed in a dual linear-flow incubation/recording chamber (Schurr et al., 1985). Each of the two compartments of the chamber was supplied with a humidified gas mixture (95% O_2/5% CO_2) through separate flow meters (2 l/min) and aCSF via a dual peristaltic pump (1 ml/min). The aCSF composition was (in mM): NaCl 124; KCl 5; NaH_2PO_4 3; $CaCl_2$ 2.5; $MgSO_4$ 2; $NaHCO_3$ 23; D-glucose 10. The aCSF had a pH of 7.3–7.4 and an osmolality of 300 ± 5 mOSM. The temperature of the incubation chamber was held at 34 ± 0.3˚C. After 60 min of incubation, the 10 mM glucose aCSF was replaced either with 2.5 mM glucose-, 5 mM Na-lactate-, or 5 mM Na-pyruvate-aCSF. A 45 min period of equilibration with the replacement medium was allowed before the beginning of electrophysiological recordings of evoked (once/min) CA1 population spike (PS, neuronal function). Each experimental protocol lasted 60 min. Glutamate (Glut; 2.5 mM) and 3-methyl-1-phenyl-2-pyrazolin-5-one (MCI-186, 33 μM), a free radical scavenger (Wu et al., 2006) were supplemented when indicated. In other experiments, 5 mM pyruvate-aCSF was replaced with either (1 mM lactate + 4 mM pyruvate)-aCSF or (0.5 mM glucose + 4 mM pyruvate)-aCSF.

ELECTROPHYSIOLOGICAL MEASUREMENTS

Continuous (45 min) extracellular recordings of electrically evoked PS in the stratum pyramidale of the hippocampal CA1 region were made from one slice in each compartment of the dual chamber using borosilicate micropipettes filled with aCSF (impedance 2–5 MΩ). A two-channel preamplifier (×100) and two field-effect transistor head stages (custom-made) were used. Bipolar stimulating electrodes were placed in the Schaffer collaterals (orthodromic stimulation) and stimulus pulses (0.1 ms in duration) of an amplitude twice threshold (∼10 V) were applied once/min to evoke a response, using two Grass S44 stimulators and two SIU-V constant voltage stimulus isolation units (Grass Technologies, West Warwick, RI, USA). The presence of neuronal function (PS of >3 mV) in each of the slices in both compartments of the dual chamber was verified prior to the beginning of the experimental protocol. The above value of the PS has been determined as our standard, based on hundreds of experiments over 25 years, as the minimum amplitude of a PS that can be accurately measured to indicate the presence of neuronal function that could safely be distinguished from an artifact. Nevertheless, the majority of viable, neuronally functional, slices typically exhibited the maximal PS amplitude in response to the chosen electrical stimulation (8–10 mV). After 45 min of continuous recording in one slice in each compartment, the rest of the slices were tested for the presence and amplitude of their PS by stimulating the Schaffer collaterals and recording the evoked response in the CA1 cell body layer, a test that lasted 10–15 min. Acquisition, analysis and storage of data was done using the CED 1401 mk II data acquisition system with Spike 2 software package (Cambridge Electronic Design corporation, Cambridge, UK). All chemicals were of analytical grade (Sigma Chemical, St. Louis, MO, USA). Each experiment (condition) was repeated three times (30–36 slices). Separate experiments (not shown here) were carried out to determine the optimal concentration of glucose, lactate, pyruvate, Glut, and MCI-186 used in this study.

DETERMINATION OF LACTATE AND GLUCOSE LEVELS IN HIPPOCAMPAL SLICES

Lactate and glucose were measured using the enzymatic kits of Sigma Chemical Co. (St. Louise, MO, USA). Slices were taken out of the incubation-recording chamber at the time points indicated, rinsed in ice-cold aCSF containing no glucose and homogenized in 0.2 ml of 8% perchloric acid. The homogenate was then neutralized with 0.1 ml of 2 M $KHCO_3$ and centrifuged for 3 min at $8000 \times g$. The supernatant (0.1 ml) was used for the analysis of both lactate and glucose. Assays were automated on the Cobas Fara centrifugal analyzer (Roche Diagnostic Systems, Branchburg, NJ, USA). The lactate kit (826-UV) uses lactate dehydrogenase to convert lactate and NAD^+ to pyruvate and NADH, respectively. The glucose kit uses hexokinase to convert glucose and ATP to glucose-6-phosphate and ADP. Glucose-6-phosphate is subsequently oxidized by glucose-6-phosphate dehydrogenase and NAD^+ to 6-phosphogluconate and NADH. In both assays, NADH

was measured fluorometrically (excitation at 340 nm and emission at 450 nm).

ROS MEASUREMENTS USING FLUORESCENT MEASUREMENTS

Reactive oxygen species generation was assessed using the fluorescent probe 2′,7′-dichlorodihydrofluorescein diacetate (H_2DCFDA; Invitrogen, Carlsbad, CA, USA) as described by Liang et al. (2005) with small modifications. The non-fluorescent H_2DCFDA, which crosses the cell membrane, is deacetylated intracellularly by non-specific endogenous esterases to its membrane impermeable form, dichlorodihydrofluorescein (H_2DCF). H_2DCF, when oxidized by ROS, is converted to the fluorescent product dichlorofluorescein (DCF). Briefly, for each experimental sample, five slices were perfused (34°C) for 45 min with aCSF containing 20 μM H_2DCFDA and the selected energy substrate (pyruvate or lactate) with or without Glut. After 45 min, slices were perfused for an additional 10 min with their respective aCSF without H_2DCFDA, then rinsed in cold aCSF and homogenized in 1 ml cold 0 mM glucose aCSF containing 40 μl of the detergent Non-idet-P40 (Roche Applied Science, Indianapolis, IN, USA). Homogenates were then spun for 20 min at 12,000 rpm (13.4 g) in 4°C. All steps and procedures of the experiments involving H_2DCFDA were performed in the dark. Excitation at 485 nm and emission at 535 nm was read using a SpectraFluor Plus spectrophotometer (Tecan, San Jose, CA, USA). Fluorescent readings from slices incubated with pyruvate (5 mM) and Glut (2.5 mM) were considered to yield the maximum DCF fluorescence level (100%; control). H_2DCFDA was dissolved in methanol as stock solution. The final concentration of methanol in the H_2DCFDA-aCSF was less than 0.2%. All samples were read for fluorescence in duplicates and each experiment was repeated at least three times.

STATISTICAL ANALYSIS

Measurements are expressed as means ± SEM. For the electrophysiological data, statistically significant differences between groups were determined using the Student's paired t-test by comparing control slices to glutamate-treated slices within each of the three groups supplemented either with glucose, lactate, or pyruvate. For the fluorescence measurements of ROS, data were assessed for statistically significant differences using paired-sample Wilcoxon signed rank test. For both tests, a value of $p \leq 0.05$ was considered to be statistically significant.

RESULTS AND DISCUSSION

LACTATE PRODUCTION AND UTILIZATION UPON NEURONAL ACTIVATION

Over a decade ago, we performed two sets of experimental paradigms in which hippocampal slices were exposed to Glut for 15 min. Slices were placed in aCSF containing 4 mM glucose for the first paradigm (A) and 10 mM for the other paradigm (B). Accordingly, slices in paradigm A were exposed to a lower Glut concentration (5 mM) than slices in paradigm B (20 mM), since the higher the glucose concentration in the aCSF, the higher Glut concentration slices could tolerate and the higher the level of lactate slices could produce during exposure to Glut (see Schurr et al., 1999a,b). It is important to emphasize that either concentration of Glut by far exceeds the intrinsic physiological concentrations of this neurotransmitter, where synaptic and extrasynaptic spaces are concerned and is thus, excitotoxic to the hippocampal slice preparation. Consequently, the PS amplitude measured during the exposure to Glut quickly falls to 0 mV, only to fully recover after 30 min of Glut washout under control conditions (see samples of PS traces in **Figure 1**). In contrast, high frequency electrical stimulation had a much less dramatic effect on the PS amplitude, as we have shown previously (Schurr et al., 1986). In each paradigm, the effect of blocking lactate transport with the monocarboxylate transporter (MCT) inhibitor α-cyano-4-hydroxycinnamate (4-CIN, Halestrap and Denton, 1975) was assessed. The blocker concentration was adjusted according to the concentration of glucose (0.25 mM 4-CIN when glucose was supplied at 4 mM, 0.5 mM 4-CIN when glucose was supplied at 10 mM). As can be seen from **Figure 1**, blockade of MCT by 4-CIN prevented the recovery of neuronal function after exposure to Glut in both paradigms. Although not shown in **Figure 1**, it is important to mention that

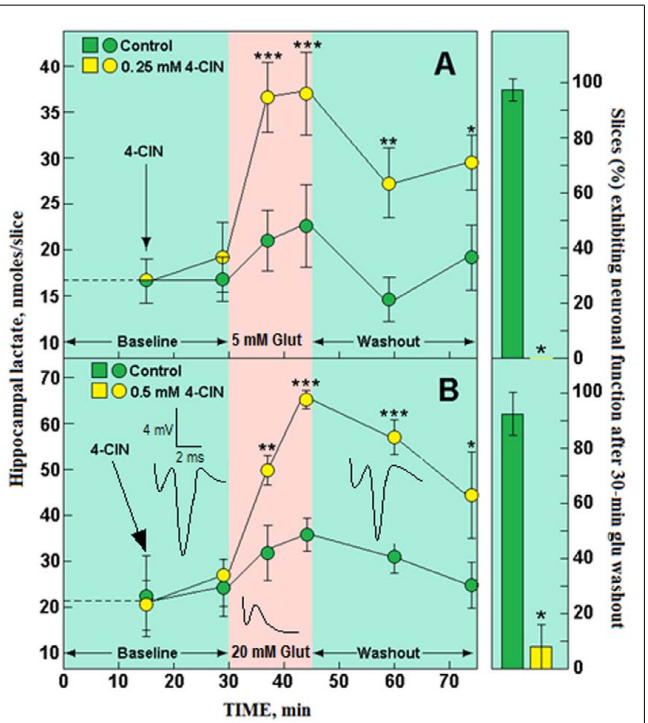

FIGURE 1 | The effect of 15 min exposure to glutamate (Glut) on the ability of hippocampal slices to recover their neuronal function following a 30 min Glut washout and on the content of tissue lactate at several time points during two experimental paradigms.
(A) Perfusion of slices with 4 mM glucose aCSF for 30 min, followed by a 15 min exposure to 5 mM Glut, followed by a 30 min washout with 4 mM glucose aCSF, either in the presence of 0.25 mM 4-CIN (yellow symbols) or in the absence of 4-CIN (green symbols); **(B)** perfusion of slices with 10 mM glucose aCSF, followed by a 15 min exposure to 20 mM Glut, followed by a 30 min washout with 10 mM glucose aCSF in the presence of 0.5 mM 4-CIN (yellow symbols) or in the absence of 4-CIN (green symbols). Also shown are sample traces of PS recorded from one hippocampal slice before and during exposure to 20 mM Glut and after Glut washout. Each data point was repeated three times (30–36 slices over all). Bars are means ± SD; significantly different from control (*$p < 0.003$; **$p < 0.01$; ***$p < 0.004$). For additional methodological details see Schurr et al., 1999a,b).

under the experimental conditions of paradigm A some diminishment in the CA1 PS amplitude occurred during the exposure to Glut, while under the conditions of paradigm B the CA1 PS amplitude quickly disappeared during the 15 min exposure to Glut regardless of the presence or absence of 4-CIN (see sample traces in **Figure 1**, paradigm B), indicating that Glut is excitotoxic at both concentrations. However, the relatively short time of exposure to Glut (15 min) did not lead to an irreversible damage, since over 90% of the slices under control conditions in both paradigms exhibited almost full recovery of neuronal function (green columns on the right side of **Figure 1**). Nevertheless, in the presence of 4-CIN, none of the slices exhibited recovery of neuronal function when supplied with 4 mM glucose and exposed to 5 mM Glut for 15 min (Paradigm A). Less than 10% of the slices showed recovery of neuronal function when supplied with 10 mM glucose and exposed to 20 mM Glut for 15 min (paradigm B; yellow columns on the right side of **Figure 1**). While the lactate content of control slices (green-filled circles in **Figure 1**) did not appear to be elevated much during Glut exposure in either paradigm, it may reflect the high rate by which neurons utilized the astrocritically produced lactate (Pellerin and Magistretti, 1994) rather than a reduction in lactate production. The significant elevation in lactate tissue content of slices treated with 4-CIN during Glut exposure demonstrates that astrocytic or more likely neuronal (Galeffi et al., 2007) lactate transport is blocked and thus was unavailable to neurons in these slices, blockade that prevented recovery of neuronal function at the end of the washout period under both paradigms.

Since lactate could not be utilized in the presence of 4-CIN, its tissue content remained elevated throughout the washout period (yellow-filled circles in **Figure 1**). As expected, the content of lactate in slices supplied with 10 mM glucose during Glut exposure in the presence of 4-CIN was almost twice as high as the content of slices supplied with 4 mM glucose, indicating that most of the glucose utilized during Glut exposure is converted to lactate. In essence, the outcome depicted in **Figure 1** strongly supports the premise of the ANLSH. These experiments with Glut (see also Schurr et al., 1999a,b) confirm that activation of neural tissue with an excitatory neurotransmitter increases glucose utilization via aerobic glycolysis, which leads to a large elevation in lactate production. Moreover, as indicated by the effects of 4-CIN in the presence of Glut, lactate is the glycolytic product that becomes the oxidative energy substrate, securing the recovery of neuronal function post-Glut activation.

In the debate that has ensued following Pellerin and Magistretti (1994) proposed ANLSH (Tsacopoulos and Magistretti, 1996; Magistretti and Pellerin, 1999; Magistretti et al., 1999; Magistretti, 2000; Chih et al., 2001; Chih and Roberts, 2003; Pellerin and Magistretti, 2003, 2004a,b; Hertz, 2004; Schurr, 2006), the skeptics tend to reject it mainly on the premise that lactate is postulated to be a major oxidative energy substrate, not necessarily on the proposed shuttle *per se*. The debate is not limited only to this hypothesis; it is still raging about a similar hypothesis concerning lactate shuttles in other tissues that preceded the one offered by Pellerin and Magistretti (see Gladden, 2004, for review). The objection to the idea of a major role for lactate in energy metabolism beyond just being a waste product or, at best, a minor player, is understandable. The dogma of glucose's obligatory role in energy metabolism in all tissues, organs, and most aerobic organisms is an inseparable part of our understanding and acceptance of this process as formulated during the first half of the twentieth century. However, a trove of experimental data have emerged over the past quarter of a century, all pointing to a major role for lactate in oxidative energy metabolism in brain, skeletal muscle, heart, and probably many other mammalian tissues. These data (Brooks, 1985, 1998, 2000, 2002a,b; Schurr et al., 1988, 1997a,b, 1999a,b; Larrabee, 1995, 1996; Hu and Wilson, 1997b; Brooks et al., 1999; Mangia et al., 2003; Kasischke et al., 2004; Ivanov et al., 2011), in addition to those found in several forgotten studies from the first half of the twentieth century (Ashford and Holmes, 1929, 1931; Holmes, 1930; Holmes and Ashford, 1930; Flock et al., 1938), prompted us to hypothesize that lactate is the end-product of both aerobic and anaerobic glycolysis and, consequently, is the ultimate cerebral oxidative energy substrate in the brain (Schurr, 2006) and possibly in other organs and tissues. The experiments described in **Figure 1** contributed greatly to the formulation of this hypothesis.

REVISITING HU AND WILSON'S STUDIES OF 1997

Among the citations cited above, the one by Hu and Wilson (1997b) carries greater importance than has been realized by both its supporters and detractors. These authors have developed both glucose and lactate, enzyme-based micro-sensors with rapid response time that allowed them direct and continuous *in vivo* measurements of lactate and glucose concentrations with high temporal resolution in rat brain extracellular fluid. Several authors (Pellerin and Magistretti, 2003; Kasischke et al., 2004; Aubert et al., 2005; Medina and Tabernero, 2005; Serres et al., 2005; Schurr, 2006) have concluded that Hu and Wilson's findings lend support to the notion that lactate is being utilized aerobically upon neuronal activation. Others (Dienel and Hertz, 2005; Fillenz, 2005; Korf, 2006) have concluded that Hu and Wilson's observations do not represent oxidative metabolism of lactate. In his commentary, Korf (2006) states that the initial drop in the hippocampal dentate gyrus lactate level following a single stimulation of the perforant pathway (Hu and Wilson, 1997b) is very small in comparison with its subsequent increase, and thus, this minor decrease cannot serve as an argument to support aerobic metabolism of lactate. As can be seen from **Figure 2**, after the first stimulation, the dip in lactate concentration was 7%, while glucose level dipped by 14%. Based on Hu and Wilson's (1997a) estimates, the lactate baseline level before stimulation was 1.19 mM and that of glucose was 2.60 mM. Hence, following the first stimulation, the levels of lactate and glucose fell by 0.08 and 0.36 mM, respectively.

One could surmise then that upon the first stimulus, a significant portion of the energy required for this activation is supplied via glycolysis (the conversion of glucose to lactate) as 0.36 mM glucose were consumed, while a smaller portion of that energy is supplied via aerobic consumption of lactate, since only 0.08 mM of the monocarboxylate were consumed. These quantities, however, could be misleading, since 0.36 mM glucose produces a net amount of 0.72 mM ATP (1 mol of glucose produces 2 mol of ATP glycolytically), while 0.08 mM lactate produces 2.72 mM ATP [1 mol of lactate produced ∼34 mol of ATP via the mitochondrial tricarboxylic acid (TCA) cycle]. Consequently, the "small" amount of lactate consumed upon the first stimulation actually

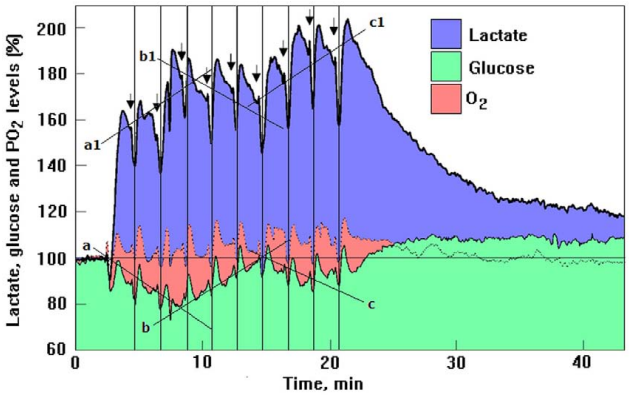

FIGURE 2 | Profiles of time course and dynamic relationships of local extracellular lactate, glucose, and PO_2 levels in the rat hippocampal dentate gyrus during a series of 5 s electrical stimulations (arrows) of the perforant pathway at 2 min rest intervals (reproduced with permission from Hu and Wilson, 1997b; copyright 1997, Blackwell, Oxford). The different diagonal lines show the trend in the mean analyte concentration during the series of stimulations. During the second to the fourth stimulations as glucose mean level gradually decreased (line a), lactate mean level gradually increased (line a1). During the next three stimulations the trend was inverted (lines b and b1) and during the 7th to the 10th stimulations the trend inverted itself again (lines c and c1). The changes in the mean concentration of glucose were always in opposite direction to the changes in mean lactate concentration. The vertical lines were drawn to indicate the simultaneous dip in all three analytes in response to each of the 10 electrical stimulations. For additional details see Hu and Wilson (1997b).

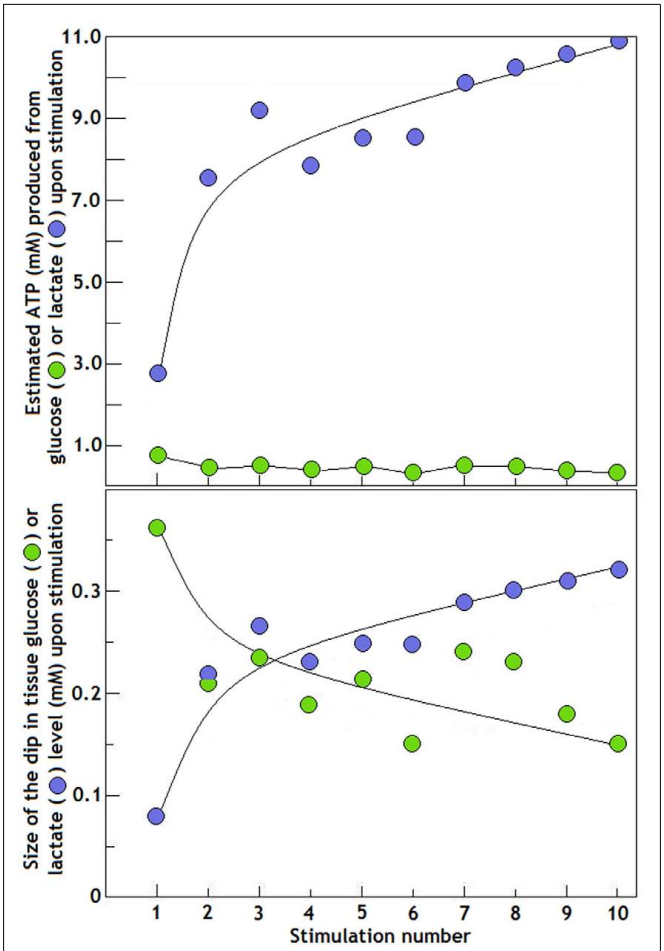

FIGURE 3 | The time course of changes in the amplitude of the dip in tissue glucose and lactate levels in the rat hippocampal dentate gyrus after each of the 10 electrical stimulations applied to the perforant pathway at intervals of 2 min (bottom panel). The amplitude of each dip (in mM) was calculated from the data of Hu and Wilson (1997b) as reproduced in **Figure 2**. The upper panel illustrates the estimated ATP amount produced based on the size of the dip (in mM) in tissue glucose and lactate levels as shown in the bottom panel. The estimated ATP levels were calculated as follows: the glucose measured dip (in mM) was multiplied by 2, which is the net formation of 2 mol of ATP for each mole of glycolytically metabolized glucose; the lactate measured dip (in mM) was multiplied by 34, which is the net formation of 34 mol of ATP for every 2 mol of lactate (formed glycolytically from 1 mol of glucose) metabolized via the mitochondrial TCA and the oxidative phosphorylation chain.

produced 3.8 times more ATP than the amount produced by the consumption of glucose upon the first stimulation. A significant fact that has been ignored by the detractors of Hu and Wilson's studies is the sharp increase in tissue lactate level immediately after the first stimulation; from 1.19 (baseline level) to 1.95 mM, a rise of 0.76 mM. Concomitantly, glucose level after the first stimulation decreased from 2.60 (baseline level) to 2.22 mM, a drop of 0.38 mM. Hence, the rise in lactate can be fully attributed to the fall in glucose, as every mole of the sugar is converted glycolytically to 2 mol of lactate. In essence, all the glucose consumed in response to the first stimulation was converted to lactate. This very stoichiometry was seen by us (**Figure 1**). Aerobic conversion of glucose to lactate rather than to pyruvate is the central theme of our hypothesis (Schurr, 2006). After the second stimulation (**Figure 2**), the amplitude of the dip in lactate level measured 0.22 mM (from 1.87 mM or 157% of the baseline level, to 1.65 mM or 139% of the baseline level), was almost threefold larger than the one that followed the first stimulation and with an estimated ATP production of 7.48 mM. Glucose dipped after the second stimulation from 2.34 (90% of the baseline level) to 2.13 mM (82% of the baseline level), a dip of 0.21 mM, an approximately 0.15 mM smaller dip (42% smaller) than the dip observed after the first stimulation and with an estimated ATP production of 0.42 mM. Thus, on the second stimulation, ATP production via lactate utilization was 18-fold greater than ATP production via glycolytic glucose utilization. Accordingly, we calculated the size of the dip for each of the ten stimulations applied by Hu and Wilson (1997b) and also estimated the resulted ATP production from glucose and lactate after each of them, calculations that are summarized in **Figure 3**. Despite the significant increases in lactate "utilization" and decreases in glucose "utilization" beginning with the second stimulation on, Korf (2006) states that there is no less glucose metabolized after repeated stimulation, since the concomitant early dips in glucose remain the same, independent of the changes in lactate. This statement is inaccurate and could be misleading, since it does not take into account the simple fact that every mole of lactate oxidized produces approximately 17 times more ATP than a mole of glucose. The breakdown of 1 mol of glucose glycolytically requires

two phosphorylation steps (2 mol of ATP) to produces two trioses, each of which later produces 2 mol of ATP for a net production of 2 mol of ATP for each mole of glucose that passes through glycolysis (Stryer, 1995; see also **Figure 4**). In contrast, upon entering the mitochondrial TCA cycle and the oxidative phosphorylation chain, the 2 mol of lactate (pyruvate) created from 1 mol of glucose via glycolysis, produce approximately 32–34 mol of ATP (Stryer, 1995) or 16–17 times more ATP than is produced from 1 mol of glucose via glycolysis. Furthermore, over the first four stimulations glucose tissue level continued to drop as lactate tissue level increased (**Figure 2**, lines a and a1), while during the next four stimulations as lactate tissue level decreased, glucose tissue level increased (**Figure 2**, lines b and b1). Hu and Wilson (1997b) found this trend noteworthy in their original paper. Although we have not analyzed quantitatively the oxygen profile produced by Hu and Wilson (1997b) in their **Figure 2**, the authors indicated that unlike the levels of glucose, O_2 levels showed essentially no decrease. Thus, one could surmise that each oxygen dip in response to an electrical stimulation signals a concomitant O_2 utilization in the mitochondrial electron transport chain with lactate utilization (via pyruvate) in the TCA cycle, the very lactate that is originating glycolytically from glucose.

A study by Mangia et al. (2003), using a time-resolved proton magnetic resonance (^{1}H-MRS) in humans, found an approximately 40% dip in lactate tissue concentration 5 s after a 1 s visual stimulation with a recovery back to baseline levels by 12 s. Due to the experimental conditions adopted by Mangia et al. (2003), any increase in lactate concentration, had it occurred, could not be measured. Nevertheless, it is interesting that both Mangia et al. (2003) and Fillenz (2005) interpreted the results of the MRS study as refutation of the ANLSH (Pellerin and Magistretti, 1994), which postulates that an increased astrocytic lactate production supports the bulk of the energy needs of Glut-activated neurons. Hence, according to Mangia et al. (2003) and Fillenz (2005) the short-lived dip in lactate concentration, which, in essence, signals lactate consumption, is sufficient to reject the ANLSH. Moreover, Fillenz (2005) takes Hu and Wilson's (1997a,b) data to demonstrate "that glucose is the main substrate used by activated neurons." In the general scheme of things, it is true that glucose is used during neural activation, but for the purpose of producing lactate, most likely by astrocytes. Considering the lopsided difference in the amount of ATP formed via lactate aerobic utilization compared to that produced via glucose glycolytic utilization (see **Figure 3**, top panel), it is apparent that more than 95% of the ATP produced and consumed by the activated neural tissue is supplied by lactate oxidation. Since the debate over the ANLSH has arguably become the basis on which the idea of lactate as an oxidative energy substrate stands or falls, some participants in this debate set aside data that could neither directly support nor refute this hypothesis. Thus, in their mathematical model, Aubert et al. (2005) selected only the lactate measurements from the data of Hu and Wilson (1997b), leaving out the measurements of glucose and oxygen that were performed concomitantly with those of lactate. Therefore, on the basis of ours and others analyses we believe that the studies of Hu and Wilson (1997a,b) should be reevaluated by those who have discounted them for one reason or another. The principle thrust of their studies is not whether they support or discredit the ANLSH, but rather that they clearly indicate that lactate, the glycolytic product of glucose, is the only substrate capable of answering all the energy needs of activated neural tissue.

LACTATE, NOT PYRUVATE IS AEROBIC GLYCOLYSIS END-PRODUCT IN THE BRAIN

Considering our own work over the past two decades and the accumulating data from a multitude of studies, the concept of lactate as an integral intermediate of normal glucose metabolism and ATP production, i.e., aerobic glycolysis and oxidative phosphorylation, has become more main stream and less controversial. Consequently, we hypothesized, as mentioned earlier, that in the brain lactate is the principal product of both aerobic and anaerobic glycolysis (**Figure 4**; Schurr, 2006).

We have tested this proposed hypothesis in a study that has provided additional evidence in its support (Schurr and Payne, 2007). A newly discovered lactate dehydrogenase inhibitor, malonate, a known competitive inhibitor of succinate dehydrogenase, has been shown to inhibit the conversion of lactate to pyruvate by Saad et al. (2006). This succinate analog is transported into neurons, astrocytes, and mitochondria via the succinate transporter (Aliverdieva et al., 2006; Yodoya et al., 2006). We used malonate in a set of experiments to test the hypothesis that lactate is the end-product of aerobic glycolysis in cerebral tissue (Schurr and Payne, 2007). As can be seen from **Figure 5**, malonate (M) drastically attenuated the amplitude of lactate-supported neuronal function (evoked hippocampal CA1 PS), as evident from the two representative traces before (L) and after 75 min exposure to the inhibitor (L + M). Lactate-supplemented slices were susceptible to LDH inhibition by malonate, exhibiting a time-dependent diminishment in the PS amplitude. However, malonate was innocuous when slices were supplemented with pyruvate (P, P + M). Thus, this LDH inhibitor appeared to be a more efficient inhibitor than any other known one, especially of mLDH, the mitochondrial form, which converts lactate to pyruvate. The inhibition of the mLDH by malonate significantly slowed down the conversion of lactate to pyruvate, resulting in the observed suppression of neuronal function. Since pyruvate can directly enter the mitochondrial TCA cycle, as it is transported by the same transporter (MCT) that transports lactate, pyruvate-supported neuronal function was unaffected by malonate. With glucose-supplemented slices the effect of malonate was significantly different. Although initially malonate suppressed the PS amplitude of both lactate-supplemented slices by 48% at 45 min incubation (45′ L + M) and of glucose-supplemented slices by 36% (45′ G + M), at 75 min however, the suppression of the PS amplitude of the lactate-supplemented slices increased to 75% (75′ L + M), while that of the glucose-supplemented slices was subsided to only 14% (75′, G + M). While all LDH inhibitors, without exception, exhibit differential inhibition toward either cLDH, the cytosolic form of the enzyme, or mLDH, the mitochondrial form, they do inhibit both forms if allowed long enough incubation time. Hence, the biphasic effect of malonate on the neuronal function of glucose-supplemented slices is predictable, since this inhibitor has stronger inhibitory potency toward mLDH than toward cLDH. Therefore, in the short run, malonate is expected to block mainly the conversion of lactate to pyruvate, which indicates that lactate is the end-product of aerobic glycolysis. If this were not the case,

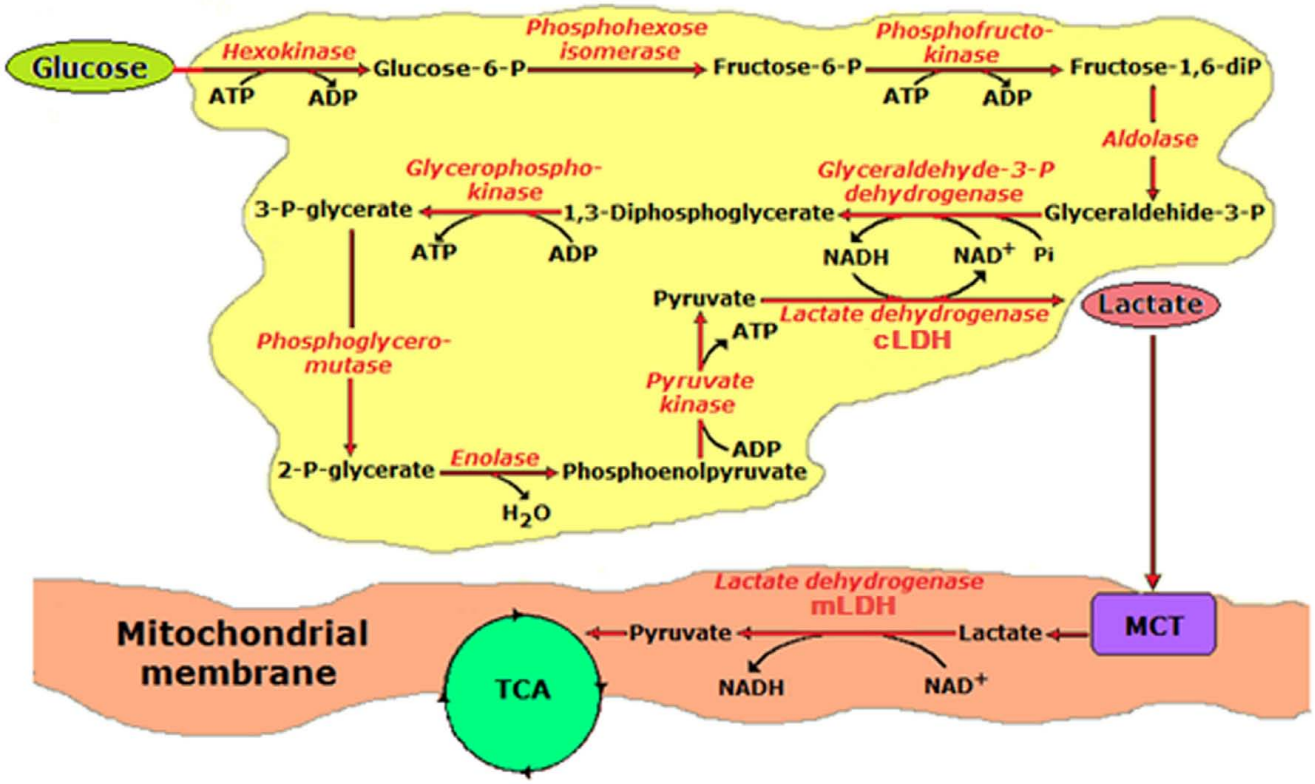

FIGURE 4 | A schematic illustration of a hypothesis first presented elsewhere (Schurr, 2006), postulating lactate, not pyruvate, to be the end-product of aerobic glycolysis. This hypothesis is founded on thermodynamic and other considerations, including data from many studies spanning almost eight decades of research by scientists in laboratories all around the world. The illustration shows the glycolytic apparatus as an aggregate of the glycolytic enzymes, all in close proximity to each other, as required by such a pathway for a maximized efficient output, with the entry of glucose into this pathway on the upper left side and an exit of lactate from the pathway on the right side through the action of cytosolic lactate dehydrogenase (cLDH). Lactate is shuttled via an intracellular shuttle to the mitochondrial membrane, where it is converted back into pyruvate via mitochondrial lactate dehydrogenase (mLDH) and into the tricarboxylic acid (TCA) cycle.

inhibition of cLDH by malonate should have no effect on glucose-supplemented slices, since according to the classic understanding of aerobic glycolysis, inhibition of cLDH should have no effect on the main aerobic glycolytic product, pyruvate, and its entry into the mitochondrial TCA cycle. Hence, the PS amplitude of glucose-supplemented slices should not at all be affected by malonate. The fact that malonate initially inhibited neuronal function of glucose-supplemented slices clearly indicates that glucose must first be glycolytically converted to lactate, a product that must then be converted by mLDH to pyruvate, a LDH form more sensitive to malonate than the cLDH form. Over a longer period of time the degree of inhibition of the cLDH form became more pronounced, such that it blocked glycolysis from continuing beyond the formation of pyruvate, practically preventing lactate production. At this point in time (75′, G + M), the accumulated glycolytic pyruvate became the main product available for mitochondrial use, which resulted in the observed recovery from malonate-induced suppression of glucose-supplemented neuronal function. The somewhat stronger inhibition of neuronal function by malonate (48%) in lactate-supported slices at 45 min (45′ L + M) than that observed in glucose-supplemented slices (36%) also indicates that already at this point in time, there was some inhibition of cLDH and thus accumulation of pyruvate, allowing glucose-supplemented slices to be affected less by malonate than the lactate-supplemented slices.

These results support the hypothesis, which postulates that lactate is the end-product of cerebral aerobic glycolysis and also confirm that its aerobic utilization first requires the conversion of lactate to pyruvate via mLDH. We performed an additional set of experiments (Schurr and Payne, 2007) that provided further support for lactate's major role in cerebral energy metabolism (**Figure 6**). In that set we combined Glut and malonate to ascertain lactate's role as a mitochondrial energy substrate for the maintenance of neuronal function during neural activation. That malonate is detrimental to neuronal viability of glutamate-activated, glucose-supported hippocampal slices was apparent from the partial recovery (50%) of the energy-dependent PS amplitude (**Figure 6**). This outcome indicates that lactate,

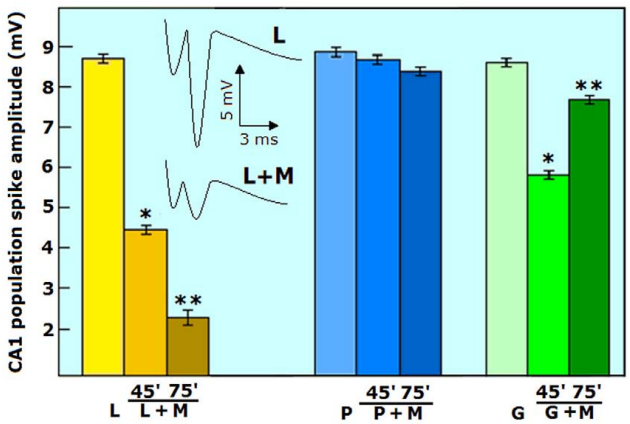

FIGURE 5 | The effect of the LDH inhibitor, malonate (M, 10 mM) on evoked CA1 population spike amplitude (neuronal function) of rat hippocampal slices maintained is aCSF containing either lactate (L, 5 mM), pyruvate (P, 5 mM), or glucose (G, 2.5 mM). Malonate progressively inhibited lactate-supported neuronal function over time and was innocuous against pyruvate-supported neuronal function. Malonate initially inhibited glucose-supported neuronal function, inhibition that was later mostly relieved. Each data point was repeated three times (30–36 slices over all). Bars are means ± SEM; *significantly different from energy substrate alone; **significantly different from energy substrate or energy substrate + malonate at 45 min ($p < 0.0001$). For additional methodological details see Schurr and Payne (2007).

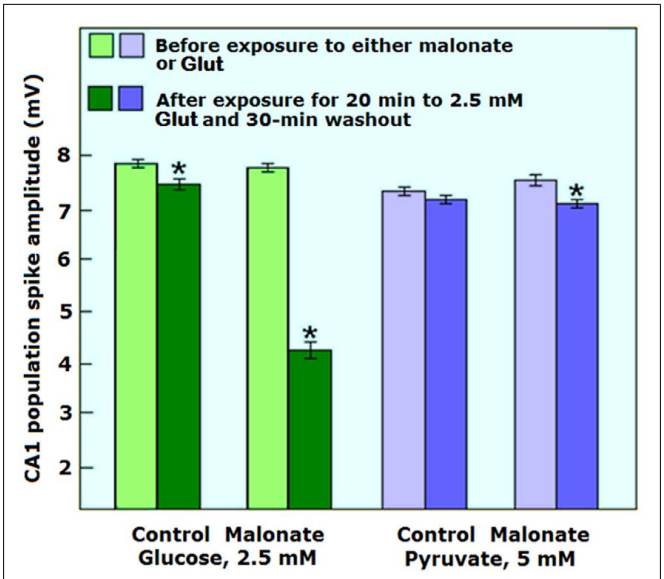

FIGURE 6 | The effect of 20 min exposure to glutamate (Glut, 2.5 mM) on hippocampal CA1 evoked population spike (PS, neuronal function) in the absence or presence of the LDH inhibitor, malonate (10 mM) when either glucose (2.5 mM) or pyruvate (5 mM) was the sole energy substrate. Slices maintained in glucose aCSF could not recover their PS amplitude following Glut washout in the presence of malonate as compared to those maintained in the absence of malonate or those maintained with pyruvate whether malonate was absent or present. Slices were exposed to malonate throughout the experimental protocol for a total of 80 min (30 min before the exposure to Glut, 20 min during the exposure to Glut and 30 min during Glut washout). Each data point was repeated three times (30–36 slices). Bars are means ± SEM; *significantly different from the mean values before exposure to either malonate or Glut ($p < 0.01$). For additional methodological details see Schurr and Payne (2007).

whether neuronal or astrocytic in origin, is crucial for neuronal viability upon activation. These results confirm both our previous findings (**Figure 1**; Schurr et al., 1999a,b) and the outcome of Hu and Wilson's (1997b) experiments. Alternatively, the outcome of our experiments could be explained by postulating an increase in astrocytic glucose utilization and lactate production in response to Glut uptake, whereupon lactate becomes a major neuronal energy substrate (Pellerin and Magistretti, 1994; Schurr et al., 1999a). Any interference with neuronal utilization of astrocytic lactate under this scenario, i.e., LDH inhibition by malonate, would suppress normal neuronal function. However, such suppression would be abolished if astrocytes, although incapable of lactate production in the presence of malonate, could produce enough pyruvate. That product, upon Glut washout, should be able to fuel the recovery of neuronal function, similar to the observed recovery in slices supplied with exogenous pyruvate (**Figure 6**). Nevertheless, such recovery did not occur, which indicates that astrocytic pyruvate, if produced during exposure to Glut and malonate, was not readily available to neurons, in contrast to the availability of astrocytic lactate and neuronal pyruvate and to the findings of Yoshioka et al. (2000).

Why was 2.5 mM glucose, in contrast to 5 mM pyruvate, unable to sustain neuronal viability in slices treated with both malonate and Glut? It is possible that not all the available glucose is converted glycolytically to pyruvate under these conditions. However, glucose-supplemented slices incubated for 20 min with both Glut and malonate should produce enough glycolytic lactate without a significant inhibition of glycolysis by malonate (see **Figure 5**). Thus, malonate, under these conditions, appears to mainly inhibit lactate conversion to pyruvate by mLDH, which would prevent the full recovery of neuronal function (**Figure 6**). One should also consider the fact that in order to meet the activated neural tissue increased energy needs, glucose cannot attenuate the rate of mitochondrial respiration through a concomitant increase in the glycolytic flux. In contrast, lactate, and most likely pyruvate, can easily do so, since they both enter the mitochondria directly. Levasseur et al. (2006) have demonstrated that glucose sustained mitochondrial respiration at low, "fixed" rate, since, despite increasing the glucose concentration nearly 100-fold, oxygen consumption was not up-regulated. However, an increase in lactate concentration did elevate mitochondrial oxygen consumption, plausibly allowing mitochondria to meet heightened energy demands. Consequently, in our experiments, glucose-supplemented and oxygenated hippocampal slices were incapable of increasing their mitochondrial respiration rate in response to activation by Glut, since they were unable to up-regulate their glycolytic flux, while at the same time could not utilize lactate directly because of the presence of malonate. Interestingly, the findings of Hu and Wilson (1997b) also agree with the interpretation of Levasseur et al. (2006). More recently, Ivanov et al. (2011) have demonstrated that lactate can cover the energy needs of activated neonatal hippocampal slices and that lactate utilization augmented oxidative phosphorylation.

Normally, both neuronal and astrocytic lactate produced from glucose would overcome this limitation (see **Figure 5**, control glucose, 2.5 mM), but in the presence of malonate this avenue is unavailable (**Figure 5**, malonate, glucose, 2.5 mM). Obviously, exogenous lactate would be useless in the presence of malonate, which is the reason no results with lactate-supported slices are shown. Nonetheless, results obtained when slices supplemented with 2.5 mM glucose were also supplemented with malonate and exposed to Glut (for 20 min; **Figure 6**) suggest an augmented shortfall in lactate (or pyruvate) supply under these conditions. This outcome emphasizes the importance of lactate both at rest and during neural activation, an outcome that cannot be explained by the classic depiction of aerobic glycolysis, where pyruvate is positioned as the glycolytic end-product. Using electrical stimulation of several durations instead of Glut application to hippocampal slices, Brennan et al. (2006) have reached a similar conclusion to ours as to the role of mitochondrial energy metabolism, not glycolysis, in supporting the need for the increase in energy supplies. Kann et al. (2011) have recently demonstrated that the induction of gamma oscillations by acetylcholine in hippocampal slices are especially energy demanding and require both high complex I expression and strong functional performance of mitochondria. These authors found that the gamma oscillation power, oxygen consumption, and Complex I expression are higher in the hippocampal subfield CA3 than in subfields CA1 and dentate gyrus and that they utilize mitochondrial oxidative capacity near its maximum limit. These studies along with other cited above and the results of our experiments with the LDH inhibitor, malonate, as summarized in **Figure 7**, strongly support our hypothesis (Schurr, 2006).

AEROBIC LACTATE UTILIZATION PROVIDES NEUROPROTECTION AGAINST GLUTAMATE-MEDIATED, ROS-INDUCED DAMAGE

The ANLSH, as proposed by Pellerin and Magistretti (1994), postulates that Glut plays a central role in the coupling between neuronal activity and energy metabolism. Accordingly, Glut, released during synaptic activity, is taken up by astrocytes via specific Glut transporters. This transport, which is sodium-dependent, triggers astrocytic aerobic glycolysis and lactate production. The ANLSH further postulates that the astrocytic lactate thus produced is

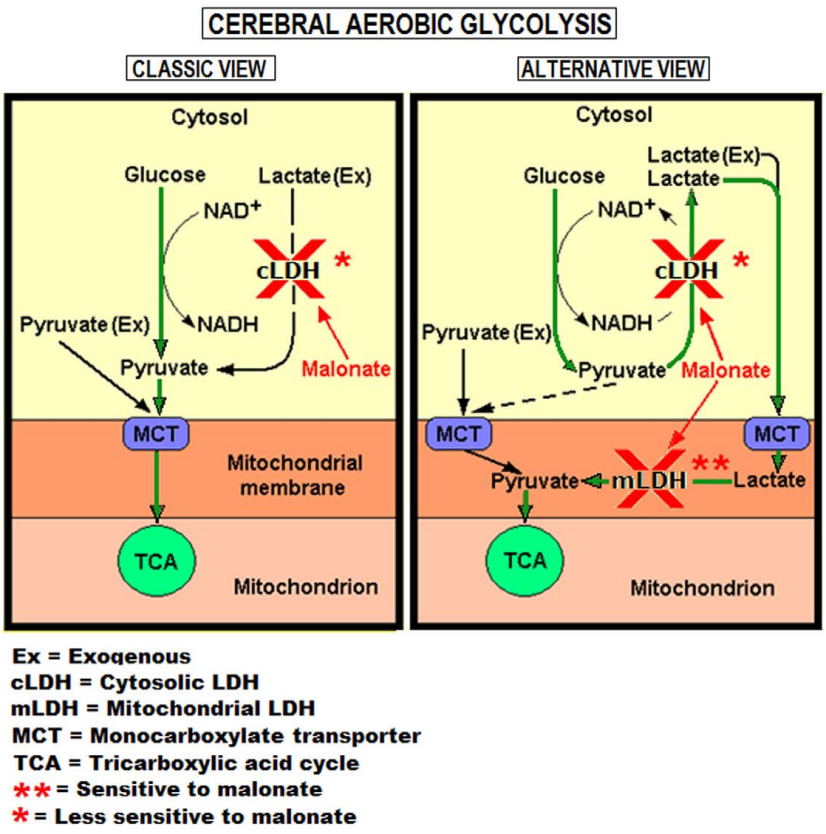

FIGURE 7 | Two views of aerobic glycolysis. The classic view depicts pyruvate as the glycolytic pathway's end-product (green arrows, left panel) and thus as the pathway that should not be affected by an LDH inhibitor such as malonate in supplying pyruvate to mitochondria. The results shown in **Figures 5** and **6** cannot be explained by this view. The alternative view of the aerobic glycolytic pathway postulates lactate to be its end-product (green arrows, right panel, Schurr, 2006). Since glycolytically produced lactate must be converted to pyruvate to allow the latter to enter the TCA cycle, this alternative view explains the ability of malonate to interfere with glucose-supported neuronal function as shown in **Figure 5** (right side histograms). However, over time, malonate's weaker inhibiting activity of the reaction converting pyruvate to lactate shifts the glycolytic conversion of glucose from lactate to pyruvate until the latter becomes the main glycolytic end-product and the mitochondrial substrate (broken arrow, right panel), relieving the suppression of neuronal function observed earlier when glucose is the energy substrate (**Figure 5**).

transported via specific monocarboxylate transporters from astrocytes to neurons, where it is utilized as an oxidative mitochondrial energy substrate (Pellerin et al., 1998; Magistretti and Pellerin, 1999). Nevertheless, Yoshioka et al. (2000), using ^{31}P-NMR and electrophysiology of granule cells in rat hippocampal slices, have concluded that, upon high K^+ stimulation, the astrocytic main product is pyruvate, not lactate, and the former, not the latter is the neuronal substrate shuttled from astrocytes to neurons. Our results, as described in the previous section refute Yoshioka et al. (2000) conclusion.

Several cellular mechanisms have been suggested over the years to explain the excitotoxicity of Glut. It is now believed that calcium uptake and overload via various glutamate receptor subtypes, a common thread of several neurodegenerative diseases where mitochondrial dysfunction and cellular apoptosis occur, leads to an oxidative stress due to elevated mitochondrial production of ROS (Krieger and Duchen, 2002; Rego and Oliveira, 2003; Emerit et al., 2004; Rosenstock et al., 2004; Lin and Beal, 2005). Acute and severe hypoxia in ischemic disease induce the release of Glut via several mechanisms and down regulate Glut transporters expression, resulting in elevated extracellular Glut (Rossi et al., 2000; Aliprandi et al., 2005; Dallas et al., 2007; Kiewert et al., 2010). The role of excitotoxicity in the pathogenesis of ischemic brain disease has been widely reported (Dirnagl et al., 1999; Kiewert et al., 2010) and elevated Glut levels have been found in plasma and in CSF of stroke patients (Aliprandi et al., 2005). The details of glial Glut sequestration have been extensively studied: GLT1 and GLAST are sodium-dependent Glut transporters that couple inward transport of one Glut molecule with inward entry of 3 Na^+, and one H^+, and outward movement of one K^+. The resulting intracellular Na^+ elevation stimulates the Na^+/K^+ ATPase pump to extrude Na^+ and the resulting energy requirement leads to enhanced glucose uptake (Pellerin and Magistretti, 1994). During ischemia, the mitochondrial respiration chain is compromised, leading to energy failure that could be aggravated by the initial increase in Glut uptake. Ischemia-induced energy failure leading to Na^+/K^+ imbalance and membrane depolarization may also reverse the transporter, carrying Glut to the extracellular space and further contributing to excitotoxicity (Nicholls and Atwell, 1990; Grewer et al., 2008). The hippocampal slice preparation has been used in our laboratory for many years to investigate and elucidate several cellular mechanisms of cerebral ischemia/hypoxia and excitotoxicity as well as in developing neuroprotective modalities against these disorders. To study the ability of each of the three energy substrates, glucose, lactate, and pyruvate, in equicaloric concentrations, to sustain neuronal function in activated neural tissue, we exposed rat hippocampal slices to a relatively low concentration of Glut (2.5 mM). In addition, we aimed to determine whether lactate or pyruvate is the astrocytic product shuttled to neurons and whether or not ROS are involved in the neuronal excitotoxicity of Glut. Hippocampal slices supplemented with either glucose (2.5 mM), pyruvate (5 mM), or lactate (5 mM) sustained their neuronal function uninterrupted throughout the duration of the experiment (60 min). Thus, a relevantly physiological concentration of glucose (2.5 mM) or an equicaloric concentration (5 mM) of either lactate or pyruvate was sufficient to support hippocampal neuronal function *in vitro* without diminution. However, when exposed to Glut (2.5 mM), pyruvate-supplemented slices (**Figures 8** and **9**) could not sustain their neuronal function, as was evidenced by the diminution in the PS amplitude. In contrast, neuronal function was diminished only slightly when glucose- or lactate-supplemented slices were exposed to Glut. Replacing a fraction of pyruvate (1/5) with lactate (1 mM) or glucose (0.5 mM) or adding the membrane-permeable ROS scavenger (MCI-186,

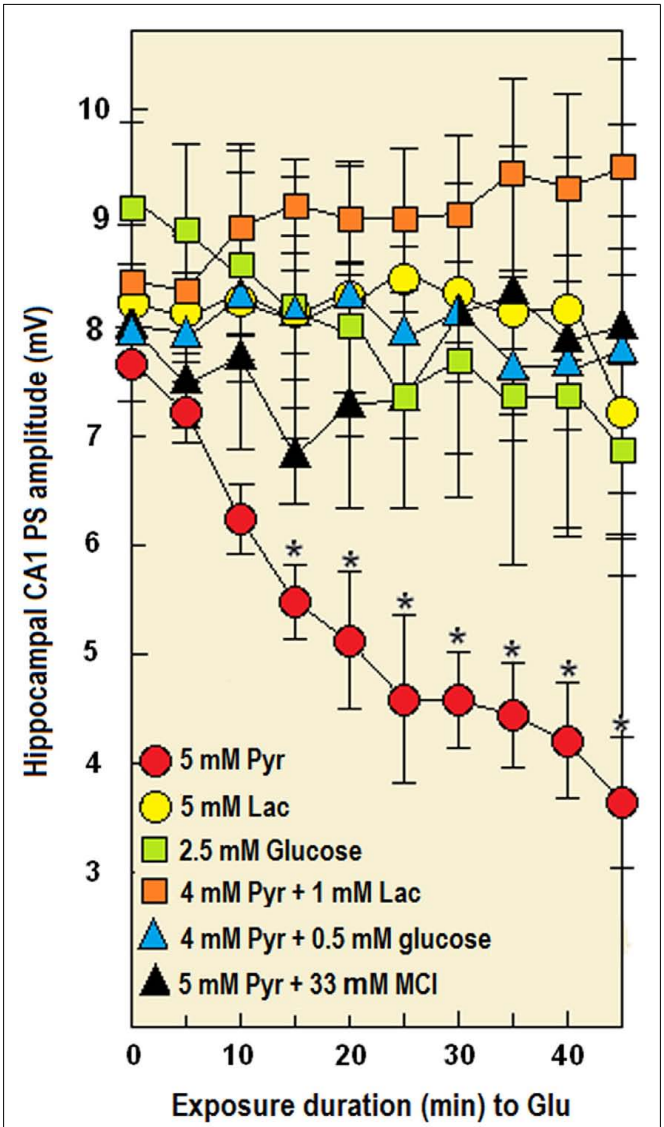

FIGURE 8 | The time-dependent effect of Glut (2.5 mM) on the amplitude of electrically evoked CA1 population spike (PS, neuronal function) in rat hippocampal slices perfused with either 5 mM pyruvate (Pyr), 5 mM lactate (Lac), a mixture of pyruvate (4 mM) with lactate (1 mM), or MCI-186 (33 μM, MCI). Pyruvate alone could not support neuronal function in the presence of glutamate, but mixing this monocarboxylate with a low concentration of either lactate, glucose, or MCI-186 overcame this inability. Each point is the mean amplitude value recorded from three separate hippocampal slices prepared from three different rat brains. Bars are SE of the mean. *Significantly different from the PS amplitude in slices perfused with pyruvate in the absence of glutamate ($p < 0.02$).

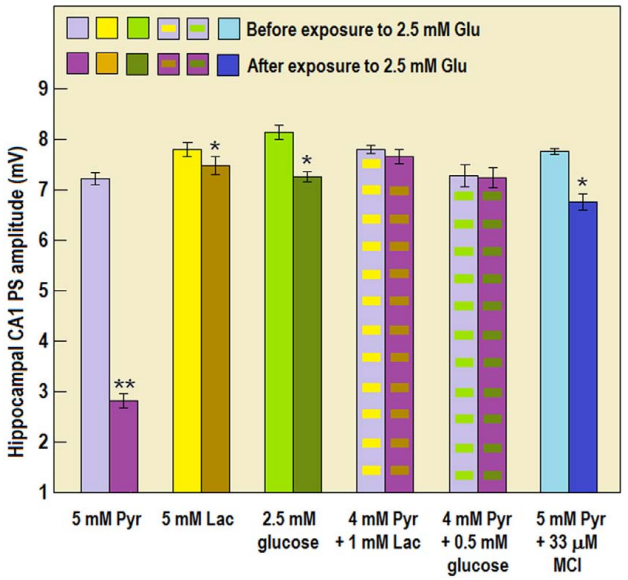

FIGURE 9 | The mean, electrically evoked, population spike (PS, neuronal function) amplitude in rat hippocampal slices perfused for at least 45 min with aCSF containing either 5 mM pyruvate (Pyr), 5 mM lactate (Lac), 2.5 mM glucose, 4 mM Pyr + 1 mM Lac, 4 mM Pyr + 0.5 mM glucose, or 5 mM Pyr + 33 μM MCI-186 (MCI) in the absence or presence of 2.5 mM Glut. Pyruvate alone could not sustain neuronal function in the presence of Glut. Pyruvate inability to sustain normal neuronal function during exposure to Glut appears to be in contrast to the results shown in **Figure 6**. However, the difference stems from the fact that in this set of experiments slices were exposed to Glut for 45 min, while in the experiments described in **Figure 6** they were exposed to Glut for only 20 min. All other treatments overcame the excitotoxicity of Glut. Each column is the mean PS amplitude recorded from at least 23 slices prepared from at least three different rat brains. Bars are SE of the mean. *Significantly different from the PS amplitude in control slices not exposed to Glut ($p < 0.004$); **significantly different from the PS amplitude in control slices not exposed to Glut ($p < 0.00006$).

33 μM; Wu et al., 2006) to pyruvate-supplemented slices during exposure to Glut, allowed the sustenance of neuronal function without any significant Glut-induced diminution in PS amplitude.

To verify that the formation of ROS contributes to the effect of Glut, ROS levels in hippocampal slices were measured using the fluorescent probe $DCFH_2$-DA, which is deacetylated in cells by non-specific endogenous esterases and oxidized by intracellular oxidant species to form the fluorescent DCF. The results shown in **Figure 10** are expressed as percent of maximum ROS production measured in slices supplemented with pyruvate (5 mM) and Glut (2.5 mM). The ROS production in these "control" slices was arbitrarily assigned a value of 100%. In the absence of Glut the level of ROS in pyruvate-supplemented slices was approximately 20% of the level measured when Glut was present ($p < 0.05$). In contrast, ROS levels in lactate-supplemented slices treated with Glut were only 25% of the levels measured in pyruvate-supplemented, Glut-treated slices ($p < 0.05$). No difference in the level of ROS was found between lactate-supplemented slices in the presence or absence of Glut. Adding the ROS scavenger MCI-186 (33 μM) to pyruvate-supplemented, Glut-treated slices reduced the level of ROS to less than 10% of control ($p < 0.05$). Replacement of only 1/5 of the pyruvate concentration in pyruvate-supplemented, Glut-treated slices with lactate (4 mM pyruvate + 1 mM lactate) was sufficient to reduce the level of ROS to 44% of control ($p < 0.05$). Thus, pyruvate when used as the sole energy substrate was unable to rescue neuronal function in rat hippocampal slices from Glut-induced, ROS-mediated damage, as was evidenced by the large diminution in PS amplitude. In contrast, lactate, even at a concentration one fifth of that of pyruvate was able to prevent Glut excitotoxicity and reduce tissue ROS levels similar to the reduction seen with the ROS scavenger, MCI-186. ROS production in neurons during a toxic Glut challenge is believed to play a central role in neuronal damage from hypoxia/ischemia and reperfusion. Glut receptor-activated neuronal cell death is attributed to a massive influx of Ca^{2+} and subsequent (within minutes) mitochondrial formation of ROS (Reynolds and Hastings, 1995; Vergun et al., 2001). In the hippocampal slice preparation, Glut-induced excitotoxic damage is expressed as a fall in PS amplitude, i.e., diminished neuronal function (Schurr et al., 1999a). Pyruvate was unable to sustain neuronal function in slices exposed to a relatively low concentration of Glut (2.5 mM), as indicated by a greater than 50% fall in PS amplitude (**Figure 9**). These results differ from the result shown in **Figure 6** only because the exposure to Glut here (45 min) was more than double the length slices in **Figure 6** were exposed to the excitotoxin (20 min). This inability of pyruvate to sustain normal neuronal function suggests that this monocarboxylate is not the substrate shuttled from astrocytes to neurons upon excitation by Glut, a finding contrasting the claim that pyruvate is the monocarboxylate shuttled from astrocytes to neurons (Yoshioka et al., 2000).

The ability of both lactate and glucose to sustain neuronal function in the presence of Glut indicates that the metabolism of these two substrates produces a by-product, which affords neuronal tissue to withstand excitotoxicity. Clearly, that by-product is not produced during pyruvate metabolism. Our results concur with the ANLSH and its postulated lactate shuttle. In light of pyruvate's inability to sustain neuronal function in the presence of Glut, we considered the only difference between the mitochondrial metabolism of pyruvate and lactate, i.e., the conversion of the latter to pyruvate via the action of the mitochondrial lactate dehydrogenase (mLDH). Reduced nicotinamide adenine dinucleotide (NADH), produced as a by-product of lactate conversion to pyruvate by both neurons (Schurr and Payne, 2007) and astrocytes, could provide the necessary reducing power to neutralize Glut-induced ROS and prevent their detrimental effect. Actually, Kirsch and De Groot (2001) were first to suggest such a role for NADH. We could not test this postulate by simply adding exogenous NADH to slices, since NADH is membrane impermeable. Nonetheless, we employed two alternative approaches to address this question. In one we replaced a small fraction of the supplied pyruvate with lactate (1 mM) or glucose (0.5 mM), fractions that by themselves could not sustain neuronal function (Schurr et al., 1988) and then exposed pyruvate-supplemented slices to Glut. In the second we treated pyruvate-supplemented slices with the membrane-permeable ROS scavenger, MCI-186 (33 μM, as determined by dose response experiments, not shown), during the exposure to Glut (**Figures 8** and **9**). When lactate (1 mM) or

glucose (0.5 mM) was mixed with pyruvate (4 mM) in the aCSF, the excitotoxicity of Glu was completely abolished, since neuronal function under these conditions remained unaffected. Adding MCI-186 (33 μM) to pyruvate-supplemented, Glut-treated slices also prevented the Glut-induced excitotoxic damage. We deem both approaches supportive of the ANLSH original postulate, according to which lactate is the astrocytic product shuttled to and utilized by neurons during activation by Glut, as lactate, not pyruvate, metabolism yields NADH that can neutralize ROS and abolish their toxicity.

To ascertain that increased ROS formation is correlated with the degree of neuronal damage measured by electrophysiological means, we employed the fluorescent probe H_2DCFDA to quantitatively measure ROS levels in hippocampal slices under several of the conditions used in the electrophysiological portion of the study. Such correlation, if exists, would support the central premise of this investigation, i.e., that lactate aerobic conversion to pyruvate and the accompanied production of the reducing agent NADH could be responsible for the neutralization of ROS. Our findings (**Figure 10**) demonstrate that pyruvate-supplemented slices treated with Glut contained ROS levels significantly higher than any other treatment combination tested. In the absence of Glut, ROS levels in pyruvate-supplemented slices were only 20% of the levels measured when Glut was present. Lactate-supported, Glut-treated slices produced significantly less ROS (25%) than their pyruvate-supported, Glut-treated counterparts, indicating that a by-product of lactate metabolism is capable of neutralizing ROS, even when the lactate concentration was as low as 1 mM, although not as efficient as the ROS scavenger, MCI-186. When interpreting these findings, it is important to consider that ROS were measured in whole slices, measurements that may have included regions where (astrocytic) lactate was not utilized during Glut excitation, but where ROS were still being produced. In contrast, the electrophysiological assessment of neuronal function was limited to the CA1 region of the hippocampal slice. Several studies have shown a correlation between ROS production in *in vitro* models of epilepsy and the ability of ROS scavengers to reduce or prevent ROS-induced neurodegeneration (Frantseva et al., 2000) and the possible role NADH [NAD(P)H] plays in neuronal survival during neurodegenerative disease and status epilepticus (Kirsch and De Groot, 2001; Heinemann et al., 2002; Kovács et al., 2002). Interestingly, Herrero-Mendez et al. (2009) have shown that neurons, unlike astrocytes, have low levels of the enzyme Pfkfb3 (6-phosphfructo-2-kinase/fructose-2,6-bisphosphatase-3), responsible for generating fructose-2,6-bisphosphate, the glycolytic product that activates the enzyme 6-phophofructo-1-kinase, the regulator of the glycolytic flux. These investigators have demonstrated that in neurons Pfkfb3 is continuously being degraded by E3 ubiquitin ligase, disabling any significant up-regulation of neuronal glycolysis. In astrocytes, the low activity of the degrading enzyme results in higher levels of Pfkfb3 that enable up-regulation of the glycolytic flux. Herrero-Mendez et al. (2009) also suggested that the low Pfkfb3 levels in neurons allow them to utilize most of their glucose via the pentose phosphate pathway, a pathway known to regenerate reduced glutathione through the oxidation of NADPH(H^+), and thus, supply the necessary neuroprotective ROS scavenger. This neuropotective mechanism could play a role

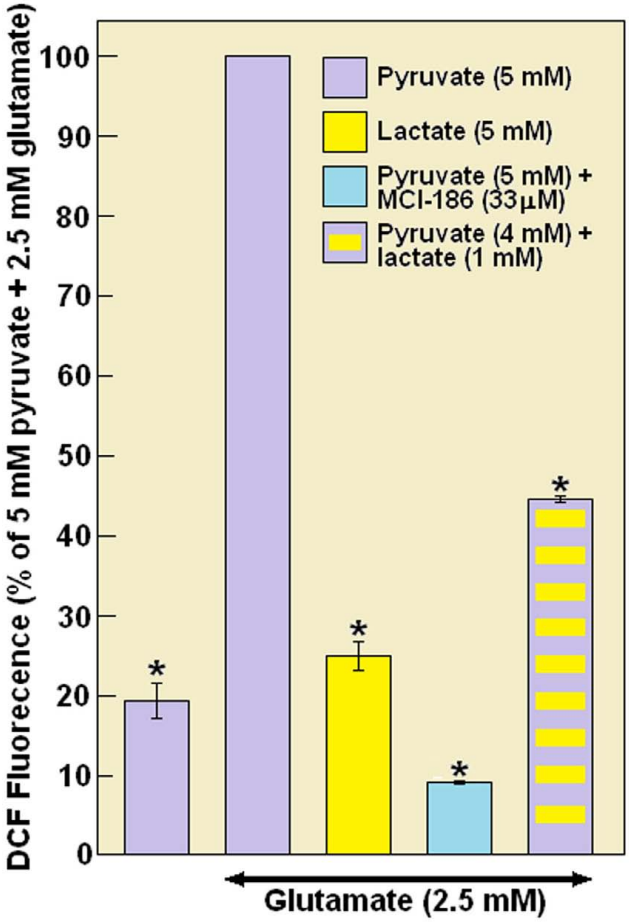

FIGURE 10 | The level of reactive oxygen species (ROS) as measured using the fluorescence of dichlorofluorescein (DCF) extracted from slices perfused with aCSF containing glutamate (2.5 mM) and either pyruvate (5 mM), lactate (5 mM), the combination of [pyruvate (4 mM) + lactate (1 mM)], or the combination of [pyruvate (5 mM) + MCI-186 (33 μM)] (see details in Materials and Methods). Also shown is a set of experiments in which Glut was omitted from the aCSF of pyruvate-supplemented slices. Glut-treated, lactate-, or MCI-186-supplemented slices exhibited significantly lower levels of ROS than pyruvate-supplemented, Glut-treated slices. Each sample for measurement of fluorescence used five slices and was prepared in duplicates. Measurements were repeated at least three times. Bars are SE of the mean. *Significantly different from pyruvate + Glut ($p < 0.05$).

in our own experimental paradigm and that of Hu and Wilson (1997b). This mechanism could also work in parallel with the neuroprotective action of NADH produced during the conversion of lactate to pyruvate by mLDH. It is possible that the mitochondrial NADH thus formed is also being used to generate reduced glutathione as the eventual ROS scavenger.

Taking together, the results of the electrophysiological measurements and those of the direct ROS formation measurements in hippocampal slices under the various treatment combinations, suggest that ROS, at least in part, are responsible for Glut excitotoxicity and neuronal damage when energy substrate availability is restricted and that pyruvate supplementation cannot overcome

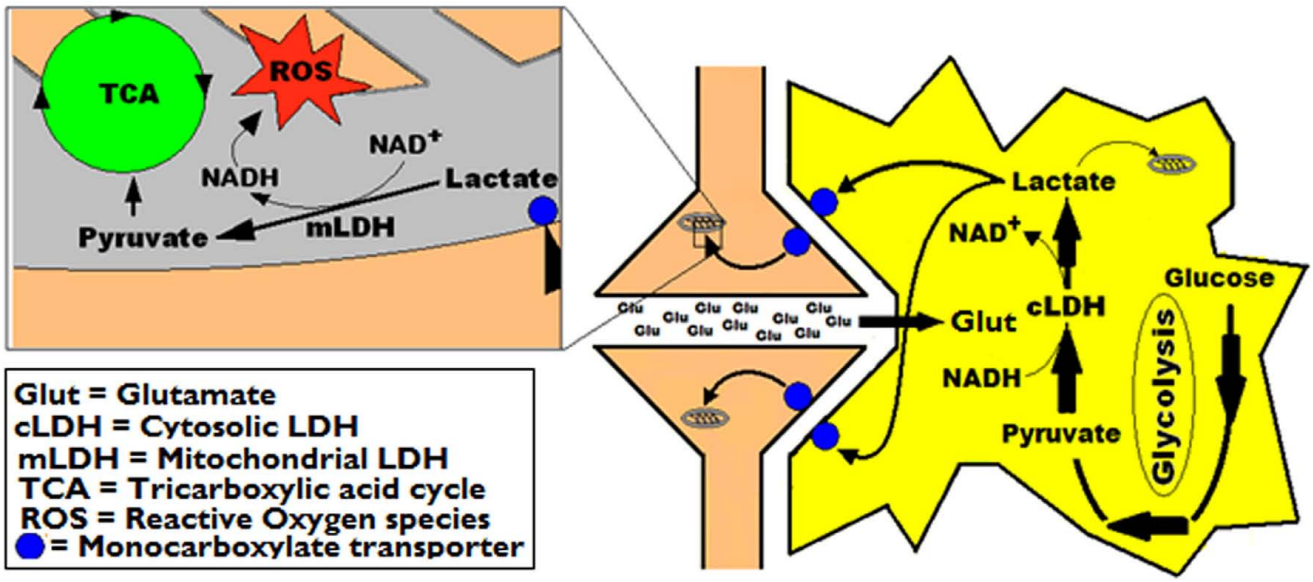

FIGURE 11 | A simplified schematic representation of the astrocytic-neuronal lactate shuttle hypothesis (ANLSH, Pellerin and Magistretti, 1994) combined with our own hypothesis that postulates lactate as the end-product of aerobic glycolysis (Figures 4 and 7). In addition, the left panel illustrate the ability of NADH, formed during lactate conversion to pyruvate in the neuronal mitochondrial membrane, to neutralize Glut-induced ROS-produced damage.

such restriction. Additionally, the results corroborate the premise of the ANLSH, according to which lactate, the astrocytic by-product of Glut uptake, is shuttled to neurons where it is utilized by mitochondria as an energy substrate. We have already provided evidence in support of aerobic neuronal production and utilization of lactate that necessitate an accompanied NADH production (**Figures 4** and **7**; Schurr, 2006; Schurr and Payne, 2007). These results provide additional support to our previous findings and indicate that the reducing agent, NADH, is a potential endogenous ROS scavenger that could protect neurons from Glut excitotoxicity (**Figure 11**).

CONCLUSION

Here we accounted for several of our studies of the last decade or so and revisited the studies of Hu and Wilson (1997a,b), proposing that their outcomes are best explained via the ANLSH (Pellerin and Magistretti, 1994). Furthermore, these experimental investigations, along with many of the cited studies by other investigators, strongly support our own hypothesis (Schurr, 2006) according to which lactate is the real glycolytic end-product both aerobically and anaerobically. Aside from the theoretical and thermodynamic considerations in support of this hypothesis (Schurr, 2006), the experimental results presented here provide scientific evidence in its support. Last, but not least, the postulate that lactate is the end-product of aerobic glycolysis means that this monocarboxylate must be converted to pyruvate by the mitochondrial LDH (mLDH) to be useful as an energy substrate. This conversion is coupled to a formation of the reducing cofactor, NADH, which we have shown here to act as a neutralizing agent of ROS, thus providing neuroprotection against Glut excitotoxicity.

REFERENCES

Aliprandi, A., Longoni, M., Stanzani, L., Remolizzo, L., Vaccaro, M., Begni, B., Galimberti, G., and Garofolo, R. (2005). Increased plasma glutamate in stroke patients might be linked to altered platelet release and uptake. *J. Cereb. Blood Flow Metab.* 25, 513–519.

Aliverdieva, D. A., Manaev, D. V., Bondarenko, D. I., and Sholtz, K. F. (2006). Properties of yeast *Saccharomyces cerevisiae* plasma membrane dicarboxylate transporter. *Biochemistry (Mosc.)* 71, 1161–1169.

Ashford, C. A., and Holmes, E. G. (1929). Contributions to the study of brain metabolism. V. Role of phosphates in lactic acid production. *Biochem. J.* 23, 748–759.

Ashford, C. A., and Holmes, E. G. (1931). Further observations on the oxidation of lactic acid by brain tissue. *Biochem. J.* 25, 2028–2049.

Atlante, A., de Bari, L., Bobba, A., Marra, E., and Passarella, S. (2007). Transport and metabolism of L-lactate occur in mitochondria from cerebellar granule cells and are modified in cells undergoing low potassium dependent apoptosis. *Biochim. Biophys. Acta* 1767, 1285–1299.

Aubert, A., Costalat, R., Magistretti, P. J., and Pellerin, L. (2005). Brain lactate kinetics: modeling evidence for neuronal lactate uptake upon activation. *Proc. Nat. Acad. Sci. U.S.A.* 102, 16448–16453.

Barros, L. F., and Deitmer, J. W. (2010). Glucose and lactate supply to the synapse. *Brain Res. Rev.* 63, 149–159.

Brennan, A. M., Connor, J. A., and Shuttleworth, C. W. (2006). NAD(P)H fluorescence transients after synaptic activity in brain slices: predominant role of mitochondrial function. *J. Cereb. Blood Flow Metab.* 26, 1389–1406.

Brooks, G. A. (1985). Lactate: glycolytic product and oxidative substrate during sustained exercise in mammals – "the lactate shuttle." in *Comparative Physiology and Biochemistry – Current Topics and Trends, Vol. A, Respiration-Metabolism-Circulation*, ed. R. Gilles (Berlin: Springer-Verlag), 208–218.

Brooks, G. A. (1998). Mammalian fuel utilization during sustained exercise. *Comp. Biochem. Physiol. B Biochem. Mol. Biol.* 120, 89–107.

Brooks, G. A. (2000). Intra- and extracellular lactate shuttles. *Med. Sci. Sports Exerc.* 32, 790–799.

Brooks, G. A. (2002a). Lactate shuttle – between but not within cells? *J. Physiol. (Lond.)* 541, 333.

Brooks, G. A. (2002b). Lactate shuttles in nature. *Biochem. Soc. Trans.* 30, 258–264.

Brooks, G. A., Dubouchaud, H., Brown, M., Sicurello, J. P., and Butz, C. E. (1999). Role of mitochondrial lactate dehydrogenase and lactate oxidation in the intracellular lactate shuttle. *Proc. Natl. Acad. Sci. U.S.A.* 96, 1129–1134.

Chih, C.-P., Lipton, P., and Roberts, E. L. Jr. (2001). Do active cerebral neurons really use lactate than glucose? *Trends Neurosci.* 24, 573–578.

Chih, C.-P., and Roberts, E. L. Jr. (2003). Energy substrates for neurons during neural activity: a critical review of the astrocyte-neuron lactate shuttle hypothesis. *J. Cereb. Blood Flow Metab.* 23, 1263–1281.

Dallas, M., Boycott, H. E., Atkinson, L., Miller, A., Boyle, J. P., Pearson, H. A., and Peers, C. (2007). Hypoxia suppresses glutamate transport in astrocytes. *J. Neurosci.* 27, 3946–3955.

Dienel, G. A., and Hertz, L. (2005). Astrocytic contributions to bioenergetics of cerebral ischemia. *Glia* 50, 362–388.

Dirnagl, U., Iadecola, C., and Moskowitz, M. A. (1999). Pathobiology of ischaemic stroke: an integrated view. *Trends Neurosci.* 22, 391–397.

Emerit, J., Edeas, M., and Bricaire, F. (2004). Neurodegenerative diseases and oxidative stress. *Biomed. Pharmacother.* 58, 39–46.

Fillenz, M. (2005). The role of lactate in brain metabolism. *Neurochem. Int.* 47, 413–417.

Flock, E., Bollman, J. L., and Mann, D. C. (1938). The utilization of pyruvic acid by the dog. *J. Biol. Chem.* 125, 49–56.

Frantseva, M. V., Perez-Velasquez, J. L., Tsorakidis, G., Mendonca, A. J., Adamchik, Y., Mills, L. R., Carlen, P. L., and Burnham, M. W. (2000). Oxidative stress is involved in seizure-induced neurodegeneration in the kindling model of epilepsy. *Neuroscience* 97, 431–435.

Galeffi, F., Foster, K. A., Sadgrove, M. P., Beaver, C. J., and Turner, D. A. (2007). Lactate uptake contributes to the NAD(P)H biphasic response and tissue oxygen response during synaptic stimulation in area CAI of rat hippocampal slices. *J. Neurochem.* 103, 2449–2461.

Gallagher, C. N., Carpenter, K. L., Grice, P., Howe, D. J., Mason, A., Teemofeev, I., Menon, D. K., Kirpatrick, P. J., Pickard, J. D., Sutherland, G. R., and Hutchinson, P. J. (2009). The human brain utilizes lactate via the tricarboxylic acid cycle: a 13C-labelled microdialysis and high-resolution nuclear magnetic resonance study. *Brain* 132, 2839–2849.

Gandhi, G. K., Cruz, N. F., Ball, K. K., and Dienel, G. A. (2009). Astrocytes are poised for lactate trafficking and release from activated brain and for supply of glucose to neurons. *J. Neurochem.* 111, 522–536.

Gladden, L. B. (2004). Lactate metabolism: a new paradigm for the third millennium. *J. Physiol. (Lond.)* 558, 5–30.

Grewer, C., Gameiro, A., Zhang, Z., Tao, Z., Braams, S., and Rauen, T. (2008). Glutamate forward and reverse transport: from molecular mechanism to transporter-mediated release after ischemia. *IUBMB Life* 60, 609–619.

Halestrap, A. P., and Denton, R. M. (1975). The specificity and metabolic implications of the inhibition of pyruvate transport in isolated mitochondria and intact tissue preparations by α-cyano-4-hydroxycinnamate and related compounds. *Biochem. J.* 148, 97–106.

Heinemann, U., Buchheim, K., Gabriel, S., Kann, O., Kovács, R., and Schuchmann, S. (2002). Cell death and the metabolic activity during epileptiform discharges and status epilepticus in the hippocampus. *Prog. Brain Res.* 135, 197–210.

Herrero-Mendez, A., Almeida, A., Fernández, E., Maestre, C., Moncada, S., and Bolanos, J. P. (2009). The bioenergetic and antioxidant statusof neurons is controlled by continuous degredation of a key glycolytic enzyme by APC/C-Cdh1. *Nat. Cell Biol.* 11, 747–752.

Hertz, L. (2004). The astrocyte-neuron lactate shuttle: a challenge of a challenge. *J. Cereb. Blood Flow Metab.* 24, 1241–1248.

Hertz, L., Peng, L., and Dienel, G. A. (2007). Energy metabolism in astrocytes: high rate of oxidative metabolism and spatiotemporal dependence on glycolysis/glycogenolysis. *J. Neurosci. Res.* 27, 219–249.

Holmes, E. G. (1930). Oxidations in central and peripheral nervous tissue. *Biochem. J.* 24, 914–925.

Holmes, E. G., and Ashford, C. A. (1930). Lactic acid oxidation in brain with reference to the "Meyerhof cycle." *Biochem. J.* 24, 1119–1127.

Hu, Y., and Wilson, G. S. (1997a). Rapid changes in local extracellular rat brain glucose observed with an in vivo glucose sensor. *J. Neurochem.* 68, 1745–1752.

Hu, Y., and Wilson, G. S. (1997b). A temporary local energy pool coupled to neuronal activity: fluctuations of extracellular lactate levels in rat brain monitored with rapid-response enzyme-based sensor. *J. Neurochem.* 69, 1484–1490.

Ivanov, A., Mukhtarov, M., Bregestovski, P., and Zilberter, Y. (2011). Lactate effectively covers energy demands during neuronal network activity in neonatal hippocampal slices. *Front. Neuroenerg.* 3:2. doi:10.3389/fnene.2011.00002

Kann, O., Huchzermeyer, C., Kovács, R., Wirtz, S., and Schuelke, M. (2011). Gamma oscillations in the hippocampus require high complex I gene expression and strong functional performance of mitochondria. *Brain* 134(Pt 2), 345–358.

Kasischke, K. A., Vishwasrao, H. D., Fisher, P. J., Zipfel, W. R., and Webb, W. W. (2004). Neural activity triggers neuronal oxidative metabolism followed by astrocytic glycolysis. *Science* 305, 99–103.

Kiewert, C., Mdzinarishvile, A., Hartmann, J., Bickel, U., and Klein, J. (2010). Metabolic and transmitter changes in core and penumbra after middle cerebral artery occlusion in mice. *Brain Res.* 1312, 101–107.

Kirsch, M., and De Groot, H. (2001). NAD(P)H, a directly operating antioxidant? *FASEB J.* 15, 1569–1574.

Korf, J. (2006). Is brain lactate metabolized immediately after neuronal activity through the oxidative pathway? *J. Cereb. Blood Flow Metab.* 26, 1584–1586.

Kovács, R., Schuchmann, S., Gabriel, S., Kann, O., Kardos, J., and Heinemann, U. (2002). Free radical-mediated cell damage after experimental status epilepticus in hippocampal slice cultures. *J. Neurophysiol.* 88, 2909–2918.

Krieger, C., and Duchen, M. R. (2002). Mitochondria, $Ca2^{+}$ and neurodegenerative disease. *Eur. J. Pharmacol.* 447, 177–188.

Larrabee, M. G. (1995). Lactate metabolism and its effects on glucose metabolism in the excised neural tissue. *J. Neurochem.* 64, 1734–1741.

Larrabee, M. G. (1996). Partitioning of CO2 production between glucose and lactate in excised sympathetic ganglia, with implications for brain. *J. Neurochem.* 67, 1726–1734.

Larsen, T. S., Rasmussen, P., Overgaard, M., Secher, N. H., and Nielsen, H. B. (2008). Non-selective β-adrenergic blockade prevents reduction of the cerebral metabolic ratio during exhaustive exercise in humans. *J. Physiol. (Lond.)* 586, 2807–2815.

Levasseur, J. E., Alessandri, B., Reinert, M., Clausen, T., Zhou, Z., Altememi, N., and Bullock, M. R. (2006). Lactate, not glucose, up-regulates mitochondrial oxygen consumption both in sham and lateral fluid percussed rat brains. *Neurosurgery* 59, 1122–1131.

Liang, H.-W., Xia, Q., and Bruce, I. C. (2005). Reactive oxygen species mediate the neuroprotection conferred by mitochondrial ATP-sensitive potassium channel opener during ischemia in the rat hippocampal slice. *Brain Res.* 1042, 169–175.

Lin, M. T., and Beal, M. F. (2005). Mitochondrial dysfunction and oxidative stress in neurodegenerative diseases. *Nature* 19, 787–795.

Magistretti, P. J. (2000). Cellular bases of functional brain imaging: insights from neuron-glia metabolic coupling. *Brain Res.* 886, 108–112.

Magistretti, P. J., and Pellerin, L. (1999). Cellular mechanisms of brain energy metabolism and their relevance to functional brain imaging. *Philos. Trans. R. Soc. Lond. B Biol. Sci.* 354, 1155–1163.

Magistretti, P. J., Pellerin, L., Rothman, D. L., and Shulamn, R. G. (1999). Energy on demand. *Science* 283, 496–497.

Malonek, D., and Grinvald, A. (1996). Interactions between electrical activity and cortical microcirculation revealed by imaging spectroscopy: implications for functional brain mapping. *Science* 272, 551–554.

Mangia, S., Garreffa, G., Bianciardi, M., Giove, F., Di Salle, F., and Maraviglia, B. (2003). The aerobic brain: lactate decrease at the onset of neural activity. *Neuroscience* 118, 7–10.

Mangia, S., Giove, F., Tkac, I., Logotetethetis, N. K., Henry, P. G., Olman, C. A., Maraviglia, B., Di Salle, F., and Ugurbil, K. (2009). Metabolic and hemodynamic events after changes in neuronal activity: current hypotheses, theoretical predictions and in vivo NMR experimental findings. *J. Cereb. Blood Flow Metab.* 29, 441–463.

Medina, J. M., and Tabernero, A. (2005). Lactate utilization by brain cells and its role in CNS development. *J. Neurosci. Res.* 79, 2–10.

Nicholls, D., and Atwell, D. (1990). The release and uptake of excitatory amino acids. *Trends Pharmacol. Sci.* 11, 462–468.

Passarella, S., de Bari, L., Valenti, D., Pizzuto, R., Paventi, G., and Atlante, A. (2008). Mitochondria and L-lactate metabolism. *FEBS Lett.* 582, 3569–3576.

Pellerin, L., Bouzier-Sore, A. K., Aubert, A., Serres, S., Merle, M., Costalat, R.,

and Magistretti, P. J. (2007). Activity-dependent regulation of energy metabolism by astrocytes: an update. *Glia* 55, 1251–1262.

Pellerin, L., and Magistretti, P. J. (1994). Glutamate uptake into astrocytes stimulates aerobic glycolysis: a mechanism coupling neuronal activity to glucose utilization. *Proc. Natl. Acad. Sci. U.S.A.* 91, 10625–10629.

Pellerin, L., and Magistretti, P. J. (2003). Food for thought: challenging the dogmas. *J. Cereb. Blood Flow Metab.* 23, 1282–1286.

Pellerin, L., and Magistretti, P. J. (2004a). Let there be (NADH) light. *Science* 305, 50–52.

Pellerin, L., and Magistretti, P. J. (2004b). Empiricism and rationalism: two paths toward the same goal. *J. Cereb. Blood Flow Metab.* 24, 1240–1241.

Pellerin, L., Pellegri, G., Bittar, P. G., Charnay, Y., Bouras, C., Martin, J. L., Stella, N., and Magistretti, P. J. (1998). Evidence supporting the existence of an activity-dependent astrocyte-neuron lactate shuttle. *Dev. Neurosci.* 20, 291–299.

Rego, A. C., and Oliveira, C. R. (2003). Mitochondrial dysfunction and reactive oxygen species in excitotoxicity and apoptosis: implications for the pathogenesis of neurodegenerative diseases. *Neurochem. Res.* 28, 1563–1574.

Reynolds, I. J., and Hastings, T. G. (1995). Glutamate induces the production of reactive oxygen species in cultured forebrain neurons following NMDA receptor activation. *J. Neurosci.* 15, 3318–3327.

Rosenstock, T. R., Carvalho, A. C., Jurkiewicz, A., Frussa-Filho, R., and Smaili, S. S. (2004). Mitochondrial calcium, oxidative stress and apoptosis in a neurodegenerative disease model induced by 3-nitropropionic acid. *J. Neurochem.* 88, 1220–1228.

Rossi, D. J., Oshima, T., and Attwell, D. (2000). Glutamate release in severe brain ischemia is mainly by reversed uptake. *Nature* 403, 316–321.

Saad, L. O., Mirandola, S. R., Maciel, E. N., and Castiho, R. F. (2006). Lactate dehydrogenase activity is inhibited by methyl malonate in vitro. *Neurochem. Res.* 31, 541–548.

Schurr, A. (2006). Lactate: the ultimate cerebral oxidative energy substrate? *J. Cereb. Blood Flow Metab.* 26, 142–152.

Schurr, A., Miller, J. J., Payne, R. S., and Rigor, B. M. (1999a). An increase in lactate output by brain tissue serves to meet the energy needs of glutamate-activated neurons. *J. Neurosci.* 19, 34–39.

Schurr, A., Payne, R. S., Miller, J. J., and Rigor, B. M. (1999b). Study of cerebral energy metabolism using the rat hippocampal slice preparation. *Methods* 18, 117–126.

Schurr, A., and Payne, R. S. (2007). Lactate, not pyruvate, is neuronal aerobic glycolysis end product: and in vitro electrophysiological study. *Neuroscience* 147, 613–619.

Schurr, A., Payne, R. S., Miller, J. J., and Rigor, B. M. (1997a). Brain lactate, not glucose, fuels the recovery of synaptic function from hypoxia upon reoxygenation: an in vitro study. *Brain Res.* 744, 105–111.

Schurr, A., Payne, R. S., Millet, J. J., and Rigor, B. M. (1997b). Brain lactate is an obligatory aerobic energy substrate for functional recovery after hypoxia: further in vitro validation. *J. Neurochem.* 69, 423–426.

Schurr, A., Reid, K. H., Tseng, M. T., Edmonds, H. L. Jr., and Rigor, B. M. (1985). A dual chamber for comparative studies using the brain slice preparation. *Comp. Biochem. Physiol.* 82A, 701–704.

Schurr, A., Reid, K. H., Tseng, M. T., Edmonds, H. L. Jr., West, C., and Rigor, B. M. (1986). Effect of electrical stimulation on the viability of the hippocampal slice preparation. *Brain Res. Bull.* 16, 299–301.

Schurr, A., West, C. A., and Rigor, B. M. (1988). Lactate-supported synaptic function in the rat hippocampal slice preparation. *Science* 240, 1326–1328.

Serres, S., Bezancon, E., Franconi, J. M., and Merle, M. (2005). Ex vivo NMR study of lactate metabolism in rat brain under various depressed states. *J. Neurosci. Res.* 79, 19–25.

Stryer, L. (1995). "Metabolic energy: generation and storage," in *Biochemistry*, 4th Edn (New York, NY: W. H. Freeman), 441–558.

Tsacopoulos, M., and Magistretti, P. J. (1996). Metabolic coupling between glia and neurons. *J. Neurosci.* 16, 877–885.

Vanzetta, I., and Grinvald, A. (1999). Increased cortical oxidative metabolism due to sensory stimulation: implications for functional brain imaging. *Science* 286, 1555–1558.

Vergun, O., Sobolevsky, A. I., Yelshansky, M. V., Keelan, J., Khodorov, B. I., and Duchen, M. R. (2001). Exploration of the role of reactive oxygen species in glutamate neurotoxicity in rat hippocampal neurones in culture. *J. Physiol. (Lond.)* 531, 147–163.

Wu, T., Ding, X.-S., Wang, W., and Wu, J. (2006). MCI-186 (3-methyl-1-phenyl-2-pyrazolin-5-one) attenuated ischemia/reperfusion injury in cultured rat hippocampal cells. *Biol. Pharm. Bull.* 29, 1613–1617.

Wyss, M. T., Jolivet, R., Buck, A., Magistretti, P. J., and Weber, B. (2011). In vivo evidence for lactate as a neuronal energy source. *J. Neurosci.* 31, 7477–7485.

Yodoya, E., Wada, M., Shimada, A., Katsukawa, H., Okada, N., Yamamoto, A., Ganaphaty, V., and Fujita, T. (2006). Functional and molecular identification of sodium-coupled decarboxylate transporters in rat primary cultured cerebrocortical astrocytes and neurons. *J. Neurochem.* 97, 162–173.

Yoshioka, K., Nishimaru, N., Yanai, S., Shimoda, H., and Yamada, K. (2000). Characteristics of monocarboxylates as energy substrates other than glucose in rat brain slices and the effect of selective glial poisoning – a 31P NMR study. *Neurosci. Res.* 36, 215–226.

Zielke, H. R., Zielke, C. L., and Baab, P. J. (2009). Direct measurement of oxidative metabolism in the living brain by microdialysis: a review. *J. Neurochem.* 109(Suppl. 1), 24–29.

Conflict of Interest Statement: The authors declare that the research was conducted in the absence of any commercial or financial relationships that could be construed as a potential conflict of interest.

Received: 07 October 2011; accepted: 23 December 2011; published online: 13 January 2012.

*Citation: Schurr A and Gozal E (2012) Aerobic production and utilization of lactate satisfy increased energy demands upon neuronal activation in hippocampal slices and provide neuroprotection against oxidative stress. Front. Pharmacol. **2**:96. doi: 10.3389/fphar.2011.00096*

This article was submitted to Frontiers in Neuropharmacology, a specialty of Frontiers in Pharmacology.

frontiers in
PHARMACOLOGY

ORIGINAL RESEARCH ARTICLE
published: 20 March 2012
doi: 10.3389/fphar.2012.00043

Cellular links between neuronal activity and energy homeostasis

Pavan K. Shetty, Francesca Galeffi and Dennis A. Turner*

Neurosurgery and Neurobiology, Research and Surgery Services, Durham VA Medical Center, Duke University, Durham, NC, USA

Edited by:
Yuri Zilberter, INSERM U751, France

Reviewed by:
Yuri Zilberter, INSERM U751, France
Muzamil Ahmad, Indian Institute of Integrative Medicine, India

***Correspondence:**
Dennis A. Turner, Neurosurgery and Neurobiology, Research and Surgery Services, Duke University, Box 3807, NSU, DUMC, Durham, NC 27710, USA.
e-mail: dennis.turner@duke.edu

Neuronal activity, astrocytic responses to this activity, and energy homeostasis are linked together during baseline, conscious conditions, and short-term rapid activation (as occurs with sensory or motor function). Nervous system energy homeostasis also varies during long-term physiological conditions (i.e., development and aging) and with adaptation to pathological conditions, such as ischemia or low glucose. Neuronal activation requires increased metabolism (i.e., ATP generation) which leads initially to substrate depletion, induction of a variety of signals for enhanced astrocytic function, and increased local blood flow and substrate delivery. Energy generation (particularly in mitochondria) and use during ATP hydrolysis also lead to considerable heat generation. The local increases in blood flow noted following neuronal activation can both enhance local substrate delivery but also provides a heat sink to help cool the brain and removal of waste by-products. In this review we highlight the interactions between short-term neuronal activity and energy metabolism with an emphasis on signals and factors regulating astrocyte function and substrate supply.

Keywords: neuronal metabolism, hippocampus, ATP, NADH, oxygen, lactate, pyruvate, cerebral metabolism

INTRODUCTION

The goal of this review is to summarize the linkage between neurons and astrocytes during both short-term perturbations in activity and metabolic function and long-term metabolic adaptation. In addition, we compare where possible observed and predicted differences in metabolic function between *in vivo* and *in vitro* preparations, since the varying methods of substrate delivery in these two conditions lead to contrasting tissue measurements in spite of well preserved neuronal function and activity. In the first section we introduce the responses associated with neuronal activation, in the second section we describe in more detail a number of signals critical for communication across the metabolic unit, and in the third section discuss long-term metabolic homeostasis.

CEREBRAL METABOLIC UNIT

The three critical cellular elements in determining the response of the brain to physiological events include: (1) neurons, which determine cerebral physiological activity based on electrical processing; (2) astrocytes and other glial cells, which directly cooperate between blood vessels and neurons for regulation of energy needs and maintenance of the extracellular environment; and (3) blood vessels for both delivery of substrate to the brain (i.e., glucose and oxygen) and removal of by-products, such as CO_2 and heat. These three elements interact for all aspects of metabolic function, forming a coherent and functional metabolic unit.

BASAL NEURONAL METABOLISM

Neurons are never completely quiescent, with modulation of action potential firing during specific brain states. For example, in the awake or conscious state there is considerable spontaneous activity, which is progressively decreased with deeper levels of anesthesia (Shulman et al., 2009) and increased with focal neuronal activation such as sensory or motor function. Neuronal and glial function is crucially dependent on the maintenance of electrochemical gradients across cellular membranes. Therefore, even during the resting state (i.e., conscious but in the absence of specific sensory, mental physical activity) a significant portion of ATP is utilized to fuel Na^+/K^+-ATPase activity to maintain sodium and potassium gradients (Pellerin and Magistretti, 1994; Chatton et al., 2000; Voutsinos-Porche et al., 2003) and also needed to maintain neurotransmitter recycling and packaging for synaptic vesicles, cell signaling pathways in both neurons and astrocytes, and repair of structural membrane, protein assemblies, and DNA. In addition, further studies have also revealed the importance of the specific composition of energy substrate pool and its utilization for controlling of neuronal excitability and maintaining resting membrane potential (Rheims et al., 2009; Holmgren et al., 2010; Zilberter et al., 2010; Ivanov and Zilberter, 2011; Mukhtarov et al., 2011). For example, lactate is utilized more effectively in the presence of glucose as an oxidative metabolic substrate, to maintain synaptic function (Ivanov et al., 2011).

Brain primarily utilizes glucose as its main energy source (in adults) to synthesize ATP (Clarke and Sokoloff, 1999) and 90% of cerebral ATP production occurs in the mitochondria though oxidative phosphorylation. Therefore, cerebral metabolic activity can be evaluated by measuring cerebral metabolic rates of glucose (CMR glucose) and oxygen (CMRO2) using either [18F]-fluoro-2-deoxy-D-glucose positron emission tomography (FDG PET) together with oxygen-15 PET or calibrated blood oxygen level dependent functional magnetic resonance imaging (BOLD fMRI) methods, respectively (Davis et al., 1998; Hoge et al., 1999). Although rates of energy turnover in the alert resting state are difficult to estimate, metabolic brain activity remains significant during this awake, non-stimulated state (Shulman et al., 2004).

Several PET and fMRI studies indicate that during the transition from the "awake state" to deeper levels of general anesthesia (Smith et al., 2002; Rothman et al., 2003; Shulman et al., 2004) there is a widespread, substantial decrease in energy demand; this decrease is larger in magnitude than the increments in energy consumption noted during activation (Hyder et al., 2001; Shulman et al., 2009).

For example, ∼15% increase in metabolic activity over baseline is observed in conscious humans during tasks to study cognitive and other neurological functions (Phelps and Mazziotta, 1985; Grafton et al., 1992; Elman et al., 1999). In contrast, after the induction of anesthesia brain oxygen and glucose consumption are reduced by ∼40–50% as revealed by PET measurements; these values decline further to ∼15–20% of baseline upon reaching deeper levels of anesthesia with pentobarbital (Shulman et al., 2009). Similarly, results from 31P magnetic resonance spectroscopy (MRS) studies, combined with magnetization transfer method to measure the rate of $P_{inorganic}$ conversion to ATP, determined that the progressive decline of ATP metabolism with increasing levels of anesthesia was parallel to the decline in brain EEG activity; at an isoelectric state the oxidative production rate of ATP was reduced to 50% compared to light isoflurane anesthesia condition (Du et al., 2008). Thus, the conscious state provides a baseline for activation but also represents a high level of spontaneous neural activity and accompanying metabolic demand, which can be substantially reduced with progressively deeper general anesthesia.

SHORT-TERM METABOLIC RESPONSES

METABOLIC EVENTS OCCURRING DURING NEURONAL ACTIVATION

Neuronal activation commonly is evoked during sensory or cognitive stimulation or motor tasks. The stimulation activates neurons in brain regions which respond to the intense incoming synaptic input, resulting typically in firing a sequence of action potentials. Moreover, intermittent periods of increased neuronal activity also can occur during the rapid-eye-movement (REM) stage of sleep, which is associated with dream formation and consolidation of learning and memory. Neuronal activation can also be evoked in *in vitro* preparations, by a short train of electrical stimulation pulses to excite axons and presynaptic terminals, resulting in postsynaptic action potentials and often a compound evoked potential response representing a combination of synaptic potentials and action potentials (Galeffi et al., 2007, 2011). The timing and density of such stimulation can be varied but commonly the duration is 5–30 s, to temporarily "activate" neurons with an intense incoming synaptic input. The energy demands associated with the neuronal activity result in a cascade of metabolic events which can be measured in a number of different ways depending on the preparation and the technique, shown on a timeline in **Figure 1** (*in vitro*) and **Figure 2** (*in vivo*). Common measurements shown include extracellular K^+, Ca^{2+}, oxygen, as well as metabolic imaging, such as NADH or FAD.

For example, trigeminal nerve or whisker stimulation increases glucose metabolism in the thalamus and brain stem (Ciricillo et al., 1994) based on the 2-deoxy-glucose imaging method (the animal equivalent to human FDG PET). Similarly, classical functional imaging studies have reported an increase in blood flow and in the metabolic rate for oxygen and glucose during a sensory, motor, or cognitive simulation after subtraction of baseline activity. However, during sensory stimulation, measurements of glucose and oxygen uptake using PET in human subjects have revealed greater glucose consumption compared to oxygen (Fox et al., 1988). Human detection methods (i.e., fMRI and PET) are sometimes insensitive to early events following neuronal activation due to the small areas involved and rapid time course. During the first few seconds (i.e., up to 10 s) intracellular Na^+ and Ca^{2+} starts to build up and K^+ is released from neurons whereas mitochondrial intermediates are rapidly oxidized (together with oxygen) for ATP generation, as noted in **Figure 1**. Real-time imaging methods are more sensitive to these early changes but typically are more invasive in nature.

For example, activity-dependent changes in NADH/NAD^+ redox state can be monitored with real-time fluorescence imaging of NADH *in vivo* as well as *in vitro*. Physiological stimulation leads to an NADH fluorescence decrease in well-oxygenated tissue (*in vitro* and *in vivo*), followed by either recovery to baseline or an increase (i.e., overshoot) above baseline (Rosenthal and Jobsis, 1971; Lothman et al., 1975; Schuchmann et al., 2001; Shuttleworth et al., 2003). Influx of glucose and lactate to neurons results in a transient decrease in lactate and glucose concentration in the extracellular space (ECS; Hu and Wilson, 1997a,b). Perfusion of the brain also depends on the tight coupling between O_2 supply and metabolic demand; stimulation of neurons results in a transient drop in O_2 concentration due to increased oxidative phosphorylation (Foster et al., 2005), which stimulates a series of reactions to increase cerebral blood flow and match demand. Increases in intracellular and mitochondrial Ca^{2+} also can enhance enzymatic activity within the tricarboxylic acid (TCA) cycle along with release of oxygen free radicals and reactive oxygen species (ROS; Duchen, 1992; Keelan et al., 1999; Kovacs et al., 2001; Schuchmann et al., 2001). Tissue oxygen measurements with NADH imaging during prolonged stimulation *in vitro* also revealed persistent NADH oxidation and O_2 utilization with continued metabolic demand (Galeffi et al., 2011).

RECOVERY AFTER NEURONAL ACTIVATION

During recovery neuronal activity is decreasing to baseline but metabolic needs can persist as well as delayed enhancement of blood flow. For example, NADH remains elevated temporarily (Foster et al., 2005; Galeffi et al., 2011) due to persistent TCA cycle dehydrogenase activity (Denton, 2009) and lactate uptake, extracellular lactate rises as astrocytic metabolism continues, and local blood flow stays elevated, while short-term intermediate molecules within the mitochondria are repleted, as noted in **Figure 1**. Eventually, neuronal activation winds down, leading to O_2 consumption trending down to basal levels as metabolism wanes, restoration of membrane potentials by pumps, stabilization of NADH and other mitochondrial intermediates once replenished, and finally decreases in local blood flow to control levels. Eventually NADH levels recover back to baseline levels (Rosenthal and Jobsis, 1971; Lothman et al., 1975; Schuchmann et al., 2001; Shuttleworth et al., 2003).

CELLULAR LOCALIZATION OF ENERGY UTILIZATION AFTER NEURONAL ACTIVATION – NEURONS VS ASTROCYTES?

Synaptic activity stimulates glucose uptake and glucose utilization by both neurons and astrocytes (Sokoloff, 1999; Chih and

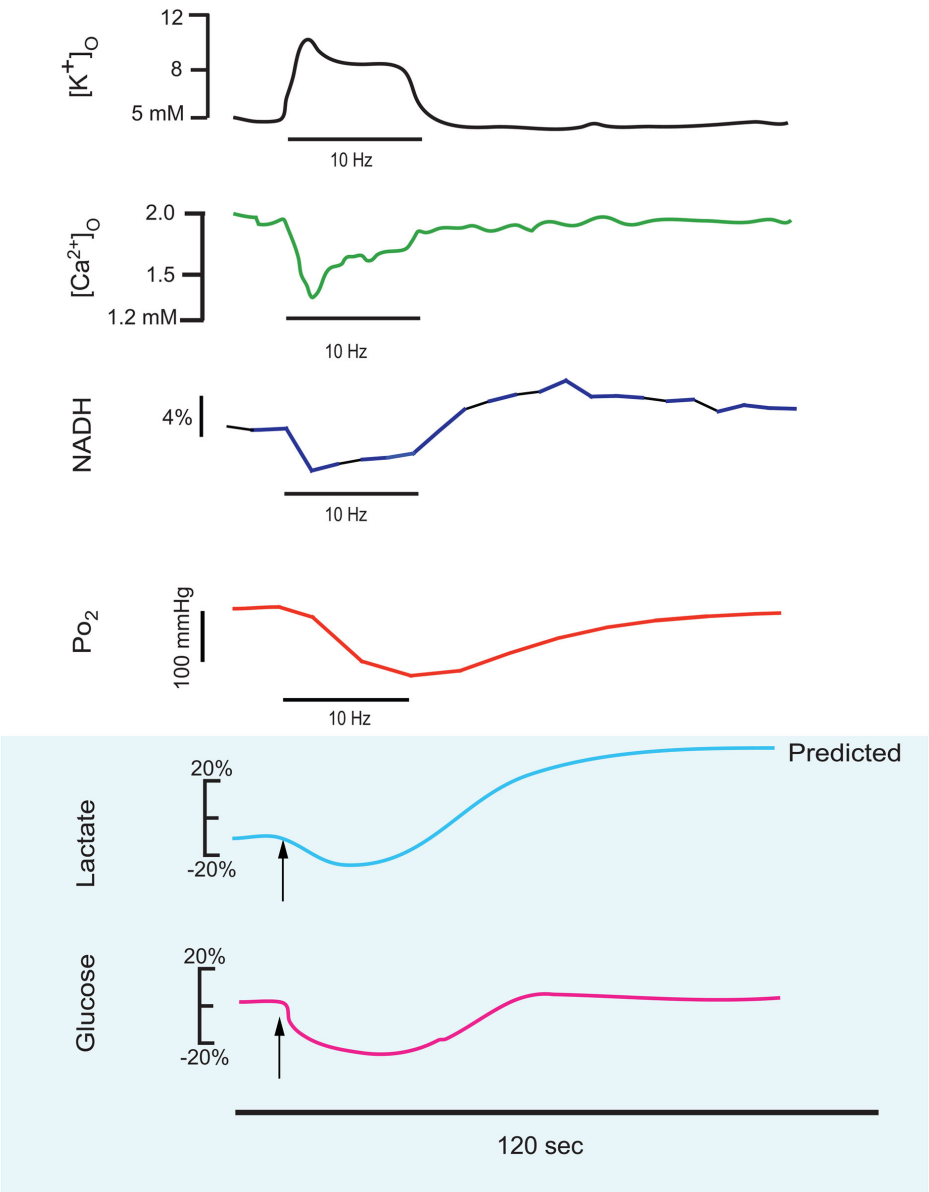

FIGURE 1 | This series of traces illustrates the response to a 10–25 short stimulus train applied to the stratum radiatum of the CA1 region of an *in vitro* hippocampal tissue slice, and the physiological responses which can be measured in real-time during this stimulus train. These reconfigured traces have been redrawn from primary sources to be on the same time scale (shown as 120 s below). Measured responses include extracellular K^+ and Ca^{2+} (Benninger et al., 1980) and NADH imaging and tissue PO_2 (Galeffi et al., 2007). Predicted *in vitro* tissue slice responses are shown below with blue shading, with lactate and glucose extrapolated from *in vivo* measurements performed by Hu and Wilson (1997a,b). Note that extracellular K^+ rises during the train and Ca^{2+} decreases, due to K^+ release from neurons and Ca^{2+} uptake into neurons. NADH shows both an oxidative phase (i.e., a decrease) and a reduction phase (i.e., an increase), whereas in tissue slices the tissue oxygen can only decrease from the baseline level. Extracellular glucose can likewise only decrease, whereas lactate synthesis (stimulated by the train) results in an initial dip (due to demand) but a subsequent elevation, as lactate is further extruded from astrocytes.

Roberts, 2003). Cellular and tissue studies show that neurons likely use a combination of extracellular lactate (derived from astrocytic glycolysis) and glucose (**Figure 3**) as their energy substrates (Galeffi et al., 2007). *In vivo* data reveals that there is a prevalence of glycolysis over oxidative phosphorylation during neuronal activation which results in increased lactate production, likely primarily within astrocytes (Dienel and Hertz, 2001).

However, evidence supporting direct lactate utilization by neurons continues to have skeptics (Korf, 2006), including data linking glucose (but not lactate) utilization with NMDA-induced neurotransmission (Bak et al., 2006, 2009). In contrast, there is activity-dependent oxidation of lactate *in vivo* (Wyss et al., 2011), whereas astrocytic-derived lactate is necessary to maintain long-term potentiation (Suzuki et al., 2011).

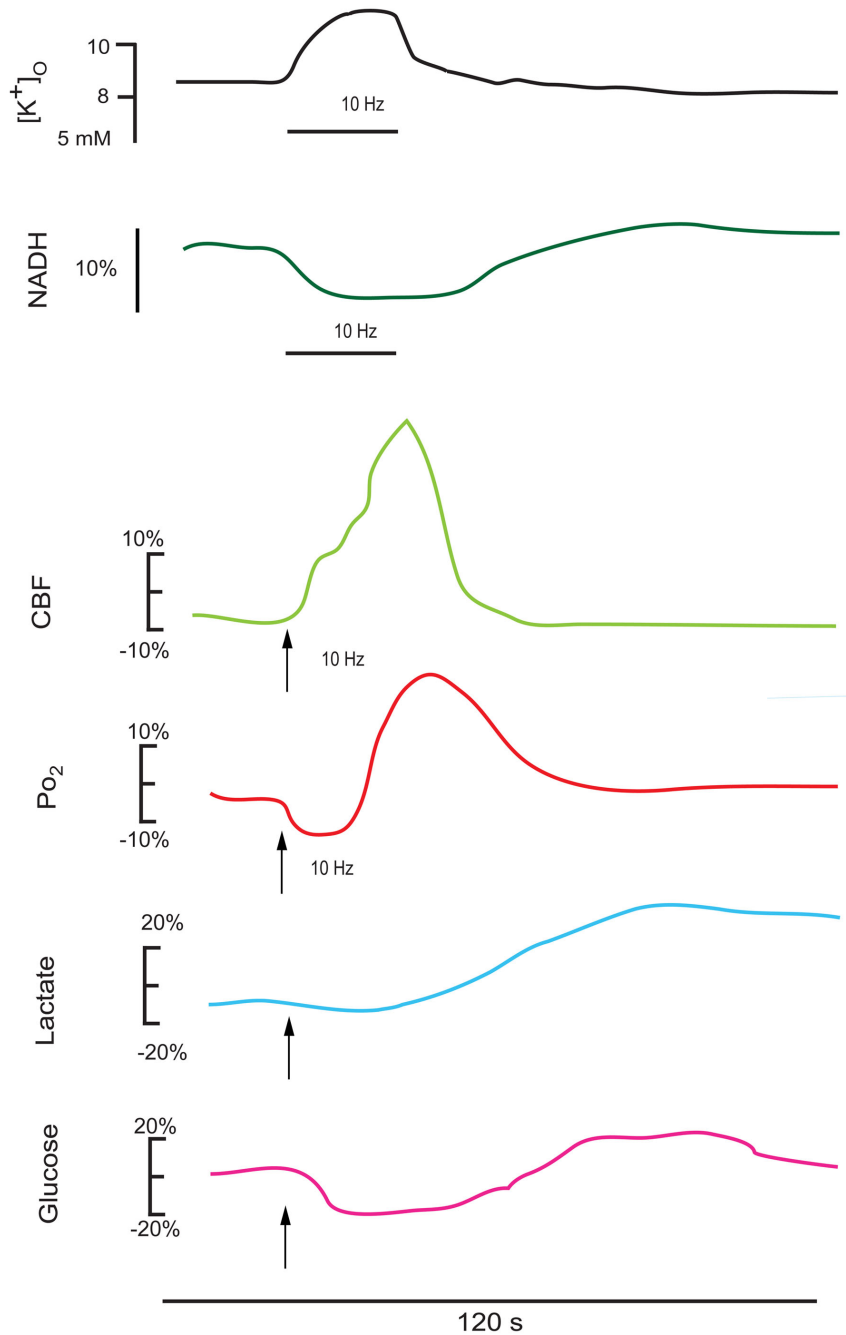

FIGURE 2 | This series of redrawn and rescaled traces show measured responses *in vivo* from intact brain (though different structures), where changes in cerebral blood flow can alter the basic responses to a stimulation train. The upper K^+ and NADH traces are in response to a 25-s stimulus train at 10 Hz in the cortex (Lothman et al., 1975), showing a consistent K^+ elevation and an NADH oxidation (Turner et al., 2007). The CBF and PO_2 responses follow a 15-s stimulation train at 10 Hz in the cerebellum (Offenhauser et al., 2005). The glucose and lactate measurements are redrawn from Hu and Wilson (1997a,b). Note that the oxygen response shows an initial dip in the activated region then an elevation as the enhanced cerebral blood flow response occurs. There is an initial decrease and a delayed enhancement in both cerebral lactate (due to astrocytic extrusion) and glucose (due to enhanced transport into the brain) as measured extracellularly.

In astrocytes, the presence of extracellular glutamate following synaptic release induces rapid glutamate uptake [through glutamate transporters (GLTs)] associated with Na^+ influx (**Figure 3**). Uptake of glutamate and its conversion to glutamine and subsequent recycling back to neurons requires energy provided by glycolysis within astrocytes (Pellerin and Magistretti, 1996, 1997). In addition, *de novo* synthesis of glutamate from glucose in astrocytes also requires ATP, through the TCA cycle

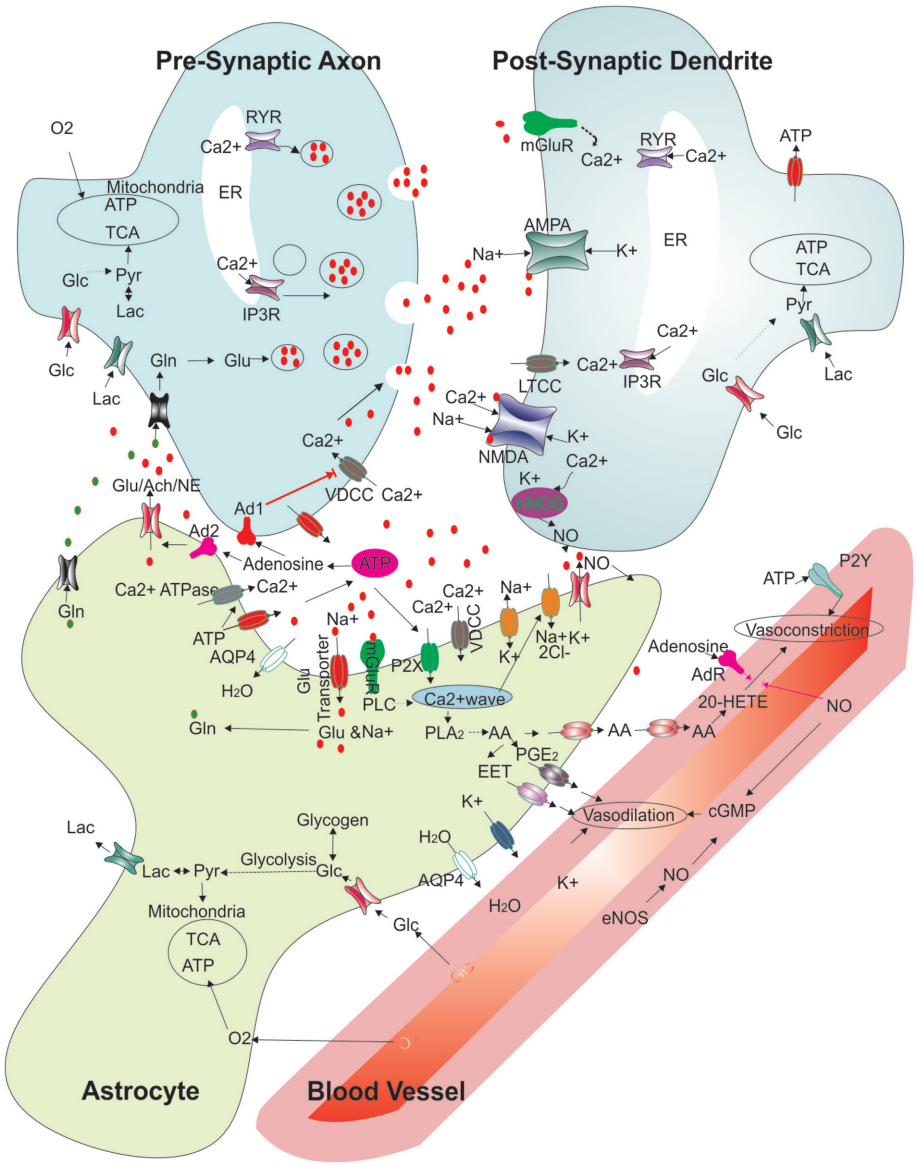

FIGURE 3 | Regulation of synaptic function and cerebral blood flow: modified schematic diagram (Attwell et al., 2010; Kapogiannis and Mattson, 2011) showing the multiple interactions between an astrocyte, neurons, and a blood vessel. The various functions depicted show presynaptic release, glutamate receptor binding and handling, various energy transport functions between blood vessels, the astrocyte and neurons, vasoconstriction and vasodilation pathways, and extracellular molecules. Abbreviations: RYR, ryanodine receptor; ER, endoplasmic reticulum; Glu, glutamate; Gln, glutamine; IP3R, Inositol 3 phosphate receptor; Lac, lactate; Glc, glucose; Pyr, pyruvate; TCA, Tricaboxylic acid cycle; ATP, adenosine 5′- tri phosphate; Ach, acetyl choline; NE, norepinephrine; No, nitric oxide; Ad1, adenosine receptor 1; Ad2, adenosine receptor 2; mGluR, metabotropic glutamate receptor; NMDAR, N-methyl-D-aspartic acid receptor; AMPAR, 2-amino-3-(5-methyl-3-oxo-1;2- oxazol-4-yl)propanoic acid receptor; nNOS, neuronal nitric oxide synthase; eNOS, endothelial nitric oxide synthase EET, epoxyeicosatrienoic acids; AA, arachidonic acid; PGE2, prostaglandin 2; 20-HETE, 20-hydroxy arachidonic acid; PLA2, phospholipase A2; cGMP,cyclic guanosine monophosphate; P2X; purinergicreceptor P2X; P2Y, purinergic receptor P2Y; PLC, phospholipase C; AQP4, aquaporin-4; VDCC, voltage dependent calcium channel; LTCC, L-type calcium channel.

intermediate α-keto-glutarate. The summary view at this time is that glucose can be metabolized by both neurons and astrocytes, but neurons utilize a large proportion of extracellular lactate for oxidative metabolism (perhaps greater than 50%, drawn from a large extracellular pool of lactate generated by astrocytes) and the balance from glucose (Zielke et al., 2007).

DIFFERENCES IN SUBSTRATE DELIVERY *IN VIVO* VS *IN VITRO* SLICE TISSUE PREPARATIONS

The large difference between the *in vivo* condition and *in vitro* slice preparations is oxygen and glucose delivery, which occurs via diffusion from tissue borders *in vitro* and through an extensive vessel and capillary network *in vivo* (Turner et al., 2007). Since there is no secondary blood flow response *in vitro*, then

the tissue levels of oxygen (Galeffi et al., 2007, 2011) and glucose can only dip to lowered levels and recover in response to the enhanced metabolic demand. In contrast to *in vivo* conditions where hemoglobin can possess high oxygen saturation and content at low PO_2 tensions, in *in vitro* preparations a high oxygen tension is needed to maintain tissue oxygen levels, since oxygen content and flux through the tissue are very low with diffusion alone, particularly at the long distances required to maintain slices (i.e., up to 400–500 μm depth). As a comparison, the oxygen dip following significant *in vivo* cortical activation may be ∼5–10 mm Hg O_2 (Thompson et al., 2003) whereas similar activation in a tissue slice can lead to ∼180 mm Hg O_2 change (Galeffi et al., 2011). This large difference in oxygen carrying capacity or content can lead to considerable confusion about what may be a "sufficient" level of oxygen in tissue slices (i.e., Gordon et al., 2008); clearly, the nature of the tissue slice preparation and the degree of neuronal activation and metabolic demand may help clarify the levels of oxygen required in the tissue bath, which should give rise to values greater than 10–15 mm Hg in the center of a slice even with significant metabolic demand. Our experience is that relatively normal neuronal function requires at least 50% ambient oxygen levels (i.e., >350 mm Hg) to maintain even low levels in the middle of slices during metabolic demand (Galeffi et al., 2011).

CEREBRAL BLOOD FLOW

Stimulation of local neuronal activity increases local blood flow through a variety of neuronal and astrocytic mechanisms (Koehler et al., 2009; Paulson et al., 2009). Metabolic signals derived from both neurons and astrocytes can modulate both blood flow and substrate availability (Furchgott and Zawadzki, 1980; Gordon et al., 2008). For example, NO generated by neurons leads to vessel dilation and acetylcholine action on muscarinic receptors of the endothelial cells can cause relaxation of vascular smooth muscle. Bradykinin is also an important vasodilator, known to induce K_{Ca} channel activation in endothelial cells through the generation of ROS (Nelson and Quayle, 1995; Sobey et al., 1997). Glutamate also has a major role in regulating blood flow by increased NO generation from neurons and arachidonic acid derived from astrocytes (Gordon et al., 2008). In astrocytes Ca^{2+} also activates phospholipase A2 and increases the production of arachidonic acid metabolites (**Figure 3**), such as prostaglandins and epoxyeicosatrienoic acids, which dilate nearby arterioles (Iadecola and Nedergaard, 2007; Koehler et al., 2009). Prostaglandins binding to the EP4 PG receptors activate protein kinase A by cAMP and thus decrease phosphorylation of myosin chains; EETs inhibit the receptors for thromboxane thereby inhibiting vasoconstriction. Adenosine, a metabolite of ATP, also modulates blood flow, through A2A receptors localized on arterioles (Gordon et al., 2008). Rapid glycolysis during neuronal activation increases the conversion of pyruvate to lactate and an increased NADH/NAD^+ ratio, which in turn increases cerebral blood flow (Ido et al., 2004; Pellerin et al., 2007; Gordon et al., 2008). A number of these mechanisms are directly in response to neuronal and astrocytic activation, linking neuronal activity to metabolic demand and supply in a number of ways (**Figure 2**). Measurements *in vivo* in intact preparations include K^+, NADH, cerebral blood flow, oxygen, as well as lactate and glucose, as shown in **Figure 2**.

HEAT PRODUCTION

Direct heat emission can reveal the source(s) of ongoing metabolism (both through ATP hydrolysis as well as mitochondrial heat release) at a cellular and circuit level, as well as the efficiency of metabolism [i.e., the coupling of mitochondrial energy with ATP production or heat release (LaManna et al., 1980, 1989; Yablonskiy et al., 2000; Trubel et al., 2005)]. Maintenance of mitochondrial membrane potential for ATP generation releases ∼33% of total energy as heat, but ATP hydrolysis also leads to heat production, whereas there is minimal heat production by anaerobic glycolysis (LaManna et al., 1980; Yablonskiy et al., 2000). The considerable resulting heat production is rapidly diffused into surrounding tissue, but since the brain resides in a closed space the heat must be dissipated by a large cerebrovascular response (LaManna et al., 1989; Trubel et al., 2005). In most instances, the cerebrovascular (dilation) response to neuronal metabolism is far out of proportion to the substrate supply need, suggesting that a secondary function of the vascular response is heat shunting (Sukstanskii and Yablonskiy, 2006). In spite of the considerable heat dissipation through the vascular system neuronal activation can still lead to up to 0.5°C temperature elevation in a local region, whereas spreading depression, seizures and recovery from ischemia can generate up to 1.0°C in intact cortex (LaManna et al., 1980, 1989). Direct heat emission imaging with specialized infrared cameras may resolve the efficiency of metabolism since uncoupling of ATP generation from mitochondrial membrane potential releases nearly all of metabolism as heat.

CHANGES IN EXTRACELLULAR SPACE

Both astrocytes and neurons swell with activation due to Na^+ and water entry, leading to shrinkage of the ECS (Bourke et al., 1980; Fayuk et al., 2002). For example, the ECS of the mature optic nerve and also hippocampus rapidly and reversibly decreases by as much as 20% (Ransom et al., 1985; Fayuk et al., 2002). Intrinsic optical signal (IOS) imaging and measurements also have revealed spontaneous neuronal hyperactivity associated with ECS shrinkage *in vitro* (Buchheim et al., 1999). This swelling is rapid and reversible and is related to duration of the physiological stimuli (Dietzel et al., 1982) but also is associated with anoxia and inflammation (Hochwald et al., 1981). The shrinkage of ECS in central nervous system is also observed developmentally due to activity-dependent changes in postnatal development (Bondareff and Pysh, 1968; Van Harreveld et al., 1969; Connors et al., 1982). Thus, ECS or IOS imaging may augment other methods of following neuronal activation and metabolism.

SUMMARY

Following neuronal activation a complex sequence of responses in neurons, astrocytes and blood vessels orchestrates enhanced substrate supply and blood flow to be able to maintain the energy requirements for the activation regardless of duration. We now summarize some of these critical intermediate signals and how they function to preserve metabolic homeostasis within the cerebral metabolic unit.

FACTORS INVOLVED IN SHORT-TERM ENERGY HOMEOSTASIS

CRITICAL INTERMEDIATE SIGNALS UNDERLYING NEURONAL–GLIAL COMMUNICATION

There are a number of factors and signals responsible for homeostatic maintenance of neuronal function and energy metabolism. As soon as neuronal activity is stimulated neurons initially show Na^+ and Ca^{2+} inward currents and then subsequently release K^+, glutamate, NO, CO_2, and H_2O_2 into the ECS; this increased neuronal activity requires increased oxygen, lactate and glucose uptake to maintain metabolic function. The neuronal uptake of metabolic substrates and the release of secondary signals (i.e., K^+, NO, and glutamate in particular) can function as intermediate cues needed for enhancement of metabolic substrate utilization. These cues then are used as signals by astrocytes and blood vessels to enhance blood flow and substrate delivery, which are amplified into secondary signals, such as ATP release, to spread within astrocytic networks. We will discuss these critical intermediate signals and the astrocytic responses which occur for short-term maintenance of metabolism.

Na^+/K^+ HOMEOSTASIS

Na^+ entry via voltage-dependent channels and action potential generation underlay the basic function of neurons for rapid communication and information processing, with a large number of K^+-voltage channels needed to repolarize neurons at various time intervals; thus, tight regulation of extracellular K^+ is important for maintaining neuronal activation through rapid membrane repolarization. Astrocytes maintain extracellular K^+ homeostasis via both passive and active mechanism of uptake through a variety of voltage-dependent channels and transporters, which is then dissipated back to the ECS, other astrocytes or blood vessels (**Figure 3**). Membrane-bound Na^+/K^+ ATPase (Skou and Esmann, 1992) is the key enzyme responsible for the maintenance of intracellular ion homeostasis in both neurons and astrocytes (Walz and Hertz, 1982). Na^+/K^+ ATPase hydrolyzes ATP to ADP in the process of extruding three Na^+ against two K^+ molecules; inhibition of Na^+/K^+ ATPase results in a marked decrease in astrocytic metabolism. Thus, astrocytes may exert considerable energy for K^+ extracellular stabilization, which helps to maintain neuronal excitability, and in turn K^+ provides an immediate extracellular signal to astrocytes demonstrating neuronal action potential firing.

GLUTAMATE METABOLISM

Glutamate uptake into astrocytes via GLT following synaptic release is another major signaling factor to astrocytes, reflecting neuronal activation (Parpura et al., 1994; Anderson and Swanson, 2000; Auger and Attwell, 2000; Danbolt, 2001; Malarkey and Parpura, 2008). Glutamate is the major excitatory neurotransmitter released throughout the brain, and glutamate action is primarily terminated by glutamate uptake into astrocytes via GLTs. Neurons express both ionotropic and metabotropic glutamate receptors, including (NMDA *N*-methyl-D-aspartate), α-amino-3-hydroxy-5-methyl-4-isoxazolepropionic acid receptor (AMPA), and kainate subtypes (**Figure 3**). Astrocytes also express metabotropic receptors (mGlur 1–8), which are a family of G protein coupled receptors, mediating effects primarily through second messengers. Astrocytes expresses mainly mGlur receptors subtypes 2, 3, and 5: mGlur 5 is coupled to phosphoinositide (PI) hydrolysis and can increase intracellular calcium, whereas mGlur 2 and 3 are negatively coupled to adenylate cyclase to inhibit cAMP formation.

In addition to glutamate actions on these receptors, astrocytes also uptake glutamate through glutamate transport protein-mediated endocytosis and then astrocytes recycle the glutamate back to neurons for further use by synthesis of glutamine (via glutamine synthetase, exclusively in astrocytes) with secondary release for neuronal uptake and repackaging of glutamate. This recycling creates a glutamate–glutamine cycle (**Figure 3**) occurring between neurons and astrocytes (Van den Berg et al., 1969; Balazs et al., 1970; Van den Berg and Garfinkel, 1971; Norenberg and Martinez-Hernandez, 1979). The vesicular uptake of glutamate requires glutamate transport protein and vacuolar-type H^+-ATPase, which couples ATP hydrolysis and glutamate transport. (Naito and Ueda, 1983; Ozkan and Ueda, 1998) and which also make the interior of the vesicle acidic. Glutamine uptake into neurons increases during hypoglycemia since glutamine can also be oxidized for energy production in low glucose conditions (Amaral et al., 2011).

Most of the glutamate taken up by the astrocytes is eventually converted to glutamine for extrusion and recycling back to neurons, via glutamine synthase. However, oxidation of glutamate can be increased up to 45% when the extracellular glutamate concentration increases beyond 100 μM (McKenna et al., 1996a,b). Exposure of cultured astrocytes to glutamate in glucose can also stimulate oxidative phosphorylation, reducing glucose utilization (Qu et al., 2001; Dienel and Cruz, 2006). Oxidation of glutamate provides more ATP than that generated from lactate, and spares the need for glucose utilization. Oxidation of glutamate in the cell can also generate pyruvate and lactate (Moreadith and Lehninger, 1984). Under steady state basal metabolism the levels of TCA derived intermediates are stable but the rate of degradation increases with neuronal activation (Gruetter et al., 2001; Sibson et al., 2001). During activation oxidation of TCA cycle derived amino acids, such as glutamate, GABA, and aspartate can provide a significant energy source. Glutamate may also be recycled in the form of lactate and alanine or other TCA cycle intermediates (Dringen et al., 1993; Westergaard et al., 1995). These intermediates may be important since neurons lack the capacity to synthesize TCA cycle constituents *de novo* due to absence of pyruvate carboxylase (Yu et al., 1983; Shank et al., 1985; Cesar and Hamprecht, 1995).

Ca^{2+} HOMEOSTASIS

The extracellular concentration of Ca^{2+} is typically ∼1.2 mM, compared to the intracellular concentration of 100 nM (Somjen, 2002). This large transmembrane gradient of Ca^{2+} can create a high inward flux and incoming Ca^{2+} ions can make a large impact on intracellular Ca^{2+} levels. The reverse transport of calcium across the membrane back into the ECS is maintained by energy dependent extrusion. For example, inward Ca^{2+} flux (**Figure 3**) via voltage sensitive calcium channels (L-type) activated by elevated K^+ stimulates both the Na^+, K^+, Cl^- co-transporter (Su et al., 2000) and also oxidative metabolism (Hertz and Dienel, 2002). These transporters are also regulated by intracellular messengers

such as cAMP, cGMP, Ca^{2+}/calmodulin and also by cell shrinkage or swelling (Jensen et al., 1993; O'Neill, 1999). The degree of calcium influx is dependent on the frequency of stimulation, particularly above 10 Hz. Increased Ca^{2+} influx promote a large number of reactions for metabolic function, particularly modulation of the rate of the TCA cycle for NADH/FAD production and ATP generation through direct influence on the dehydrogenase reactions.

Tight buffering of cytoplasmic Ca^{2+} is maintained by Ca^{2+} extrusion, sequestration with Ca^{2+} binding molecules, and uptake into organelles including endoplasmic reticulum (ER) and mitochondria. Each molecule of Ca^{2+} transported either into endoplasmic reticulum or out of the plasma membrane requires one molecule of ATP, through Ca^{2+} ATPase activity or the Na^{+}/Ca^{2+} exchanger. Influx of Ca^{2+} is important for initiation of long-term neuronal signaling (i.e., long-term potentiation) and also for activation of TCA cycle enzymes and mitochondrial oxidative phosphorylation. Buffering of mitochondrial Ca^{2+} is important to prevent toxic effects exerted by increased ROS generation and loss of signaling efficacy. However, extrusion of Ca^{2+} from mitochondria occurs at time points when Ca^{2+} levels in the cytosol return to baseline and when ATP demand and O_2 consumption are low, through either a mitochondrial Ca^{2+} proton exchanger or the mitochondrial permeability transition pore (MTP). The kinetics of transport for these exchangers is low, which can enhance Ca^{2+} overload in mitochondria. During neuronal activation astrocytes show elevation of intracellular Ca^{2+}, which may be spontaneous or triggered by ATP released extracellularly (Charles et al., 1991). In neurons Ca^{2+} influx occurs at synapses via NMDA receptors and L-type calcium channels (LTCCs). CaV1.2 is a widely expressed LTCC in the brain, localized mainly at dendritic shafts and spines (Hell et al., 1993; Clark et al., 2003; Obermair et al., 2004; Schlick et al., 2010); this LTCC can be internalized through tumor suppressor eIF3e mediated calcium and dynamin-dependent endocytosis (Green et al., 2007; Di Biase et al., 2011).

ATP SIGNALING

Both neurons and astrocytes can release ATP during basal metabolic activity and during neuronal activation. ATP acts as a neurotransmitter by binding to purinergic receptors (Burnstock, 1999; Fields and Stevens, 2000). However, ATP release from astrocytes is likely the main source of extracellular ATP (Butt, 2011) and is mediated by exocytosis (Pangrsic et al., 2007). ATP can also trigger a rise in intracellular calcium within astrocytes, particularly as a delayed Ca^{2+} wave (**Figure 3**). This action is mediated by an elevation in nicotinic acid-adenine dinucleotide phosphate by ATP (Barceló-Torns et al., 2011). Purinergic receptors are either ionotropic (P2X) or metabotropic (P2Y). P2X receptors consists of seven transmembrane subunits (P2 × 1–P2 × 7) involved in fast synaptic transmission (Bardoni et al., 1997). Metabotropic receptors (P2Y1, Y2, Y4, Y6, Y11) are abundant throughout the nervous system (Abbracchio and Burnstock, 1994; Cook et al., 1997) and are coupled with Gq/G11 proteins which activate phospholipase c/inositol triphosphate pathways to increase intracellular Ca^{2+} (Kastritsis et al., 1992). In contrast, P2Y receptors are linked to GI/0 proteins.

Quantal release of ATP from neuronal synaptic terminals has been characterized by the analysis of P2X receptor-mediated evoked and spontaneous miniature excitatory postsynaptic currents (mEPSCs) in hippocampal neurons (Pankratov et al., 2006). P2X mediated mEPSCs are different from glutamate mediated mEPSCs in terms of amplitude and kinetics. It has been speculated that ATP is released either from a separate pool of vesicles (White and MacDonald, 1990) or vesicles associated with acetylcholine, GABA, or glutamate (William, 2003; Pankratov et al., 2006). Astrocytes also release ATP from vesicles containing SNARE complexes; the release of ATP is suppressed in transgenic mice expressing a dominant negative SNARE domain (Pascual et al., 2005). ATP is also a potent vasoconstrictor and astrocytes demonstrate secondary Ca^{2+} waves through highly enriched purinergic receptors (P2Y2 and 4; Butt, 2011). However, ATP as a vasoconstrictor is opposed by adenosine, a metabolite of ATP, which acts as a potent vasodilator; the relative balance of these two metabolites at the astrocytic-vascular interface plays an important role in neurovascular coupling mechanisms (Butt, 2011).

ADENOSINE

Adenosine, a metabolite of ATP, exerts potent vasodilation effects and inhibits neuronal transmission via AD1 receptors (**Figure 3**); this can result in inhibition of glutamate release at presynaptic terminals of Schaffer collaterals in the CA1 hippocampus and reduce the release of glutamate from these fibers (Fowler, 1992; Lupica et al., 1992; Zhu and Krnjevic, 1993; Butt, 2011). Adenosine can also enhance the release of several neurotransmitters, such as acetylcholine, glutamate, and noradrenaline, via AD2 receptors (Sebastiao and Ribeiro, 1996). Extracellular adenosine formation from ATP/ADP/AMP depends upon the activity of ecto-5′-nucleotidase and the overall levels of energy metabolism and ATP levels. Extracellular concentration of adenosine is maintained by specific nucleoside transporters present in both neurons and astrocytes and by its conversion to inosine. For example, insulin-induced hypoglycemia increases extracellular adenosine levels and depresses evoked synaptic potentials (Chapman et al., 1981; Fan et al., 1988).

Addition of alternative substrates, such as lactate, during glucose deprivation can maintain ATP levels and significantly reduce adenosine levels, leading to improved neuronal function (Fowler, 1993). Addition of AD1 receptor antagonists also can extend synaptic activity for a limited period of time in low glucose conditions, suggesting that adenosine levels rise before complete energy failure occurs (Shetty et al., 2012). Adenosine can also block voltage-dependent calcium channels (Phillis and Wu, 1981; Scholz and Miller, 1991; Bennett and Ho, 1992; Mogul et al., 1993) and thereby inhibits presynaptic calcium fluxes. Differential effects of adenosine on calcium channels depends on adenosine receptor subtype activation and has significant implications for neuronal excitability (Mogul et al., 1993). Adenosine also activates presynaptic potassium channels and can attenuate evoked neurotransmitter release by hyperpolarizing the presynaptic membrane during aglycemia (Bachelard et al., 1984; Knopfel et al., 1990).

GLYCOGEN UTILIZATION AND SYNAPTIC ACTIVITY

Though brain utilizes glucose for its energy substrate there is also the capacity to store glucose in the form of glycogen. Although the enzyme for glycogen formation, glycogen synthase, is present in both astrocytes and neurons glycogen storage capability and glycogen degrading enzymes are localized only in astrocytes (Vilchez et al., 2007). However, innate glycogen levels in the brain appear small compared to liver and muscle glycogen content (3–12 μmol glycosyl units/g; Cataldo and Broadwell, 1986; Cruz and Dienel, 2002; Choi and Gruetter, 2003; Suh et al., 2007). In certain conditions glycogen levels can be augmented; for example, between periods of intermittent hypoglycemia glycogen levels can increase above normal levels (termed supercompensation). The ability of brain tissue to accumulate extra glycogen has been also demonstrated in brain slices following supplementation with extra glucose, pyruvate, or lactate (Shetty et al., 2012). Because glycogen is stored only in astrocytes, its utilization by neurons (likely as extruded lactate) reveals highly coordinated energy metabolism interactions between astrocytes and neurons (Suzuki et al., 2011).

Astrocytic stored glycogen can be rapidly converted directly into pyruvate via glycolysis or perhaps glucose (Ghosh et al., 2005). Glycogen storage is advantageous in some ways since no further ATP is required to initiate metabolism, unlike glucose and fatty acids (Hertz et al., 2007). Glycogen-derived lactate is likely released into the ECS (**Figure 3**) and taken up by neurons for energy, particularly in low glucose conditions where glycogenolysis is initiated (Dringen et al., 1993; Pellerin and Magistretti, 1994; Magistretti and Pellerin, 1999; Brown et al., 2004). In contrast, the utilization of glycogen during euglycemic conditions is controversial. Inhibition of glycogen breakdown by 1,4-dideaxy-1, 4-imino-D-arabinitol (DAB; glycogen phosphorylase inhibitor) did not suppress ongoing neuronal activity during euglycemic conditions (Shetty et al., 2012). In contrast, blocking glycogen metabolism *in vivo* with DAB may impair hippocampal memory formation (Suzuki et al., 2011). Glycogen may also be utilized for glutamate and glutamine synthesis (Gibbs et al., 2006, 2007; Sickmann et al., 2009). Glycogen-derived energy is also involved in the uptake of glutamate, since inhibition of glycogen breakdown impairs the uptake of the glutamate analog D-[3H]aspartate irrespective of the presence of glucose in cultured astrocytes (Sickmann et al., 2009). Glycogenolysis can be stimulated directly by low glucose levels, norepinephrine, and vasoactive intestinal peptide (VIP) (Magistretti et al., 1998; Magistretti, 2006).

SUMMARY

Short-term regulation of the metabolic unit occurs through tight regulation of these multiple local factors, acting between neurons, astrocytes and blood vessels, on the time scale of seconds to minutes. Some factors, such as glycogen, can also potentially help prevent substrate starvation over a period of up to an hour. However, during long-term issues such as development and aging there are a number of other cues needed to maintain homeostasis, beyond these factors implicated in short-term regulation of metabolism.

LONG-TERM REGULATION OF CNS ENERGY METABOLISM

Complex neuronal networks regulate long-term energy homeostasis, using a variety of peripheral and brain derived hormones to regulate appetite and body weight. For example, brain function responds to changes in insulin, leptins, orexin, neuropeptide Y, propiomelanocortin, epinephrine, norepinephrine, glucagon, glutamate, and a wide variety of other systemic stimuli and regulatory molecules, some of which can act as growth factors for long-term support of the brain. We discuss a few of these factors relevant to energy homeostasis in the brain.

LEPTIN

Leptin and orexin are involved in long-term weight regulation. Leptin functions to regulate body fat, but leptin receptors are widely expressed throughout the CNS, particularly in hippocampus, cerebellum, brain stem and amygdala (Elmquist et al., 1998; Hakansson et al., 1998; Harvey, 2003), suggesting that leptin may be involved in other roles in CNS function. Leptin can increase memory formation and hippocampal synaptic plasticity through facilitation of Ca^{2+} influx via NMDA receptors (Shanley et al., 2001), functioning by phosphorylation of MAPK, Src, or PI3 Kinase mediated pathways. However, incubation of leptin with brain slices at resting conditions without glutamate failed to increase Ca^{2+} concentrations. Leptin can also inhibit mTOR and can function as an antiepileptogenic hormone. Leptin also activates AMP-activated protein kinase (AMPK) and Silent information regulator proteins (Sirtuins) in neurons and is neuroprotective (Greco et al., 2011). Sirtuins are histone deacetylases and are dependent on nicotinamide adenine dinucleotide (NAD^+) and upregulation of proteins required for energy metabolism and survival (Zhang et al., 2011).

INSULIN

The hormone insulin, which has the ability to activate cell signaling pathways similar to leptin and can function as a neurotrophic factor, facilitates NMDA receptor-mediated responses. Insulin may also decrease Alzheimer pathology by regulating tau phosphorylation and by inhibiting GSK-3 function (Greco et al., 2009, 2011). Neurons can secrete insulin in a calcium-dependent manner when depolarized but this appears to be more of a neurotrophic role rather than associated with energy homeostasis. Insulin can inhibit neuronal activity by activating the Ca^{2+} activated potassium channel via mitogen activated protein kinase dependent process. There are now trials beginning administering intranasal insulin for possible treatment of Alzheimer's disease, since this may be a less invasive method of delivery.

STARVATION AND KETOSIS RESPONSES

During severe fasting or with rigorous exercise circulating blood glucose levels fall, leading to initiation of regulatory responses by the liver, particularly increased glucose synthesis and glycogen degradation (Amiel, 1997). Activation of sympathetic neurons, stimulation of adrenalin, cortisol, and enhanced growth hormone secretion all favor increased blood glucose but through different mechanisms, after a more prolonged period of fasting (i.e., 8–12 h); growth hormone in particular can liberate fat from lipid

stores as ketone bodies, beta-hydroxybutyrate and acetoacetate. Brain can utilize ketone bodies as a alternative energy source during starvation or hypoglycemia. Because of their permeability through the blood brain barrier via monocarboxylate transporters, these compounds do have ready access to the nervous system and are easily metabolized by the brain (Puchowicz et al., 2007). Beta-hydroxybutyrate, the major ketone body in the circulation, can preserve ATP levels in the brain during low glucose conditions and early development. The rate of utilization of beta-hydroxybutyrate is very high during brain development, particularly during postnatal suckling in mammals, but reduced as animals wean from breast milk after P14 in rats (Izumi et al., 1998). Thus, during starvation a long-term series of changes occur in metabolism to adapt to different energy sources, and particularly to utilize internal fat and eventually protein for energy substrates.

ROLE OF SIRTUINS

Sirtuins (Sirt) are a family of nicotinamide adenine nucleotide (NAD) dependent deacetylases, which are implicated in energy metabolism and life span (Michan and Sinclair, 2007; Yu and Auwerx, 2009). Among the known Sirt isoforms (Sirt1–7), Sirt3 has been identified as a stress responsive deacetylase recently shown to have a role in protecting cells under stress conditions (Sundaresan et al., 2008; Kim et al., 2011). Sirt3 was shown to regulate the activity of acetyl-CoA synthetase 2 (AceCS2), an important mitochondrial enzyme involved in generating acetyl-CoA for the TCA cycle. In these studies, Sirt3 knockout resulted in a marked decrease of basal ATP level *in vivo* (Hirschey et al., 2010, 2011b; Shimazu et al., 2010). Overexpression of Sirt1 and the use of the Sirt1 agonist, resveratrol, were neuroprotective against amyloid beta toxicity by reducing microglial NF-kappaB signaling (Chen et al., 2005). Mitochondrial protein acetylation is markedly elevated in Sirt3(−/−) tissues (Ahn et al., 2008; Sundaresan et al., 2008; Huang et al., 2010). NAD-dependent deacetylation regulates energy homeostasis and the absence of the deacetylase leads to a marked reduction in ATP. Complex I activity can be regulated by acetylation and deacetylation, a posttranslational modification, and Sirt3 also deacetylates GDH and AceCS2 (Hallows et al., 2006; Hirschey et al., 2011a). Sirt has been implicated in caloric restriction as a treatment to enhance life span during aging as well (Someya et al., 2010; Hallows et al., 2011; Shetty et al., 2011; Zhang et al., 2011). This is one of several regulatory molecules spanning the gap between nuclear regulation of metabolism and actual metabolic processing.

PATHOLOGICAL CONDITIONS LEADING TO ENERGY CRISES

Inadequate supply of oxygen and glucose to the brain can lead to impaired brain function, and if sustained, to permanent cell loss and damage. The clinical conditions where this occurs are usually termed stroke, which commonly arises from changes in blood vessels, such as thrombosis or embolic reasons. Energy metabolism deficits during ischemia can inhibit Na^+/K^+ ATPase activity and lead to increased ROS generation. Drugs that increase Na^+/K^+ ATPase activity have a positive effect on neuronal energy metabolism during oxidative stress (Simao et al., 2011). During hypoxia, decreased ATP content leads to rapid depression of the evoked synaptic potentials (Lipton and Whittingham, 1979, 1982). The brain can eventually adapt to these energy crises by increasing collateral blood flow and eventually demarcating regions of the brain into areas with partial or intact neuronal function, separating out regions of permanent damage.

CONCLUSION

Energy homeostasis is an ongoing process under baseline conscious conditions, during and after brief periods of neuronal activation with accompanying changes in metabolic demand and supply, and also over long-term periods. There are multiple links between neurons, astrocytes, and blood vessels to maintain homeostasis during a wide range of energy demand and supply conditions in the nervous system. Some of these links can now be directly measured by *in vivo* or *in vitro* imaging techniques, including PET, fMRI, intrinsic fluorescent imaging (such as NADH or FAD), direct imaging of ion fluxes (i.e., Na^+, Ca^{2+}, Cl^-), ECS imaging (with IOS), blood flow and oxygen or nitric oxide tissue measurements, and possibly direct heat emission imaging, taking advantage of the large heat signature released by metabolism.

ACKNOWLEDGMENTS

This work was supported by NIH Grant AG037599 and a VA Merit Review Award.

REFERENCES

Abbracchio, M. P., and Burnstock, G. (1994). Purinoceptors: are there families of P2X and P2Y purinoceptors? *Pharmacol. Ther.* 64, 445–475.

Ahn, B. H., Kim, H. S., Song, S., Lee, I. H., Liu, J., Vassilopoulos, A., Deng, C. X., and Finkel, T. (2008). A role for the mitochondrial deacetylase Sirt3 in regulating energy homeostasis. *Proc. Natl. Acad. Sci. U.S.A.* 105, 14447–14452.

Amaral, A. I., Teixeira, A. P., Sonnewald, U., and Alves, P. M. (2011). Estimation of intracellular fluxes in cerebellar neurons after hypoglycemia: importance of the pyruvate recycling pathway and glutamine oxidation. *J. Neurosci. Res.* 89, 700–710.

Amiel, S. A. (1997). Hypoglycaemia in diabetes mellitus – protecting the brain. *Diabetologia* 40(Suppl. 2), S62–S68.

Anderson, C. M., and Swanson, R. A. (2000). Astrocyte glutamate transport: review of properties, regulation, and physiological functions. *Glia* 32, 1–14.

Attwell, D., Buchan, A. M., Charpak, S., Lauritzen, M., Macvicar, B. A., and Newman, E. A. (2010). Glial and neuronal control of brain blood flow. *Nature* 468, 232–243.

Auger, C., and Attwell, D. (2000). Fast removal of synaptic glutamate by postsynaptic transporters. *Neuron* 28, 547–558.

Bachelard, H. S., Cox, D. W., and Drower, J. (1984). Sensitivity of guinea-pig hippocampal granule cell field potentials to hexoses in vitro: an effect on cell excitability? *J. Physiol.* 352, 91–102.

Bak, L. K., Schousboe, A., Sonnewald, U., and Waagepetersen, H. S. (2006). Glucose is necessary to maintain neurotransmitter homeostasis during synaptic activity in cultured glutamatergic neurons. *J. Cereb. Blood Flow Metab.* 26, 1285–1297.

Bak, L. K., Walls, A. B., Schousboe, A., Ring, A., Sonnewald, U., and Waagepetersen, H. S. (2009). Neuronal glucose but not lactate utilization is positively correlated with NMDA-induced neurotransmission and fluctuations in cytosolic Ca2+ levels. *J. Neurochem.* 109(Suppl. 1), 87–93.

Balazs, R., Machiyama, Y., Hammond, B. J., Julian, T., and Richter, D. (1970). The operation of the gamma-aminobutyrate bypath of the tricarboxylic acid cycle in brain tissue in vitro. *Biochem. J.* 116, 445–461.

Barceló-Torns, M., Lewis, A. M., Gubern, A., Barneda, D., Bloor-Young, D., Picatoste, F., Churchill, G. C., Claro, E., and Masgrau, R. (2011). NAADP mediates ATP-induced Ca2+ signals in astrocytes. *FEBS Lett.* 585, 2300–2306.

Bardoni, R., Goldstein, P. A., Lee, C. J., Gu, J. G., and Macdermott, A. B. (1997). ATP P2X receptors mediate fast synaptic transmission in the dorsal horn of the rat spinal cord. *J. Neurosci.* 17, 5297–5304.

Bennett, M. R., and Ho, S. (1992). Adenosine modulation of potassium currents in preganglionic nerve terminals of avian ciliary ganglia. *Neurosci. Lett.* 137, 41–44.

Benninger, C., Kadis, J., and Prince, D. A. (1980). Extracellular calcium and potassium changes in hippocampal slices. *Brain Res.* 187, 165–182.

Bondareff, W., and Pysh, J. J. (1968). Distribution of the extracellular space during postnatal maturation of rat cerebral cortex. *Anat. Rec.* 160, 773–780.

Bourke, R. S., Kimelberg, H. K., Nelson, L. R., Barron, K. D., Auen, E. L., Popp, A. J., and Waldman, J. B. (1980). Biology of glial swelling in experimental brain edema. *Adv. Neurol.* 28, 99–109.

Brown, A. M., Baltan Tekkok, S., and Ransom, B. R. (2004). Energy transfer from astrocytes to axons: the role of CNS glycogen. *Neurochem. Int.* 45, 529–536.

Buchheim, K., Schuchmann, S., Siegmund, H., Gabriel, H. J., Heinemann, U., and Meierkord, H. (1999). Intrinsic optical signal measurements reveal characteristic features during different forms of spontaneous neuronal hyperactivity associated with ECS shrinkage in vitro. *Eur. J. Neurosci.* 11, 1877–1882.

Burnstock, G. (1999). Current status of purinergic signalling in the nervous system. *Prog. Brain Res.* 120, 3–10.

Butt, A. M. (2011). ATP: a ubiquitous gliotransmitter integrating neuron-glial networks. *Semin. Cell Dev. Biol.* 22, 205–213.

Cataldo, A. M., and Broadwell, R. D. (1986). Cytochemical identification of cerebral glycogen and glucose-6-phosphatase activity under normal and experimental conditions. II. Choroid plexus and ependymal epithelia, endothelia and pericytes. *J. Neurocytol.* 15, 511–524.

Cesar, M., and Hamprecht, B. (1995). Immunocytochemical examination of neural rat and mouse primary cultures using monoclonal antibodies raised against pyruvate carboxylase. *J. Neurochem.* 64, 2312–2318.

Chapman, A. G., Westerberg, E., and Siesjo, B. K. (1981). The metabolism of purine and pyrimidine nucleotides in rat cortex during insulin-induced hypoglycemia and recovery. *J. Neurochem.* 36, 179–189.

Charles, A. C., Merrill, J. E., Dirksen, E. R., and Sanderson, M. J. (1991). Intercellular signaling in glial cells: calcium waves and oscillations in response to mechanical stimulation and glutamate. *Neuron* 6, 983–992.

Chatton, J.-Y., Marquet, P., and Magistretti, P. J. (2000). A quantitative analysis of l-glutamate-regulated Na+ dynamics in mouse cortical astrocytes: implications for cellular bioenergetics. *Eur. J. Neurosci.* 12, 3843–3853.

Chen, J., Zhou, Y., Mueller-Steiner, S., Chen, L. F., Kwon, H., Yi, S., Mucke, L., and Gan, L. (2005). SIRT1 protects against microglia-dependent amyloid-beta toxicity through inhibiting NF-kappaB signaling. *J. Biol. Chem.* 280, 40364–40374.

Chih, C.-P., and Roberts, E. L. Jr. (2003). Energy substrates for neurons during neural activity: a critical review of the astrocyte-neuron lactate shuttle hypothesis. *J. Cereb. Blood Flow Metab.* 23, 1263–1281.

Choi, I. Y., and Gruetter, R. (2003). In vivo 13C NMR assessment of brain glycogen concentration and turnover in the awake rat. *Neurochem. Int.* 43, 317–322.

Ciricillo, S. P., Hill, M. P., Gonzalez, M. F., Smalley, S., Morton, M. T., and Sharp, F. R. (1994). Whisker stimulation metabolically activates thalamus following cortical transplantation but not following cortical ablation. *Neuroscience* 59, 975–992.

Clark, N. C., Nagano, N., Kuenzi, F. M., Jarolimek, W., Huber, I., Walter, D., Wietzorrek, G., Boyce, S., Kullmann, D. M., Striessnig, J., and Seabrook, G. R. (2003). Neurological phenotype and synaptic function in mice lacking the CaV1.3 alpha subunit of neuronal L-type voltage-dependent Ca2+ channels. *Neuroscience* 120, 435–442.

Clarke, D., and Sokoloff, L. (1999). "Circulation and energy metabolism of the brain," in *Basic Neurochemistry: Molecular, Cellular, and Medical Aspects*, 5th Edn, eds G. Siegel, B. Agranoff, R. W. Albers, and P. Molinoff (New York: Raven Press), 645-680.

Connors, B. W., Ransom, B. R., Kunis, D. M., and Gutnick, M. J. (1982). Activity-dependent K+ accumulation in the developing rat optic nerve. *Science* 216, 1341–1343.

Cook, S. P., Vulchanova, L., Hargreaves, K. M., Elde, R., and Mccleskey, E. W. (1997). Distinct ATP receptors on pain-sensing and stretch-sensing neurons. *Nature* 387, 505–508.

Cruz, N. F., and Dienel, G. A. (2002). High glycogen levels in brains of rats with minimal environmental stimuli: implications for metabolic contributions of working astrocytes. *J. Cereb. Blood Flow Metab.* 22, 1476–1489.

Danbolt, N. C. (2001). Glutamate uptake. *Prog. Neurobiol.* 65, 1–105.

Davis, K. D., Kwan, C. L., Crawley, A. P., and Mikulis, D. J. (1998). Functional MRI study of thalamic and cortical activations evoked by cutaneous heat, cold, and tactile stimuli. *J. Neurophysiol.* 80, 1533–1546.

Denton, R. M. (2009). Regulation of mitochondrial dehydrogenases by calcium ions. *Biochim. Biophys. Acta* 1787, 1309–1316.

Di Biase, V., Tuluc, P., Campiglio, M., Obermair, G. J., Heine, M., and Flucher, B. E. (2011). Surface traffic of dendritic CaV1.2 calcium channels in hippocampal neurons. *J. Neurosci.* 31, 13682–13694.

Dienel, G. A., and Cruz, N. F. (2006). Astrocyte activation in working brain: energy supplied by minor substrates. *Neurochem. Int.* 48, 586–595.

Dienel, G. A., and Hertz, L. (2001). Glucose and lactate metabolism during brain activation. *J. Neurosci. Res.* 66, 824–838.

Dietzel, I., Heinemann, U., Hofmeier, G., and Lux, H. D. (1982). Stimulus-induced changes in extracellular Na+ and Cl- concentration in relation to changes in the size of the extracellular space. *Exp. Brain Res.* 46, 73–84.

Dringen, R., Wiesinger, H., and Hamprecht, B. (1993). Uptake of L-lactate by cultured rat brain neurons. *Neurosci. Lett.* 163, 5–7.

Du, F., Zhu, X.-H., Zhang, Y., Friedman, M., Zhang, N., Ugurbil, K., and Chen, W. (2008). Tightly coupled brain activity and cerebral ATP metabolic rate. *Proc. Natl. Acad. Sci. U.S.A.* 105, 6409–6414.

Duchen, M. R. (1992). Ca(2+)-dependent changes in the mitochondrial energetics in single dissociated mouse sensory neurons. *Biochem. J.* 283(Pt 1), 41–50.

Elman, I., Sokoloff, L., Adler, C. M., Weisenfeld, N., and Breier, A. (1999). The effects of pharmacological doses of 2-deoxyglucose on cerebral blood flow in healthy volunteers. *Brain Res.* 815, 243–249.

Elmquist, J. K., Maratos-Flier, E., Saper, C. B., and Flier, J. S. (1998). Unraveling the central nervous system pathways underlying responses to leptin. *Nat. Neurosci.* 1, 445–450.

Fan, P., O'Regan, P. A., and Szerb, J. C. (1988). Effect of low glucose concentration on synaptic transmission in the rat hippocampal slice. *Brain Res. Bull.* 21, 741–747.

Fayuk, D., Aitken, P. G., Somjen, G. G., and Turner, D. A. (2002). Two different mechanisms underlie reversible, intrinsic optical signals in rat hippocampal slices. *J. Neurophysiol.* 87, 1924–1937.

Fields, R. D., and Stevens, B. (2000). ATP: an extracellular signaling molecule between neurons and glia. *Trends Neurosci.* 23, 625–633.

Foster, K. A., Beaver, C. J., and Turner, D. A. (2005). Interaction between tissue oxygen tension and NADH imaging during synaptic stimulation and hypoxia in rat hippocampal slices. *Neuroscience* 132, 645–657.

Fowler, J. C. (1992). Escape from inhibition of synaptic transmission during in vitro hypoxia and hypoglycemia in the hippocampus. *Brain Res.* 573, 169–173.

Fowler, J. C. (1993). Purine release and inhibition of synaptic transmission during hypoxia and hypoglycemia in rat hippocampal slices. *Neurosci. Lett.* 157, 83–86.

Fox, P. T., Mintun, M. A., Reiman, E. M., and Raichle, M. E. (1988). Enhanced detection of focal brain responses using intersubject averaging and change-distribution analysis of subtracted PET images. *J. Cereb. Blood Flow Metab.* 8, 642–653.

Furchgott, R. F., and Zawadzki, J. V. (1980). The obligatory role of endothelial cells in the relaxation of arterial smooth muscle by acetylcholine. *Nature* 288, 373–376.

Galeffi, F., Foster, K. A., Sadgrove, M. P., Beaver, C. J., and Turner, D. A. (2007). Lactate uptake contributes to the NAD(P)H biphasic response and tissue oxygen response during synaptic stimulation in area CA1 of rat hippocampal slices. *J. Neurochem.* 103, 2449–2461.

Galeffi, F., Somjen, G. G., Foster, K. A., and Turner, D. A. (2011). Simultaneous monitoring of tissue PO2 and NADH fluorescence during synaptic stimulation and spreading depression reveals a transient dissociation between oxygen utilization and mitochondrial redox state in rat hippocampal slices. *J. Cereb. Blood Flow Metab.* 31, 626–639.

Ghosh, A., Cheung, Y. Y., Mansfield, B. C., and Chou, J. Y. (2005). Brain contains a functional glucose-6-phosphatase complex capable of endogenous glucose production. *J. Biol. Chem.* 280, 11114–11119.

Gibbs, M. E., Anderson, D. G., and Hertz, L. (2006). Inhibition of

glycogenolysis in astrocytes interrupts memory consolidation in young chickens. *Glia* 54, 214–222.

Gibbs, M. E., Lloyd, H. G., Santa, T., and Hertz, L. (2007). Glycogen is a preferred glutamate precursor during learning in 1-day-old chick: biochemical and behavioral evidence. *J. Neurosci. Res.* 85, 3326–3333.

Gordon, G. R., Choi, H. B., Rungta, R. L., Ellis-Davies, G. C., and Macvicar, B. A. (2008). Brain metabolism dictates the polarity of astrocyte control over arterioles. *Nature* 456, 745–749.

Grafton, S. T., Mazziotta, J. C., Presty, S., Friston, K. J., Frackowiak, R. S., and Phelps, M. E. (1992). Functional anatomy of human procedural learning determined with regional cerebral blood flow and PET. *J. Neurosci.* 12, 2542–2548.

Greco, S. J., Hamzelou, A., Johnston, J. M., Smith, M. A., Ashford, J. W., and Tezapsidis, N. (2011). Leptin boosts cellular metabolism by activating AMPK and the sirtuins to reduce tau phosphorylation and beta-amyloid in neurons. *Biochem. Biophys. Res. Commun.* 414, 170–174.

Greco, S. J., Sarkar, S., Casadesus, G., Zhu, X., Smith, M. A., Ashford, J. W., Johnston, J. M., and Tezapsidis, N. (2009). Leptin inhibits glycogen synthase kinase-3beta to prevent tau phosphorylation in neuronal cells. *Neurosci. Lett.* 455, 191–194.

Green, E. M., Barrett, C. F., Bultynck, G., Shamah, S. M., and Dolmetsch, R. E. (2007). The tumor suppressor eIF3e mediates calcium-dependent internalization of the L-type calcium channel CaV1.2. *Neuron* 55, 615–632.

Gruetter, R., Seaquist, E. R., and Ugurbil, K. (2001). A mathematical model of compartmentalized neurotransmitter metabolism in the human brain. *Am. J. Physiol. Endocrinol. Metab.* 281, E100–E112.

Hakansson, M. L., Brown, H., Ghilardi, N., Skoda, R. C., and Meister, B. (1998). Leptin receptor immunoreactivity in chemically defined target neurons of the hypothalamus. *J. Neurosci.* 18, 559–572.

Hallows, W. C., Lee, S., and Denu, J. M. (2006). Sirtuins deacetylate and activate mammalian acetyl-CoA synthetases. *Proc. Natl. Acad. Sci. U.S.A.* 103, 10230–10235.

Hallows, W. C., Yu, W., Smith, B. C., Devries, M. K., Ellinger, J. J., Someya, S., Shortreed, M. R., Prolla, T., Markley, J. L., Smith, L. M., Zhao, S., Guan, K. L., and Denu, J. M. (2011). Sirt3 promotes the urea cycle and fatty acid oxidation during dietary restriction. *Mol. Cell* 41, 139–149.

Harvey, J. (2003). Novel actions of leptin in the hippocampus. *Ann. Med.* 35, 197–206.

Hell, J. W., Westenbroek, R. E., Warner, C., Ahlijanian, M. K., Prystay, W., Gilbert, M. M., Snutch, T. P., and Catterall, W. A. (1993). Identification and differential subcellular localization of the neuronal class C and class D L-type calcium channel alpha 1 subunits. *J. Cell Biol.* 123, 949–962.

Hertz, L., and Dienel, G. A. (2002). Energy metabolism in the brain. *Int. Rev. Neurobiol.* 51, 1–102.

Hertz, L., Peng, L., and Dienel, G. A. (2007). Energy metabolism in astrocytes: high rate of oxidative metabolism and spatiotemporal dependence on glycolysis/glycogenolysis. *J. Cereb. Blood Flow Metab.* 27, 219–249.

Hirschey, M. D., Shimazu, T., Capra, J. A., Pollard, K. S., and Verdin, E. (2011a). SIRT1 and SIRT3 deacetylate homologous substrates: AceCS1,2 and HMGCS1,2. *Aging (Albany NY)* 3, 635–642.

Hirschey, M. D., Shimazu, T., Huang, J. Y., Schwer, B., and Verdin, E. (2011b). SIRT3 regulates mitochondrial protein acetylation and intermediary metabolism. *Cold Spring Harb. Symp. Quant. Biol.* doi: 10.1101/sqb.2011.76.010850. [Epub ahead of print].

Hirschey, M. D., Shimazu, T., Goetzman, E., Jing, E., Schwer, B., Lombard, D. B., Grueter, C. A., Harris, C., Biddinger, S., Ilkayeva, O. R., Stevens, R. D., Li, Y., Saha, A. K., Ruderman, N. B., Bain, J. R., Newgard, C. B., Farese, R. V. Jr., Alt, F. W., Kahn, C. R., and Verdin, E. (2010). SIRT3 regulates mitochondrial fatty-acid oxidation by reversible enzyme deacetylation. *Nature* 464, 121–125.

Hochwald, G. M., Nakamura, S., and Camins, M. B. (1981). The rat in experimental obstructive hydrocephalus. *Z. Kinderchir.* 34, 403–410.

Hoge, R. D., Atkinson, J., Gill, B., Crelier, G. R., Marrett, S., and Pike, G. B. (1999). Stimulus-dependent BOLD and perfusion dynamics in human V1. *Neuroimage* 9, 573–585.

Holmgren, C. D., Mukhtarov, M., Malkov, A. E., Popova, I. Y., Bregestovski, P., and Zilberter, Y. (2010). Energy substrate availability as a determinant of neuronal resting potential, GABA signaling and spontaneous network activity in the neonatal cortex in vitro. *J. Neurochem.* 112, 900–912.

Hu, Y., and Wilson, G. S. (1997a). Rapid changes in local extracellular rat brain glucose observed with an in vivo glucose sensor. *J. Neurochem.* 68, 1745–1752.

Hu, Y., and Wilson, G. S. (1997b). A temporary local energy pool coupled to neuronal activity: fluctuations of extracellular lactate levels in rat brain monitored with rapid-response enzyme-based sensor. *J. Neurochem.* 69, 1484–1490.

Huang, J. Y., Hirschey, M. D., Shimazu, T., Ho, L., and Verdin, E. (2010). Mitochondrial sirtuins. *Biochim. Biophys. Acta* 1804, 1645–1651.

Hyder, F., Kida, I., Behar, K. L., Kennan, R. P., Maciejewski, P. K., and Rothman, D. L. (2001). Quantitative functional imaging of the brain: towards mapping neuronal activity by BOLD fMRI. *NMR. Biomed.* 14, 413–431.

Iadecola, C., and Nedergaard, M. (2007). Glial regulation of the cerebral microvasculature. *Nat. Neurosci.* 10, 1369–1376.

Ido, Y., Chang, K., and Williamson, J. R. (2004). NADH augments blood flow in physiologically activated retina and visual cortex. *Proc. Natl. Acad. Sci. U.S.A.* 101, 653–658.

Ivanov, A., Mukhtarov, M., Bregestovski, P., and Zilberter, Y. (2011). Lactate effectively covers energy demands during neuronal network activity in neonatal hippocampal slices. *Front Neuroenergetics* 3:2. doi:10.3389/fnene.2011.00002

Ivanov, A., and Zilberter, Y. (2011). Critical state of energy metabolism in brain slices: the principal role of oxygen delivery and energy substrates in shaping neuronal activity. *Front Neuroenergetics* 3:9. doi:10.3389/fnene.2011.00009

Izumi, Y., Ishii, K., Katsuki, H., Benz, A. M., and Zorumski, C. F. (1998). beta-Hydroxybutyrate fuels synaptic function during development. Histological and physiological evidence in rat hippocampal slices. *J. Clin. Invest.* 101, 1121–1132.

Jensen, B. S., Jessen, F., and Hoffmann, E. K. (1993). Na+, K+, Cl- cotransport and its regulation in Ehrlich ascites tumor cells. Ca2+/calmodulin and protein kinase C dependent pathways. *J. Membr. Biol.* 131, 161–178.

Kapogiannis, D., and Mattson, M. P. (2011). Disrupted energy metabolism and neuronal circuit dysfunction in cognitive impairment and Alzheimer's disease. *Lancet Neurol.* 10, 187–198.

Kastritsis, C. H., Salm, A. K., and Mccarthy, K. (1992). Stimulation of the P2Y purinergic receptor on type 1 astroglia results in inositol phosphate formation and calcium mobilization. *J. Neurochem.* 58, 1277–1284.

Keelan, J., Vergun, O., and Duchen, M. R. (1999). Excitotoxic mitochondrial depolarisation requires both calcium and nitric oxide in rat hippocampal neurons. *J. Physiol. (Lond.)* 520(Pt 3), 797–813.

Kim, S. H., Lu, H. F., and Alano, C. C. (2011). Neuronal Sirt3 protects against excitotoxic injury in mouse cortical neuron culture. *PLoS ONE* 6, e14731. doi:10.1371/journal.pone.0014731

Knopfel, T., Spuler, A., Grafe, P., and Gahwiler, B. H. (1990). Cytosolic calcium during glucose deprivation in hippocampal pyramidal cells of rats. *Neurosci. Lett.* 117, 295–299.

Koehler, R. C., Roman, R. J., and Harder, D. R. (2009). Astrocytes and the regulation of cerebral blood flow. *Trends Neurosci.* 32, 160–169.

Korf, J. (2006). Is brain lactate metabolized immediately after neuronal activity through the oxidative pathway? *J. Cereb. Blood Flow Metab.* 26, 1584–1586.

Kovacs, R., Schuchmann, S., Gabriel, S., Kardos, J., and Heinemann, U. (2001). Ca2+ signalling and changes of mitochondrial function during low-Mg2+-induced epileptiform activity in organotypic hippocampal slice cultures. *Eur. J. Neurosci.* 13, 1311–1319.

LaManna, J. C., Mccracken, K. A., Patil, M., and Prohaska, O. J. (1989). Stimulus-activated changes in brain tissue temperature in the anesthetized rat. *Metab. Brain Dis.* 4, 225–237.

LaManna, J. C., Rosenthal, M., Novack, R., Moffett, D. F., and Jobsis, F. F. (1980). Temperature coefficients for the oxidative metabolic responses to electrical stimulation in cerebral cortex. *J. Neurochem.* 34, 203–209.

Lipton, P., and Whittingham, T. S. (1979). The effect of hypoxia on evoked potentials in the in vitro hippocampus. *J. Physiol. (Lond.)* 287, 427–438.

Lipton, P., and Whittingham, T. S. (1982). Reduced ATP concentration as a basis for synaptic transmission failure during hypoxia in the in vitro guinea-pig hippocampus. *J. Physiol. (Lond.)* 325, 51–65.

Lothman, E., Lamanna, J., Cordingley, G., Rosenthal, M., and Somjen, G. (1975). Responses of electrical potential, potassium levels, and oxidative metabolic activity of the

cerebral neocortex of cats. *Brain Res.* 88, 15–36.

Lupica, C. R., Proctor, W. R., and Dunwiddie, T. V. (1992). Presynaptic inhibition of excitatory synaptic transmission by adenosine in rat hippocampus: analysis of unitary EPSP variance measured by whole-cell recording. *J. Neurosci.* 12, 3753–3764.

Magistretti, P. J. (2006). Neuron-glia metabolic coupling and plasticity. *J. Exp. Biol.* 209, 2304–2311.

Magistretti, P. J., Cardinaux, J. R., and Martin, J. L. (1998). VIP and PACAP in the CNS: regulators of glial energy metabolism and modulators of glutamatergic signaling. *Ann. N. Y. Acad. Sci.* 865, 213–225.

Magistretti, P. J., and Pellerin, L. (1999). Cellular mechanisms of brain energy metabolism and their relevance to functional brain imaging. *Philos. Trans. R. Soc. Lond. B Biol. Sci.* 354, 1155–1163.

Malarkey, E. B., and Parpura, V. (2008). Mechanisms of glutamate release from astrocytes. *Neurochem. Int.* 52, 142–154.

McKenna, M. C., Sonnewald, U., Huang, X., Stevenson, J., and Zielke, H. R. (1996a). Exogenous glutamate concentration regulates the metabolic fate of glutamate in astrocytes. *J. Neurochem.* 66, 386–393.

McKenna, M. C., Tildon, J. T., Stevenson, J. H., and Huang, X. (1996b). New insights into the compartmentation of glutamate and glutamine in cultured rat brain astrocytes. *Dev. Neurosci.* 18, 380–390.

Michan, S., and Sinclair, D. (2007). Sirtuins in mammals: insights into their biological function. *Biochem. J.* 404, 1–13.

Mogul, D. J., Adams, M. E., and Fox, A. P. (1993). Differential activation of adenosine receptors decreases N-type but potentiates P-type Ca2+ current in hippocampal CA3 neurons. *Neuron* 10, 327–334.

Moreadith, R. W., and Lehninger, A. L. (1984). The pathways of glutamate and glutamine oxidation by tumor cell mitochondria. Role of mitochondrial NAD(P)+-dependent malic enzyme. *J. Biol. Chem.* 259, 6215–6221.

Mukhtarov, M., Ivanov, A., Zilberter, Y., and Bregestovski, P. (2011). Inhibition of spontaneous network activity in neonatal hippocampal slices by energy substrates is not correlated with intracellular acidification. *J. Neurochem.* 116, 316–321.

Naito, S., and Ueda, T. (1983). Adenosine triphosphate-dependent uptake of glutamate into protein I-associated synaptic vesicles. *J. Biol. Chem.* 258, 696–699.

Nelson, M. T., and Quayle, J. M. (1995). Physiological roles and properties of potassium channels in arterial smooth muscle. *Am. J. Physiol.* 268, C799–C822.

Norenberg, M. D., and Martinez-Hernandez, A. (1979). Fine structural localization of glutamine synthetase in astrocytes of rat brain. *Brain Res.* 161, 303–310.

Obermair, G. J., Szabo, Z., Bourinet, E., and Flucher, B. E. (2004). Differential targeting of the L-type Ca2+ channel alpha 1C (CaV1.2) to synaptic and extrasynaptic compartments in hippocampal neurons. *Eur. J. Neurosci.* 19, 2109–2122.

Offenhauser, N., Thomsen, K., Caesar, K., and Lauritzen, M. (2005). Activity-induced tissue oxygenation changes in rat cerebellar cortex: interplay of postsynaptic activation and blood flow. *J. Physiol.* 565, 279–294.

O'Neill, W. C. (1999). Physiological significance of volume-regulatory transporters. *Am. J. Physiol.* 276, C995–C1011.

Ozkan, E. D., and Ueda, T. (1998). Glutamate transport and storage in synaptic vesicles. *Jpn. J. Pharmacol.* 77, 1–10.

Pangrsic, T., Potokar, M., Stenovec, M., Kreft, M., Fabbretti, E., Nistri, A., Pryazhnikov, E., Khiroug, L., Giniatullin, R., and Zorec, R. (2007). Exocytotic release of ATP from cultured astrocytes. *J. Biol. Chem.* 282, 28749–28758.

Pankratov, Y., Lalo, U., Verkhratsky, A., and North, R. (2006). Vesicular release of ATP at central synapses. *Pflügers Arch.* 452, 589–597.

Parpura, V., Basarsky, T. A., Liu, F., Jeftinija, K., Jeftinija, S., and Haydon, P. G. (1994). Glutamate-mediated astrocyte-neuron signalling. *Nature* 369, 744–747.

Pascual, O., Casper, K. B., Kubera, C., Zhang, J., Revilla-Sanchez, R., Sul, J.-Y., Takano, H., Moss, S. J., Mccarthy, K., and Haydon, P. G. (2005). Astrocytic purinergic signaling coordinates synaptic networks. *Science* 310, 113–116.

Paulson, O. B., Hasselbalch, S. G., Rostrup, E., Knudsen, G. M., and Pelligrino, D. (2009). Cerebral blood flow response to functional activation. *J. Cereb. Blood Flow Metab.* 30, 2–14.

Pellerin, L., Bouzier-Sore, A. K., Aubert, A., Serres, S., Merle, M., Costalat, R., and Magistretti, P. J. (2007). Activity-dependent regulation of energy metabolism by astrocytes: an update. *Glia* 55, 1251–1262.

Pellerin, L., and Magistretti, P. J. (1994). Glutamate uptake into astrocytes stimulates aerobic glycolysis: a mechanism coupling neuronal activity to glucose utilization. *Proc. Natl. Acad. Sci. U.S.A.* 91, 10625–10629.

Pellerin, L., and Magistretti, P. J. (1996). Excitatory amino acids stimulate aerobic glycolysis in astrocytes via an activation of the Na+/K+ ATPase. *Dev. Neurosci.* 18, 336–342.

Pellerin, L., and Magistretti, P. J. (1997). Glutamate uptake stimulates Na+, K+ -ATPase activity in astrocytes via activation of a distinct subunit highly sensitive to ouabain. *J. Neurochem.* 69, 2132–2137.

Phelps, M. E., and Mazziotta, J. C. (1985). Positron emission tomography: human brain function and biochemistry. *Science* 228, 799–809.

Phillis, J. W., and Wu, P. H. (1981). The role of adenosine and its nucleotides in central synaptic transmission. *Prog. Neurobiol.* 16, 187–239.

Puchowicz, M. A., Xu, K., Sun, X., Ivy, A., Emancipator, D., and Lamanna, J. C. (2007). Diet-induced ketosis increases capillary density without altered blood flow in rat brain. *Am. J. Physiol. Endocrinol. Metab.* 292, E1607–E1615.

Qu, H., Eloqayli, H., Unsgard, G., and Sonnewald, U. (2001). Glutamate decreases pyruvate carboxylase activity and spares glucose as energy substrate in cultured cerebellar astrocytes. *J. Neurosci. Res.* 66, 1127–1132.

Ransom, B. R., Yamate, C. L., and Connors, B. W. (1985). Activity-dependent shrinkage of extracellular space in rat optic nerve: a developmental study. *J. Neurosci.* 5, 532–535.

Rheims, S., Holmgren, C. D., Chazal, G., Mulder, J., Harkany, T., Zilberter, T., and Zilberter, Y. (2009). GABA action in immature neocortical neurons directly depends on the availability of ketone bodies. *J. Neurochem.* 110, 1330–1338.

Rosenthal, M., and Jobsis, F. F. (1971). Intracellular redox changes in functioning cerebral cortex. II. Effects of direct cortical stimulation. *J. Neurophysiol.* 34, 750–762.

Rothman, D. L., Behar, K. L., Hyder, F., and Shulman, R. G. (2003). In vivo NMR studies of the glutamate neurotransmitter flux and neuroenergetics: implications for brain function. *Annu. Rev. Physiol.* 65, 401–427.

Schlick, B., Flucher, B. E., and Obermair, G. J. (2010). Voltage-activated calcium channel expression profiles in mouse brain and cultured hippocampal neurons. *Neuroscience* 167, 786–798.

Scholz, K. P., and Miller, R. J. (1991). Analysis of adenosine actions on Ca2+ currents and synaptic transmission in cultured rat hippocampal pyramidal neurones. *J. Physiol.* 435, 373–393.

Schuchmann, S., Kovacs, R., Kann, O., Heinemann, U., and Buchheim, K. (2001). Monitoring NAD(P)H autofluorescence to assess mitochondrial metabolic functions in rat hippocampal-entorhinal cortex slices. *Brain Res. Brain Res. Protoc.* 7, 267–276.

Sebastiao, A. M., and Ribeiro, J. A. (1996). Adenosine A2 receptor-mediated excitatory actions on the nervous system. *Prog. Neurobiol.* 48, 167–189.

Shank, R. P., Bennett, G. S., Freytag, S. O., and Campbell, G. L. (1985). Pyruvate carboxylase: an astrocyte-specific enzyme implicated in the replenishment of amino acid neurotransmitter pools. *Brain Res.* 329, 364–367.

Shanley, L. J., Irving, A. J., and Harvey, J. (2001). Leptin enhances NMDA receptor function and modulates hippocampal synaptic plasticity. *J. Neurosci.* 21, RC186.

Shetty, P. K., Galeffi, F., and Turner, D. A. (2011). Age-induced alterations in hippocampal function and metabolism. *Aging Dis.* 2, 196–218.

Shetty, P. K., Sadgrove, M. P., Galeffi, F., and Turner, D. A. (2012). Pyruvate incubation enhances glycogen stores and sustains neuronal function during subsequent glucose deprivation. *Neurobiol. Dis.* 45, 177–187.

Shimazu, T., Hirschey, M. D., Hua, L., Dittenhafer-Reed, K. E., Schwer, B., Lombard, D. B., Li, Y., Bunkenborg, J., Alt, F. W., Denu, J. M., Jacobson, M. P., and Verdin, E. (2010). SIRT3 deacetylates mitochondrial 3-hydroxy-3-methylglutaryl CoA synthase 2 and regulates ketone body production. *Cell Metab.* 12, 654–661.

Shulman, R. G., Hyder, F., and Rothman, D. L. (2009). Baseline brain energy supports the state of consciousness. *Proc. Natl. Acad. Sci. U.S.A.* 106, 11096–11101.

Shulman, R. G., Rothman, D. L., Behar, K. L., and Hyder, F. (2004). Energetic basis of brain activity: implications for neuroimaging. *Trends Neurosci.* 27, 489–495.

Shuttleworth, C. W., Brennan, A. M., and Connor, J. A. (2003). NAD(P)H

fluorescence imaging of postsynaptic neuronal activation in murine hippocampal slices. *J. Neurosci.* 23, 3196–3208.

Sibson, N. R., Mason, G. F., Shen, J., Cline, G. W., Herskovits, A. Z., Wall, J. E., Behar, K. L., Rothman, D. L., and Shulman, R. G. (2001). In vivo (13)C NMR measurement of neurotransmitter glutamate cycling, anaplerosis and TCA cycle flux in rat brain during. *J. Neurochem.* 76, 975–989.

Sickmann, H. M., Walls, A. B., Schousboe, A., Bouman, S. D., and Waagepetersen, H. S. (2009). Functional significance of brain glycogen in sustaining glutamatergic neurotransmission. *J. Neurochem.* 109(Suppl. 1), 80–86.

Simao, F., Matte, A., Matte, C., Soares, F. M., Wyse, A. T., Netto, C. A., and Salbego, C. G. (2011). Resveratrol prevents oxidative stress and inhibition of Na(+)K(+)-ATPase activity induced by transient global cerebral ischemia in rats. *J. Nutr. Biochem.* 22, 921–928.

Skou, J. C., and Esmann, M. (1992). The Na, K-ATPase. *J. Bioenerg. Biomembr.* 24, 249–261.

Smith, A. J., Blumenfeld, H., Behar, K. L., Rothman, D. L., Shulman, R. G., and Hyder, F. (2002). Cerebral energetics and spiking frequency: the neurophysiological basis of fMRI. *Proc. Natl. Acad. Sci. U.S.A.* 99, 10765–10770.

Sobey, C. G., Heistad, D. D., and Faraci, F. M. (1997). Mechanisms of bradykinin-induced cerebral vasodilatation in rats. Evidence that reactive oxygen species activate K+ channels. *Stroke* 28, 2290–2294; discussion 2295.

Sokoloff, L. (1999). Energetics of functional activation in neural tissues. *Neurochem. Res.* 24, 321–329.

Someya, S., Yu, W., Hallows, W. C., Xu, J., Vann, J. M., Leeuwenburgh, C., Tanokura, M., Denu, J. M., and Prolla, T. A. (2010). Sirt3 mediates reduction of oxidative damage and prevention of age-related hearing loss under caloric restriction. *Cell* 143, 802–812.

Somjen, G. G. (2002). Ion regulation in the brain: implications for pathophysiology. *Neuroscientist* 8, 254–267.

Su, G., Haworth, R. A., Dempsey, R. J., and Sun, D. (2000). Regulation of Na(+)-K(+)-Cl(-) cotransporter in primary astrocytes by dibutyryl cAMP and high [K(+)](o). *Am. J. Physiol. Cell Physiol.* 279, C1710–C1721.

Suh, S. W., Hamby, A. M., and Swanson, R. A. (2007). Hypoglycemia, brain energetics, and hypoglycemic neuronal death. *Glia* 55, 1280–1286.

Sukstanskii, A. L., and Yablonskiy, D. A. (2006). Theoretical model of temperature regulation in the brain during changes in functional activity. *Proc. Natl. Acad. Sci. U.S.A.* 103, 12144–12149.

Sundaresan, N. R., Samant, S. A., Pillai, V. B., Rajamohan, S. B., and Gupta, M. P. (2008). SIRT3 is a stress-responsive deacetylase in cardiomyocytes that protects cells from stress-mediated cell death by deacetylation of Ku70. *Mol. Cell. Biol.* 28, 6384–6401.

Suzuki, A., Stern, S. A., Bozdagi, O., Huntley, G. W., Walker, R. H., Magistretti, P. J., and Alberini, C. M. (2011). Astrocyte-neuron lactate transport is required for long-term memory formation. *Cell* 144, 810–823.

Thompson, J. K., Peterson, M. R., and Freeman, R. D. (2003). Single-neuron activity and tissue oxygenation in the cerebral cortex. *Science* 299, 1070–1072.

Trubel, H. K. F., Sacolick, L. I., and Hyder, F. (2005). Regional temperature changes in the brain during somatosensory stimulation. *J. Cereb. Blood Flow Metab.* 26, 68–78.

Turner, D. A., Foster, K. A., Galeffi, F., and Somjen, G. G. (2007). Differences in O2 availability resolve the apparent discrepancies in metabolic intrinsic optical signals in vivo and in vitro. *Trends Neurosci.* 30, 390–398.

Van den Berg, C. J., and Garfinkel, D. (1971). A stimulation study of brain compartments. Metabolism of glutamate and related substances in mouse brain. *Biochem. J.* 123, 211–218.

Van den Berg, C. J., Krzalic, L., Mela, P., and Waelsch, H. (1969). Compartmentation of glutamate metabolism in brain. Evidence for the existence of two different tricarboxylic acid cycles in brain. *Biochem. J.* 113, 281–290.

Van Harreveld, A., Khattab, F. I., and Steiner, J. (1969). Extracellular space in the central nervous system of the leech, *Mooreobdella fervida*. *J. Neurobiol.* 1, 23–40.

Vilchez, D., Ros, S., Cifuentes, D., Pujadas, L., Valles, J., Garcia-Fojeda, B., Criado-Garcia, O., Fernandez-Sanchez, E., Medrano-Fernandez, I., Dominguez, J., Garcia-Rocha, M., Soriano, E., Rodriguez de Cordoba, S., and Guinovart, J. J. (2007). Mechanism suppressing glycogen synthesis in neurons and its demise in progressive myoclonus epilepsy. *Nat. Neurosci.* 10, 1407–1413.

Voutsinos-Porche, B., Bonvento, G., Tanaka, K., Steiner, P., Welker, E., Chatton, J. Y., Magistretti, P. J., and Pellerin, L. (2003). Glial glutamate transporters mediate a functional metabolic crosstalk between neurons and astrocytes in the mouse developing cortex. *Neuron* 37, 275–286.

Walz, W., and Hertz, L. (1982). Ouabain-sensitive and ouabain-resistant net uptake of potassium into astrocytes and neurons in primary cultures. *J. Neurochem.* 39, 70–77.

Westergaard, N., Sonnewald, U., and Schousboe, A. (1995). Metabolic trafficking between neurons and astrocytes: the glutamate/glutamine cycle revisited. *Dev. Neurosci.* 17, 203–211.

White, T. D., and MacDonald, W. F. (1990). Neural release of ATP and adenosinea. *Ann. N. Y. Acad. Sci.* 603, 287–298.

William, V. D. K. (2003). Loading and recycling of synaptic vesicles in the Torpedo electric organ and the vertebrate neuromuscular junction. *Prog. Neurobiol.* 71, 269–303.

Wyss, M. T., Jolivet, R., Buck, A., Magistretti, P. J., and Weber, B. (2011). In vivo evidence for lactate as a neuronal energy source. *J. Neurosci.* 31, 7477–7485.

Yablonskiy, D. A., Ackerman, J. J., and Raichle, M. E. (2000). Coupling between changes in human brain temperature and oxidative metabolism during prolonged visual stimulation. *Proc. Natl. Acad. Sci. U.S.A.* 97, 7603–7608.

Yu, A. C., Drejer, J., Hertz, L., and Schousboe, A. (1983). Pyruvate carboxylase activity in primary cultures of astrocytes and neurons. *J. Neurochem.* 41, 1484–1487.

Yu, J., and Auwerx, J. (2009). The role of sirtuins in the control of metabolic homeostasis. *Ann. N. Y. Acad. Sci.* 1173(Suppl. 1), E10–E19.

Zhang, D., Liu, Y., and Chen, D. (2011). SIRT-ain relief from age-inducing stress. *Aging (Albany NY)* 3, 158–161.

Zhu, P. J., and Krnjevic, K. (1993). Adenosine release is a major cause of failure of synaptic transmission during hypoglycemia in rat hippocampal slices. *Neurosci. Lett.* 155, 128–131.

Zielke, H. R., Zielke, C. L., Baab, P. J., and Tildon, J. T. (2007). Effect of fluorocitrate on cerebral oxidation of lactate and glucose in freely moving rats. *J. Neurochem.* 101, 9–16.

Zilberter, Y., Zilberter, T., and Bregestovski, P. (2010). Neuronal activity in vitro and the in vivo reality: the role of energy homeostasis. *Trends Pharmacol. Sci.* 31, 394–401.

Conflict of Interest Statement: The authors declare that the research was conducted in the absence of any commercial or financial relationships that could be construed as a potential conflict of interest.

Received: 21 December 2011; accepted: 24 February 2012; published online: 20 March 2012.

Citation: Shetty PK, Galeffi F and Turner DA (2012) Cellular links between neuronal activity and energy homeostasis. Front. Pharmacol. ***3****:43. doi: 10.3389/fphar.2012.00043*

This article was submitted to Frontiers in Neuropharmacology, a specialty of Frontiers in Pharmacology.

frontiers in
PHARMACOLOGY

ORIGINAL RESEARCH ARTICLE
published: 15 June 2012
doi: 10.3389/fphar.2012.00105

Deciphering the neuronal circuitry controlling local blood flow in the cerebral cortex with optogenetics in PV::Cre transgenic mice

Alan Urban*, Armelle Rancillac, Lucie Martinez and Jean Rossier*

Laboratoire de Neurobiologie, Equipe Optogenetics and Brain Imaging, CNRS UMR 7637, Ecole Supérieure de Physique et de Chimie Industrielles ParisTech, PARIS, France

Edited by:
Yuri Zilberter, Institut National de la Santé et de la Recherche Médicale, France

Reviewed by:
Enrico Sanna, University of Cagliari, Italy
Piotr Bregestovski, Institut de Neurobiologie de la Méditerranée Marseille, France

****Correspondence:***
Alan Urban and Jean Rossier, Laboratoire de Neurobiologie, Optogenetics and Brain Imaging, CNRS UMR 7637, Ecole Supérieure de Physique et de Chimie Industrielles ParisTech, 10 rue Vauquelin, 75005 PARIS, France.
e-mail: alan.urban@espci.fr; jean.rossier@espci.fr

Although it is know since more than a century that neuronal activity is coupled to blood supply regulation, the underlying pathways remains to be identified. In the brain, neuronal activation triggers a local increase of cerebral blood flow (CBF) that is controlled by the neurogliovascular unit composed of terminals of neurons, astrocytes, and blood vessel muscles. It is generally accepted that the regulation of the neurogliovascular unit is adjusted to local metabolic demand by local circuits. Today experimental data led us to realize that the regulatory mechanisms are more complex and that a neuronal system within the brain is devoted to the control of local brain-blood flow. Recent optogenetic experiments combined with functional magnetic resonance imaging have revealed that light stimulation of neurons expressing the calcium binding protein parvalbumin (PV) is associated with positive blood oxygen level-dependent (BOLD) signal in the corresponding barrel field but also with negative BOLD in the surrounding deeper area. Here, we demonstrate that in acute brain slices, channelrhodopsin-2 (ChR2) based photostimulation of PV containing neurons gives rise to an effective contraction of penetrating arterioles. These results support the neurogenic hypothesis of a complex distributed nervous system controlling the CBF.

Keywords: neurovascular coupling, interneurons, optogenetics, parvalbumin, barrel cortex, infrared video microscopy

INTRODUCTION

Although the tight coupling between neuronal activity and local cerebral blood flow (CBF) control is known since a century, little is yet known on the mechanisms involved. For a long time the attention of scientists was focused at the neurogliovascular unit composed of terminals of neurons, astrocytes, and blood vessel muscles. The regulation was triggered by local demand and controlled at the local level. Today we realize that the system is more complex. We have changed paradigm and view this system as a distributed nervous system within the brain specialized in the control of local blood flow (Kleinfeld et al., 2011). The brain activation is followed by a change in tone of smooth muscles that wrap around arterioles and thus control the amount of blood flowing in a particular capillary bed. A single stimulus, such as stimulation of the whisker pad in rodents, will be associated with local increase in the corresponding barrel field and decrease in the surrounding deeper area and in the opposite barrel field (Alonso Bde et al., 2008; Boorman et al., 2010). Moreover, this complex response is clearly dependent of the brain state (Martin et al., 2006) and not restricted to the homotypic barrel field but extended to other brain area (Wiest et al., 2005).

The hypothesis that a specified neuronal circuit is involved in the regulation of local blood was emphasized by recent *in vivo* studies using optogenetics (Lee et al., 2010; Desai et al., 2011; Kahn et al., 2011). In the last few years, optogenetic has become the method of choice to trace functional neurocircuit in the brain (Urban and Rossier, 2012). One of the many advantages that optogenetic has over others methods like electrical stimulation is the minimally invasive and precise spatiotemporal activation/silencing of specific cell types (Chow et al., 2010; Zhang et al., 2010). In their recent paper, Lee et al. (2010) have used optogenetic to investigate the blood oxygen level-dependent (BOLD) response after light stimulation of different areas in adult rat brain. In their experiments, pyramidal cells of the primary motor cortex (M1) were specifically labeled after injection of an adeno-associated viral vector (AAV) AAV5-CaMKIIα::ChR2 (H134R)-EYFP in this area. In this construct, the channelrhodopsin-2 (ChR2) is expressed under the control of the promoter derived from alpha Ca^{2+}/calmodulin-dependent protein kinase II (CaMKIIα) particularly active in pyramids but not in GABAergic or glial cells. After validation of the correct specificity, sensitivity, and spatial distribution of the chimera channelrhodopsin-2 with enhanced yellow fluorescent protein (ChR2-EYFP) by using both

Abbreviations: AAV, adeno-associated viral vector; BOLD, blood oxygen level-dependent signal; CaMKIIα, Ca^{2+}/calmodulin-dependent protein kinase II alpha subunit; CBF, cerebral blood flow; ChETA, engineered E123T Accelerated variant of ChR2; ChR2, channelrhodopsin-2; ChR2-EYFP, channelrhodopsin-2 with enhanced yellow fluorescent protein; DIO, double inverted open reading frame; FLEX, flip-excision switch; fMRI, functional magnetic resonance imaging; FS-PV, fast-spiking parvalbumin; M1, motor cortical area; ofMRI (optofMRI), method combining optogenetic with fMRI; PV, parvalbumin; PV::Cre, transgenic mouse expressing Cre recombinase under the control of the parvalbumin promoter.

immunochemistry and fluorescence microscopy, they proceed to 20 Hz blue laser stimulation (473 nm, 15 ms pulse width, 85 mW mm^{-2}) of transfected pyramids through an implanted optrode. Lee and colleagues performed experiments combining optogenetic with functional magnetic resonance imaging (ofMRI) in an anesthetized animal (7.0 T, gradient echo planar imaging, 0.5 mm × 0.5 mm × 0.5 mm, 3 s repetition time). They observed that light stimulation of transfected pyramids resulted in positive BOLD signals in the infected motor cortical area (M1) and in the non-illuminated thalamus. Comparable of MRI results were also observed after activation of pyramidal cells expressing ChR2 in S1 barrel cortex with significantly increased BOLD response in awake as compared to anesthetized mice (Desai et al., 2011; Kahn et al., 2011).

Lee et al. (2010) also studied the BOLD effect after light stimulation of fast-spiking inhibitory interneurons. To overcome the low level of opsin produced when a PV promoter fragment drives its expression, they devised a new strategy combining transgenic mice expressing Cre recombinase under the control of the PV promoter (PV::Cre; Hippenmeyer et al., 2005) and a Cre-dependant AAV. The specificity of this system called flip-excision switch (FLEX) or double inverted open (DIO) reading frame is very high by the introduction of two pairs of heterotypic and antiparallel loxP/lox2272 recombination sites that prevent transcriptional read-through observed with classic lox-STOP-lox cassette (Atasoy et al., 2008; Sohal et al., 2009). Moreover, this system decouples transcriptional strength from the specificity of the PV promoter, allowing expression of ChR2-EYFP by the strong EF1α promoter. Thus, the expression of the Cre recombinase directly under the control of the endogenous PV locus restricts the expression of ChR2-EYFP to PV-expressing cells (**Figure 1**). Consequently, if neurons are infected by DIO/FLEX ChR2-EYFP rAAV but devoid of Cre recombinase, they cannot process the cassette and will not express any of the genetic tools carried by the viral construct.

When the motor cortex of infected PV::Cre mice was illuminated, complex responses were observed in BOLD and intracortical electrical signals. BOLD of MRI activation map shows positive BOLD in the illuminated area while a negative BOLD was observed in the flanking region. In the same time, extracellular optrode recording revealed a neuronal excitation in superficial cortical layers and inhibition in deeper layers.

This observation of a possible role of PV-expressing cells in the local control of blood flow was puzzling. PV-expressing cells were never proposed to be involved in local blood control. Indeed, they do not contain vasoactive neuropeptides although a subclass of parvalbumin interneurons contains nitric oxide synthase. It is thus possible that stimulation of parvalbumin interneurons could induce vasodilation by release of NO. The unexpected results of Lee et al. (2010) with PV::Cre mice prompted us to further investigate these optogenetic experiments in an *ex vivo* set-up used since many years in the laboratory. Here we report that photostimulation of PV containing neurons gives rise to an effective contraction of penetrating arterioles in brain slices. We observed that PV expression is not restricted to fast-spiking GABAergic interneurons (FS-PV) but is also present in a subclass of glutamatergic pyramidal neurons projecting to the thalamus. We therefore conclude that either FS-PV interneurons or PV-positive pyramids could be implied in vasoconstriction of penetrating arterioles and proposes an efficient optogenetic strategy to address this question.

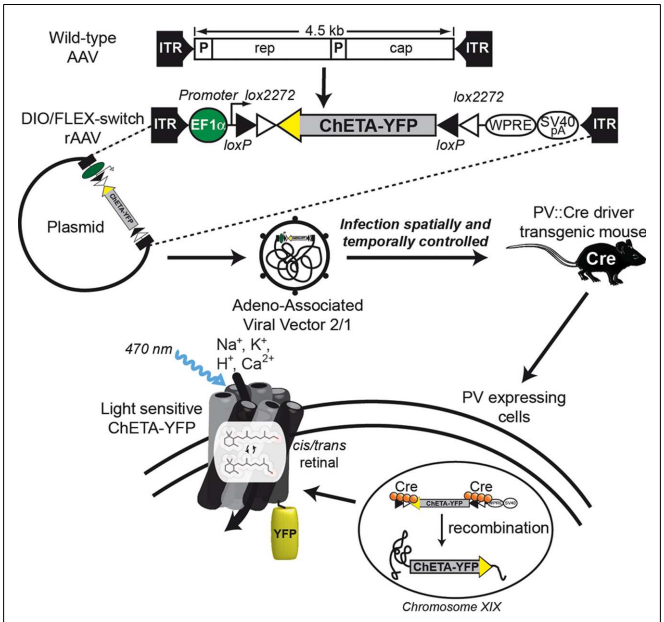

FIGURE 1 | Schematic representation of DIO/FLEX system to express ChETA-EYFP in PV::Cre mouse by rAAV infection. This strategy is based on two components: a Cre-dependant virus containing ChETA-EYFP expression cassette under the control of an ubiquitous EF1α promoter and a driver transgenic mouse expressing Cre recombinase in neurons containing parvalbumin. The transgene integrates into the host genome allowing stable expression of a fusion protein of ChETA and yellow fluorescent protein (EYFP).

MATERIALS AND METHODS

ANIMALS

All experiments were carried out in accordance with the European Communities Council Directive of November 24 1986 (86/609/EEC). Transgenic B6;129P2-Pvalbtm1(cre)Arbr/J (PV::Cre) mice were kindly provided by Dr. Poncer (Institut du Fer-à-Moulin, FR). All animals were housed with controlled temperature (23–25°C) and lighting (12-h dark/light cycle) with food and water available *ad libitum*.

OPTOGENETIC CONSTRUCT

Fast-spiking GABAergic interneurons interneurons are divided in several morphological subtypes in the hippocampus and cortex but they share many electrophysiological properties such as short-duration action potentials, no spike-frequency adaptation during short depolarizing current pulses and a spike-frequency up to 200 Hz (Kawaguchi and Kubota, 1993; Thomson et al., 1996). To be able to study the effects of optogenetic stimulation over a broad range of frequencies, we therefore decide to use an engineered ChR2-E123T Accelerated variant (ChETA). This mutant does feature a higher single-channel conductance, but also a much faster on/off-kinetics, resulting in high fidelity light-driven spiking over

pulse trains up to 200 Hz (Gunaydin et al., 2010). Similarly to the genetic construct used in of MRI experiments, the expression of our light sensitive ion channel ChETA was under control of an EF1α promoter and depends on the presence of Cre recombinase.

ANIMAL ANESTHESIA AND SURGERY

Prior to surgery, animals were anesthetized with intraperitoneal injections of ketamine (100 mg/kg), xylazine (10 mg/kg) with additional doses administered if required. The animals were placed in a stereotaxic frame on a homeothermic blanket (WPI Stoelting, USA) to maintain body temperature at 37˚C throughout surgical procedure. Just before viral injection and in order to get a larger infection efficacy, mice received a single systemic intraperitoneal injection of mannitol (Carty et al., 2010). Recombinant AAV2/1-EF1α::ChETA-EYFP was produced by the Laboratoire de Thérapie Génique – UMR649 (INSERM, Nantes, France) at a titer of 4.3×10^{11} GC/ml and according to protocol previously described (Hildinger et al., 2001). Thin holes were drilled through the skull under the guidance of a stereomicroscope. After the motorized 34-gage Hamilton syringe was positioned in the center of the barrel field, 1 µl of rAAV was injected unilaterally at P30 (**Figure 2B**) at constant speed with over a 5-min period (Cetin et al., 2006).

SLICE PREPARATION AND ELECTROPHYSIOLOGICAL RECORDINGS

Two weeks after rAAV injection, PV::Cre mice (P45) were decapitated and brains were quickly removed. A block of tissue containing the S1BF was trimmed, kept in ice-cold artificial cerebro-spinal fluid (aCSF) containing 126 mM NaCl, 2.5 mM KCl, 1.25 mM NaH_2PO_4, 2 mM $CaCl_2$, 1 mM $MgCl_2$, 26 mM $NaHCO_3$, 10 mM glucose, 15 mM sucrose, 1 mM kynurenic acid, and bubbled with O_2–CO_2 (95–5%). Then, coronal slices (300 µm thick) were prepared as described previously (Schubert et al., 2001). For whole-cell patch-clamp experiments, slices were transferred in the recording chamber and superfused (1–2 ml/min) with oxygenated aCSF. Patch pipettes (4–8 MΩ) pulled from borosilicate glass were filled with internal solution containing 144 mM *K*-gluconate, 3 mM $MgCl_2$, 0.2 mM EGTA, 10 mM HEPES, pH 7.2 (285/295 mOsm). Electrophysiological recordings were performed at a holding potential of −60 mV in current-clamp mode at room temperature (24.5 ± 1.5˚C) using a patch-clamp amplifier (Multiclamp 700B; Molecular Devices, UK). Data were filtered at 5 kHz and digitized at 50 kHz using an acquisition board (Digidata 1440A/pCLAMP10; Molecular Devices).

LIGHT STIMULATION AND VASCULAR REACTIVITY

Blood vessels with >50 µm of their length in focus and exhibiting a well-defined luminal diameter (8–30 µm) were selected for vascular reactivity. Images of blood vessels were acquired every 15 s using Image Pro Plus 6.1 (Media Cybernetics, San Diego, CA, USA), and baselines was determined for 5 min. Blood vessels with unstable baseline were discarded from the analyses. Optical stimulation of FS-PV interneurons was performed using the optoLED system (Cairn Research, Faversham, UK), consisting of a 470-nm, 3.5 W LED mounted on an BX51WI microscope (Olympus) equipped with infrared DIC optics (900 nm) and epifluorescence (**Figure 3C**). Targeted optogenetic stimulation was applied during 2 min (20 Hz, 5 ms pulse width). The illuminated spot was around 2 mm (**Figure 3A**) corresponding to the area of the slice visualized using a 40×/0.8 numerical aperture water-immersion objective. Luminal diameter changes were quantified off-line at different locations along the blood vessel using custom written routines running within Igor Pro software (WaveMetrics, Portland, OR, USA) to determine the spot of maximum diameter change.

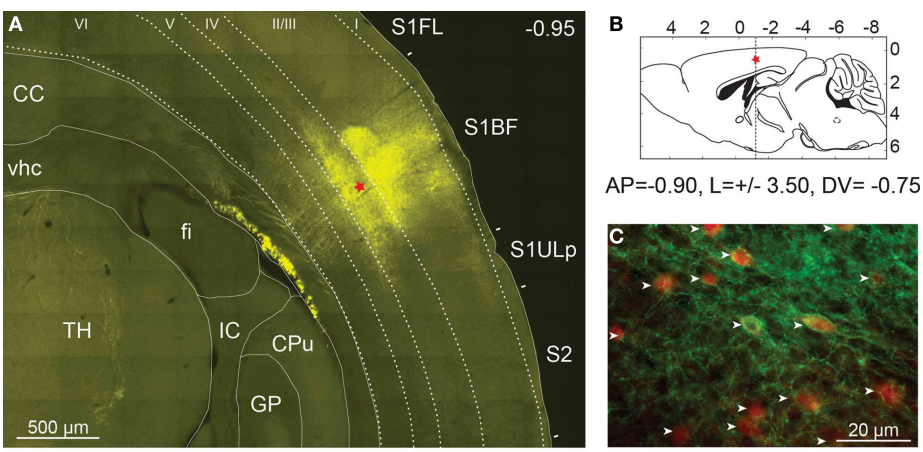

FIGURE 2 | Expression of ChETA-EYFP in the cerebral cortex of mice. **(A)** High resolution mosaic images of around 100 individual frames obtained from a 50-µm thick coronal section of PV::Cre mouse cerebral cortex after 14 days of rAAV infection. Level of expression in somatosensory cortex was controlled by fluorescence microscopy (EYFP filter). The red star indicates the injection site. TH, thalamus; fi, fimbria of hippocampus; vhc, ventral hippocampal commissure; CC, corpus callosum; GP, globus pallidus; IC, internal capsule; CPu, caudate putamen, S1FL, primary somatosensory forelimb cortex; S1BF, primary somatosensory barrel field cortex; S2, secondary somatosensory cortex; S1ULp, primary somatosensory upper limb cortex. **(B)** Diagram of a sagittal brain slice showing the injection site in the S1BF of the transgenic mouse brain. **(C)** The cell-type specificity of the viral expression was assayed using immunocytochemistry with an anti-parvalbumin antibody coupled to Alexa Fluor 568 (in red). EYFP expression was found to be largely restricted to parvalbumin expressing neurons (white arrow) in layer 2/3 of PV::Cre mouse somatosensory cortex.

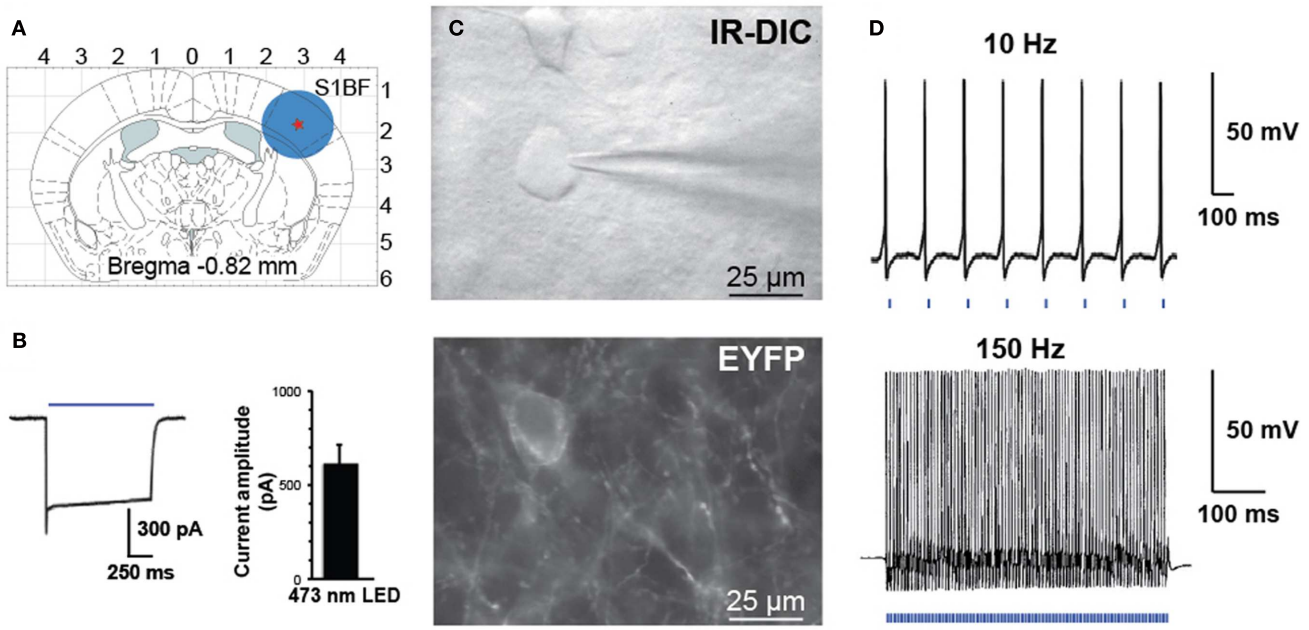

FIGURE 3 | Activation of PV interneurons by blue light. (A) Schematic diagram of a coronal brain slice used in our study. A blue circle represents the size of illuminated area. **(B)** Voltage-clamp recording demonstrating inward current induced by blue laser light (left). Histogram of peak steady-state photocurrent in response to light stimulation (mean 600 ± 120 pA, $n = 7$ FS cells in three animals, 1 s stimulus, 35 mW mm^{-2} output power). **(C)** Bright field (top panel IR-DIC) and fluorescence (bottom panel EYFP) images in the region of recorded neurons. **(D)** Whole-cell current-clamp recording of PV interneuron expressing ChETA-EYFP in response to patterned light stimulation at 10 or 150 Hz.

RESULTS

CELL-TYPE-SPECIFIC EXPRESSION OF ChETA-EYFP

Because successful use of optogenetic techniques relies on sufficient levels and correct expression of the light-activated channels, we performed various controls to evaluate the efficiency of our infection protocol. One advantage of AAV compared to others viruses is the broader spatial spread of transgene expression as confirmed by our observations at both macro and microscopic scales.

Pictures of the exposed skull were taken 2 weeks after viral infection at a 1.25× magnification using a MZ10F fluorescence stereomicroscope (Leica Microsystems, Wetzlar, Germany) equipped with GFP Plant filter set (Ex: 470/40, Dichroic: 495, Em: 525/50 nm) and interfaced to a Retiga-SRV CCD camera (Q-Imaging, Surrey, Canada). rAAV injection led to a large expression of ChETA-EYFP in the S1BF over a distance of up to 2 mm around the injection site (data not shown). The animals were then fixed by intracardiac perfusion with 4% paraformaldehyde and brain was cut in 40 µm coronal sections. Fluorescence microscopy and automated mosaic imaging of the whole brain at low magnification revealed a strong ChETA-EYFP fluorescent area of 500 µm diameter clearly visible in layers 2/3 and 4 around the injection site (**Figure 2A**). Fluorescent neuronal fibers were also detected in layers 5 and 6, in the corpus callosum and in the thalamus. In contrast, no fluorescent signal was observed in the same area on the opposite hemisphere (data not shown).

The cell-type specificity of the viral expression was assayed using immunocytochemistry with a monoclonal primary antibody specific for parvalbumin (Swant, Bellinzona, Switzerland) and an Alexa Fluor 568-coupled secondary antibody (Invitrogen, CA, USA). Using two-color fluorescent microscopy we demonstrated that the expression of transgene was largely restricted to PV-expressing neurons as 95% (361/380) of ChETA-EYFP expressing cells were also PV-positive in layer 2/3 of PV::Cre mouse somatosensory cortex (**Figure 2C**). Moreover at high magnification, ChETA-EYFP channels appear distributed over both cell body on plasma membranes and neurites (**Figure 2C**).

OPTOGENETIC STIMULATION OF PV-POSITIVE NEURONS

Controlled illumination of slices expressing ChETA-EYFP led to spike activity in a temporally precise fashion. In response to blue light stimulation during whole-cell voltage-clamp recordings, FS-PV interneurons exhibit large inward photocurrents (mean 600 ± 120 pA, $n = 7$ FS cells in three animals, 1 s stimulus, 35 mW mm^{-2} output power, **Figure 3B**). FS-PV interneurons reliably fired action potentials in response to patterned blue light stimulation (5 ms pulse width is presented by the blue bars at the bottom of the electrophysiological recordings, 35 mW mm^{-2} output power) up to 150 Hz (**Figure 3D**). As described by Gunaydin et al. (2010) for ChETA-EYFP, responses to light were straightforward with neither missed spikes nor plateau potentials over all frequencies tested between 10 and 150 Hz. Light stimulation induced inhibitory postsynaptic potentials (IPSP) on nearby pyramidal cells (data not shown).

STIMULATION OF PARVALBUMIN EXPRESSING NEURONS ELICITS VASOCONSTRICTION

In their report Lee et al. have demonstrate with of MRI that activation of parvalbumin-positive cells induce a positive BOLD and a concomitant increase of local neuronal excitation in the illuminated area. More intriguing, they also observed a negative BOLD in the flanking regions (Lee et al., 2010). These results led us to investigate in slices if stimulation of PV-expressing neurons gives rise to a change on the diameters of perforating arterioles. Using infrared video microscopy, we demonstrated that optogenetic stimulation of PV-positive neurons lead to a strong decrease of the diameter of arterioles (**Figure 4A**). Vasomotor responses were plotted as a percentage relative to the mean diameter measured during the control period (**Figure 4B**). From Poiseuille's law, it is known that the radius of the blood vessels plays by far the most prominent role in determining the amount of blood flow, $Q = (\frac{kP}{l})d^4$ where Q is flow, P is the pressure difference, d is the diameter, l is the length, and k is a constant depending of the viscosity. After 6 min, we observed a 5% contraction of vessels ($n = 5$; $p < 0.05$) what represents a significant decrease of blood flow by a value of more than 20%. Although all recording of vessels were performed in brain slices, these results are in agreement with those measured in the cerebral cortex *in vivo* (Stefanovic et al., 2008; Mace et al., 2011).

DISCUSSION

HOW ACTIVATION OF THE BRAIN TRANSMUTES IN FUNCTIONAL HYPEREMIA: NEUROGENIC VS. METABOLIC HYPOTHESIS

Precise mechanisms involved in functional hyperemia are still poorly understood. At present, an intense debate among neuroscientists exists with two hypotheses, the "metabolic" and the "neurogenic" (Estrada and DeFelipe, 1998; Hamel, 2006). Neuronal activity is the principal energy-consuming process in the brain. The metabolic hypothesis assumes a causal link between neuronal energy demand and regulation of local CBF. The general assumption, which is supported by positron emission tomography (PET) findings showing comparable functional increases in blood flow and glucose uptake (Raichle and Mintun, 2006), is that CBF is coupled to regional glucose utilization, which in turn is directly related to neuronal activity (Magistretti, 2006). Excitatory neuronal activity releases glutamate that activates glia through metabotropic glutamate receptors. The activation of glial cells will induce at the same time an increase in the diameter of nearby blood vessels and increase of glucose uptake. In this metabolic hypothesis, the activity-dependent regulation of local CBF is a feedback mechanism that does not anticipate possible demand (Rossier, 2009). In contrast with this metabolic feedback hypothesis, the neurogenic hypothesis (Estrada and DeFelipe, 1998; Hamel, 2006) describes a feed forward mechanism where the hyperemia evoked by cerebral activation is linked to neuronal synaptic signaling rather than to the metabolic needs of the tissue (Leithner et al., 2010; Lindauer et al., 2010). Previous studies demonstrated three neuronal elements that are candidate for controlling local CBF: interneurons (Abounader and Hamel, 1997; Cauli et al., 2004), pyramids (Abounader and Hamel, 1997; Zonta et al., 2003; Filosa et al., 2006; Iadecola and Nedergaard, 2007; Lecrux et al., 2011), and subcortical nuclei afferent pathways (Raichle et al., 1975; Cohen et al., 1996; Abounader and Hamel, 1997; Krimer et al., 1998; Yamada et al., 2001; Hamel, 2004; Gordon et al., 2008; Jones et al., 2008).

RECENT *IN VIVO* EXPERIMENTS IN RODENTS INDICATE THE POSSIBLE EXISTENCE OF AN INTRINSIC BRAIN NEURONAL NETWORK THAT CONTROLS THE NEOCORTICAL LOCAL BLOOD FLOW

Several *in vivo* experiments with various techniques have already indicated that whisker pad stimulation is accompanied by blood flow increase in the contralateral barrel field but also by blood flow decrease in other part of the brain. In two recent reports, one from (Alonso Bde et al., 2008; Boorman et al., 2010) describing fMRI experiments with the rodent whisker-to-barrel system, whisker pad stimulation was accompanied by a positive BOLD in the homotypic contralateral barrel field but also by a negative BOLD in the ipsilateral primary somatosensory cortex (S1) and/or in deeper surrounding areas of the contralateral cortex.

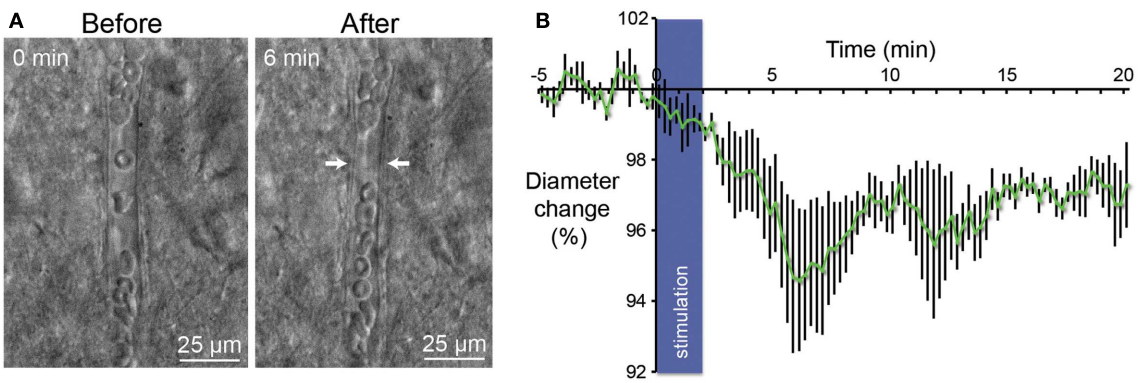

FIGURE 4 | Vasoconstriction induced by optogenetic stimulation of PV-expressing neurons. (A) Infrared microscopy images of a blood vessel in the somatosensory cortex showing changes of the luminal diameter after light stimulation of PV interneurons. Images of the microvessels were acquired every 15 s after a control period of 5 min. Arrows indicate region of high vascular reactivity. Note the accumulation of red blood cells on both sides of the arrows in the right panel. **(B)** Mean vascular constriction ± SEM ($n = 5$) induced by 2 min stimulation at 20 Hz (473 nm, 5 ms pulse width, 35 mW mm^{-2}) in the layer II/III of the somatosensory cortex.

In order to explain these data we propose that a neuronal circuitry is devoted to an exquisite regulation of the local blood flow. Kleinfeld et al. (2011) also proposed the idea that a specialized neuronal system is locked to the precise local blood flow control in a recent review. Almost 10 years ago, several fMRI studies had already described that besides positive BOLD and blood flow signal changes in the activated area, robust negative responses can be detected independently in the absence or simultaneously with the positive responses (Brefczynski and DeYoe, 1999; Allison et al., 2000; Shmuel et al., 2002). More recently Devor et al. (2008) reached the same conclusion by intrinsic optical spectroscopic imaging when they measured hemodynamic changes in response to forepaw stimulation. They showed that an increase of blood perfusion in the contralateral cortex is followed by a decrease in the ipsilateral somatosensory cortex (Devor et al., 2008).

In conclusion, changes in the redistribution of the cerebral local blood flow following brain activation are much more complex than initially anticipated. If activation of pyramids and release of glutamate could explain the positive BOLD response via the stimulation of astrocytes, it could not explain the negative BOLD response in the surrounding areas and in the ipsilateral cortex. Negative BOLD is generally considered to be the manifestation of an increase activity of GABAergic inhibitory interneurons (Logothetis et al., 2001; Logothetis, 2008). The puzzling problem is to understand what classes of interneurons are activated and how their activation is mediated. In the present general knowledge, the local blood flow redistribution after brain activation appears complex with a simultaneous increase in some regions of the brain and a decrease in others. The network controlling local blood flow could be considered as a connected regulatory system in his own right. The neurovascular regulatory system could not be explained solely by local circuitry involving interneurons and pyramidal cells. Possible long projections are to be taken into account to explain the decreased perfusion in the ipsilateral cortex observed by several investigators. Direct transcallosal projections between the two somatosensory cortices are a possibility although multisynaptic connections via the motor cortex or the thalamus have also to be taken into account. Here we enter in an uncharted territory.

If we restrict our analysis to the identification of the last neuronal relays, i.e., interneurons and pyramids, many *ex vivo* experiments from our group have clearly demonstrated that distinct subclasses of interneurons containing VIP, NOS, SOM, and NPY control directly the tone of the smooth muscles of the arterioles (Cauli et al., 2004; Rancillac et al., 2006). Indeed, smooth muscles of the penetrating arterioles are ideally localized to be the main regulators of blood flow and pressure in the cortical cortex (Hillman, 2007; Nishimura et al., 2007). This regulation occurs at the precapillary level through sphincters that are involved in a localized control of capillary tone (Peppiatt et al., 2006; Attwell et al., 2010; Hamilton et al., 2010).

OPTOGENETIC STIMULATION OF PV CONTAINING NEURONS AND THE CONTROL LOCAL BLOOD FLOW

One main advantage of our experiments in slices is the direct visualization of parenchymal microvessels movements. Although the blood vessels in this preparation lack intraluminal flow and pressure, which have been shown to play a role in the regulation of tone (Johansson, 1989; Mellander, 1989), the physiologic reactivity of vessels in the brain slice preparation has been demonstrated (Sagher et al., 1993; Fergus et al., 1996). Moreover, it was previously reported that vascular responses observed *ex vivo* are really slow compared to *in vivo* responses (5 min vs. 1 s respectively; Cauli et al., 2004; Rancillac et al., 2006). Our results in **Figure 4** show that increased activity of cells expressing PV results in vasoconstriction in neighboring perforating arterioles. How to explain these results? PV interneurons were never described to mediate vascular responses. Moreover, PV interneurons do not contain any known vasoactive peptides although a subpopulation expresses nitric oxide synthase. If NO was release by a subpopulation of PV interneurons, a vasodilatation should have been expected and not a vasoconstriction as observed in our experiments. It is unlikely that PV interneurons regulates directly CBF but they could act as a relay to inhibit local or distal interneuron involved in a vasodilation tone. FS-PV interneurons could thus lead to vasoconstriction by a decreased release of VIP and/or NOS following inhibition of interneurons containing these vasodilatating substances. PV interneurons could also be in the middle of an inhibitory loop whose final effect could relief the inhibition of neurogliaform interneurons releasing the potent vasoconstrictor peptide NPY.

Another possible explanation could be that these vasoconstrictions are not generated by PV interneurons but by PV-expressing pyramidal neurons. This hypothesis is supported by previous studies showing that a subset of pyramids from the primary somatosensory, motor, and visual areas expresses PV (McMullen et al., 1994; Preuss and Kaas, 1996; Tanahira et al., 2009). Indeed as shown in **Figure 2A**, we observed efferent fibers projecting from the cortical layer V and VI of the cortex to the ventral posterolateral nucleus (VPL) of the thalamus and through the corpus callosum, while the virus was injected into S1BF. This result suggests that these long projection neurons could belong to a subset of pyramids expressing PV. In this scenario, pyramidal cell could therefore be implicated in vasoconstriction observed after by light stimulation of ChETA-EYFP in slices. This assumption about involvement of pyramids in CBF control is consistent with previous studies that demonstrate their roles either directly by the release of COX-2-derived dilatory prostaglandins or indirectly by astrocytic release of EETs (Lecrux et al., 2011). Nevertheless, the proposal that a subset of pyramids expressing PV is part of the neuronal system controlling blood flow is still intriguing.

Together, vasoconstrictions following optogenetic stimulation of PV-expressing neurons could results from interneurons and/or pyramids activation. Our results are in accordance with the role of local cortical neurons in the regulation of CBF since all afferent and efferent fibers between the cortex and others subcortical nuclei are cut in coronal brain slices used in these experiments. These findings bring new insight to the complex mechanisms of the neurovascular coupling and require further investigation.

ACKNOWLEDGMENTS

We thank Marcel Leopoldie for animal husbandry. This work was supported by the French National Research Agency (ANRSVSE4-BRAINVASC) and by the Fondation Pour les Sciences du Cerveau.

REFERENCES

Abounader, R., and Hamel, E. (1997). Associations between neuropeptide Y nerve terminals and intraparenchymal microvessels in rat and human cerebral cortex. *J. Comp. Neurol.* 388, 444–453.

Allison, J. D., Meador, K. J., Loring, D. W., Figueroa, R. E., and Wright, J. C. (2000). Functional MRI cerebral activation and deactivation during finger movement. *Neurology* 54, 135–142.

Alonso Bde, C., Lowe, A. S., Dear, J. P., Lee, K. C., Williams, S. C., and Finnerty, G. T. (2008). Sensory inputs from whisking movements modify cortical whisker maps visualized with functional magnetic resonance imaging. *Cereb. Cortex* 18, 1314–1325.

Atasoy, D., Aponte, Y., Su, H. H., and Sternson, S. M. (2008). A FLEX switch targets Channelrhodopsin-2 to multiple cell types for imaging and long-range circuit mapping. *J. Neurosci.* 28, 7025–7030.

Attwell, D., Buchan, A. M., Charpak, S., Lauritzen, M., Macvicar, B. A., and Newman, E. A. (2010). Glial and neuronal control of brain blood flow. *Nature* 468, 232–243.

Boorman, L., Kennerley, A. J., Johnston, D., Jones, M., Zheng, Y., Redgrave, P., and Berwick, J. (2010). Negative blood oxygen level dependence in the rat: a model for investigating the role of suppression in neurovascular coupling. *J. Neurosci.* 30, 4285–4294.

Brefczynski, J. A., and DeYoe, E. A. (1999). A physiological correlate of the "spotlight" of visual attention. *Nat. Neurosci.* 2, 370–374.

Carty, N., Lee, D., Dickey, C., Ceballos-Diaz, C., Jansen-West, K., Golde, T. E., Gordon, M. N., Morgan, D., and Nash, K. (2010). Convection-enhanced delivery and systemic mannitol increase gene product distribution of AAV vectors 5, 8, and 9 and increase gene product in the adult mouse brain. *J. Neurosci. Methods* 194, 144–153.

Cauli, B., Tong, X. K., Rancillac, A., Serluca, N., Lambolez, B., Rossier, J., and Hamel, E. (2004). Cortical GABA interneurons in neurovascular coupling: relays for subcortical vasoactive pathways. *J. Neurosci.* 24, 8940–8949.

Cetin, A., Komai, S., Eliava, M., Seeburg, P. H., and Osten, P. (2006). Stereotaxic gene delivery in the rodent brain. *Nat. Protoc.* 1, 3166–3173.

Chow, B. Y., Han, X., Dobry, A. S., Qian, X., Chuong, A. S., Li, M., Henninger, M. A., Belfort, G. M., Lin, Y., Monahan, P. E., and Boyden, E. S. (2010). High-performance genetically targetable optical neural silencing by light-driven proton pumps. *Nature* 463, 98–102.

Cohen, Z., Bonvento, G., Lacombe, P., and Hamel, E. (1996). Serotonin in the regulation of brain microcirculation. *Prog. Neurobiol.* 50, 335–362.

Desai, M., Kahn, I., Knoblich, U., Bernstein, J., Atallah, H., Yang, A., Kopell, N., Buckner, R. L., Graybiel, A. M., Moore, C. I., and Boyden, E. S. (2011). Mapping brain networks in awake mice using combined optical neural control and fMRI. *J. Neurophysiol.* 105, 1393–1405.

Devor, A., Hillman, E. M., Tian, P., Waeber, C., Teng, I. C., Ruvinskaya, L., Shalinsky, M. H., Zhu, H., Haslinger, R. H., Narayanan, S. N., Ulbert, I., Dunn, A. K., Lo, E. H., Rosen, B. R., Dale, A. M., Kleinfeld, D., and Boas, D. A. (2008). Stimulus-induced changes in blood flow and 2-deoxyglucose uptake dissociate in ipsilateral somatosensory cortex. *J. Neurosci.* 28, 14347–14357.

Estrada, C., and DeFelipe, J. (1998). Nitric oxide-producing neurons in the neocortex: morphological and functional relationship with intraparenchymal microvasculature. *Cereb. Cortex* 8, 193–203.

Fergus, A., Jin, Y., Thai, Q. A., Kassell, N. F., and Lee, K. S. (1996). Tonic protein kinase C-mediated vasoconstriction is unmasked when nitric oxide synthase is inhibited in cerebral microvessels. *Neuroscience* 74, 927–934.

Filosa, J. A., Bonev, A. D., Straub, S. V., Meredith, A. L., Wilkerson, M. K., Aldrich, R. W., and Nelson, M.T. (2006). Local potassium signaling couples neuronal activity to vasodilation in the brain. *Nat. Neurosci.* 9, 1397–1403.

Gordon, G. R., Choi, H. B., Rungta, R. L., Ellis-Davies, G. C., and Macvicar, B. A. (2008). Brain metabolism dictates the polarity of astrocyte control over arterioles. *Nature* 456, 745–749.

Gunaydin, L. A., Yizhar, O., Berndt, A., Sohal, V. S., Deisseroth, K., and Hegemann, P. (2010). Ultrafast optogenetic control. *Nat. Neurosci.* 13, 387–392.

Iadecola, C., and Nedergaard, M. (2007). Glial regulation of the cerebral microvasculature. *Nat. Neurosci.* 10, 1369–1376.

Hamel, E. (2004). Cholinergic modulation of the cortical microvascular bed. *Prog. Brain Res.* 145, 171–178.

Hamel, E. (2006). Perivascular nerves and the regulation of cerebrovascular tone. *J. Appl. Physiol.* 100, 1059–1064.

Hamilton, N. B., Attwell, D., and Hall, C. N. (2010). Pericyte-mediated regulation of capillary diameter: a component of neurovascular coupling in health and disease. *Front. Neuroenergetics* 2:5. doi:10.3389/fnene.2010.00005

Hildinger, M., Auricchio, A., Gao, G., Wang, L., Chirmule, N., and Wilson, J. M. (2001). Hybrid vectors based on adeno-associated virus serotypes 2 and 5 for muscle-directed gene transfer. *J. Virol.* 75, 6199–6203.

Hillman, E. M. (2007). Optical brain imaging in vivo: techniques and applications from animal to man. *J. Biomed. Opt.* 12, 051402.

Hippenmeyer, S., Vrieseling, E., Sigrist, M., Portmann, T., Laengle, C., Ladle, D. R., and Arber, S. (2005). A developmental switch in the response of DRG neurons to ETS transcription factor signaling. *PLoS Biol.* 3, e159. doi:10.1371/journal.pbio.0030159

Johansson, B. (1989). Myogenic tone and reactivity: definitions based on muscle physiology. *J. Hypertens. Suppl.* 7, S5–S8; discussion S9.

Jones, M., Devonshire, I. M., Berwick, J., Martin, C., Redgrave, P., and Mayhew, J. (2008). Altered neurovascular coupling during information-processing states. *Eur. J. Neurosci.* 27, 2758–2772.

Kahn, I., Desai, M., Knoblich, U., Bernstein, J., Henninger, M., Graybiel, A. M., Boyden, E. S., Buckner, R. L., and Moore, C. I. (2011). Characterization of the functional MRI response temporal linearity via optical control of neocortical pyramidal neurons. *J. Neurosci.* 31, 15086–15091.

Kawaguchi, Y., and Kubota, Y. (1993). Correlation of physiological subgroupings of nonpyramidal cells with parvalbumin- and calbindin D28k-immunoreactive neurons in layer V of rat frontal cortex. *J. Neurophysiol.* 70, 387–396.

Kleinfeld, D., Blinder, P., Drew, P. J., Driscoll, J. D., Muller, A., Tsai, P. S., and Shih, A. Y. (2011). A guide to delineate the logic of neurovascular signaling in the brain. *Front Neuroenergetics* 3:1. doi:10.3389/fnene.2011.00001

Krimer, L. S., Muly, E. C. III, Williams, G. V., and Goldman-Rakic, P. S. (1998). Dopaminergic regulation of cerebral cortical microcirculation. *Nat. Neurosci.* 1, 286–289.

Lecrux, C., Toussay, X., Kocharyan, A., Fernandes, P., Neupane, S., Levesque, M., Plaisier, F., Shmuel, A., Cauli, B., and Hamel, E. (2011). Pyramidal neurons are "neurogenic hubs" in the neurovascular coupling response to whisker stimulation. *J. Neurosci.* 31, 9836–9847.

Lee, J. H., Durand, R., Gradinaru, V., Zhang, F., Goshen, I., Kim, D. S., Fenno, L. E., Ramakrishnan, C., and Deisseroth, K. (2010). Global and local fMRI signals driven by neurons defined optogenetically by type and wiring. *Nature* 465, 788–792.

Leithner, C., Muller, S., Fuchtemeier, M., Lindauer, U., Dirnagl, U., and Royl, G. (2010). Determination of the brain-blood partition coefficient for water in mice using MRI. *J. Cereb. Blood Flow Metab.* 30, 1821–1824.

Lindauer, U., Dirnagl, U., Fuchtemeier, M., Bottiger, C., Offenhauser, N., Leithner, C., and Royl, G. (2010). Pathophysiological interference with neurovascular coupling – when imaging based on hemoglobin might go blind. *Front Neuroenergetics* 2:25. doi:10.3389/fnene.2010.00025

Logothetis, N. K. (2008). What we can do and what we cannot do with fMRI. *Nature* 453, 869–878.

Logothetis, N. K., Pauls, J., Augath, M., Trinath, T., and Oeltermann, A. (2001). Neurophysiological investigation of the basis of the fMRI signal. *Nature* 412, 150–157.

Mace, E., Montaldo, G., Cohen, I., Baulac, M., Fink, M., and Tanter, M. (2011). Functional ultrasound imaging of the brain. *Nat. Methods* 8, 662–664.

Magistretti, P. J. (2006). Neuron-glia metabolic coupling and plasticity. *J. Exp. Biol.* 209, 2304–2311.

Martin, C., Martindale, J., Berwick, J., and Mayhew, J. (2006). Investigating neural-hemodynamic coupling and the hemodynamic response function in the awake rat. *Neuroimage* 32, 33–48.

McMullen, N. T., Smelser, C. B., and Rice, F. L. (1994). Parvalbumin expression reveals a vibrissa-related pattern in rabbit SI cortex. *Brain Res.* 660, 225–231.

Mellander, S. (1989). Functional aspects of myogenic vascular control. *J. Hypertens. Suppl.* 7, S21–S30; discussion S31.

Nishimura, N., Schaffer, C. B., Friedman, B., Lyden, P. D., and Kleinfeld, D. (2007). Penetrating arterioles are a bottleneck in the perfusion of neocortex. *Proc. Natl. Acad. Sci. U.S.A.* 104, 365–370.

Peppiatt, C. M., Howarth, C., Mobbs, P., and Attwell, D. (2006). Bidirectional control of CNS capillary diameter by pericytes. *Nature* 443, 700–704.

Preuss, T. M., and Kaas, J. H. (1996). Parvalbumin-like immunoreactivity of layer V pyramidal cells in the motor and somatosensory cortex

of adult primates. *Brain Res.* 712, 353–357.

Raichle, M. E., Hartman, B. K., Eichling, J. O., and Sharpe, L. G. (1975). Central noradrenergic regulation of cerebral blood flow and vascular permeability. *Proc. Natl. Acad. Sci. U.S.A.* 72, 3726–3730.

Raichle, M. E., and Mintun, M. A. (2006). Brain work and brain imaging. *Annu. Rev. Neurosci.* 29, 449–476.

Rancillac, A., Rossier, J., Guille, M., Tong, X. K., Geoffroy, H., Amatore, C., Arbault, S., Hamel, E., and Cauli, B. (2006). Glutamatergic control of microvascular tone by distinct GABA neurons in the cerebellum. *J. Neurosci.* 26, 6997–7006.

Rossier, J. (2009). Wiring and plumbing in the brain. *Front. Hum. Neurosci.* 3:2. doi:10.3389/neuro.09.002.2009

Sagher, O., Zhang, X. Q., Szeto, W., Thai, Q. A., Jin, Y., Kassell, N. F., and Lee, K. S. (1993). Live computerized videomicroscopy of cerebral microvessels in brain slices. *J. Cereb. Blood Flow Metab.* 13, 676–682.

Schubert, D., Staiger, J. F., Cho, N., Kotter, R., Zilles, K., and Luhmann, H. J. (2001). Layer-specific intracolumnar and transcolumnar functional connectivity of layer V pyramidal cells in rat barrel cortex. *J. Neurosci.* 21, 3580–3592.

Shmuel, A., Yacoub, E., Pfeuffer, J., Van De Moortele, P. F., Adriany, G., Hu, X., and Ugurbil, K. (2002). Sustained negative BOLD, blood flow and oxygen consumption response and its coupling to the positive response in the human brain. *Neuron* 36, 1195–1210.

Sohal, V. S., Zhang, F., Yizhar, O., and Deisseroth, K. (2009). Parvalbumin neurons and gamma rhythms enhance cortical circuit performance. *Nature* 459, 698–702.

Stefanovic, B., Hutchinson, E., Yakovleva, V., Schram, V., Russell, J. T., Belluscio, L., Koretsky, A. P., and Silva, A. C. (2008). Functional reactivity of cerebral capillaries. *J. Cereb. Blood Flow Metab.* 28, 961–972.

Tanahira, C., Higo, S., Watanabe, K., Tomioka, R., Ebihara, S., Kaneko, T., and Tamamaki, N. (2009). Parvalbumin neurons in the forebrain as revealed by parvalbumin-Cre transgenic mice. *Neurosci. Res.* 63, 213–223.

Thomson, A. M., West, D. C., Hahn, J., and Deuchars, J. (1996). Single axon IPSPs elicited in pyramidal cells by three classes of interneurones in slices of rat neocortex. *J. Physiol. (Lond.)* 496(Pt 1), 81–102.

Urban, A., and Rossier, J. (2012). "Genetic targeting of specific neuronal cell types in the cerebral cortex," in *Progress in Brain Research*, Chapter 9, eds K. P. Thomas and S. B. Edward (Paris: Elsevier), 163–192.

Wiest, M. C., Bentley, N., and Nicolelis, M. A. (2005). Heterogeneous integration of bilateral whisker signals by neurons in primary somatosensory cortex of awake rats. *J. Neurophysiol.* 93, 2966–2973.

Yamada, M., Lamping, K. G., Duttaroy, A., Zhang, W., Cui, Y., Bymaster, F. P., Mckinzie, D. L., Felder, C. C., Deng, C. X., Faraci, F. M., and Wess, J. (2001). Cholinergic dilation of cerebral blood vessels is abolished in M(5) muscarinic acetylcholine receptor knockout mice. *Proc. Natl. Acad. Sci. U.S.A.* 98, 14096–14101.

Zhang, F., Gradinaru, V., Adamantidis, A. R., Durand, R., Airan, R. D., De Lecea, L., and Deisseroth, K. (2010). Optogenetic interrogation of neural circuits: technology for probing mammalian brain structures. *Nat. Protoc.* 5, 439–456.

Zonta, M., Angulo, M. C., Gobbo, S., Rosengarten, B., Hossmann, K. A., Pozzan, T., and Carmignoto, G. (2003). Neuron-to-astrocyte signaling is central to the dynamic control of brain microcirculation. *Nat. Neurosci.* 6, 43–50.

Conflict of Interest Statement: The authors declare that the research was conducted in the absence of any commercial or financial relationships that could be construed as a potential conflict of interest.

Received: 26 January 2012; paper pending published: 13 February 2012; accepted: 16 May 2012; published online: 15 June 2012.

Citation: Urban A, Rancillac A, Martinez L and Rossier J (2012) Deciphering the neuronal circuitry controlling local blood flow in the cerebral cortex with optogenetics in PV::Cre transgenic mice. Front. Pharmacol. ***3****:105. doi: 10.3389/fphar.2012.00105*

This article was submitted to Frontiers in Neuropharmacology, a specialty of Frontiers in Pharmacology.

frontiers in
NEUROENERGETICS

ORIGINAL RESEARCH ARTICLE
published: 01 February 2012
doi: 10.3389/fnene.2012.00002

Energetics based spike generation of a single neuron: simulation results and analysis

Nagarajan Venkateswaran[1]*, Sudarshan Sekhar[2], Thiagarajan Thirupatchur Sanjayasarathy[2], Sharath Navalpakkam Krishnan[2], Dinesh Kannan Kabaleeswaran[2], Subbu Ramanathan[2], Narendran Narayanasamy[2], Sharan Srinivas Jagathrakshakan[2] and S. R. Vignesh[2]

[1] *WAran Research FoundaTion, Chennai, India*
[2] *Charaka Group – Computational Neuroscience, WAran Research FoundaTion, Chennai, India*

Edited by:
Yuri Zilberter, Institut National de la Santé et de la Recherche Médicale U751, France

Reviewed by:
Tibor Kristian, University of Maryland School of Medicine, USA
Fahmeed Hyder, Yale University, USA

****Correspondence:***
Nagarajan Venkateswaran, WAran Research FoundaTion, No. 46B, Mahadevan Street, West Mambalam, Chennai, Tamil Nadu, India.
e-mail: warft.backup@gmail.com

Existing current based models that capture spike activity, though useful in studying information processing capabilities of neurons, fail to throw light on their internal functioning. It is imperative to develop a model that captures the spike train of a neuron as a function of its intracellular parameters for non-invasive diagnosis of diseased neurons. This is the first ever article to present such an integrated model that quantifies the inter-dependency between spike activity and intracellular energetics. The generated spike trains from our integrated model will throw greater light on the intracellular energetics than existing current models. Now, an abnormality in the spike of a diseased neuron can be linked and hence effectively analyzed at the energetics level. The spectral analysis of the generated spike trains in a time–frequency domain will help identify abnormalities in the internals of a neuron. As a case study, the parameters of our model are tuned for Alzheimer's disease and its resultant spike trains are studied and presented. This massive initiative ultimately aims to encompass the entire molecular signaling pathways of the neuronal bioenergetics linking it to the voltage spike initiation and propagation; due to the lack of experimental data quantifying the inter dependencies among the parameters, the model at this stage adopts a particular level of functionality and is shown as an approach to study and perform disease modeling at the spike train and the mitochondrial bioenergetics level.

Keywords: neuroenergetics, mitochondria, Alzheimer's disease, Krebs cycle, wavelet transformations, Petri nets, voltage spike, ATP

INTRODUCTION

Over the past decades, neuroscience research has witnessed myriad deterministic (Hodgkin and Huxley, 1952; Fitzhugh, 1955; Oja, 1982; Buchholtz et al., 1992), stochastic (Fienberg, 1974; Harrison et al., 2005), electrical (Rall, 1957, 1959, 1960) models, which have delved into the functional aspects of spatio-temporal characteristics of a network of ion channels (Babinec and Babincov, 2002), dendritic arborization (van Pelt et al., 2001), the dynamics of a single synapse (Reutimann, 1999; Attwell and Gibb, 2005), and calcium wave oscillations (Volman et al., 2007) in response to neurotransmitter release. These models abstract the characteristics of either a specific function of a single neuron or deal with the fundamental characteristics of the neuron on a dynamic scale which is furnished in the concomitant voltage spike response.

On the other hand, with the advent of advanced experimentation techniques, metabolic pathways which co-exist within the cell characterizing the intracellular energetics of the cell organelles, have been identified and studied extensively (Duchen, 2000; Green and Green, 2005; Shulman and Rothman, 2005). This research into the deeper aspects of intracellular interactions has paved the way for elaborate models which describe the chemical kinetics of the intracellular reactions of the mitochondria (Krebs cycle, electron transport chain, B-Oxidation) and other organelles (Baker et al., 2002; Mogilevskaya et al., 2006), through deterministic differential equations, predominantly the Michaelis–Menten kinetics (Beard and Qian, 2008).

However, a common feature of these models has been the lack of improvisation to connect and establish the missing link between the spike generation of the neuron to its underlying biophysical and the biochemical processes in its intracellular compartments. An unmistakable gap exists between the spike generation activities and energetics of a single neuron. Alzheimer's, Huntington's, Parkinson's, and other degenerative terminal brain diseases are characterized by a cascade of affirmative changes at the energetics level of the cell (Hirai et al., 2001; Zeviani and Di Donato, 2004; Mattson et al., 2008) which is expressed in the voltage spike activity of the neuron. This research work presented here is an attempt at bridging that lacuna, probing into the unknown, and establishing the connect between electrical, biophysical, and biochemical pathways of a single neuron thus providing a better and a comprehensive working platform toward disease modeling and drug testing.

The pivotal role of the mitochondria during the degenerate mode of a single neuron in times of Alzheimer's cannot be ignored (Hirai et al., 2001; Zeviani and Di Donato, 2004; Mattson et al., 2008). It thus becomes indispensable that the dynamics of the mitochondrial behavior needs to be captured through a mathematical model and linked to the spike generation of the neuron.

The resulting time–frequency analysis of the voltage spike presented in the following section reflect the fine changes in the mitochondrial energetics leading to a better understanding and comprehension of the disease and its intracellular potency.

The model, with respect to energetics is restricted to the mitochondria and does not deal with the entire set of parameters involved in the Alzheimer's disease but still gives a fair understanding (Hardy and Selkoe, 2002). Limitations and further extensions have been discussed in the final section.

A major limiting factor during the simulation phase of the model has been the non-availability of realistic values for certain intracellular parameters for specific types of neurons. In fact, this model makes use of a few intracellular parameters obtained from the mitochondria belonging to hepatocytes (Mogilevskaya et al., 2006). A generic, ubiquitous model has thus been proposed which can be fine-tuned to work for a particular type of neuron depending upon the level of experimentation available.

The concept that, the dynamics of the mitochondrial energetics is captured in the voltage spike of the neuron adds a powerful dimension to disease modeling. The non-invasive technique is strengthened by the fact that intracellular pathways can be analyzed comprehensively through the spike response of the neuron. It narrows down the field of experimentation and calls for establishing greater synergy between computational and clinical neuroscientists – working toward disease modeling and drug discovery, and ultimately yielding better results.

The integrated voltage spike – energetics model along with the mathematical concepts and simulation framework has been presented at the International Neuroinformatics Conference, 2010 at Kobe, Japan (Mohan et al., 2010a,b). However, this is the first time that the simulation results of the integrated model are presented, discussed, and analyzed.

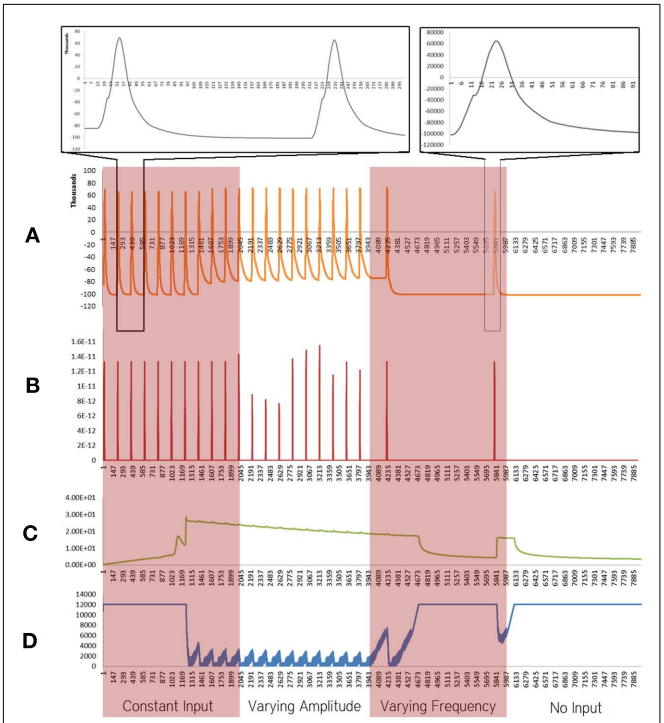

FIGURE 1 | Simulation results using the energetics based single neuron simulator, for a pyramidal neuron over four stages of input under healthy conditions. (A) Difference in ionic concentration across the membrane (voltage spike; μM) vs timestamp. **(B)** Input neurotransmitters to the neuron (μM) vs timestamp corresponding to various input bands. **(C)** Krebs cycle activity (pyruvate consumed in μM per timestamp) vs timestamp. **(D)** Total intracellular ATP concentration (μM) vs timestamp.

RESULTS

The simulated voltage spike (**Figure 1A**) was analyzed under varying concentrations and frequencies of neurotransmitter input and intracellular parameters corresponding to a pyramidal neuron. Alternate methods (discussed further) were adopted to determine values of a few intracellular parameters which were unavailable. Preliminary Disease Modeling was performed by identifying the parameters that are responsible for Alzheimer's (**Figures 2**, **3**, **4**, and **5B**). These parameters and associated constants 38 were then altered to match the abnormalities found in a diseased neuron. The simulation was then repeated to get the spike train of the diseased neuron. The variations of all parameters were tracked using the simulator. The rate and quantity of injected neurotransmitters to the neuron was spread over four bands, i.e., constant rate and quantity, varying quantity, varying rate, and null input conditions. The Krebs Cycle Activity is represented as the micromoles of pyruvate used per timestamp. ATP concentration represents the total intracellular ATP concentration in micromoles.

HEALTHY NEURON

For a constant neurotransmitter input to the simulator (**Figure 1**, Constant Input Band), it was found that the voltage spike had a constant frequency and small variation in amplitude (**Figure 1A**). The Krebs Cycle Activity (**Figure 1C**) increased with deviation of ionic concentration of Na^+ and K^+ from equilibrium state; a gradual decrease in Krebs cycle activity is observed thereafter. Further, activation of the Krebs cycle correlated with a decrease in the ATP concentration (**Figure 1D**). When the amplitude of neurotransmitter input was varied (**Figure 1**, Varying Amplitude Band), all the above phenomena were observed, with a constant amplitude of the spike train, which resulted in similar graphs for Krebs Cycle Activity (**Figure 1C**) and ATP concentration (**Figure 1D**). A fixed concentration of neurotransmitter input with varied frequency (**Figure 1**, Varying Frequency Band) caused a variation in the frequency of spikes (**Figure 1A**) and similar variations in the frequency of Krebs Cycle Activity (**Figure 1C**). Also, when the frequency of neurotransmitter input decreases, Krebs cycle activity is observed to decrease, correlating with increased ATP concentration. Finally, when the neurotransmitter input was removed (**Figure 1**, No Input Band); the ionic concentration was restored to its equilibrium and ATP concentration became constant.

ALZHEIMER'S AFFECTED NEURON

Neurons affected by Alzheimer's disease were modeled as a combination of two important factors, decreased activity of the Electron Transport Chain (Mattson et al., 2008) and an increased formation of Oxide ions (O^{2-}; Mattson et al., 2008). These factors and their implications are discussed in the Section "Discussion." In

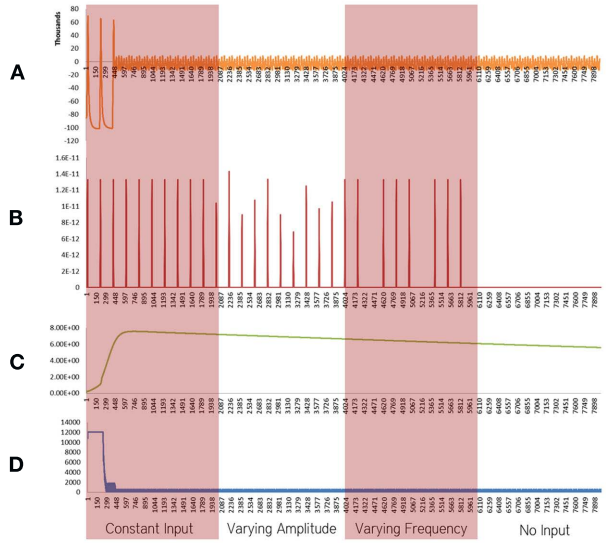

FIGURE 2 | Simulation results using the energetics based single neuron simulator, for a pyramidal neuron over four stages of input affected by Alzheimer's disease. (A) Ionic concentration across the membrane (Voltage Spike; μM) vs timestamp. **(B)** Input neurotransmitters to the neuron (μM) vs Timestamp corresponding to various input bands. **(C)** Krebs cycle activity (NADH produced in μM/timestamp) vs timestamp. **(D)** Total intracellular ATP concentration (μM) vs timestamp.

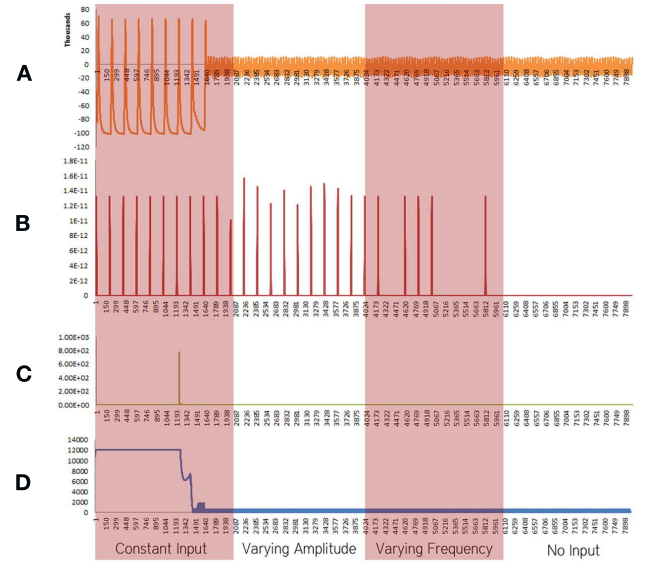

FIGURE 3 | Simulation results using the energetics based single neuron simulator, for a pyramidal neuron over four stages of input affected by a decrease in the rate of the electron transport chain. (A) Ionic concentration across the membrane (voltage spike; μM) vs timestamp. **(B)** Input neurotransmitters to the neuron (μM) vs timestamp corresponding to various input bands. **(C)** Krebs cycle activity (NADH produced in μM/timestamp) vs timestamp. **(D)** Total intracellular ATP concentration (μM) vs timestamp.

our simulations of a defective neuron (**Figure 2**), it was found that the Krebs Cycle Activity (**Figure 2C**) increased. However, a corresponding drop in ATP concentration (**Figure 2D**) was observed. Spiking activity was prevalent for the initial 200 time stamps, followed by a breakdown of ionic concentration gradients (**Figures 2A–D**). These results are discussed in the Section "Discussion."

DECREASED ACTIVITY OF ELECTRON TRANSPORT CHAIN

When the decrease in the activity of the Electron Transport Chain was considered in isolation, excluding the effect of increased rate of formation of Oxide ions (O^{2-}), breakdown of ionic concentration gradient was observed, however, it took a longer time when compared with the results obtained from the Alzheimer's neuron affected by the combination of both the parameters – decreased activity of ETC and increased superoxide production (**Figure 3**).

INCREASED RATE OF FORMATION OF OXIDE IONS

When the increase in rate the formation of superoxide anion radicals was considered in isolation, excluding the effect of decrease in the activity of ETC, breakdown of ionic concentration gradient was observed, however, it took a longer time when compared with the results obtained from the Alzheimer's neuron affected by the combination of both the parameters – decreased activity of ETC and increased superoxide production and shorter time than results obtained from the decreased activity of ETC (**Figure 4**).

WAVELET ANALYSIS

The Fourier transform has been traditionally used for various signal analysis, but it only gives the frequency–amplitude relationship

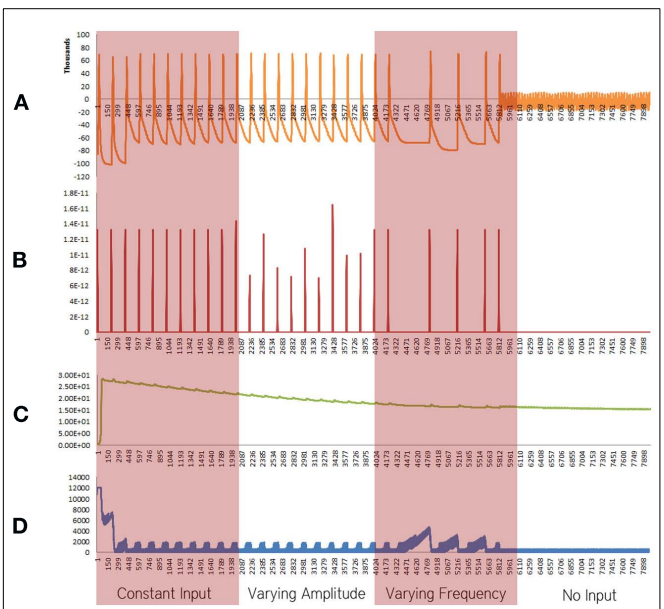

FIGURE 4 | Simulation results using the energetics based single neuron simulator, for a pyramidal neuron over four stages of input affected by an increased formation of oxide ions. (A) Ionic concentration across the membrane (voltage spike; μM) vs timestamp. **(B)** Input neurotransmitters to the neuron (μM) vs timestamp corresponding to various input bands. **(C)** Krebs cycle activity (NADH produced in μM/timestamp) vs timestamp. **(D)** Total intracellular ATP concentration (μM) vs timestamp.

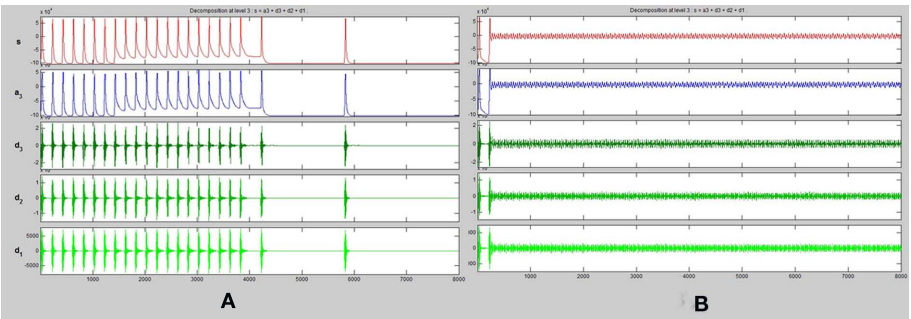

FIGURE 5 | One dimensional wavelet transform (up to three frequency levels) of spike trains obtained from (A) energetics based simulation of a healthy pyramidal neuron. (B) Energetics based simulation of a pyramidal neuron affected by Alzheimer's disease.

of the given signal. It throws no light on the time–frequency variations present in the signal.

This Achilles' heel is overcome with the use of Wavelet transforms (Tsodyks et al., 2000; Sklar, 2001), by using a varying scale window function, we are able to obtain a time–frequency analysis of the signal. Here the high frequency components are analyzed with a high time resolution and a low frequency resolution while the low frequency components are analyzed with a low time resolution and high frequency resolution.

A one dimensional wavelet transform resolved to three frequency levels is applied to the spike train of both the healthy and diseased simulated neurons. We compare the results of this transformation (**Figures 5A,B**)

It can be observed that across all input conditions, the wavelet transformation of the diseased neuron (**Figure 5B**) indicates a complete lack of activity as compared to that of the healthy neuron (**Figure 5A**). The reasons and implications of this observation are discussed in detail in Section "Discussion."

MATERIALS AND METHODS

A Petri-net based environment was adopted to model the various biophysical processes using applied stochastic differential equations. The places represent the concentration of reactants and products, while the transitions capture the kinetics of the biophysical and biochemical reactions. A single neuron Petri-net model realizes biological concepts such as the Krebs Cycle Activity, Electron Transport Chain, and Oxidative Phosphorylation, etc.

We shall now go on to describe the various biochemical pathways considered in the model. We leave out housekeeping activities of the neuron since these processes are highly dependent on the DNA and DNA transcription rates. As we do not have a model for this at the present, we shall be implementing these models in the future.

ATP CONSUMING PATHWAYS

Restoration of ionic gradients in the post-synapse

When neurotransmitters from the cleft dock on AMPA receptors present on the post-synapse, the receptors open up and allow Na^+ ions to move in. As the voltage increases (caused by this increased Na^+ gradient), the Mg^{2+} ions which block NMDA channels get released leading to increased calcium ions influx.

CaMKII present in the synapse is activated by the calcium ions. CaMKII, when activated increase the number of AMPA receptors and also increase their *open* time by phosphorylating them. This helps bring about Long-Term Potentiation.

When the synapse is activated for a continuous period of time, the G-Proteins are also activated. The G-Protein upon activation activates both the IP3 and the DAG. Activated IP3 leads to the release of calcium stored in the endoplasmic reticulum. DAG activates PKC, which then attaches itself to the AMPA receptors and decreases the number of AMPA receptors by internalizing them. This helps bring about Long-Term Depression (Hayashi et al., 2000; Attwell and Laughlin, 2001; Linden, 2001; Yu et al., 2001; Weber et al., 2003; Steinberg et al., 2004; Remy and Spruston, 2007).

Due to the influx of sodium and calcium ions, the gradient has been lost and must be restored. This is an energy consuming process. These activities of the synapse have been modeled by us. The mathematical model formed to represent these pathways will be detailed later in this section.

Restoration of ionic gradients in the soma

This inflow of sodium and calcium ions will lead to a Voltage Spike if the voltage generated exceeds a threshold level. This threshold will lead to the opening up of the voltage gated sodium and potassium ion channels which cause spike propagation (Kandel et al., 1991). Restoration of these ionic gradients in the soma is also an ATP consuming process.

Packaging of neurotransmitters inside vesicles by Golgi apparatus and pumping the vesicles with H^+ ions

The packaging of the neurotransmitters inside vesicles by Golgi apparatus is an energy consuming process. The vesicles have to be pumped with H^+ ions in order to create a gradient so that the neurotransmitters in the pre-synaptic site leave the neuron with a particular force. This enables them to make it across the synaptic cleft and hence dock onto the receptors on the post-synaptic neuron (Südhof, 2004).

Absorption of neurotransmitters from the synaptic cleft by the glial cells

The neurotransmitters are active at the post-synaptic site only for a short interval. After this the neurotransmitters are absorbed by the glial cells. The glial cell absorbs them based on the sodium

concentration difference present between the extracellular and intracellular part of the glial cell. The greater concentration of sodium outside the glial cell pushes the neurotransmitters into the glial cells where they are recycled and sent back to the neuron. In order to restore the sodium gradient ATP is required.

Over the years there has been a drastic change in the view of what role glial cells play in the central nervous system. Once thought of as just passive members of the CNS providing a supporting framework to a network of neurons, new evidence suggests that the glial cells are involved in higher level activities such as plasticity regulation of synapses and recycling of the neurotransmitter glutamate released by the synapse. This glutamate absorbed by the glial cells gets converted to glutamite. This glutamite is released back to the neuron, which is then reconverted to glutamate. Thus glial cells have been known to be suppliers of neurotransmitter glutamate to the neuron. As scientific estimates show that glial cells account for only maximum 20% of total neuronal glutamate, we decided to exclude the recycling of neurotransmitters from the pilot simulation. Thus the glial cells play a minimal role in our model. Their only main function is to absorb the glutamate released into the cleft. The recycling process has not yet been modeled. However even though it accounts for only a maximum of 20% of neurotransmitters the neuron–glial interactions cannot be ignored and will be incorporated along with their role in plasticity regulation and calcium waves (Tsodyks et al., 2000; Schulman and Rothman, 2004; Sherwood et al., 2006; Volman et al., 2007; Cloutier et al., 2009).

MITOCHONDRIAL RESPIRATION PATHWAYS

Calcium exchange between endoplasmic reticulum and mitochondria

When the IP3 molecules dock on the endoplasmic reticulum (ER) due to repeated synaptic activity, the calcium reserves of the ER are released, which is then absorbed by the mitochondria. Absorption of calcium by the mitochondria increases its rate of respiration by depolarization of the mitochondrial membrane. This is one way in which the mitochondria are able to sense the increase in activity of the neuron (Yu et al., 2001; Weber et al., 2003; Steinberg et al., 2004; Remy and Spruston, 2007).

Adenosine mono-phosphate activated protein kinase enzyme

The AMPK is known as the master switch or the master regulator. AMPK has been identified as a key metabolic regulator in the neuron. It senses the difference between the ATP and AMP concentration levels. The AMPK has two binding sites. When the ATP concentration is very high (i.e., the cell is inactive) both the binding sites are occupied by ATP which renders the AMPK inactive. However during periods of high frequency neuronal firing/activity, the ADP formed does not recycle back to ATP quick enough. In this case, ADP molecules begin reacting with each other. Two ADP molecules combine together, leading to the formation of one molecule each of AMP and ATP. This process is favored only under high stress. This is because it is *almost* impossible to recycle the AMP back to ATP. However, this process is faster than the normal Krebs cycle.

$$ADP + ADP \Leftrightarrow ATP + AMP$$

Thus as the AMP concentration increases, the AMPK gets activated as both the docking sites are now occupied by AMP. Upon activation, the AMPK simultaneously increase the rate of Beta Oxidation and increases the number of glucose transporters available. The Beta Oxidation of the fatty acids increases the hydrogen ion gradient. Beta oxidation is not a major process in the brain but it does exist. And we believe if we are going to model the energetics of the single neuron it is a good idea to include these processes even if it has a negligible effect as long as they exist, and we can get data about them. To take this into consideration the Beta oxidation process in our simulations was not anyway a major producer of ATP and compared to the actual Krebs cycle it was much smaller. Moreover due to the increase in the glucose transporters more glucose is transported to the neuron, thus it can produce more ATP (Hayashi et al., 2000; Zong et al., 2002; Jäger et al., 2007).

Uncoupling protein

The UCP is a mitochondrial transport protein present in the inner membrane of the mitochondria (Rousset et al., 2004). It is activated by high superoxide concentration. Superoxides are formed by complexes I and III in the respiratory chain through a non-enzymatic process. These superoxides are highly reactive and can lead to cell death (Turrens, 1997). To prevent the toxic effects of the superoxide anion radical ion, Manganese Superoxide dismutase catalyze the dismutation of superoxides into oxygen and hydrogen peroxide. The hydrogen peroxide, formed as a result of the redox reaction is further reduced to water by glutathione peroxidase. As the Krebs cycle rate increases, so does the superoxide formation. At some point the rate of superoxide formation increases beyond the rate at which MnSOD and glutathione peroxidase can detoxify them to water. This is when the UCP comes into play. It is activated by the Superoxides and opens up. H^+ ions will now flow through the opening created by the UCP (Echtay et al., 2002). This leads to the *short-circuiting* of the ATPase enzyme. Activation of the UCP and its functioning as a proton carrier results in a thermogenic process where the oxidation energy is dissipated as heat, enhancing, and stimulating respiration (Turrens, 1997; Rousset et al., 2004).

PETRI NETS BASED MODELING

We shall now view the mathematical Petri nets based model that is used to represent these various biochemical pathways. **Figures 6**, **8**, and **9** represent the Petri net system divided into various sections. As explained earlier, the places represent parameter concentrations, activation levels, and rate depending on the context. The transitions represent the various equations used to model the relations. To maintain the brevity of this paper, the transition equations and Initial Ionic Concentrations are not mentioned here. However, the equations and Initial state conditions (concentrations) used may be viewed online at http://www.warftindia.org/equations.pdf.

Synaptic cleft and post-synaptic dynamics

The input to the neuron is through the place titled neurotransmitter input. Neurons have excitatory synapses in their apical dendrites and inhibitory synapses on their basal dendrites. For a given neurotransmitter input the ratio of excitatory synapses activated to

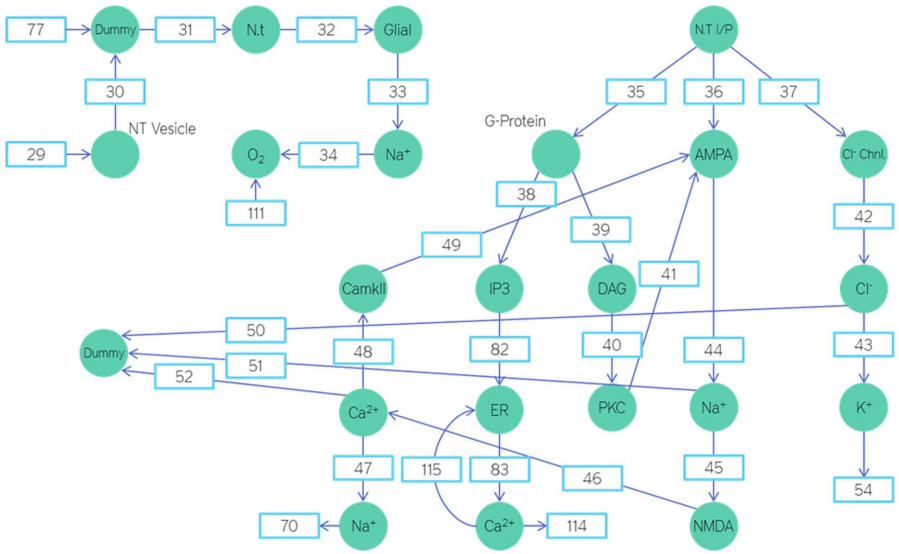

FIGURE 6 | Petri nets based energetics model depicting the post-synapse and glial cells.

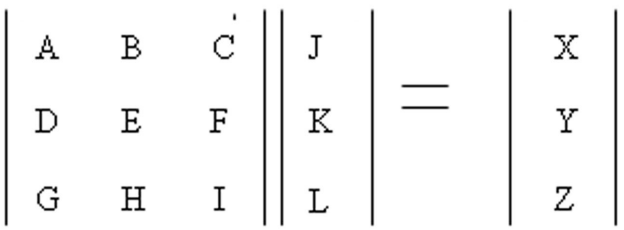

FIGURE 7 | Transition probability matrix.

inhibitory synapses activated is 7:2. A 10th of the neurotransmitter input is used to activate the G-Proteins (**Figure 6**).

The AMPA receptors upon activation give rise to an influx of Na^+ ions. This influx was modeled using a transition probability matrix. In **Figure 7**, the matrix on the left is the transition probability matrix and the one in the middle is the conditional probability matrix. The matrix to the extreme right is the dwell time matrix.

The elements in the first row of this matrix represent the probability of making a transition from a given state (This is determined by the element number. For example the letter C represents the third state of conduction) of ion channel conduction to the first state namely the closed state.

The elements of the second and third row represent the same thing except it is for their respective states namely the half open (second state) and the fully open (third state).

The matrix in the middle has elements which represent the conditional probability. Its values represent the probability of being in that particular state. Thus the product of these two matrices gives rise to the dwell matrix. It represents the probability of finding the ion channel in a given conducting state in the next instant of time. Multiplication of each state probability with its conductance gives rise to total conductance of the channel in the next instance of time (Keizer, 2002; Beard and Qian, 2008). Similarly, the AMPA and Chlorine channels were modeled this way.

The G-protein upon release diffuses into the cell fluid and docks on the IP3 and DAG proteins activating them. IP3 upon activation sits on the endoplasmic reticulum and releases the internal calcium reserves. The released calcium ions activate the CaMKII. The CaMKII then phosphorylate the AMPA receptors, increasing the time they spend in the open state and their numbers.

Similarly the DAG upon activation diffuses into the cell fluid and docks on the PKC activating it. Upon activation the PKC attaches itself to the AMPA receptors and internalizes them.

Each of these transitions has been modeled such that the new product formed is equal to the amount of substrate released.

The chlorine ions that enter the neuron from the synaptic cleft are transported out with the help of the potassium gradient. This fall in potassium gradient is then restored by the ATPase pump. Similarly the Sodium–Calcium exchanger pushes the calcium out and the sodium in. This sodium is then pushed back out using the ATPase pump. The restoration of the Sodium–Potassium gradient consumes ATP. The equation to govern this ATP consumption will be explained subsequently.

In our model the plasticity effects on the AMPA receptors are brought about by the CaMKII. As the calcium concentration inside the cell increases so does the number of activated CaMKII.

Based on the amount of activated CaMKII the time in each element of the array for the AMPA channels was changed. As the CaMKII concentration increased the time spent in the open state of the AMPA channel was increased and that in the closed state was correspondingly decreased.

Similarly based on the amount of activated PKC the time in each element of the array for the AMPA channels was changed. As the PKC concentration increased the time spent in the open state of the AMPA channel was decreased and that in the closed state was correspondingly increased.

This was how we brought in the plasticity variation of synapses.

The equation used is like an AND function. Only if there are three or more sodium ions and two or more potassium ions, will the equation return true. And whenever it does, an ATP is consumed and three sodium ions are transported outside and two potassium ions are transported inside. The time dependency of this process has not yet been studied by us. Hence we have assumed it to be a time independent or instantaneous process. However it will be improved in the future.

The endoplasmic reticulum releases calcium. The endoplasmic reticulum is where the ribosomes are attached. The ribosomes are the organelles where the various proteins in the body are manufactured. The ribosomes attach themselves to the rough endoplasmic reticulum. The endoplasmic reticulum consists of two parts, the rough endoplasmic reticulum and the smooth endoplasmic reticulum. The smooth endoplasmic reticulum is a store house of calcium ions.

The endoplasmic reticulum is known to play a role in the regulation of synaptic plasticity. When the IP3 protein is activated it will sit on the receptors on the surface of the smooth endoplasmic reticulum. When this happens the channels connected to the receptors open up and calcium ions are released. These calcium ions are crucial in the strengthening of synapses.

The endoplasmic reticulum also plays an important role in increasing the Krebs cycle rate in response to activity. Under physical duress when the ATP demand is high, the mitochondrial respiration should be increased. One of the ways to increase mitochondrial respiration rate is through the endoplasmic reticulum. When the endoplasmic reticulum releases calcium it is absorbed by the mitochondria. The calcium absorbed by the mitochondria depolarizes its membrane, leading to increased ETC activity (Jouaville et al., 1999; Arnaudeau et al., 2001; Parekh, 2003).

The mitochondria and endoplasmic reticulum interact through calcium ion exchange. The calcium released by the endoplasmic reticulum is absorbed by the mitochondria. This calcium is then again released by the mitochondria. This will then be re-absorbed by the endoplasmic reticulum. In this fashion gradually reducing calcium waves are set up between the two organelles.

The NMDA receptors are blocked by magnesium ions. They can start conduction only if this magnesium block is relieved by heavy sodium influx.

Mitochondrial regulation

The ATP is consumed when the ATPase pumps try to restore the ionic gradients. They are also consumed while pumping the neurotransmitter vesicles with hydrogen ions, in order to package the neurotransmitters. This is why there is a transition from the Golgi apparatus to the ATP (Shulman and Rothman, 2005). Simultaneously the number of ADP produced is also increased (**Figure 8**).

Thus the only change here is that as the Golgi activation increases so does the number of ADP.

The number of Golgi apparatus activated depends on the number of neurotransmitters produced by the Krebs cycle at a particular instant. It represents how the Golgi apparatus activity changes per neurotransmitter packaged. For the time being due to a lack of experimental evidence we are assuming such processes to be linear time variant. As we garner more information through experiments our models will also improve to incorporate this new information.

The neurotransmitters are produced from the alpha-ketoglutarate in the Krebs cycle. This is a chemical reaction and the proportionality constant is calculated from the Gibbs free energy value.

The ATP is produced by the ATPase enzyme using the ADP and the H^+ ions. Only if the H^+ ions have a high enough concentration can enough energy be provided to the ATPase enzyme to produce the required ATP. Thus as the H^+ and Ca^{2+} gradient increases the amount of ATP produced also increases.

Consider the equation,

$$ADP + ADP \Leftrightarrow AMP + ATP$$

The Gibbs free energy for ADP + ADP is calculated and using this, the rate reaction constant is obtained. The amount of ATP produced will be equal to amount of AMP produced. This AMP is used to activate the AMPK (metabolic switch). This process is also modeled using a linear differential equation. This AMPK activation leads to the phosphorylation and hence inhibition of acetyl CoA carboxylase.

The inhibition of acetyl CoA carboxylase leads to the inhibition of malanoyl CoA carboxylase production. Inhibition of malanoyl CoA carboxylase leads to an increase in the number of CPTI enzymes which move across the mitochondrial membrane and increase the transport of fatty acids into the mitochondria. These fatty acids are then broken down by Beta Oxidation to increase the number of NADH and FADH2.

The above modeled reactions are all part of the Beta Oxidation process and will be modeled in greater depth in the future. As of now a more simplistic approach has been adopted due to the lack of knowledge on the precise dynamics and all the contributing factors (Jäger et al., 2007).

Adenosine mono-phosphate activated protein kinase also increases the number of glutamate transporters and hence increases the amount of glucose transported into the neuron.

The increase in the amount of glucose transporter production will definitely involve an increase in the transcription rate of the DNA. As our nucleus model is still in the development phase there is no way of incorporating the chemical pathway which eventually increases the rate of glucose transporter transcription. Moreover the chemical pathway linking the increased AMPK activation to the increase in transcription of glucose transporter is not yet known. That is why we have a simplified equation to govern the increase in glucose transporters.

This motion of glucose transporters and CPTI enzymes across the membrane is done using the Michaelis–Menten kinetics (Beard and Qian, 2008).

The increase in glucose leads to an increase in pyruvate. This is modeled using the Gibbs free energy of pyruvate production. The increase in pyruvate leads to an increase in Acetyl CoA. This is also modeled using Gibbs free energy.

This is based on the fact that longer the molecule, lower the stability, and hence faster the cleaving of two carbon atoms. But as the length of the fatty acid decreases the rate at which it is

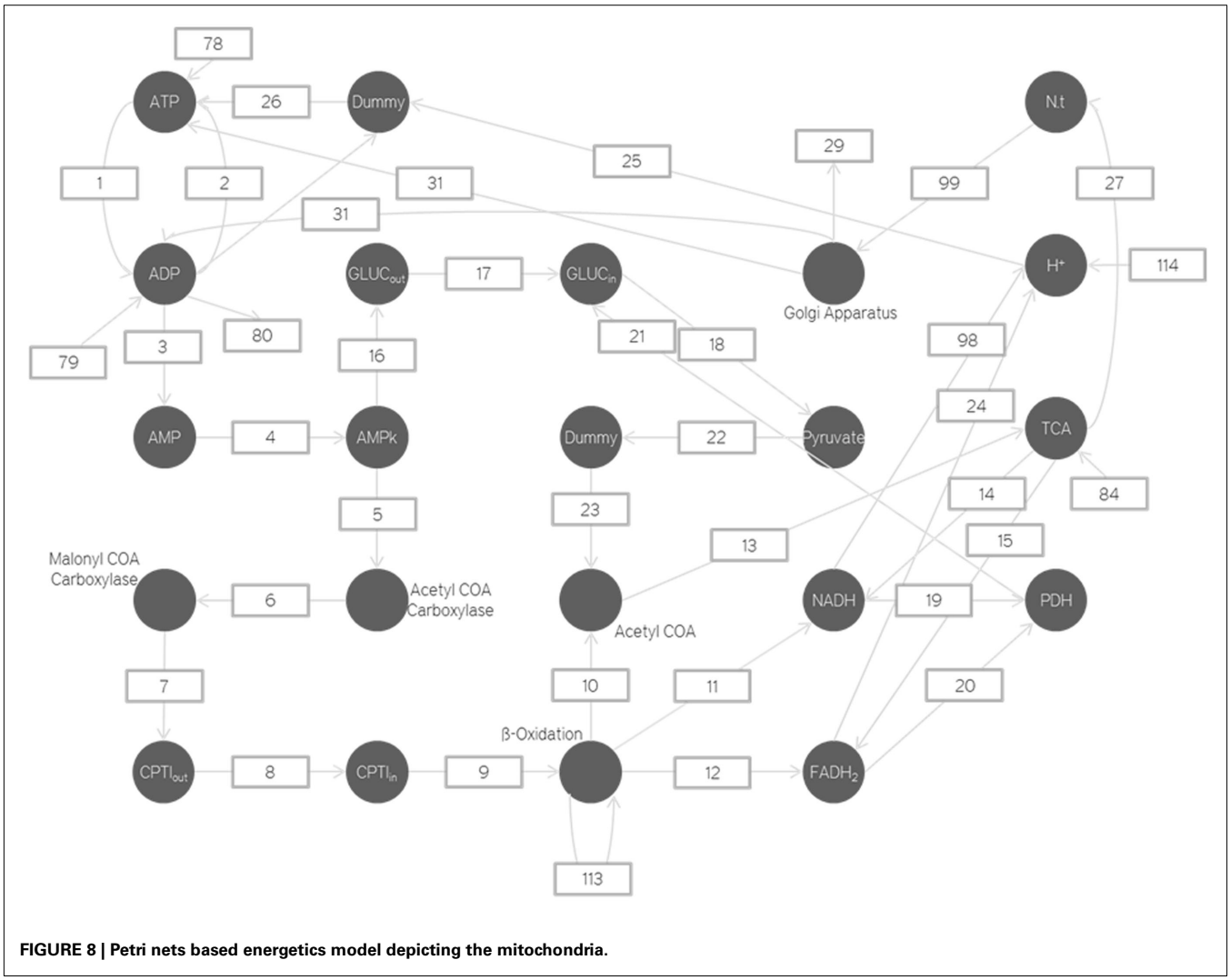

FIGURE 8 | Petri nets based energetics model depicting the mitochondria.

broken down also decreases. The FADH2, NADH, and acetyl CoA produced depend directly on the amount of fatty acid produced.

The Krebs cycle rate increases with the amount of Acetyl CoA produced. This increase is modeled using the Gibbs free energy for acetyl CoA to citrate. The rate of formation of the NADH and FADH2 is modeled using the Gibbs free energy obtained from the transition malate to oxaloacetate. This is the transition responsible for the rate of H^+ ions released. So based on the rate of this reaction we determine the rate of formation of NADH and FADH2. The H^+ ions formation from FADH2 and NADH is also modeled using the Gibbs free energy for releasing the H^+ ions. The NADH and FADH2 inversely affect the amount of PDH. They are PDH inhibitors.

The currents generated due to the sodium, calcium, and chlorine influx in the pre-synaptic sites are added up and the net voltage generated due to them is calculated. This voltage generated is then passed to the voltage gated sodium, potassium, and chlorine channels. The number of ion channels activated will depend on the magnitude of the voltage due to the synaptic currents. It is assumed to be linearly dependent. The influx of ions is used to calculate the Voltage Spike. The equation used to govern this process is the Langevin equation inspired transporter equation (Schuss et al., 2001; Keizer, 2002; Beard and Qian, 2008). The Voltage Spike is used to calculate the number of calcium channels that are open. The calculation of Voltage Spike has been discussed earlier. The number of calcium channels is used to determine the number of calcium ions based on the conductance of each ion channel. This process is also implemented by the Langevin inspired transporter equation (Schuss et al., 2001; Keizer, 2002; Beard and Qian, 2008). The number of neurotransmitters released depends on the amount of activated SNARE proteins which in turn depends on the amount of calcium ions.

Spike activity and pre-synaptic dynamics

Similarly the amount the number of ROS generated is considered directly proportional to the amount of H^+ ions generated. Where we could not scientifically determine a rate constant a value of 0.1 was chosen. A part of these oxygen ions is detoxified by the mitochondrial MnSOD and converted to less reactive water. But a part of these oxygen ions are also used to activate the UCP (**Figure 9**).

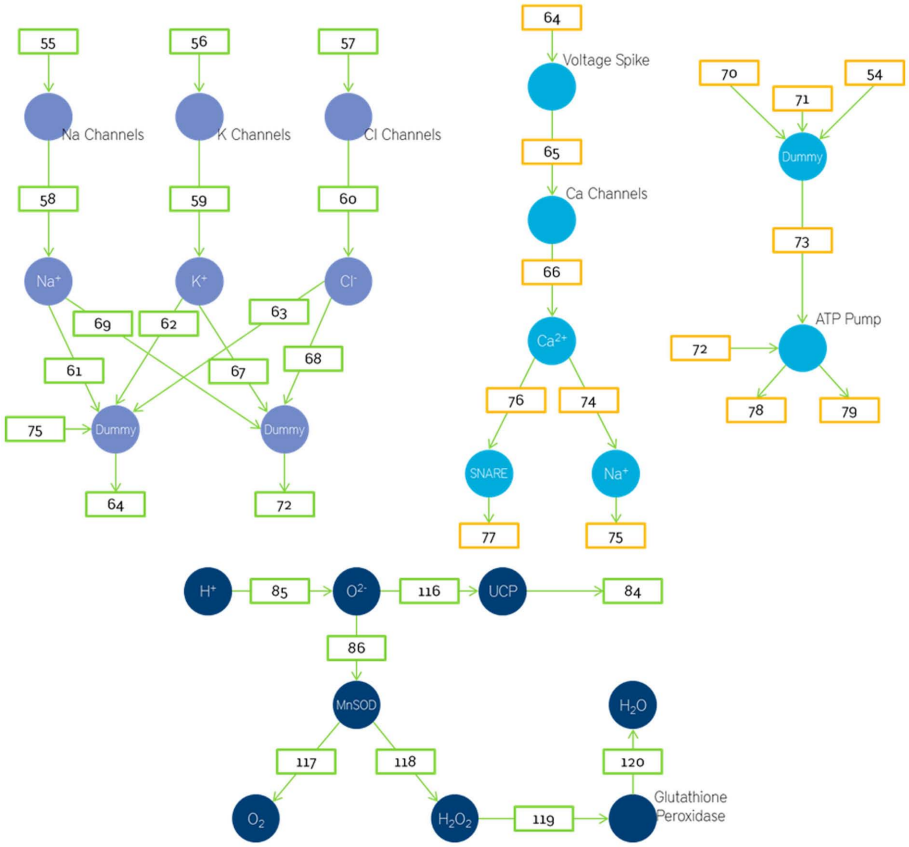

FIGURE 9 | Petri nets based energetics model depicting the pre synapse and spike generation.

The number of output neurotransmitters will depend on the amount of activated SNARE and the number of vesicles. Assuming there is approximately 1 SNARE protein per vesicle the number of output neurotransmitters will be determined by whichever of the two (vesicles or SNARE) is smaller.

The number of activated glial cells will vary linearly with number of neurotransmitters in cleft. This is then assumed to cause a linear decrease in number of sodium ions. As this leads to a loss in the gradient the amount of oxygen required is also increased. Thus the oxygen required depends on both the acetyl CoA and sodium ions used up. In this model we have used a place called dummy. Dummy is used when the number of fan-ins is more than the number of fan-outs. In such cases we store the fan-ins in dummy and then execute the function. This is done to maintain the property that edges are alone transitions.

We are aware that there are more biochemical pathways that regulate mitochondrial respiration. However we have at present only considered the pathways mentioned above. In the future, we will be expanding our model to include the nucleus, transcription rates of proteins, housekeeping activities, and in-depth models of the Endoplasmic Reticulum, Peroxisome, and Golgi apparatus.

The modeling of the various biochemical reactions in the model was done based on the Gibbs free energies of the respective reactions. The rate constants for these biochemical reactions were calculated from the Gibbs free energy values.

However while modeling the biophysical processes several difficulties were faced when trying to determine the values for the various constants, used in the equations.

This problem was particularly pronounced when voltage gated ion channels, the contribution of calcium to the increase in electron transport chain, uncoupling protein activation, DAG activation, PKC activation, and CaMKII activation were being modeled. The problem stemmed from the lack of experimental data that quantified how sensitive one parameter was to another.

To be more precise, we could not find data that indicated how many ion channels per unit area are activated for a 1-mV increase in the voltage difference across the membrane or at the least if this dependency was non-linear or linear by nature. Similarly the contribution of calcium to the increase in the rate of electron transport chain was also unknown. Likewise for the synaptic parameters (Südhof, 2004) listed above.

In such cases a method of repeated simulations and analysis was adopted to obtain a realistic voltage spike. Repeated simulations were carried out to compare the output of the model to the experimental values and to get the appropriate rate constants in our simulator. We are also working on modeling the inter relation of heat with chemical reactions as we believe this would be

a key to study thermogenic processes**.** Presently we are modeling the rate constants as a function of temperature and pH and will be incorporating it into the energetics model in the near future.

DISCUSSION

The graphs indicate, the activity of the Krebs cycle directed toward spike generation, without taking into consideration housekeeping activities. The results obtained from the simulation indicate a healthy correlation between the Krebs Cycle Activity and the spiking activity of the neuron. Further, a significant correlation between the Krebs Cycle Activity and intracellular ATP concentration was observed. ATP is consumed quickly during the voltage spike, and rises immediately after the Krebs Cycle Activity increases. When the neurotransmitter input was removed, the ATP gradually restores itself to its equilibrium condition.

Our preliminary effort toward disease modeling considers Alzheimer's disease as a combination of two factors, decrease in the activity of the Electron Transport Chain (Mattson et al., 2008) and an increased formation of Oxide ions (Mattson et al., 2008) Other parameters such as a large increase in intracellular and mitochondrial calcium have been identified (Mattson et al., 2008) .However; the model in its current state cannot accommodate the variations of these parameters. Thus, further work at WARFT, is directed toward expanding the model and thus increasing its ability to accurately model diseases.

The simulations of a diseased neuron, in its preliminary form, indicate complete breakdown of the ionic concentration gradient across the neuronal membrane. This is due to severe inhibition of the ATP Synthase Enzyme which inhibits the activity of the ATP Pump. We believe that experimentations to capture the spike train of a defective single neuron could produce similar voltage spikes.

An important consideration in disease modeling is the quantitative variation in the considered parameters. Due to lack of accurate experimental data, we are forced to quantify this variation with assumptions. We find that even a small change in amplitude of this variation affects the severity of its deviation from that of healthy neurons. Since the model is still in its pilot phase, we are currently working on expanding the model to include all parameters that are responsible for such diseases. This would aid us in working on disease modeling using a method of optimization to quantify the deviation of rate constants dependencies described in detail at the end of this section.

As the voltage spike in the model is a function of the neuronal energetics through several biophysical and biochemical processes, we hope to be able to predict the concentrations of the various intracellular parameters and the nature of the various reactions taking place within the neuron based on the spike output of the integrated energetics model.

No doubt, this will pave the way for non-invasive testing of patients for diseases and could possibly be used in the future for accurate modeling of diseases. Such a model also promises several benefits toward a non-invasive simulation technique for drug testing and discovery.

A study in the potency of the drug could be done with no danger to the patient using such a model and its subsequent simulation. A time–frequency analysis of both the healthy and diseased simulated neuron can taken (**Figure 5**). Further, a neuron can be tested to see whether it is in a degenerate state or not by taking a time–frequency analysis of its spiking activity and comparing it with those of the simulated neurons. If there is a high correlation with that of the healthy simulated neuron it would indicate that the neuron is not degenerate.

The model that has been discussed in this paper relates the spike activity of a single neuron to its energetics. We would no doubt like to extend the single neuron model to a network level. The results that we get by studying a network of neurons would be comparatively simpler to verify experimentally than that of a single neuron because of the current limitations in experimental methods. Moreover the devastating effect of a disease are felt only when a network of degenerate neurons are considered as compared to a single degenerate neuron.

However, there were several practical difficulties that were encountered while trying to extend to a network model**.** The most significant being the lack of experimental data detailing the spatial distribution of mitochondria and other such organelles and chemicals within the neuron. As such information could not be found, a lumped model for the mitochondria and various intracellular chemicals, proteins such as voltage gated ion channels, ligand gated ion channels etc., was developed. To develop a network model we would in particular need precise and accurate information on the distribution of inhibitory and excitatory receptors on the dendritic tree. However as this information was hard to come by the ion channels were modeled lumped in nature. Needless to say a lumped ion channel model would make the spatio-temporal summation of input by dendrites (an essential feature of a network of neurons), impossible to bring in, thereby negating the very essence of a network of neurons.

Another important simplification we have made is with respect to the rate constants. With more than 80 interdependent parameters in our model the rate constants governing the various biochemical reactions take up a pivotal role. As explained earlier, these values were obtained by a process of repeated simulation and analysis.

Current work at WARFT aims at integrating this Voltage-Spike Energetics Model to a network of neurons generated in a neurogenesis inspired structure generation manner. The biochemical signaling pathways responsible for the growth of neurons are linked with the geometrical properties of the neuronal network. The cell growth and division, neurite outgrowth, axon selection and guidance, synapse and spine formation, and other anatomical parameters are modeled as function of the concentration of proteins and enzymes responsible for their development (Venkateswaran et al., 2011). In this regard, deeper models that investigate the distribution and movement of mitochondria within a neuron, distribution of ion channels across the neuronal surface and a spike propagation model that combines both these models are being simultaneously investigated.

As explained earlier, the unavailability of detailed information regarding the positioning and distribution of various organelles and chemicals and their inter relationship hold back the model. Thus immediate work aims at developing a robust optimization paradigm that would effectively optimize

these parameter values as a function of the voltage spike. A two level Simulated Annealing – Game Theory optimization approach is being currently investigated based upon. (Mohan, 2008).

COMPUTATIONAL ASPECTS

A framework for large scale simulation is presented here. A hyper graph data structure captures the neuronal network information. The hyper nodes and hyper edges represent the neurons and their synaptic connectivity while the sub level nodes and sub level edges represent the neuronal parameters and their dependency relations. The energetic based simulation is currently being executed over an arbitrary neuronal network which can be tuned to a specific connectivity.

At every timestamp, a centralized control triggers execution of energetics model across partitions of neuronal network. Within a neuronal partition, the computations performed and communications established are in parallel (Ramanathan, 2011).

Deeper investigation into simulation techniques to decide on event driven or data driven, centralized or distributed controls etc., are currently under research.

The parallel environment for the large scale simulation is facilitated by a hierarchy of host and node processes (Venkateswaran et al., 2008).

The intra and inter regional synaptic connectivity (communications within and across partitions) contribute to the communication complexity while computationally significant single neuron models capturing the dynamics spanning from molecular, cellular, and network levels contribute to the computational complexity. The enormity lies in managing these high communication and computational complexities pertaining to a dynamic system.

This research initiative demands a global database of experimental results and deeper experiments to capture energetic parameters. The enormity of this project calls for global support.

ACKNOWLEDGMENTS

We would like to extend our heartfelt thanks to the two reviewers whose comments and suggestions enhanced the quality of this research. We would also like to thank Dr. Yuri Zilberter, Editor of this research topic for encouraging our work. Further, We are thankful to the Frontiers Foundation for providing us with a complete waiver for the publication of this paper.

REFERENCES

Arnaudeau, S., Kelley, W. L., Walsh, J. V. Jr., and Demaurex, N. (2001). Mitochondria recycle Ca(2+) to the endoplasmic reticulum and prevent the depletion of neighboring endoplasmic reticulum regions. *J. Biol. Chem.* 276, 29430–29439.

Attwell, D., and Gibb, A. (2005). Neuroenergetics and the kinetic design of excitatory synapses. *Nat. Rev. Neurosci.* 6, 841–849.

Attwell, D., and Laughlin, S. B. (2001). An energy budget for signaling in the grey matter of the brain. *J. Cereb. Blood Flow Metab.* 21, 1133–1145.

Babinec, P., and Babincov, M. (2002). Spatial distribution of ion channel activity in biological membranes: the role of noise. *Bioelectrochemistry* 56, 167–170.

Baker, H. L., Errington, R. J., Davies, S. C., and Campbel, A. K. (2002). A mathematical model predicts that calreticulin interacts with the endoplasmic reticulum Ca2+–ATPase. *Biophys. J.* 82, 582–590.

Beard, D. A., and Qian, H. (2008). *Chemical Biophysics: Quantitative Analysis of Cellular Systems.* Cambridge: Cambridge University Press.

Buchholtz, F., Golowasch, J., Epstein, I. R., and Marder, E. (1992). Mathematical model of an identified stomatogastric ganglion neuron. *J. Neurophysiol.* 67, 332–340.

Cloutier, M., Bolger, F. B., Lowry, J. P., and Wellstead, P. (2009). An integrative dynamic model of brain energy metabolism using in vivo neurochemical measurements. *J. Comput. Neurosci.* 27, 391–414.

Duchen, M. R. (2000). Mitochondria and calcium: from cell signalling to cell death. *J. Physiol. (Lond.)* 529, 57–68.

Echtay, K. S., Murphy, M. P., Smith, R. A. J., Talbot, D. A., and Brand, M. D. (2002). Superoxide activates mitochondrial uncoupling protein 2 from the matrix side. *J. Biol. Chem.* 277, 47129–47135.

Fienberg, S. E. (1974). Stochastic models for single neuron firing trains: a survey. *Biometrics* 30, 399–427.

Fitzhugh, R. (1955). Mathematical models of threshold phenomena in the nerve membrane. *Bull. Math. Biophys.* 17, 257–278.

Green, D. R., and Green, D. R. (2005). Apoptotic pathways: ten minutes to dead. *Cell* 121, 671–674.

Hardy, J., and Selkoe, D. J. (2002). The amyloid hypothesis of Alzheimer's disease: progress and problems on the road to therapeutics. *Science* 297, 2209.

Harrison, L. M., David, O., and Fritson, K. J. (2005). Stochastic models of neuronal dynamics. *Philos. Trans. R. Soc. Lond. B Biol. Sci.* 360, 1075–1091.

Hayashi, Y., Shi, S. H., Esteban, J. A., Piccini, A., Poncer, J. C., and Malinow, R. (2000). Driving AMPA receptors into synapses by LTP and CaMKII: requirement for GluR1 and PDZ domain interaction. *Science* 287, 2262–2267.

Hirai, K., Aliev, G., Nunomura, A., Fujioka, H., Russell, R. L., Atwood, C. S., Johnson, A. B., Kress, Y., Vinters, H. V., Tabaton, M., Shimohama, S., Cash, A. D., Siedlak, S. L., Harris, P. L., Jones, P. K., Petersen, R. B., Perry, G., and Smith, M. A. (2001). Mitochondrial abnormalities in Alzheimer's disease. *J. Neurosci.* 21, 3017–3023.

Hodgkin, A. L., and Huxley, A. F. (1952). A quantitative description of membrane current and its application to conduction and excitation in nerve. *J. Physiol. (Lond.)* 117, 500–544.

Jäger, S., Handschin, C., St-Pierre, J., and Spiegelman, B. M. (2007). AMP-activated protein kinase (AMPK) action in skeletal muscle via direct phosphorylation of PGC-1α. *PNAS* 104, 12017–12022.

Jouaville, L. S., Pinton, P., Bastianutto, C., Rutter, G. A., and Rizzuto, R. (1999). Regulation of mitochondrial ATP synthesis by calcium: evidence for a long-term metabolic priming. *Proc. Natl. Acad. Sci. U.S.A.* 96, 13807–13812.

Kandel, E. R., Schwartz, J., and Jessell, T. (1991). *Principles of Neuroscience,* 4th Edn. New York: McGraw-Hill.

Keizer, K. (2002). *Computational Cell Biology.* New York: Springer Publications.

Linden, D. J. (2001). The expression of cerebellar LTD in culture is not associated with changes in AMPA-receptor kinetics, agonist affinity, or unitary conductance. *Proc. Natl. Acad. Sci. U.S.A.* 98, 14066–14071.

Mattson, M. P., Gleichmann, M., and Cheng, A. (2008). Mitochondria in neuroplasticity and neurological disorders. *J. Neurosci.* 60, 748–766.

Mogilevskaya, E., Demin, O., and Goryanin, I. (2006). Kinetic model of mitochondrial Krebs cycle: unraveling the mechanism of salicylate hepatotoxic effects. *J. Biol. Phys.* 32, 245–271.

Mohan, A. (2008). *The MMINi-DASS Simulator and its Application to Visual Pathway Connectivity Prediction.* [A thesis submitted to WAran Research FoundaTion]. Available at: http://www.warftindia.org/Ashutosh.pdf

Mohan, A., Nagarajan, V., Sekhar, S., Sharath, N. K., Thiagarajan, T. S., Ramanathan, S., and Kannan, D. (2010a). "Energetics based simulation of large-scale 3D neuronal network: energetics-based models," in *Frontiers Neuroscience Conference Abstract: Neuroinformatics 2010,* Kobe. doi: 10.3389/conf.fnins.2010.13.00092

Mohan, A., Nagarajan, V., Ramanathan, S., Sekhar, S., Thiagarajan, T. S., Kannan, D., and Sharath, N. K. (2010b). "Energetics-based simulation of 3D neuronal network: neurogenesis-inspired structure generation," in *Frontiers Neuroscience Conference Abstract: Neuroinformatics 2010,* Kobe. doi: 10.3389/conf.fnins.2010.13.00097

Oja, E. (1982). A simplified neuron model as a principal component analyzer. *J. Math. Biol.* 15, 267–273.

Parekh, A. B. (2003). Mitochondrial regulation of intracellular Ca2+ signaling: more than just simple Ca2+ buffers. *News Physiol. Sci.* 18, 252–256.

Rall, W. (1957). Membrane time constant of motoneurons. *Science* 126, 454.

Rall, W. (1959). Branching dendritic trees and motoneuron membrane resistivity. *Exp. Neurol.* 1, 491–527.

Rall, W. (1960). Membrane potential transients and membrane time constant of motoneurons. *Exp. Neurol.* 2, 503–532.

Ramanathan, S. (2011). *3D Neuronal Structure: Towards Generation, Simulation and Optimization for Brain Specific Region.* [A thesis submitted to WAran Research FoundaTion]. Available at: www.warftindia.org/Subbu.pdf

Remy, S., and Spruston, N. (2007). Dendritic spikes induce single-burst long-term potentiation. *Proc. Natl. Acad. Sci. U.S.A.* 104, 17192–17197.

Reutimann, J. A. (1999). Model of synaptic short-term plasticity and its adaptation.

Rousset, S., Alves-Guerra, M. C., Mozo, J., Miroux, B., Cassard-Doulcier, A. M., Bouillaud, F., and Ricquier, D. (2004). The biology of uncoupling proteins. *Diabetes* 53(Suppl. 1), S130–S135.

Schulman, R. G., and Rothman, D. L. (2004). *Brain Energetics and Neuronal Activity*. Chichester: Wiley.

Schuss, Z., Nadler, B., and Eisenberg, R. S. (2001). Derivation of Poisson and Nernst-Planck equations in a bath and channel from a molecular model. *Phys. Rev. E Stat. Nonlin. Soft Matter Phys.* 64, 036116.

Sherwood, C. C., Stimpson, C. D., Raghanti, M. N., Wildman, D. E. Uddin, M., Grossman, L. I., Goodman, M., Redmond, J. C., Bonar, C. J., Erwin, J. M., and Hof, P. R. (2006). Evolution of increased glia–neuron ratios in the human frontal cortex. *Proc. Natl. Acad. Sci. U.S.A.* 103, 13606–13611.

Shulman, R. G., and Rothman, D. L. (eds) (2005). *Brain Energetics, and Neuronal Activity*. Chichester: John Wiley and Sons Limited, 315.

Sklar, B. (2001). *Digital Communications: Fundamentals and Applications*. New Jersey: Prentice Hall.

Steinberg, J. P., Huganir, R. L., and Linden, D. J. (2004). N-ethylmaleimide-sensitive factor is required for the synaptic incorporation and removal of AMPA receptors during cerebellar long-term depression. *Proc. Natl. Acad. Sci. U.S.A.* 101, 18212–18216.

Südhof, T. C. (2004). The synaptic vesicle cycle. *Annu. Rev. Neurosci.* 27, 509–547.

Tsodyks, M., Uziel, A., and Markram, H. (2000). Synchrony generation in recurrent networks with frequency-dependent synapses. *J. Neurosci.* 20, RC50.

Turrens, J. F. (1997). Superoxide production by the mitochondrial respiratory chain. *Biosci. Rep.* 17, 3–8.

van Pelt, J., van Ooyen, A., and Uylings, H. B. M. (2001). "Modeling dendritic geometry and the development of nerve connections," in *Computational Neuroscience: Realistic Modeling for Experimentalists*, ed. E. De Schutter (Boca Raton: CRC Press), 179–208.

Venkateswaran, N., Elangovan, V. K., Ganesan, K., Sagar, T. R. S., Aananthakrishanan, S., Ramalingam, S., Gopalakrishnan, S., Manivannan, M., Srinivasan, D., Krishnamurthy, V., Chandrasekar, K., Venkatesan, V., Subramaniam, B., Sangkar, V., Vasudevan, A., Ganapathy, S., Murali, S., and Thyagarajan, M. (2008). "On the concept of simultaneous execution of multiple applications on hierarchically based cluster and the silicon operating system," in *IEEE International Symposium on Parallel and Distributed Processing, 2008*, Miami, FL.

Venkateswaran, N., Kabaleeswaran, D. K., Vignesh, S. R., Ramanathan, S., Jagathrakshakan, S. S., Narayanasamy, N., Sekhar, S., Krishnan, N. S., and Thiagarajan, T. S. (2011). "Single neuron development – a neurogenesis inspired structure generation model," in *Frontiers Neuroinformatics Conference Abstract*, Boston. doi: 10.3389/conf.fninf.2011.08.00162

Volman, V., Ben-Jacob, E., and Levine, H. (2007). The astrocyte as a gatekeeper of synaptic information transfer. *Neural. Comput.* 19, 303–326.

Weber, J. T., De Zeeuw, C. I., Linden, D. J., and Hansel, C. (2003). Long-term depression of climbing fiber-evoked calcium transients in Purkinje cell dendrites. *Proc. Natl. Acad. Sci. U.S.A.* 100, 2878–2883.

Yu, T. P., McKinney, S., Lester, H. A., and Davidson, N. (2001). γ-Aminobutyric acid type A receptors modulate cAMP-mediated long-term potentiation and long-term depression at monosynaptic CA3–CA1 synapses. *Proc. Natl. Acad. Sci. U.S.A.* 98, 5264–5269.

Zeviani, M., and Di Donato, S. (2004). Mitochondrial disorders. *Brain* 127, 2153–2172.

Zong, H., Ren, J. M., Young, L. H., Pypaert, M., Mu, J., Birnbaum, M. J., and Shulman, G. I. (2002). AMP kinase is required for mitochondrial biogenesis in skeletal muscle in response to chronic energy deprivation. *Proc. Natl. Acad. Sci. U.S.A.* 99, 15983–15987.

Conflict of Interest Statement: The authors declare that the research was conducted in the absence of any commercial or financial relationships that could be construed as a potential conflict of interest.

Received: 22 September 2011; accepted: 12 January 2012; published online: 01 February 2012.

Citation: Venkateswaran N, Sekhar S, Thirupatchur Sanjayasarathy T, Krishnan SN, Kabaleeswaran DK, Ramanathan S, Narayanasamy N, Jagathrakshakan SS and Vignesh SR (2012) Energetics based spike generation of a single neuron: simulation results and analysis. Front. Neuroenerg. ***4****:2. doi: 10.3389/fnene.2012.00002*

frontiers in
NEUROENERGETICS

OPINION ARTICLE
published: 20 December 2011
doi: 10.3389/fnene.2011.00008

Carbohydrate-biased control of energy metabolism: the darker side of the selfish brain

Tanya Zilberter*

Infotonic Consultancy, Stockholm, Sweden
**Correspondence: zilberter@gmail.com*

INTRODUCTION

There is evidence that the brain favors consumption of carbohydrates (CHO) rather than fats, this preference resulting in glycolysis-based energy metabolism domination. This metabolic mode, typical for consumers of the "Western diet" (Cordain et al., 2005; Seneff et al., 2011), is characterized by over-generation of reactive oxygen species and advanced glycation products both of which are implicated in many of the neurodegenerative diseases (Tessier, 2010; Vicente Miranda and Outeiro, 2010; Auburger and Kurz, 2011). However, it is not CHO but fat that is often held responsible for metabolic pathologies. This paper, based on analysis of experimental data, offers an opinion that the obesogenic and neurodegenerative effects of dietary fat in the high-fat diets (HFD) cannot be separated from the effects of the CHO compound in them. Since this is not a comprehensive literature review, only essential research results are presented.

It is general knowledge that the glucose homeostasis possesses very limited buffering capacities, while energy homeostasis in its fat-controlling part enjoys practically unlimited energy stores. Logically, a control system with a limited buffer should thoroughly defend the "consumption" part. Indeed, existing experimental data (briefly reviewed here later) show important properties of the CHO intake control that is different from or not shown for the fat intake control:

(1) A mere oral sensation of CHO elicits physiological anticipation response (cephalic phase) that is either inborn or rapidly conditioned.
(2) Oral CHO sensation stimulates reward-specific brain areas.
(3) CHO addiction is essentially similar to typical drug addictions.

These peculiarities can explain the physiologically and metabolically opposite effects of obesogenic HFD versus the ketogenic diet (KD), which is also HFD but lower in CHO.

THE SELFISH BRAIN CONCEPT: TWO MEANINGS

There are two ways to look at the CHO-biasing trait of the brain.

(1) The "Selfish Brain" is a term coined by Robert L. DuPont in the title of his book where he wrote: "With respect to aggression, fear, feeding, and sexuality, the brain is selfish. It simply wants what it wants right now" (DuPont, 1997). We must add, "if the environment permits, the brain gets it." The bad news is, in the long run the body can be harmed as the result.
(2) An elaborate (and rare for modern physiology) systemic concept explaining the fundamental ability of the brain to control priorities of energy allocation has been proposed by Peters and colleagues who also titled their theory the Selfish Brain. They wrote referring to DuPont's book: "The brain looks after itself first. Such selfishness is reminiscent of an earlier concept in which the brain's selfishness was addressed with respect to addiction. We chose our title by analogy but applied it in a different context, i.e., the competition for energy resources" (Peters et al., 2004).

These two meaning of the Selfish Brain have important common points if we consider the addiction (highly non-homeostatic) as a result of the "push" principle borrowed from the economic "push–pull" paradigm of supply chains. As early as in 1998, Hill and Peters wrote: "According to the 'push' principle, the environment pushes excess amounts of energy into the organism" (Hill and Peters, 1998).

They also share a common mechanism – reward. According to DuPond, "What makes a drug addictive is not that it is 'psychoactive' but that it produces specific brain reward. It is not withdrawal that hooks the addict, it is reward" (DuPont, 2008). This reward is hard-wired in the brain, in the loci where both "pull" and "push" systems might be converging, something that is discussed within the Selfish Brain paradigm as the comforting effect of food (Peters et al., 2007), particularly, the CHO-rich foods (Hitze et al., 2010).

PUSH AND PULL PARTS OF ENERGY SUPPLY CONTROL SYSTEM

The role of depots, as determined by a general principle in economic supply chains, is energy buffering in unstable environments (Fischer et al., 2011). Peters and Langemann (2009) analyzed two concepts of environment–organism relationship with opposite views at depots:

(1) An environment offering abundant energy beyond homeostatic need "pushes" it into the body via some evolutionary appropriate gateway. The surplus, naturally, goes into depots. Peters and Langemann, however, remained in doubt about this concept partly due to the fact that this "push" does not work invariably for all animal or human subjects (Martin et al., 2010; Cao et al., 2011).
(2) A somewhat alternative concept, well accepted for the last 50 years, concerns the "pull" character of the open system "organism–environment," supposedly in accordance with homeostatic needs. In this system, either the size of fat depot (Kennedy, 1953; Woods and Ramsay, 2011) or glucose levels (Mayer, 1953) are being controlled.

The role of CHO depot was not conferred, perhaps due to its negligible storing capacities. Indeed, the sizes of CHO and fat depots are incomparable. In the survival terms, CHO can provide energy support for less than 2 days (Bilsborough and Crowe, 2003), while a year-long complete

water–vitamin fast, with body fat as a sole energy source, has been reported (Stewart and Fleming, 1973).

NON-HOMEOSTATIC EFFECTS OF CHO VERSUS FAT

From the teleological standpoint, the strong drive for CHO intake beyond homeostatic needs exists very likely due to limited CHO-storing capacities. For fat with its vast depots, there is less (or none at all) evidence for a drive of similar magnitude. It seems to contradict the overwhelming reports on obesogenic properties of HFD but we shall see later that in reality there is no conflict.

Oral stimulation with both sweet and non-sweet CHO activated brain regions associated with reward – insula/frontal operculum, orbitofrontal cortex, and striatum. These regions were unresponsive to sweet, non-CHO stimulation with saccharin (Jeukendrup and Chambers, 2010). On the other hand, experiments with the no-calorie fat substitute (Olestra) revealed an impaired ability to use sensory cues associated with fat to predict caloric outcomes (Swithers et al., 2011). In humans, the intra-amniotic injection of fat (Lipiodol) reduced fetal drinking, while injection of sodium saccharin stimulated it; infants consumed the same amounts of milk formulas with different fat contents. Oral fat stimulation had no positive or negative mood-related effects, whereas sucrose shifted emotional spectrum toward positive scores (Mattes, 2005). CHO-rich food intake (buffet, KR 0.511:1) relieved neuroglycopenic and mood responses to stress independently from oral or i.v. administration of energy (Hitze et al., 2010).

Besides, HFD often fails in inducing obesity. Consequently, it is not uncommon in diet-induced obesity experiments that obesity-resistant subjects are eliminated from analysis or CHO are added to the diet to encourage overeating. Also, more accurate approximation of biologically adequate environments, e.g., allowing voluntary exercising, prevented HFD-induced obesity through radical modulation of hypothalamic control of fat metabolism (Cao et al., 2011).

To sum it up, fat *per se* is neither as highly rewarding as CHO nor it is as addictive (Wojnicki et al., 2008; Avena et al., 2009; Pickering et al., 2009; Berthoud et al., 2011). But why, then, it is the dietary fat that is blamed for overconsumption, obesity, and neuro-deteriorating effects?

THE ROLE OF MACRONUTRIENT COMPOSITION

Interestingly, the diet categorization (HFD, low-CHO, KD, etc.) is not fixed and varies from author to author (**Figure 1B**) although there is a clear-cut tool for labeling a diet according to its metabolic consequences.

A century ago, Woodyatt wrote: "antiketogenesis is an effect due to certain products which occur in the oxidation of glucose, an interaction between these products on the one hand and one or more of the acetone bodies on the other" (Woodyatt, 1910). Shaffer (1921) calculated the number of "ketogenic" molecules versus molecules of glucose and concluded that the maximal ratio compatible with the oxidation of the "ketogenic" molecules becomes possible when their ratio is at least 1:1. Later, Woodyatt (1921) suggested the following equation for calculating KD composition:

$$KR = (0.46\ pg + 0.90\ fg):(1.0\ cg + 0.58\ pg + 0.1\ fg)$$

Where KR is "ketogenic ratio," g is grams, P is protein, F is fat, and C is CHO.

Wilder and Winter (1922) defined the threshold of ketogenesis explaining it from the standpoint of condition where either ketone bodies or glucose can be oxidized. They arrived, together with Shaffer and Woodyatt, at the conclusion that KR for induction of ketogenesis should be 2:1 or higher.

This is a very important point, not only methodologically, but also ideologically. The KR invariably indicates whether the CHO proportion is low enough for allowing the fat-mobilizing pathway and ketogenesis, or high enough for blocking it and supporting glycolysis instead. The latter option opens the energy "push" opportunity through CHO intake gateway with the consequences discussed above. On the other hand, ketogenesis introduces a fuel alternative to glucose, which can be crucial in metabolic pathologies.

In the clinical KD, KR is usually 4:1; in the experimental KD, it's often 6:1 or higher. KR of HFD is more often than not undeclared, making it difficult to compare effects of different HFD – unless diet composition is known and calculation of KR is possible.

KETOGENESIS-TO-ANTIKETOGENESIS RATIOS: THE PHYSIOLOGICAL EFFECTS

Using the Woodyartt's equation, I calculated KR of 45 experimental works (2005–2011), wherever there was enough information regarding macronutrient composition. It is evident (**Figure 1B**) that in the HFD, KR is almost uniformly below the threshold of ketogenesis indicating a too-high proportion of CHO. It is interesting that even below the ketogenic threshold, the lower CHO proportion was, the higher neuroprotective effects were reported, e.g., against hypoxia (Puchowicz et al., 2007, 2008).

Among the most frequently reported consequences of HFD are features typical for metabolic syndrome – increased hunger/appetite, insulin resistance, elevated body fat deposition, and glucose intolerance along with decreased neuronal resistance to damaging conditions. A set of completely opposite effects is well documented for KD – decreased hunger/appetite, decreased levels of glucose and insulin in the blood, lower body fat deposition, increased neuronal resistance to damaging conditions (**Figure 1A**). The metabolic state caused by KD (**Figure 1C**) was called "unique" (Kennedy et al., 2007) and it closely resembles effects of calorie restriction (Domouzoglou and Maratos-Flier, 2011).

THE KETOGENIC RATIO AND THE "PUSH" COMPONENT OF ENERGY METABOLISM

The environment in Western-type societies can be characterized as "pushing" the energy into our organisms via activation of reward and addiction circuits of our selfish brains. In the standard experimental "Western Diet" (5TJN) with KR close to 1:1, CHO proportion is high enough to continuously maintain glycolysis, overconsumption, and the subsequent chain of events resulting in metabolic disturbances detrimental for the brain (Langdon et al., 2011).

Interestingly, this view of the environmental "push" is in line with a socio-economic explanation of the modern obesity epidemic. The NHANES surveys of 1971–2006 (Austin et al., 2011) revealed that in the USA population, the trend toward increased CHO intake and decreased fat intake (KR shift from 0.716 to 0.620) resulted in the increase of obesity

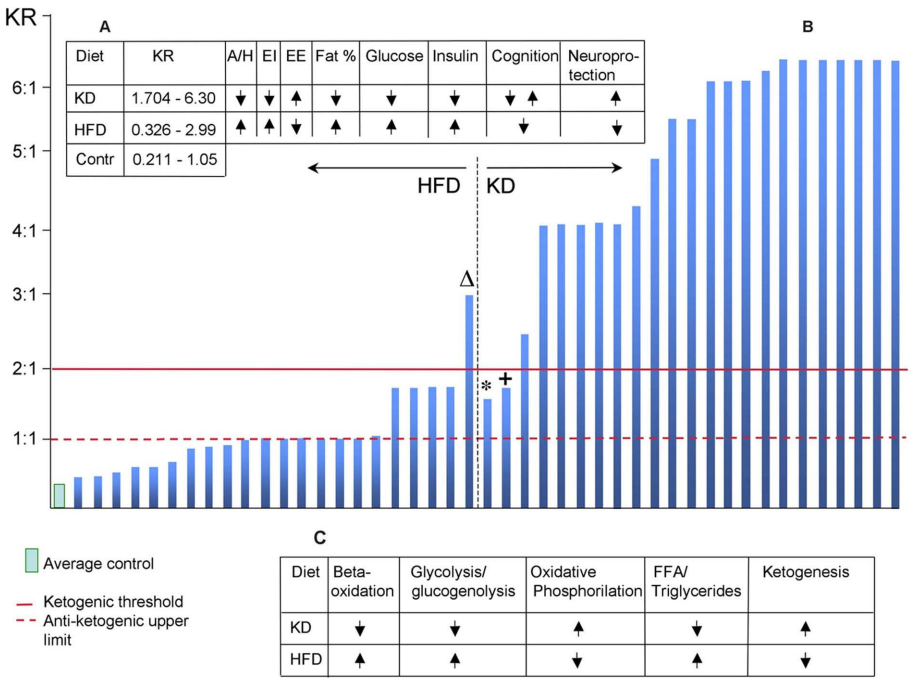

FIGURE 1 | (A) Summary of major physiological effects of HFD and KD. KR, ketogenic ratio; A/H, appetite/hunger; EI, energy intake; EE, energy expenditure. **(B)** Ketogenic ratio distribution of diets classified by authors as HFD or KD. ΔDiet defined as HFD (Holloway et al., 2011); KR = 2.994:1, resulted in cognitive impairment. The diet's duration was 5 days or within the adaptation period for KD when it does not exert its neuroprotective properties (Brinkworth et al., 2009). *Diet defined as KD (Johnstone et al., 2008); KR = 1.545:1 and gradually decreasing in the course of 10-week study since five extra grams of CHO was added each week. +Diet defined as KD (Johnstone et al., 2008); KR = 0.704:1 and 0.525:1 in two series. This finding is in agreement with (Puchowicz et al., 2008). **(C)** Metabolic profiles of HFD and KD (based on Kennedy et al., 2007).

incidence. In a recent article entitled "Using Marketing Muscle to Sell Fat: The Rise of Obesity in the Modern Economy," J. Zimmerman wrote: "In this paradigm, overeating results from more extensive advertising, new product development, increased portion sizes, and other tactics of food marketers that have caused shifts in the underlying demand for total food calories" (Zimmerman, 2011).

On the other hand, the diets with KR of 2:1 or higher are repeatedly described as metabolically beneficial, non-addictive, hunger–reducing, and neuroprotective (**Figure 1A**). In this, they mimic many of the effects of calorie restriction (Kennedy et al., 2007; Domouzoglou and Maratos-Flier, 2011) and are seen as evolutionary and genetically adequate but "no longer adaptive under current circumstances" (Stranahan and Mattson, 2011).

CONCLUSION

Homeostatic control of energy metabolism aims to maintaining energy balance and as soon as it is achieved, energy intake might be expected to decrease or stop. However, this is possible only in deterministic environments. In variable environments, energy storage becomes advantageous and approximately equal parts of energy are allocated for maintenance, reproduction, and depots (Fischer et al., 2011). Energy intake beyond rigid homeostatic regulation relies on behaviors with hedonic, rewarding, and addictive nuances more characteristic for CHO than for fat. Their traits notwithstanding, these behaviors are highly evolutionary significant: "Although at first glance, hijacking of the homeostatic regulatory mechanisms by its hedonic counterpart may seem conflicting, it should be borne in mind that during evolution, humans have lived in an environment where food availability was restricted and uncertain (e.g., hunter–gatherers) and the biological system has been 'hard-wired' to maximize energy stores" (Pandit et al., 2011).

To maximize energy stores, energy intake relies on CHO-driven behaviors to allow the environmental "push." Therefore: (1) dietary fat is not to blame for the diet-induced obesity; it is CHO that is not limited enough in HFD; (2) KR may be an element of common language in experiments with different methodological approaches.

REFERENCES

Auburger, G., and Kurz, A. (2011). The role of glyoxalases for sugar stress and aging, with relevance for dyskinesia, anxiety, dementia and Parkinson's disease. *Aging (Albany NY)* 3, 5–9.

Austin, G. L., Ogden, L. G., and Hill, J. O. (2011). Trends in carbohydrate, fat, and protein intakes and association with energy intake in normal-weight, overweight, and obese individuals: 1971–2006. *Am. J. Clin. Nutr.* 93, 836–843.

Avena, N. M., Rada, P., and Hoebel, B. G. (2009). Sugar and fat bingeing have notable differences in addictive-like behavior. *J. Nutr.* 139, 623–628.

Berthoud, H. R., Lenard, N. R., and Shin, A. C. (2011). Food reward, hyperphagia, and obesity. *Am. J. Physiol. Regul. Integr. Comp. Physiol.* 300, R1266–R1277.

Bilsborough, S. A., and Crowe, T. C. (2003). Low-carbohydrate diets: what are the potential short- and long-term health implications? *Asia Pac. J. Clin. Nutr.* 12, 396–404.

Brinkworth, G. D., Noakes, M., Buckley, J. D., Keogh, J. B., and Clifton, P. M. (2009). Long-term effects of a very-low-carbohydrate weight loss diet compared with an isocaloric low-fat diet after 12 mo. *Am. J. Clin. Nutr.* 90, 23–32.

Cao, L., Choi, E. Y., Liu, X., Martin, A., Wang, C., Xu, X., and During, M. J. (2011). White to brown fat phenotypic switch induced by genetic and environmental activation of a hypothalamic-adipocyte axis. *Cell Metab.* 14, 324–338.

Cordain, L., Eaton, S. B., Sebastian, A., Mann, N., Lindeberg, S., Watkins, B. A., O'keefe, J. H., and Brand-Miller, J. (2005). Origins and evolution of the Western diet: health implications for the 21st century. *Am. J. Clin. Nutr.* 81, 341–354.

Domouzoglou, E., and Maratos-Flier, E. (2011). Fibroblast growth factor 21 is a metabolic regulator that plays a role in the adaptation to ketosis. *Am. J. Clin. Nutr.* 93(Suppl.), 901S–905S.

DuPont, R. (2008). Addiction in medicine. *Trans. Am. Clin. Climatol. Assoc.* 119, 227–241.

DuPont, R. L. (1997). *The Selfish Brain: Learning from Addiction.* Center City, MN: Hazelden.

Fischer, B., Dieckmann, U., and Taborsky, B. (2011). When to store energy in a stochastic environment. *Evolution* 65, 1221–1232.

Hill, J. O., and Peters, J. C. (1998). Environmental contributions to the obesity epidemic. *Science* 280, 1371–1374.

Hitze, B., Hubold, C., Van Dyken, R., Schlichting, K., Lehnert, H., Entringer, S., and Peters, A. (2010). How the selfish brain organizes its supply and demand. *Front. Neuroenergetics* 2:7. doi: 10.3389/fnene.2010.00007

Holloway, C. J., Cochlin, L. E., Emmanuel, Y., Murray, A., Codreanu, I., Edwards, L. M., Szmigielski, C., Tyler, D. J., Knight, N. S., Saxby, B. K., Lambert, B., Thompson, C., Neubauer, S., and Clarke, K. (2011). A high-fat diet impairs cardiac high-energy phosphate metabolism and cognitive function in healthy human subjects. *Am. J. Clin. Nutr.* 93, 748–755.

Jeukendrup, A. E., and Chambers, E. S. (2010). Oral carbohydrate sensing and exercise performance. *Curr. Opin. Clin. Nutr. Metab. Care* 13, 447–451.

Johnstone, A. M., Horgan, G. W., Murison, S. D., Bremner, D. M., and Lobley, G. E. (2008). Effects of a high-protein ketogenic diet on hunger, appetite, and weight loss in obese men feeding ad libitum. *Am. J. Clin. Nutr.* 87, 44–55.

Kennedy, A. R., Pissios, P., Otu, H., Roberson, R., Xue, B., Asakura, K., Furukawa, N., Marino, F. E., Liu, F. F., Kahn, B. B., Libermann, T. A., and Maratos-Flier, E. (2007). A high-fat, ketogenic diet induces a unique metabolic state in mice. *Am. J. Physiol. Endocrinol. Metab.* 292, E1724–E1739.

Kennedy, G. (1953). The role of depot fat in the hypothalamic control of food intake in the rat. *Proc. R. Soc. Lond. B Biol. Sci.* 140, 578–596.

Langdon, K. D., Clarke, J., and Corbett, D. (2011). Long-term exposure to high fat diet is bad for your brain: exacerbation of focal ischemic brain injury. *Neuroscience* 182, 82–87.

Martin, B., Ji, S., Maudsley, S., and Mattson, M. P. (2010). "Control" laboratory rodents are metabolically morbid: why it matters. *Proc. Natl. Acad. Sci. U.S.A.* 107, 6127–6133.

Mattes, R. D. (2005). Fat taste and lipid metabolism in humans. *Physiol. Behav.* 86, 691–697.

Mayer, J. (1953). Genetic, traumatic and environmental factors in the etiology of obesity. *Physiol. Rev.* 33, 472–508

Pandit, R., De Jong, J. W., Vanderschuren, L. J., and Adan, R. A. (2011). Neurobiology of overeating and obesity: the role of melanocortins and beyond. *Eur. J. Pharmacol.* 660, 28–42.

Peters, A., and Langemann, D. (2009). Build-ups in the supply chain of the brain: on the neuroenergetic cause of obesity and type 2 diabetes mellitus. *Front. Neuroenergetics* 1:2. doi: 10.3389/neuro.14.002.2009

Peters, A., Pellerin, L., Dallman, M. F., Oltmanns, K. M., Schweiger, U., Born, J., and Fehm, H. L. (2007). Causes of obesity: looking beyond the hypothalamus. *Prog. Neurobiol.* 81, 61–88.

Peters, A., Schweiger, U., Pellerin, L., Hubold, C., Oltmanns, K. M., Conrad, M., Schultes, B., Born, J., and Fehm, H. L. (2004). The selfish brain: competition for energy resources. *Neurosci. Biobehav. Rev.* 28, 143–180.

Pickering, C., Alsio, J., Hulting, A. L., and Schioth, H. B. (2009). Withdrawal from free-choice high-fat high-sugar diet induces craving only in obesity-prone animals. *Psychopharmacology (Berl.)* 204, 431–443.

Puchowicz, M. A., Xu, K., Sun, X., Ivy, A., Emancipator, D., and Lamanna, J. C. (2007). Diet-induced ketosis increases capillary density without altered blood flow in rat brain. *Am. J. Physiol. Endocrinol. Metab.* 292, E1607–E1615.

Puchowicz, M. A., Zechel, J. L., Valerio, J., Emancipator, D. S., Xu, K., Pundik, S., Lamanna, J. C., and Lust, W. D. (2008). Neuroprotection in diet-induced ketotic rat brain after focal ischemia. *J. Cereb. Blood Flow Metab.* 28, 1907–1916.

Seneff, S., Wainwright, G., and Mascitelli, L. (2011). Nutrition and Alzheimer's disease: the detrimental role of a high carbohydrate diet. *Eur. J. Intern. Med.* 22, 134–140.

Shaffer, P. A. (1921). Antiketogenesis. I. An in vitro analogy. *J. Biol. Chem.* xlvii, 433.

Stewart, W. K., and Fleming, L. W. (1973). Features of a successful therapeutic fast of 382 days' duration. *Postgrad. Med. J.* 49, 203–209.

Stranahan, A. M., and Mattson, M. P. (2011). Bidirectional metabolic regulation of neurocognitive function. *Neurobiol. Learn. Mem.* 96, 507–516.

Swithers, S. E., Ogden, S. B., and Davidson, T. L. (2011). Fat substitutes promote weight gain in rats consuming high-fat diets. *Behav. Neurosci.* 125, 512–518.

Tessier, F. J. (2010). The Maillard reaction in the human body. The main discoveries and factors that affect glycation. *Pathol. Biol. (Paris)* 58, 214–219.

Vicente Miranda, H., and Outeiro, T. F. (2010). The sour side of neurodegenerative disorders: the effects of protein glycation. *J. Pathol.* 221, 13–25.

Wilder, R., and Winter, M. (1922). The threshold of ketogenesis. *J. Biol. Chem.* 52, 393–401.

Wojnicki, F. H., Charny, G., and Corwin, R. L. (2008). Binge-type behavior in rats consuming trans-fat-free shortening. *Physiol. Behav.* 94, 627–629.

Woods, S. C., and Ramsay, D. S. (2011). Food intake, metabolism and homeostasis. *Physiol. Behav.* 104, 4–7.

Woodyatt, R. (1910). The action of glycol aldehyd and glycerin aldehyd in diabetes mellitus and the nature of antiketogenesis. *J. Am. Med. Assoc.* 1, 2109.

Woodyatt, R. (1921). Objects and methods of diet adjustment in diabetes. *Arch. Intern. Med* 28, 125.

Zimmerman, F. J. (2011). Using marketing muscle to sell fat: the rise of obesity in the modern economy. *Annu. Rev. Public Health* 32, 285–306.

Received: 10 October 2011; accepted: 02 December 2011; published online: 20 December 2011.

Citaiton: Zilberter T (2011) Carbohydrate-biased control of energy metabolism: the darker side of the selfish brain. Front. Neuroenerg. ***3****:8. doi: 10.3389/fnene.2011.00008*